



Breast Cancer and Oxidative Stress

Maryam Afzal

Doctor of Philosophy (PhD)

January 2010

*TENOVUS Centre for Cancer Research,
Cardiff University, King Edward VII Avenue, Cardiff, CF10 3XF*

UMI Number: U584391

All rights reserved

INFORMATION TO ALL USERS

The quality of this reproduction is dependent upon the quality of the copy submitted.

In the unlikely event that the author did not send a complete manuscript and there are missing pages, these will be noted. Also, if material had to be removed, a note will indicate the deletion.



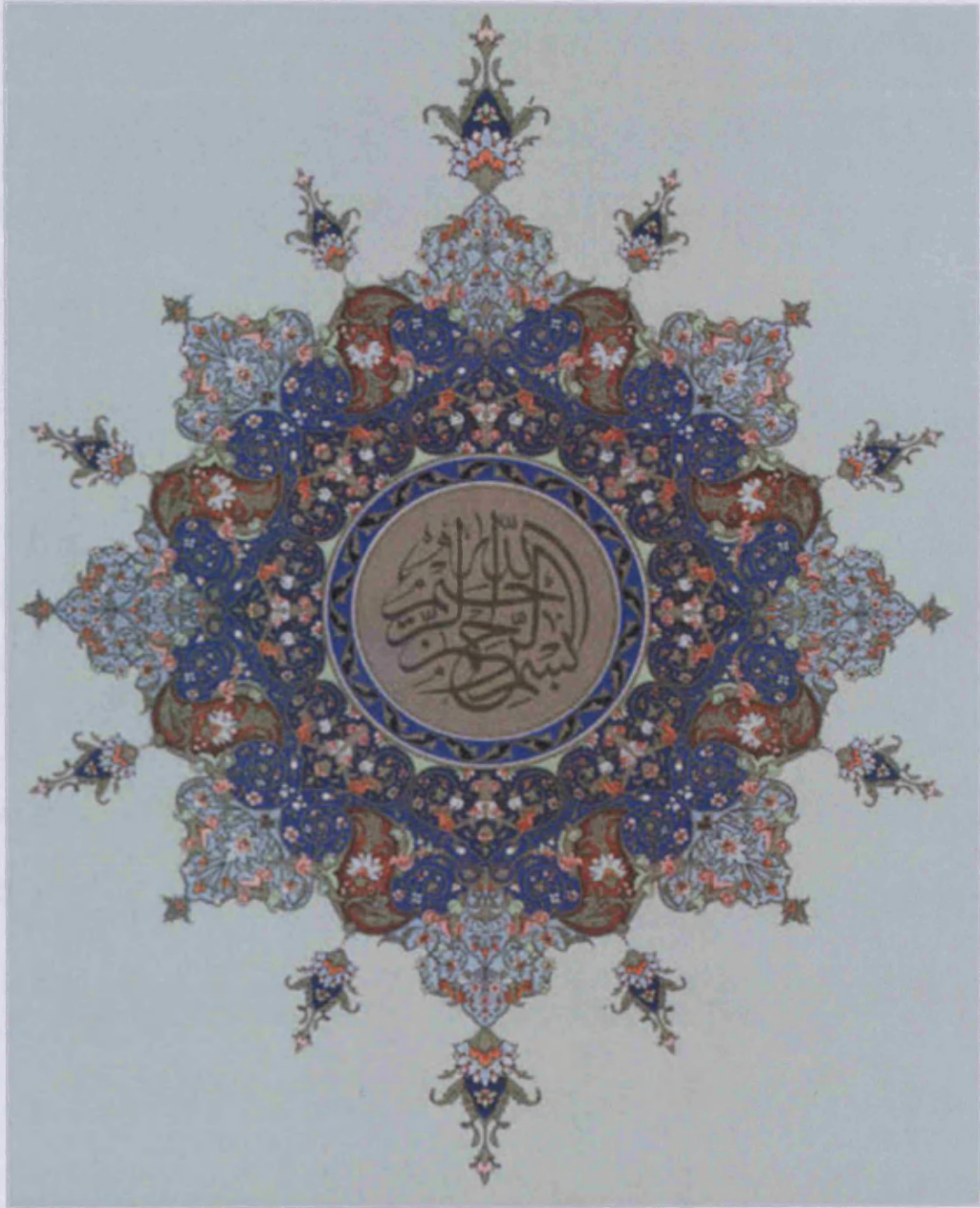
UMI U584391

Published by ProQuest LLC 2013. Copyright in the Dissertation held by the Author.
Microform Edition © ProQuest LLC.

All rights reserved. This work is protected against
unauthorized copying under Title 17, United States Code.




ProQuest LLC
789 East Eisenhower Parkway
P.O. Box 1346
Ann Arbor, MI 48106-1346




Declaration

This work has not previously been accepted in substance for any degree and is not concurrently submitted in candidature for any degree.

Signed..... (candidate) Date ...15:01:10....


Statement 1

This thesis is being submitted in partial fulfilment of the requirements for the degree of PhD

Signed..... (candidate) Date ...15:01:10....

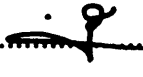
Statement 2

This thesis is the result of my own independent work/investigation, except where otherwise stated. Other sources are acknowledged by explicit references.

Signed..... (candidate) Date ...15:01:10....

Statement 3

I hereby give consent for my thesis , if accepted, to be available for photocopying and for inter-library loan, and for the title and abstract to be made available to outside organisations.

Signed..... (candidate) Date ...15:01:10....

Abstract

Endocrine and anti-EGFR strategies are used to treat breast cancer. Unfortunately, resistance can be acquired. Deciphering resistance mechanisms remains essential to design treatments for this adverse state. Oxidative stress is the cellular imbalance of pro-oxidants (promoting cell death) and antioxidants (facilitating cell survival and chemotherapy/radiotherapy resistance). However, it remains unexplored whether endocrine or anti-EGFR resistance also associates with altered redox balance. In this project, redox balance was examined using *in vitro* human resistant breast cancer models TAMR, FASR, X-MCF and NEW DUBS, comparing with responsive w/tMCF7 cells using microarray analysis, PCR, and TAC, ROS, or MTT assays. Pro-oxidant levels increased significantly in all resistant models but this did not impact adversely on growth. Significantly increased antioxidant levels were also observed in all resistant models, perhaps limiting pro-oxidant increases to maintain cell survival. Antioxidants were also significantly induced by antihormones in w/tMCF7 cells that may limit apoptosis with early treatment. Expression of 15 antioxidant genes increased in resistant cells spanning multiple resistant states. While gefitinib challenge revealed many antioxidant genes were EGFR/kinase signalling-regulated in TAMR cells, gefitinib and further signal transduction inhibitors (STIs) indicated total antioxidant capacity was not. Thus, additional genes/signalling probably drive increased antioxidants in resistant cells; future deciphering and depletion of antioxidants could feasibly block cell survival in multiple resistant states. Several STIs further increased pro-oxidants in TAMR cells, indicating oxidative stress was also not EGFR/kinase-promoted; since STIs also further increased antioxidant capacity, this may again limit pro-oxidant increases and hence apoptotic effect. Importantly, the thesis revealed resistant cells may be particularly sensitive to agents inducing excessive oxidative stress. Redox balance and feasibility of agents influencing redox remains complex. However, new findings and concepts emerging from this thesis are worthy of future exploration for potential treatments for resistance to endocrine/anti-EGFR agents.

Acknowledgments

I would like to begin by thanking most sincerely Dr Julia MW Gee for her supervision, guidance and contribution to the evolution of this research project. Expressing thanks also to Professor Robert I Nicholson for his helpful guidance during the course of this research.

Special thanks are due to Staff and Students (past and present) at the TENOVUS Centre for Cancer Research who had made a valuable contribution to the development of this thesis including Richard, Carol, Huw, Sue, Sara, Pete

With particular thanks to those who had made a contribution to *my* development over the years, never forgetting Siân, Sioned, Steve, Ross, Ian, Valery, and the brightest star of all, Laura Jane Lewis!

This thesis is dedicated to: my Father, Dr M. Reza Afzal-khoshkbijari and Mother, Afsaneh Derakhshan, for whom I initiated the process in the first place; my Brothers Hamed and Saeed who encouraged me through it; my soul mate Mahdi Damghani and first born Ibrahim who made me complete it; and to my grandmother Aziz and grandfather Haji. This is for you

Contents

Abstract	ii
-----------------	----

Acknowledgments	iii
------------------------	-----

Contents	iv
-----------------	----

Abbreviations	x
----------------------	---

Chapter 1 – Introduction

Breast Cancer and Oxidative Stress: the Role of Pro-oxidants in Promoting Tumours as well as Cell Death, and the Potential Role of Antioxidants in Promoting Tumour Cell Survival and Resistance	1
---	---

1.1 Introduction	2
1.2 Breast Cancer	4
1.2.1 Oestrogen Receptor	5
1.2.2 Oestrogen Receptor Signalling	8
1.2.3 Endocrine Therapy in Breast Cancer	10
1.2.4 Resistance Acquired to Endocrine Therapy	13
1.3 Oxidative Stress	20
1.3.1 Pro-Oxidant Mechanisms of ROS Production	22
1.3.2 Downstream Cellular Effects of Oxidative Stress	27
1.3.2.1 Lipid Peroxidation	27
1.3.2.2 Oxidative DNA Damage	29
1.3.2.3 Activation of Signalling Pathways	30
1.3.3 Antioxidants	31
1.3.3.1 Enzymatic Antioxidants	32
1.3.3.1.1 Superoxide Dismutase (SOD)	32
1.3.3.1.2 Catalase (CAT)	34
1.3.3.1.3 Glutathione Peroxidase (GPX)	35
1.3.3.2 Non-Enzymatic Antioxidants	36

1.3.3.2.1	<i>Thiol Antioxidants – Glutathione (GSH) Network</i>	36
1.3.3.2.2	<i>Thiol Antioxidants – Thioredoxin (TXN)</i>	39
1.3.3.2.3	<i>Peroxiredoxins (PRDX) and their interplay with TXN</i>	41
1.4	Hypothesis and Aims	42
Chapter 2 – Methodology		45
<hr/>		
2.1	Cell Culture studies	46
2.1.1	Materials	46
2.1.1.1	<i>Cell culture reagents and Plasticware</i>	46
2.1.1.2	<i>Cell lines, anti-oestrogens, signal transduction inhibitors, and drugs impacting on oxidative stress</i>	47
2.1.1.3	<i>Reagents used for MTT growth assays</i>	47
2.1.1.4	<i>Reagents used for TAC analysis</i>	48
2.1.1.5	<i>Reagents and plasticware used for ROS detection</i>	48
2.1.1.6	<i>Reagents and glassware used for Ki67 immuno staining</i>	48
2.1.1.7	<i>Reagents used in apoptosis analysis</i>	49
2.1.2	Methodology	49
2.1.2.1	<i>Development of acquired resistant breast cancer cell models</i>	49
2.1.2.2	<i>Maintenance of w/t MCF7 and acquired resistant breast cancer cell models</i>	51
2.1.2.3	<i>Coulter Counting Growth experiment in responsive and acquired resistant cell lines</i>	52
2.1.2.4	<i>MTT assay to evaluate basal growth of acquired resistant versus responsive cells and in the presence of tyrosine kinase inhibitors (TKI),</i>	

	<i>signal transduction inhibitors (STIs), Antioxidant inhibitor (BSO), or oxidative stress inducer</i>	
	<i>Menadione (MSB)</i>	53
	<i>2.1.2.5 TAC analysis</i>	57
	<i>2.1.2.6 ROS detection</i>	60
	<i>2.1.2.7 Ki67 immunostaining for proliferation</i>	61
	<i>2.1.2.8 ApoAlert assay (MMS) for apoptosis</i>	62
2.2	Affymetrix microarray analysis	64
2.2.1	Materials	64
	<i>2.2.1.1 Cell culture reagents and plasticware for microarrays</i>	64
	<i>2.2.1.2 RNA purification kits</i>	64
2.2.2	Methodology	64
	<i>2.2.2.1 RNA extraction from cell lines</i>	65
	<i>2.2.2.2 Hybridisation to Affymetrix Chips and expression database construction for expression studies in the cell lines</i>	66
	<i>2.2.2.3 Creating new projects for expression analysis</i>	68
	<i>2.2.2.4 Initial interrogation of gene of known expression profile (quality control step)</i>	73
	<i>2.2.2.5 Interrogation of antioxidant gene expression profile</i>	73
	<i>2.2.2.6 Multiple probe analysis for antioxidant genes (quality control)</i>	75
2.3	RT-PCR studies of selected antioxidant gene expression	79
2.3.1	Materials	79
	<i>2.3.1.1 Cell culture reagents and plasticware for PCR studies</i>	79
	<i>2.3.1.2 Enzymes and inhibitors</i>	79
	<i>2.3.1.3 PCR reagents</i>	79
	<i>2.3.1.4 Equipment</i>	80
2.3.2	Methodology	80

2.3.2.1 Polymerase Chain Reaction (PCR)	81
2.3.2.1.1 Reverse transcription (RT) of cDNA templates	81
2.3.2.1.2 Oligonucleotide primer design and PCR amplification from cDNA	83
2.3.2.1.3 Visualisation of PCR Products	89

Chapter 3 – Results

Antioxidants and Oxidative stress in Resistant and Responsive Breast Cancer Cells	91
--	----

3.1 Total Antioxidant Capacity (TAC) measured in ER+ Tamoxifen resistant versus Endocrine responsive MCF-7 breast cancer cells, and further antihormone and anti-EGFR resistant models	92
3.2 Affymetrix Microarray mRNA profiling to determine Antioxidant gene expression in antihormone resistance	100
3.2.2 GeneSifter analysis of antioxidant gene category	104
3.3 PCR Verification studies for the 11 induced Antioxidant genes increased in resistance	113
3.4 TAC and Antioxidant gene expression during initial treatment of w/t MCF7 cells with anti-hormonal agents	127
3.5 Impact of EGFR inhibitor Gefitinib on antioxidant gene expression in TAMR cells	146
3.6 Impact of EGFR inhibitor gefitinib and further growth factor signalling inhibitors on TAC in TAMR cells	155
3.7 Impact of glutathione (GSH) pathway depletion using BSO +/- EGFR blockade in TAMR cells	161
3.8 Oxidative stress (ROS) measured in TAMR cells versus w/t MCF-7 cells	164
3.9 ROS measurements in other acquired resistant models versus w/t MCF7 cells	168

3.9.1	ROS measurement in FASR cells versus w/tMCF7	168
3.9.2	ROS measurement in X-MCF cells versus w/tMCF7	168
3.9.3	ROS measurement in NEW DUBS cells versus w/tMCF7	169
3.10	Examination of ROS in w/t MCF7 cells during initial treatment with antihormonal agents	173
3.11	Impact of Inhibitors of growth factor signalling pathways on ROS level in TAMR cells	174
3.12	TAMR growth sensitivity to excess oxidative stress	180
3.13	Growth sensitivity of further acquired resistant models to excess oxidative stress	184
Chapter 4 –Discussion		189
<hr/>		
4.1	Discussion and future studies	190
4.2	Summary of potential redox mechanism in acquired resistant breast cancer cells and therapeutic implications:	222
Chapter 5 – References		228
<hr/>		

Appendix I – Compilation of Signal Transduction pathway genes related to Oxidative Stress (n =117)

Appendix II – Methodology Recipes

Abbreviations

8-oxo-G	8-Oxoguanine
ABTS	2,2'-azino-bis(3-ethylbenzthiazoline-6-sulfonic acid)
AF1	Activation function 1
AF2	Activation function 2
Akt	serine/threonine protein kinase
ARE	Antioxidant response elements
AW464	4-(benzothiazol-2-yl)-4-hydroxycyclohexa-2,5-dienone
β actin	Beta actin
BH ₄	6(R)-tetrahydro-L-biopterin
BSO	L-Buthionine sulfoximine
CAT	Catalase
Cu/Zn-SOD	
/or SOD1	Cytosolic copper/zinc superoxide dismutase
CYP450	Cytochrome P450
DCF	2',7'-dichlorofluorescein
DMSO	Dimethyl sulfoxide
DNA	Deoxyribonucleic acid
E ₂	Oestradiol
EC-SOD	Extracellular superoxide dismutase
EDTA	Ethylenediaminetetraacetic acid (Disodium salt)
EGFR	Epidermal growth factor receptor
eNOS	Endothelial nitric oxide synthase
EPHX2	Epoxide hydrolase 2
ER	Oestrogen receptor
ER ⁻	Oestrogen receptor negative
ER ⁺	Oestrogen receptor positive
ERE	Oestrogen response elements
ESR	Electron spin resonance spectroscopy
EtBr	Ethidium bromide

ETC	Electron transport chain
FAS	Faslodex
FCS	Foetal calf serum
G6PD	Glucose-6-phosphate 1-dehydrogenase
GEF	Gefitinib
GLRX	Glutaredoxin
GPX	Glutathione peroxidases
GPX2	Glutathione peroxidases 2
GSH	Glutathione
GST	Glutathione-S-transferase
GSTA4	Glutathione S-transferase A4
GSTM3	Glutathione-S-transferase M3
GSTT2	Glutathione S-transferase theta 2
H₂DCF-DA	2',7'-dichlorodihydrofluorescein diacetate
H₂O₂	Hydrogen peroxide
HO-1	Heme oxygenase-1
HNE	4-hydroxy-2-nonenal
IC₅₀	Inhibitory concentration to 50% of cells
IGF	Insulin-like growth factor
IGFR	Insulin-like growth factor receptor
iNOS	Inducible nitric oxide synthase
Keap1	Kelch-like ECH-associated protein 1
MAPK	Mitogen-activated protein kinase
MDA	Malondialdehyde
Mn-SOD	
/or SOD2	Mitochondrial magnesium superoxide dismutase
MMS	Mitochondrial membrane sensor
MSB	Menadione-sodium-Bisulfite
MTT	(3-(4,5-dimethylthiazol-2-yl)-2, 5-diphenyltetrazolium bromide)
Ni	Nickel
nNOS	Neuronal nitric oxide synthase
NO•	Nitric oxide

NOS	Nitric oxide synthase
NQO1	NAD(P)H dehydrogenase, quinone 1
Nrf2	Nuclear factor-erythroid-2-related factor 2
¹O₂	Singlet oxygen
O₂	Molecular oxygen
O₂[•]	Superoxide
O₂^{•-}	Superoxide anion
OH[•]	Hydroxyl radicals
OONO[•]	Peroxynitrite
PARTH	Parthenolide
PBS	Phosphate buffer solution
PCR	Polymerase chain reaction
PRDX	Peroxiredoxins
PRDX1-6	Peroxiredoxin 1-6
pS2	see TF1
R-COO[•]	Peroxyl radicals
RNA	Ribonucleic acid
RNS	Reactive nitrogen species
ROOH	Organic peroxide
ROS	Reactive oxygen species
RT	Reverse transcription
RTKs	Receptor tyrosine kinases
SD	Standard deviation
SEM	Standard error of mean
SERD	selective oestrogen receptor down-regulator
SERMs	Selective oestrogen receptor modulators
SOD	Superoxide dismutase
Src	Steroid receptor co-activator protein
STIs	Signal transduction inhibitors
TAC	Total antioxidant capacity
TAE	Tris acetate buffer
TAM	Tamoxifen

TESPA	3-Aminopropyltriethoxysilane
TF1	Trefoil factor 1 (pS2)
TKI	Tyrosine kinase inhibitor
TXN	Thioredoxin
TXNRD	Thioredoxin reductase
TXNRD1	Thioredoxin reductase 1
TXNRD2	Thioredoxin reductase 2
UGT1A6	UDP glycosyltransferase 1 family, polypeptide A6
UV	Ultra violet
WORT	Wortmannin
w/t	Wild type

Chapter 1 – Introduction

Breast Cancer and Oxidative Stress: the Role of Pro-oxidants in Promoting Tumours as well as Cell Death, and the Potential Role of Antioxidants in Promoting Tumour Cell Survival and Resistance

1.1 Introduction

Various endocrine strategies, notably anti-oestrogen and oestrogen deprivation treatments, have been designed to compromise oestrogen signalling and are valuable in treating oestrogen receptor positive (ER+) breast cancer (Dowsett et al., 2005; Gee et al., 2005; Nicholson & Johnson, 2005). However, despite initial responses, resistance is commonly acquired during treatment where this event can be associated with poorer prognosis (Katzenellenbogen et al., 1995). Therefore, discovery of the mechanisms driving endocrine resistant growth is essential to design therapies to better treat this adverse state.

The Tenovus Centre for Cancer Research (and others) have previously identified through use of *in vitro* models that epidermal growth factor receptor (EGFR) signalling is one factor that can be important in acquired tamoxifen (TAM) resistance. EGFR and its associated signalling is hence being targeted in clinical trials using anti-EGFR agents such as gefitinib and further ErbB inhibitors and signal transduction inhibitors (STIs) (Gee et al., 2003; Hiscox et al., 2004; Jones et al., 2004; Gee et al., 2005; Jones et al., 2005). However, emerging experience indicates that such newer targeted agents will not be spared the phenomenon of resistance. Therefore, continued deciphering of the biology underlying resistant states remains essential to reveal ways to improve treatment. This investigation will look at the role of oxidative stress in endocrine and anti-EGFR resistant states by studying various acquired resistant breast cancer models *in vitro*.

Oxidative stress can be defined as an imbalance of pro-oxidants and antioxidants within the cell. An excess of oxidants, such as superoxide ($O_2^{\cdot-}$), hydrogen peroxide (H_2O_2), and hydroxyl radicals (OH^{\cdot}), can promote DNA damage and lipid peroxidation leading to cell death (Mathews CK, *et al.*, 1999). However, there is an increase in antioxidants generated by the cell in response to oxidative stress such as: superoxide dismutase (SOD) (Housset, 1987; Pani *et al.*, 2004); catalase (CAT) (Spitz *et al.*, 1993; Suematsu *et al.*, 2002); peroxiredoxins (PRDX) (Iwao-Koizumi *et al.*, 2005); glutathione peroxidases (GPX) (Housset, 1987; Szatrowski & Nathan, 1991; Toyokuni *et al.*, 1994); and thioredoxin (TXN) (Yokomizo *et al.*, 1995; Sinha *et al.*, 1998; Gorgan *et al.*, 2000; Hedley *et al.*, 2004; Ahmadi *et al.*, 2006), that can facilitate cell survival. Indeed, the antioxidant response has in some instances been reported to confer resistance to chemotherapeutics whose anti-tumour mechanism is known to involve the induction of oxidative stress (Toyokuni *et al.*, 1994).

While previously not significantly explored, endocrine or anti-EGFR agent treatments and subsequently acquired resistance might also feasibly be associated with changes in redox balance. Antioxidants might thus again actively contribute to cell survival in the presence of such drugs and hence contribute to resistant growth. In this project, the relevance of antioxidants to resistant growth and also evaluation of oxidative stress will be assessed with the aim of determining new mechanisms and thereby potential future therapeutic approaches for resistant states.

1.2 Breast Cancer

An Egyptian papyrus first referred to tumours of the breast between 3000–1500 BC (CancerStats: a brief history of cancer–UK, 2006). The Greek physician Hippocrates, the "Father of Medicine", was the first to recognise the difference between benign and malignant tumours around 400 BC (Adams, 2004; CancerStats: a brief history of cancer–UK, 2006). He named malignant tumours "Carcinos" (crab/crayfish), resembling their appearance, and later this included the suffix –oma (swelling), giving the name "Carcinoma" (Adams, 2004). Breast carcinoma is now the most common cancer in the UK, and in 2006, over 45,500 women and 300 men were diagnosed with breast cancer. (CancerStats: Breast Cancer-UK, 2006). Mortality rates have declined by 25% since 1987 due to earlier detection and improved treatment, notably including the endocrine agent tamoxifen (TAM) (Lacey et al., 2005; CancerStats: a brief history of cancer–UK, 2006). However, there are still many deaths associated with the disease (12,400 annually (30% of all breast cancer patients) CancerStats: Breast Cancer-UK, 2006), and so improved treatments remain critical.

Breast cancer has been related to increased age, alcohol consumption, diet, and genetic make-up. However, in particular female steroid hormones are implicated in breast cancer development and subsequent growth, as women are clearly at a higher risk of developing the disease than men (99% of sufferers being women, and only 1% being men) (Brekelmans, 2003; CancerStats: Breast Cancer-UK, 2006). There is much evidence supporting the fact that

breast cancer is a disease related to the steroid hormone oestrogen and its signalling, with a higher risk of developing the disease associated with a women's increased lifetime exposure to oestrogen, for example associating with an early menarche, late menopause, or reproductive factors such as late first pregnancy (Madigan et al., 1995; Brekelmans, 2003), as well as exposure to exogenous steroid hormones through use of hormone replacement therapy (Brekelmans, 2003). In 1896, Sir George Beatson reported regression of an advanced mammary cancer in one of his patients (Murphy, 1998). This was achieved by surgical removal of the ovaries, the organs now known to comprise the predominant source of oestrogen in the premenopausal woman, data directly associating this steroid hormone with maintenance of some established mammary tumours. Such findings also had therapeutic implications, although nowadays emphasis is placed on the use of pharmacological inhibitors of oestrogen production as well as drugs to interfere with the oestrogen signalling mechanism (Murphy, 1998).

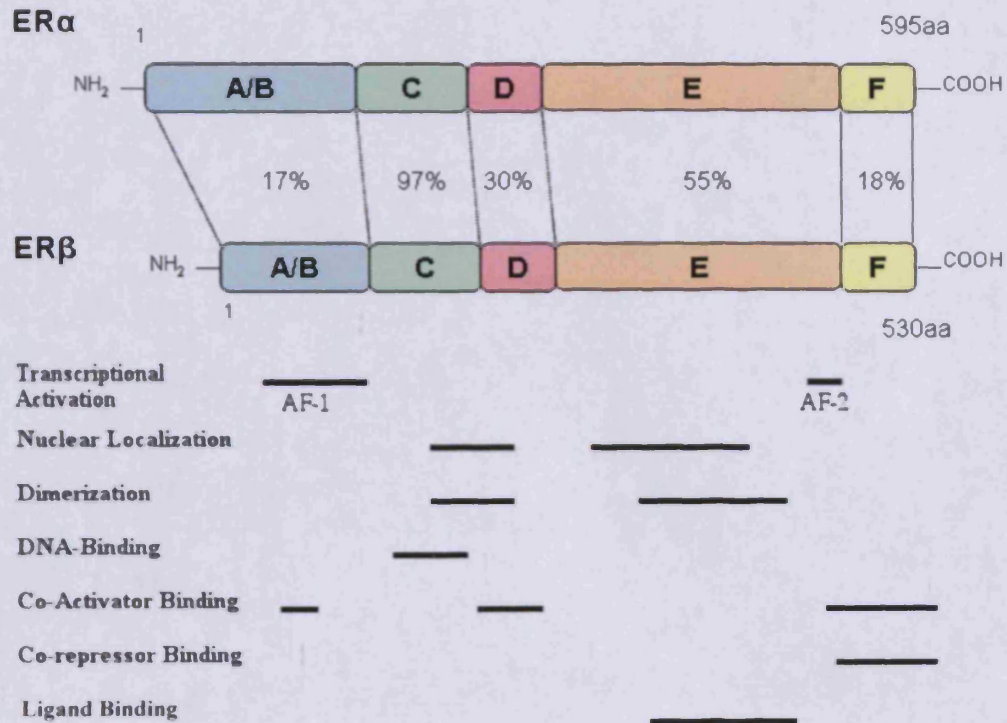
1.2.1 Oestrogen Receptor

There are two receptors by which oestrogen can signal to promote its cellular actions, namely ER α and ER β (Jenson & Jacobson, 1962; Kuiper et al, 1996). These receptor proteins have some homology as members of the steroid receptor superfamily (Figure 1.1), however, they are encoded on different chromosomes and have distinct patterns of distribution, differences in structure, and ligand binding affinity (Kuiper et al., 1997). The ratio of ER α to ER β at a target site might be significant in tissue modulation, as predominance of

functional ER α to ER β correlates with very high levels of proliferation, whereas a high ER β over ER α correlates with low levels of proliferation (Roger et al., 2001; Shaaban et al., 2003; Paruthiyil et al., 2004; Acconcia et al., 2005). However, it is ER α that is the most predominant receptor protein in breast cancer, expressed in at least 70% of tumours in the breast cancer epithelial cell nuclei (Green et al., 1986; Kuiper et al., 1997; Fuqua et al., 2003) and conferring an “ER positive” (ER⁺) tumour status.

The ER α protein (subsequently referred to as ER in this thesis) is somewhat larger than ER β , containing 595 versus 530 amino acids respectively (Figure 1.1) (Fuqua et al., 1999; Fuqua et al., 2003). Like other steroid hormone receptors, ER is a nuclear transcription factor with an NH₂-terminal (A/B) domain bearing a ligand-independent transcriptional activation function 1 (AF-1), a ligand-binding (E) domain near the COOH-terminal with a hormone-dependent transcriptional activation function 2 (AF-2), a central DNA-binding domain (C) and a hinge domain (D) permitting dimerisation of the receptor (Tsai et al., 1994; Ribeiro et al., 1995; Fuqua et al., 2003). The AF-1 and AF-2 regions are crucial for interactions with other co-regulatory proteins to subsequently drive gene transcription activity that can promote cell survival and proliferation of breast cancer cells (Jordan, 2007).

Figure 1.1 Functional Domains of, and % homology between, ER α and ER β



Schematic representation of the human oestrogen receptors ER α and ER β . The percentage identity between the two receptors is indicated. Both receptors consist of functional domains, comprising the ligand-independent activation function AF-1 in the aminoterminal domain (A/B), DNA-binding domain (C), hinge (D), the ligand-dependent activation function AF-2 at the ligand-binding domain (E), as well as agonist/antagonist distinction site (F). This diagram is adapted from Kling (2000).

1.2.2 Oestrogen Receptor Signalling

In the absence of a ligand the ER is found in the cell nuclei within an inhibitory protein complex of heat shock proteins 90 and 70, and cyclophilin-40 and p23 (Pratt & Toft, 1997). Classical ligand dependant signalling of the ER is induced in the presence of oestradiol. The steroid hormone diffuses through the cell plasma membrane to translocate to the nucleus, and binds to the ER causing subsequent alterations to the ligand binding domain and phosphorylation of the ER, releasing it from the inactive oligomeric complex (Roa, 1981; Osborne & Schiff, 2005). This allows ER dimerisation and DNA binding of the ER to the oestrogen receptor elements (ERE) in the promoter sequence of oestrogen responsive genes (Osborne & Schiff, 2005). Once attached to the DNA and through specific recruitment of co-regulatory transcription factors, the receptor complex can regulate target gene transcription via synergistic activity of AF-2 and AF-1. There are ER co-regulators such as Co-Activators or Co-Repressors that can influence recruitment of the general transcriptional machinery and other co-factors, modifying the chromatin environment surrounding the promoter of the targeted gene to further facilitate gene activation or inactivation respectively (McKenna et al., 1999; Kling, 2001; Dobrzycka et al., 2003). In the presence of oestrogens, predominant Co-Activator recruitment to the ER facilitates increased gene transcription of ER-regulated genes (McKenna et al., 1999; Kling, 2001; Dobrzycka et al., 2003).

In breast cancer, non-classical ER signalling can also occur when ligand bound nuclear ER can interact with other DNA bound transcription factors, such as c-fos and c-jun, to promote the expression of genes that contain the AP-1 response element in their promoter region, such as cyclin D1, and the growth factor ligand IGF-1 (Kushner et al., 2000). The endpoint of oestrogen/ER signalling in breast cancer is expression of genes that can promote tumour cell proliferation and survival (McKenna et al., 1999; Kling, 2001; Dobrzycka et al., 2003).

In addition to nuclear ER, however, cytoplasmic ER and plasma membrane ER have also been found to be present at low levels in breast cancer cells (Losel et al., 2003). Interestingly, the membrane ER (probably identical to ER α) has experimentally been shown to be able to activate growth factor signalling pathways, such as the epidermal growth factor receptor (EGFR), where membrane ER has been linked to very rapid cellular responses to steroid hormone (Filardo et al., 2000; Levin, 2003; Gee et al., 2005). This crosstalk with growth factor receptors is reported to result in the downstream activation of mitogen activated protein kinase (MAPK) and serine/threonine protein kinase (Akt) signalling pathways, elements that in turn can activate nuclear ER by phosphorylation of the Ser118 and Ser167 residues present in the AF-1 domain of the ER receptor to trigger gene transcription (Martin et al., 2000; Kato et al., 1995).

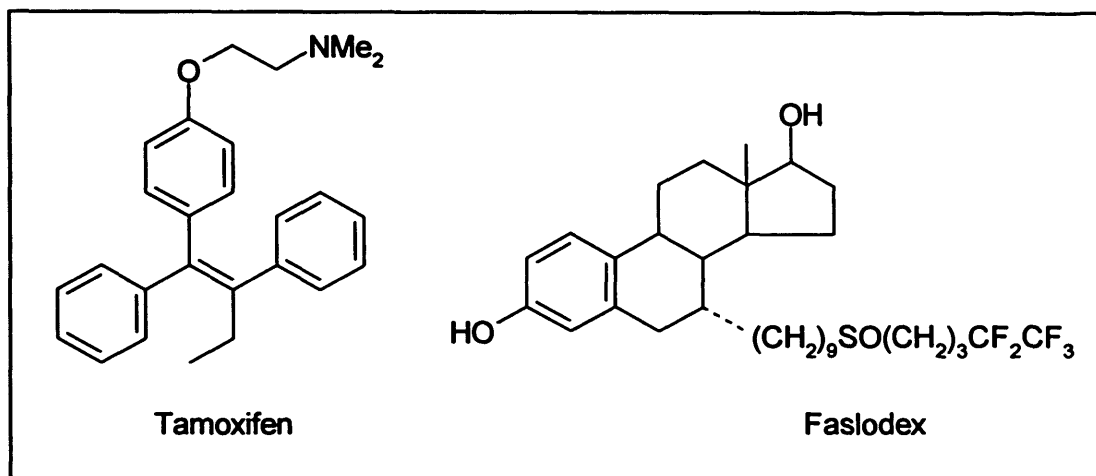
1.2.3 Endocrine Therapy in Breast Cancer

The development of endocrine therapies to block the activation of ER signalling by steroid hormone, either by competitively inhibiting oestrogen binding to ER and depleting activity (and in some instances level) of the ER, or by depleting oestrogen in the body, has proven valuable in treating breast cancers that express ER and hence may use signalling via this receptor for their growth (ER⁺ disease). Tumours lacking the receptor (ER⁻) are inappropriate for endocrine treatment, being inherently resistant and thus to date suitable only for chemotherapy.

Tamoxifen was until recently the gold standard endocrine agent for the treatment or prevention of ER⁺ breast cancer (Fisher et al., 1998). Tamoxifen is a non-steroidal triphenylethylene derivative that acts by competitive blockade of the ER, and is hence an “anti oestrogen” (Figure 1.2) (Katzenellenbogen et al., 1995; Nicholson & Johnson, 2005). Tamoxifen competes with oestrogen for binding to ER, changing the receptor conformation and thus blocking AF2 function to limit subsequent ER-regulated gene expression. Proliferation can thus be substantially inhibited in ER⁺ breast cancer cells, resulting in a positive therapeutic response in ~60% of ER⁺ breast cancer patients (Gee et al., 2005). However, ligand-independent AF-1 activity remains unchanged and in some tissues such as uterus and bone (where coactivator / kinase complement is appropriate to allow constitutive AF-1 phosphorylation and subsequent transcriptional activation), tamoxifen behaves

as an agonist. Because of this mixed antagonist/agonist profile, tamoxifen has therefore been termed a selective ER modulator (SERM) (Santen et al., 2003).

Figure 1.2 Structure of the antioestrogens tamoxifen and faslodex



However, ~40% of ER⁺ disease patients are intrinsically (*de novo*) resistant to tamoxifen, and moreover despite initial responses many more patients eventually progress on such treatment since their tumour cells acquire resistance to tamoxifen, despite their tumours commonly retaining ER (Katzenellenbogen et al., 1995). The requirement for a novel drug that would potentially improve the response rate in ER⁺ women by treating ER⁺ tamoxifen resistant breast cancer, while also avoiding unwanted agonist effects on the uterus, led to the synthesis of the steroidal ER antagonist fulvestrant, referred to in this report as faslodex (FAS) (Figure 1.2) (Dowsett et al., 2005; Nicholson & Johnson, 2005). Faslodex proved a more effective anti-oestrogen than tamoxifen in ER⁺ breast cancer cells (such as MCF-7 cells) *in vitro*. It has a higher affinity for ER with a binding affinity of 0.89, versus tamoxifen's

binding affinity of 0.025 (Wakeling et al., 1991; Osborne et al., 1995). Faslodex thus more effectively competes with oestrogen to bind to ER and prevents oestrogen signalling. Faslodex also radically alters the ER conformation, preventing receptor dimerisation and also blocking AF1 function as well as AF2 function, such that any FAS-ER complex formed that enters the nucleus is transcriptionally inactive (Dowsett et al., 2005). Critically however, faslodex also results in a reduction of ER protein level (and so has been termed a selective oestrogen receptor down-regulator or 'SERD'), and in total therefore, there is very effective inhibition of oestrogen signalling with this agent (Robertson, 2001; Osborne et al., 2004). Moreover, unlike tamoxifen, faslodex is not associated with agonist activity but is a pure anti-oestrogen (Wakeling et al., 1991; Robertson et al., 2003; Dowsett et al., 2005). The agent can bring about responses in tamoxifen (or aromatase inhibitor – see below) ER⁺ resistant disease clinically, and is thus approved in 2nd and 3rd line treatment in ER⁺ breast cancer (Wakeling et al., 1991; Robertson et al., 2003; Dowsett et al., 2005). It is currently undergoing further trials to examine if it has potential in additional aspects of ER⁺ disease management (Wakeling et al., 1991; Robertson et al., 2003; Dowsett et al., 2005).

Of further interest in the treatment of ER⁺ breast cancer is an alternative endocrine therapeutic approach, oestrogen deprivation, that is increasingly replacing tamoxifen as the gold standard postmenopausal endocrine approach. Synthesis of residual oestrogen from androgens persists in postmenopausal women through activation of the cytochrome P450 (CYP450) enzyme

aromatase in peripheral tissues, where this enzyme is also found in some ER⁺ breast cancers (Nicholson & Johnston, 2005). Therefore, aromatase inhibitors, now having reached potent ‘third generation’ agents such as the steroidal agent exemestane and the non-steroidal agent anastrozole (Nicholson & Johnston, 2005), have been developed to suppress aromatase activity in postmenopausal ER⁺ breast cancer patients, profoundly reducing oestrogen levels in the body and therefore depriving the ER⁺ breast cancer cells of their growth input (Smith & Dowsett, 2003). Such oestrogen deprivation is proving highly effective in treating ER⁺ postmenopausal breast cancer, without conferring unwanted uterine agonistic effects (Lønning & Kvinnsland, 1998; Lønning, 1999). Of note, in ER⁺ premenopausal breast cancer patients, oestrogen deprivation can also be effective, but in this instance by use of the Gonadotropin-releasing hormone 1 (GNRH1) agonist Zoladex that acts centrally to block hypothalamic/pituitary regulation of oestrogen synthesis by the ovaries during the menstrual cycle (Lønning & Kvinnsland, 1998; Lønning, 1999).

1.2.4 Resistance Acquired to Endocrine Therapy

Unfortunately, aromatase inhibitors have not been spared the phenomenon of acquired resistance (Lønning & Kvinnsland, 1998; Lønning, 1999), and groups including the Tenovus Centre for Cancer Research have previously identified, through use of *in vitro* models, that resistance is also acquired to treatment with faslodex, where clinical experiences confirm this phenomena also occurs during therapy (McClelland et al., 2001; Robertson, 2001). The exact mechanisms driving resistance to endocrine therapy and thus ER⁺ relapse

during treatment remain elusive. Some tamoxifen resistant cells have been shown from experimental and clinical evidence to have acquired the ability to be stimulated, rather than inhibited, by tamoxifen after prolonged treatment (Legault-Poisson et al., 1979; Gottardis et al., 1988; Osborne et al., 1991; Osborne et al., 1994; Osborne et al., 1995). DeGregorio and colleagues found that treatment with tamoxifen suppressed tumour growth for several months; however, growth eventually resumed, stimulated by tamoxifen (Osborne et al., 1991). Several early studies using breast cancer *in vivo* models explored potential mechanisms for resistant growth including altered hormone (tamoxifen) uptake, metabolism, and altered ER (Legault-Poisson et al., 1979; Gottardis et al., 1988; Osborne et al., 1994; Osborne & Fuqua, 1994; Wolf et al., 1994; Osborne et al., 1995), although in general none revealed mechanisms that proved clinically relevant.

More recently, increased understanding of growth factor pathways has highlighted the importance of such signalling, and its interplay with ER in driving growth of ER⁺ tamoxifen resistant cell lines. Deregulation of growth factor pathways and ER-growth factor receptor cross-talk is thought to be one of the determinants of tamoxifen resistance that can either be apparent at primary (*de novo*) ER⁺ resistance or be acquired by responsive ER⁺ breast cancer cells after varying durations of tamoxifen treatment (Nicholson et al., 2004). Of particular relevance to tamoxifen resistance is increased EGFR / ErbB2 signaling. The ErbB family of the receptor tyrosine kinases (RTKs) comprises EGFR (ErbB1 or HER1, a 175kDa protein), ErbB2 (HER2/Neu,

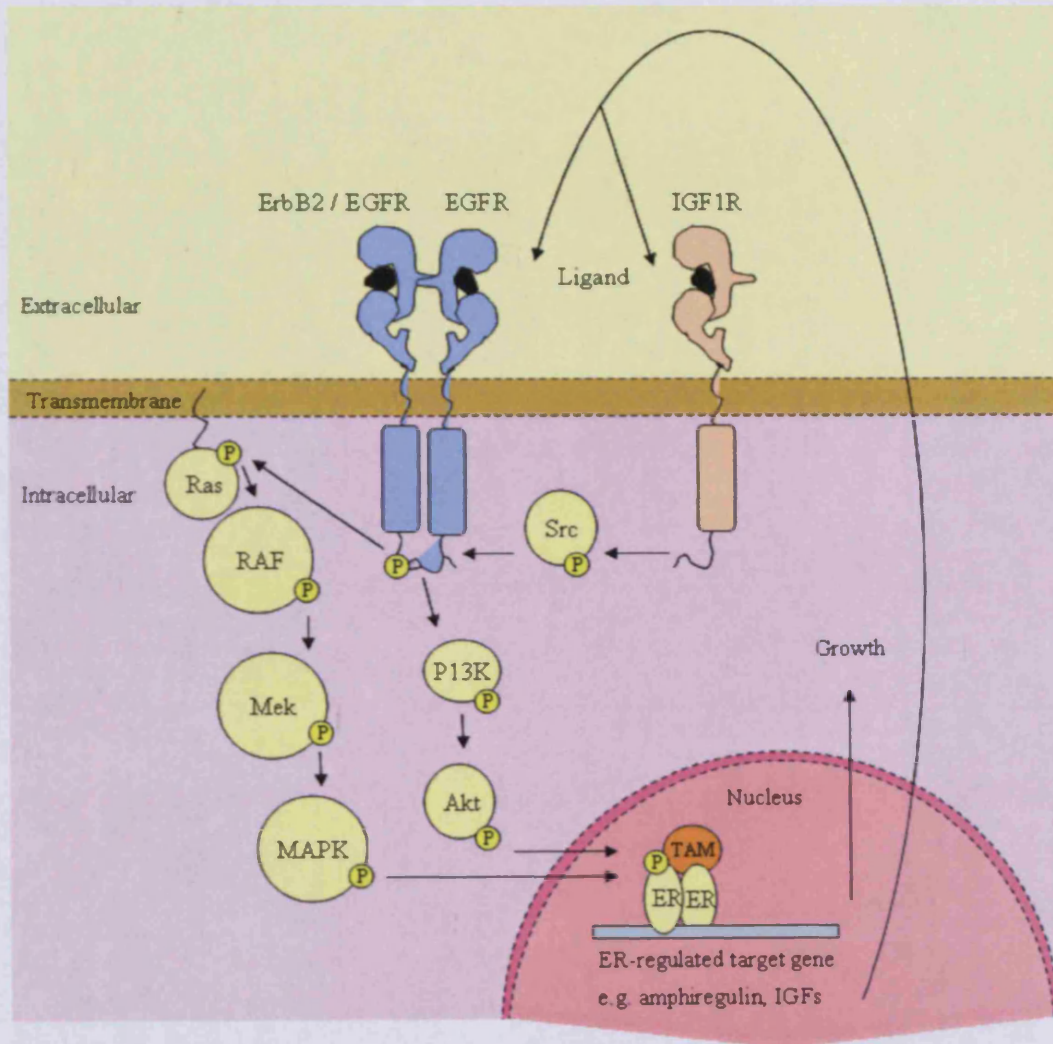
185kDa protein), ErbB3 and ErbB4 (HER3, and HER4 respectively, 180-190kDa proteins) that play a key role in cell growth, proliferation, differentiation, and cell survival. The increased kinase signalling of such receptors, in particular EGFR and ErbB2, has been implicated in the development of some types of endocrine resistance, notably to antioestrogens in *in vitro* and *in vivo* models but also with emerging evidence in clinical *de novo* and acquired resistance to tamoxifen (Ullrich et al., 1984; Nicholson et al., 2001; Gee et al., 2003; Knowlden et al., 2003; Nicholson et al., 2004; Gee et al., 2005; Rhee et al., 2005). For example, increased EGFR and ErbB2 can clinically be associated with reduced anti-proliferative effect of tamoxifen in ER⁺ tumours (Dowsett et al., 2005), where in addition there is an established relationship between elevated EGFR and ER⁻ disease (Nicholson et al., 2001). Increased levels of EGFR and ErbB2 have also been reported in the acquired TAMR *in vitro* tamoxifen resistant model from Knowlden and colleagues (2003), where such receptors can heterodimerise and become activated, triggering downstream kinases and tamoxifen resistant cell proliferation and survival, such cells also gaining invasive behaviour via additional increases in c-Src activity (Knowlden et al, 2003; Hiscox et al., 2004; Hiscox et al., 2006).

It is known from *in vitro* models, such as these acquired TAMR cells from Knowlden and colleagues (2003), that increased EGFR/ErbB2 signalling gained by such cells can crosstalk with ER to promote tamoxifen resistant growth. In this model, MAPK and Akt activity promoted by the increased upstream EGFR/ErbB2 activity augment the ligand-independent transactivation

function of nuclear ER α in the presence of tamoxifen through their phosphorylation of Ser167 and Ser118 within the ER AF1 domain (Figure 1.3) (Masuhiro et al., 2005; Britton et al., 2006; Kim et al., 2006). This results in increased ER-regulated expression of growth factor ligands such as the EGFR ligand amphiregulin, which further drives elevated EGFR signalling, and also IGF production (Britton et al., 2006). The agonistic effect of TAM/ER can thus be further enhanced by increases in interplay with insulin like growth factor receptor (IGFR) signalling, which further facilitates EGFR activity via Src (Knowlden et al., 2003, 2005). Thus there is an autocrine growth regulatory pathway in the TAMR model since EGFR driven crosstalk with ER promotes ER-regulated growth factors that in turn facilitate EGFR/IGFR signalling that impact on ER despite the presence of tamoxifen. The resultant effect of this autocrine loop is increased proliferation in the presence of tamoxifen and hence resistant growth (Knowlden *et al.*, 2003, 2005).

The Tenovus Centre for Cancer Research has targeted EGFR in these TAMR cells using a selective EGFR tyrosine kinase inhibitor (TKI), gefitinib (Gee et al., 2003; Knowlden et al., 2003; Hiscox et al., 2004; Jones et al., 2004; Gee et al., 2005; Jones et al., 2005). This agent (as well as others targeting the downstream kinases, and also targeting of Src or ErbB2) promotes substantial inhibition of TAMR models, confirming the EGFR signalling loop is dominant in driving growth (Knowlden et al., 2003). Of note, there is also some contribution for increased EGFR in some FASR models *in vitro*, where EGFR signalling can again be increased (McClelland, et al., 2001).

Figure 1.3 Increased EGFR and ER crosstalk in Tamoxifen resistant ER⁺ breast cancer cells *in vitro*.



Moreover, altered growth factor signalling has also been implicated in ER⁺ breast cancer with acquired resistance to oestrogen deprivation, as evident by models such as the long term oestrogen deprived LTED models from Martin and colleagues (2003), and Santen and colleagues (2004), where increased ErbB2 and IGFR downstream kinase signalling have been implicated in nuclear ER crosstalk and also crosstalk with membrane ER to trigger resistant growth (Martin et al., 2003; Santen et al., 2004). Again growth inhibitory responses to anti-growth factor agents such as gefitinib, anti-IGFR, and also various kinase inhibitors (e.g. MAPK, PI3K/Akt pathways) can invariably be observed in these resistant models (Martin et al., 2003; Santen et al., 2004). These models are usually derived in the presence of serum growth factors that could feasibly force the resistance mechanism towards growth factor signalling. However, the Tenovus Centre for Cancer Research developed a new *in vitro* model, MCF-7X (referred to in this report as X-MCF), under conditions of severe oestrogen and growth factor depletion. Although not driven by classical growth factor receptors, again these acquired oestrogen deprivation resistant cells respond to PI3K/Akt blockade and there is kinase crosstalk with nuclear ER to drive their resistant growth (Staka et al., 2005).

Clearly, growth factor signalling can contribute to endocrine resistant growth and its targeting may be of therapeutic value, an area currently being explored through many clinical trials (Johnston, 2005). However, emerging clinical and experimental experience indicates that anti growth factor strategies will also not be spared the phenomenon of resistance, exemplified by studies with the

EGFR-TKI gefitinib (Jones et al., 2004). By example, in the Tenovus Centre for Cancer Research, a model (NEW DUBS), of acquired resistance to gefitinib was successfully developed followed prolonged treatment of TAMR cells with this EGFR-TKI, despite initial tumour cell responsiveness. Furthermore, gefitinib resistance frequently occurs in the clinic in cancer patients (Jones et al., 2004). Again, *in vitro* gefitinib resistance can be promoted by further growth factor pathway deregulation, for example by increased IGFR receptor signalling in NEW DUBS where some growth inhibitory responses to anti-IGFR agents are consequently observed (Jones et al., 2004; Knowlden et al., 2003). However, since resistance can again emerge after such STI treatment (Jones et al., 2004), it is clear that continued deciphering of the biology underlying these various acquired endocrine and anti-EGFR therapeutic resistant states remains essential to reveal new ways of improving treatment, particularly as studies in Tenovus Centre for Cancer Research have shown both endocrine and anti-EGFR resistance is associated with increased invasive capacity (Hiscox et al., 2004; Jones et al., 2004).

1.3 Oxidative Stress

Commoner and colleagues first discovered the presence of highly reactive molecules, termed 'free radicals', in biological materials just over 50 years ago (Commoner et al., 1954). Soon thereafter in 1956, Denham Harman hypothesized that these free radicals may be formed as by-products of enzymic reactions *in vivo*, namely from the mitochondria and termed 'reactive oxygen species' or ROS. He suggested that such free radicals, when excessive, might contribute to gross cellular damage, mutagenesis, cancer, and the degenerative process of biological aging (Harman, 1956; Harman, 1981). Numerous researchers have since linked dysregulation of redox homeostasis with over 100 disease states. The main diseases identified include cancer, diabetes mellitus, hypoxia, atherosclerosis, neurodegenerative disease, ischemia / reperfusion injury, inflammatory dysfunction, and aging (Cai & Harrison, 2000; Batandier et al., 2002). Imbalances in the redox homeostasis are now referred to as 'oxidative stress', and are known to be caused either by an increase in ROS produced by pro-oxidant mechanisms, or by insufficient endogenous antioxidants, which are produced by cells in response to oxidative stress in an attempt to quench ROS (Mathews et al., 2000; Lee et al., 2001). Any deregulated ROS can potentially cause damage to the cells own DNA, proteins, and essential fatty acids, leading to oxidative DNA damage and lipid peroxidation (Cai & Harrison, 2000; Batandier et al., 2002).

ROS can also influence the balance of cell proliferation, differentiation and cell survival or death (Eyries et al., 2004). While ROS is produced for the

phagocyte “oxygen burst reaction” as a normal host defence mechanism by the cell against invading microorganisms (Hensley et al., 2000; Suematsu, et al., 2002), production of ROS also plays an important role in many biological processes such as modulating signal transduction pathways that may lead to the proliferation of cancer cells (Droge, 2002). Indeed, it was more recently found that human tumour cells (such as prostate cancer cells) have elevated levels of ROS, such as O_2^{\cdot} and H_2O_2 (Kurdi & Booz, 2007; Lien et al., 2008). However, excessive ROS can cause cell death, exemplified by the impact of chemotherapy/radiotherapy, which in some instances exerts its anti-tumour effect via increasing ROS (Szatrowski & Nathan, 1991; Spitz et al., 1993; Toyokuni S, et al., 1994).

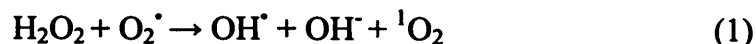
Of note, increased antioxidant levels occur within tumour cells in response to chemotherapy/radiotherapy, and interestingly, this may ultimately lead to resistance of tumour cells to these therapies whose mechanism relies on the induction of oxidative stress (Szatrowski & Nathan, 1991; Spitz et al., 1993; Toyokuni S, et al., 1994). Spitz and colleagues found that in such instances, tumour cells were found to have acquired resistance by up regulating their CAT and glutathione (GSH) antioxidant activity levels (Spitz et al., 1993; Suematsu et al., 2002). While largely unexplored, it is feasible that changes in redox balance may also be relevant to further therapeutic strategies and contribute to associated resistance.

1.3.1 Pro-Oxidant Mechanisms of ROS Production

A key site of ROS production within the cell is the electron transport chain (ETC) in the mitochondria in living cells. Approximately 1 – 3 % of the total molecular oxygen (O_2) consumed by the mitochondria is incompletely reduced leading to ROS production (Boveris et al., 1972; Boveris & Chance, 1973). ROS is formed as a result of “electron leakage” during mitochondrial respiration, where the primary radical superoxide anion ($O_2^{\cdot-}$) is generated by the addition of a single electron to an oxygen molecule (Boveris et al., 1972; Loschen et al., 1974; Chance et al., 1979; Babior, 1999; Cai & Harrison 2000). The transfer of a single free electron to molecular oxygen occurs at the level of NADH CoQ reductase (Complex I) and CoQ cytochrome C reductase (Complex III), generating $O_2^{\cdot-}$ and indirectly further potent oxidants such as H_2O_2 , OH^{\cdot} and peroxynitrite ($OONO^{\cdot}$) (Boveris et al., 1972; Loschen et al., 1974; Chance et al., 1979; Cai & Harrison 2000).

Moreover, the addition of two electrons to molecular oxygen can form peroxide, which then undergoes protonation to yield the further oxidant H_2O_2 (Ushio-Fukai et al., 1998). H_2O_2 is not a free radical; however it is still a ROS and a detrimental oxidant that through a variety of mechanisms, including the Haber-Weiss reaction (Figure 1.4), can produce a very short lived and reactive form of oxygen named singlet oxygen (1O_2) (Zalba et al., 2001).

Haber-Weiss reaction:



The addition of a third electron to molecular oxygen can yield a further oxidant, OH^\bullet , through the Fenton reaction shown below (Toufektsian et al., 2001). The majority of OH^\bullet formed *in vivo* can lead to inflammation, and comes from the metal-catalysed breakdown of hydrogen peroxide according to this reaction (Figure 1.4).

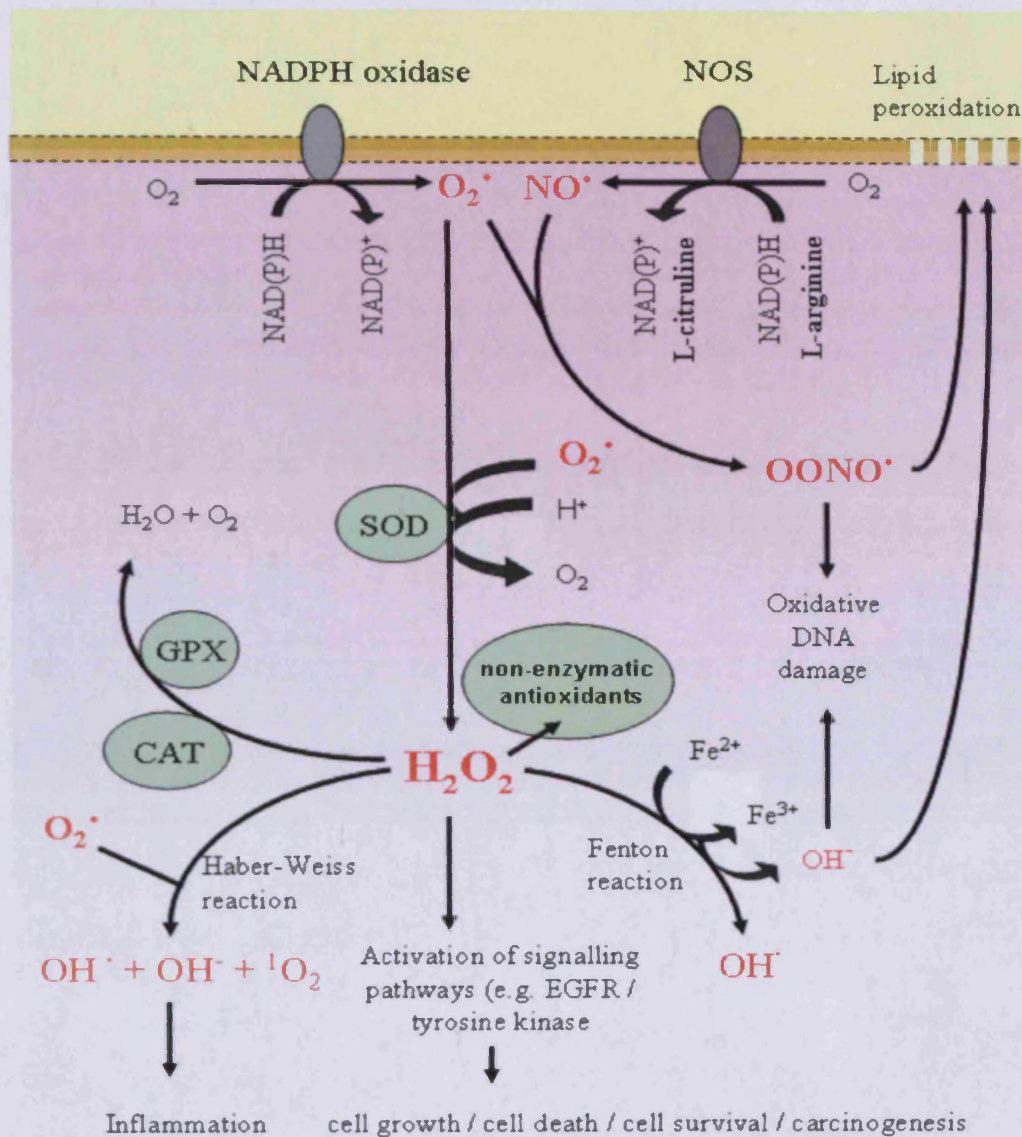
Fenton reaction:



Here, M^{n+} is a transition metal ion, and *in vivo* production of OH^\bullet through the Fenton reaction is most common when M^{n+} is iron or copper, chromium, cobalt, or other metals (Platenik et al., 2001; Liochev & Fridovich, 2002). OH^\bullet generated by iron catalysis of H_2O_2 (from tissue ferritin) reacts with biological targets at $10^9 \text{ M}^{-1} \text{ Sec}^{-1}$, making it more reactive than other free radicals such as O_2^\bullet (rate constant $2.9 \times 10^9 \text{ M}^{-1} \text{ Sec}^{-1}$) (Biemond et al., 1986; Toufektsian et al., 2001).

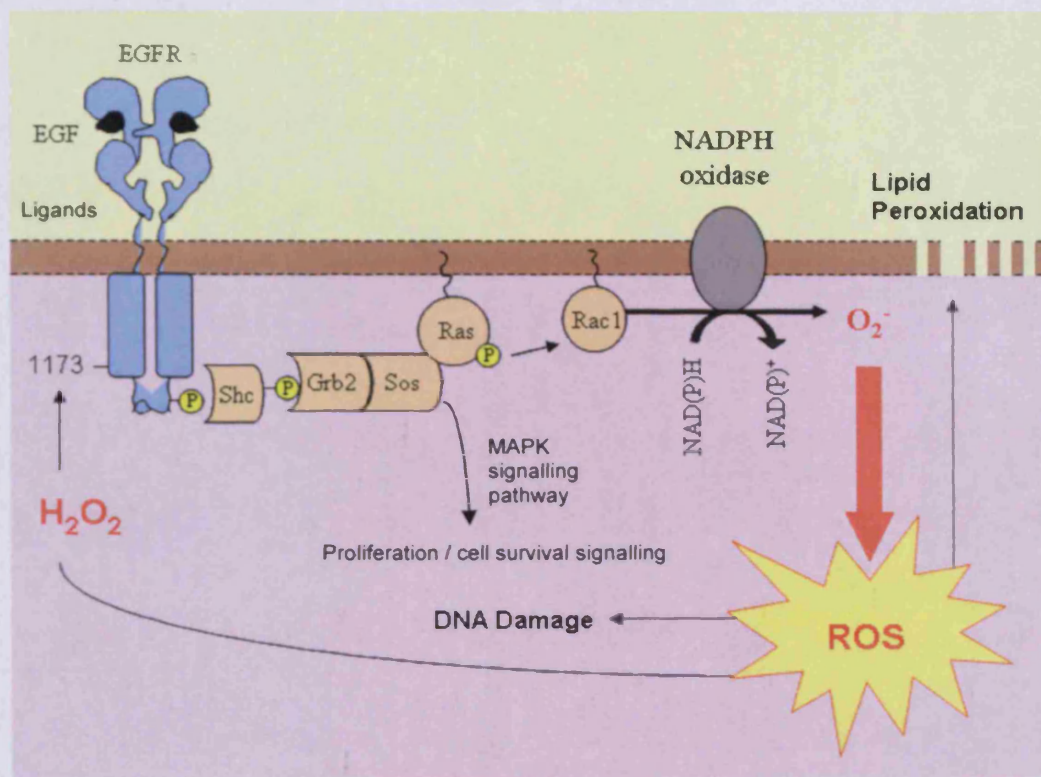
ROS formation can also be achieved within the cell through enzyme systems such as nitric oxide synthase (NOS), cytochrome P450s, xanthine, amino acid, and NADH / NAD(P)H oxidases, arachidonic acid pathway enzymes, cyclooxygenase, as well as through exposure to cytokines and growth factor signalling (Babior, 1999; Sakai et al., 2003; Eyries et al., 2004). For example, Nitric oxide (NO^\bullet), a reactive nitrogen species (RNS), is synthesised from O_2 by NOSs that can be membrane associated endothelial NOS (eNOS), inducible NOS (iNOS), or cytosolic neuronal NOS (nNOS), where NOS function requires the co-factors L-arginine or 6(R)-tetrahydro-L-biopterin (BH_4) (Figure 1.4) (Xiong et al., 2005). NO^\bullet regulates the function of the endothelium (Oberley & Oberley, 1997), along with other useful biological activities that include inhibition of platelet and leukocyte activation, attenuation of smooth muscle cell proliferation, and vasorelaxation depending on soluble guanylate cyclase (Auch-Schwelk et al., 1992). However, in the absence of the co-factors L-arginine and BH_4 , NO^\bullet can be very detrimental as eNOS can become uncoupled and produce O_2^\bullet resulting in H_2O_2 production. The ROS free radical O_2^\bullet can also readily react with NO^\bullet to form further RNS OONO^\bullet (Figure 1.4) (Beckman et al., 1990; Subbarao & Richardson, 1990). Interestingly, growth factor signalling has also been documented to be able to promote ROS. For example, activated EGFR can facilitate the formation of ROS *via* its well documented Ras/Rac pathway (Figure 1.5) (Rao, 1996). In addition to enzyme and growth factor mechanisms, exogenous inducers of ROS also exist and can be used to treat tumour cells, including chemotherapy and radiotherapy (Tokoyuni et al., 1995; La Torre et al., 1997).

Figure 1.4 General overview of oxidative stress pathways



$O_2^{\bullet -}$ (and other ROS in red) produced either by NADPH oxidase or free in the cytosol can be dismutated by the antioxidant SOD to form O_2 and H_2O_2 . $O_2^{\bullet -}$ is converted to NO^{\bullet} through NOS in the presence of cofactor L-arginine, and can react with $O_2^{\bullet -}$ to form $OONO^{\bullet}$. H_2O_2 generates the very reactive OH^{\bullet} through the Fenton reaction, or 1O_2 in conjugation with $O_2^{\bullet -}$ by the Haber-Weiss reaction. Further antioxidants (green), such as enzymatic antioxidants CAT and GPX are shown here to be able to convert 'key player' H_2O_2 into H_2O and O_2 , or H_2O_2 can be quenched as shown by non-enzymatic antioxidants such as GSH, TXN, and PRDX that trap H_2O_2 before it can enter the Fenton or Haber-Weiss reactions. Any unquenched ROS can activate events such as Lipid peroxidation, DNA damage and cell death, but also triggers growth promoting signalling pathways by activating tyrosine kinases such as EGFR as well as carcinogenic events.

Figure 1.5 EGFR induced generation of ROS and its potential cellular consequences.



EGFR is activated either by its family of EGF-like ligands or at its 1173 autophosphorylation site by H₂O₂ resulting in the RAS/RAC pathway as shown. O₂⁻ produced as a result of subsequently activated NADPH oxidase promotes further ROS, as shown in Figure 1.4. ROS (red) can go on to have detrimental effects on cellular components through activation of tyrosine kinases, lipid peroxidation (resulting in the production of further reactive species HNE and MDA) and DNA damage, also potentially further promoting signalling through growth factor pathways (including back onto EGFR signalling via H₂O₂) to impact on proliferation and cell survival.

1.3.2 Downstream Cellular Effects of Oxidative Stress

In the presence of increased oxidative stress (for example, where antioxidants are insufficient at quenching the free radicals), formation of cellular ROS can go on to initiate cell death by lipid peroxidation in cells (Biemond et al., 1986). ROS can also react with all components of the DNA molecule, damaging purine and pyrimidine bases along with the deoxyribose backbone that in excess can also lead to cell death (Figure 1.4) (Dizdaroglu et al., 2002). Increases of oxidised DNA damage in living systems may thus be due to an increase in the steady state level of ROS, and/or to a decrease in the antioxidant capacity of the cell (Brown & Borutaite, 2001). In addition to ROS, RNS such as NO[•] and OONO[•] have also been implicated in both lipid peroxidation and DNA damage (Brown & Borutaite, 2001), where the RNS OONO[•] is reported to also induce lipid peroxidation and initiate single stranded breakage of DNA (Figure 1.4) (Backman et al., 1990; Subbarao & Richardson, 1990). However, in addition to the events that can promote cell death, ROS can influence signalling pathways in cells that impact on cell proliferation and cell survival, as well as mutagenic events, leading to cancer formation (Yang et al., 2003).

1.3.2.1 Lipid Peroxidation

Lipid peroxidation involves three main stages of initiation, propagation and termination in a chain reaction, commonly initiated by the ROS OH[•] (Pinchuk et al., 1998; Mathews et al., 2000; Nyska & Kohen, 2002). Lipid radicals produced by lipid peroxidation have a myriad of adverse effects on cellular function including alteration in ion channel configuration and hence altered ion

flux, leakage of plasmalemma, and membrane bound receptor dysfunction all implicated in cell death (Cai & Harrison, 2000; Nelson et al., 2005). Fatty acids in membrane lipids are oxidised by OH^\bullet in the first instance to generate further radicals such as fatty acid peroxy radical (R-COO^\bullet) (Mathews et al., 2000). Once formed, R-COO^\bullet is rearranged by a cyclisation reaction to form endoperoxides that are precursors of malondialdehyde (MDA) that can be mutagenic and carcinogenic (Marnett, 1999). This is thus an example of one way in which excess ROS can also promote cancer.

R-COO^\bullet can initiate a further peroxidation reaction by attacking adjacent fatty acid side chains (Herbst et al., 1999). These lipid peroxidation chain reaction mechanisms can go on for some time following initiation, resulting in the accumulation of fatty acid hydroperoxides and phospholipid hydroperoxides (Herbst et al., 1999; Yang et al., 2003; Nelson et al., 2005). Fatty acid carbon chains are also cleaved during lipid peroxidation yielding highly reactive compounds including exocyclic DNA adducts, pentane radical, ethane radical, and α,β -unsaturated aldehydes such as 4-hydroxy-2-nonenal (HNE) (Yang et al., 2003). HNE is thus found at high levels in biological membranes under oxidative stress (Yang et al., 2003). HNE is weakly mutagenic and has the same triggering effects on EGFR signalling as H_2O_2 , therefore having the potential to influence signal transduction pathways that have major effects on the phenotypic characteristics of cells and cancer growth as shown in Figures 1.4 and 1.5 (see below, section 1.3.2.3) (Yang et al., 2003).

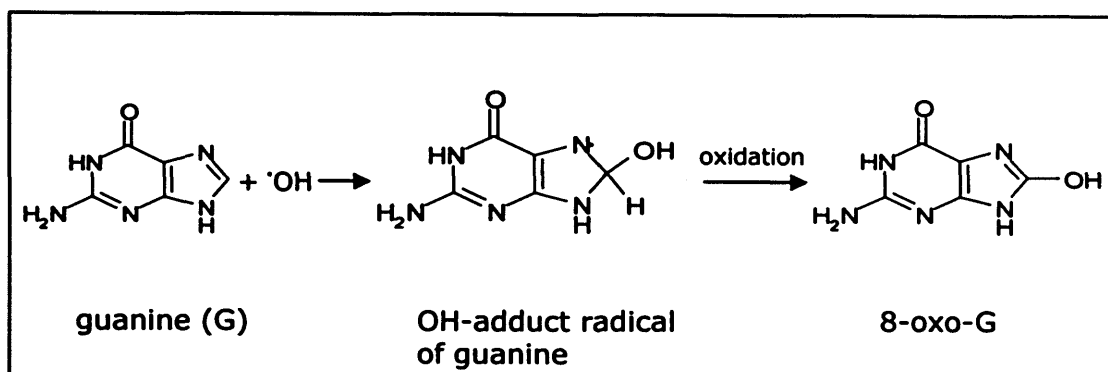
1.3.2.2 Oxidative DNA Damage

Oxidative DNA damage that can also be a consequence of ROS is the first step involved in mutagenesis and carcinogenesis. Over 100 products have been identified from the oxidation of DNA to date, resulting from ROS-induced single- or double-stranded DNA breaks, DNA cross-links, purine, pyrimidine, and deoxyribose modifications (Marnett, 2000; Cooke et al., 2003). Oxidative DNA damage can result in induction of signal transduction pathways, either causing arrest or induction of transcription, replication errors and genomic instability, which are all associated with carcinogenesis (Marnett, 2000; Cooke et al., 2003). ROS-induced lipid peroxidation products such as MDA can also have detrimental effects on cells as it can react with DNA bases G, C, and A to form adducts M₁G, M₁C, and M₁A respectively (Marnett, 1999). M₁G adducts, for example, have been detected in breast cancer tissue using ³²P-post-labeling, at levels up to 1.2 adducts per 10⁶ nucleotides, which corresponds approximately to 6000 adducts per cell (Wang et al., 1996).

Besides the effects lipid peroxidation products have on DNA, ROS can also directly affect DNA in the form of the very reactive OH[•] that can be incorporated into the double bonds of DNA bases (Dizdaroglu et al., 2002). OH[•] can abstract a hydrogen atom from the methyl group of thymine, along with five carbon atoms of 2' deoxyribose (Dizdaroglu et al., 2002). An additional reaction generates OH-adduct radicals of DNA bases, and the allylic radical 8-hydroxyguanine (8-OH-G/8-oxo-G) is derived from thymine and carbon-centred sugar radicals through abstraction reactions (Figure 1.6)

(Mathews et al., 2000; Dizdaroglu et al., 2002). 8-oxo-G is a biomarker of oxidative stress, and as such is perceived as a potential biomarker of carcinogenesis (Halliwell & Gutteridge, 1999).

Figure 1.6 Reaction of guanine with OH[•].



1.3.2.3 Activation of Signalling Pathways

Autophosphorylation or ligand-independent phosphorylation of a number of RTKs, including the EGFR family, is known to be enhanced by the pro-oxidant H₂O₂ (Figures 1.4 and 1.5) (King et al., 1989; Knebel et al., 1996; Rao, 1996). Indeed, chronic levels of H₂O₂ can alter gene expression and act as intracellular second messenger to activate a wide range of intracellular signalling proteins and nuclear transcription factors such as AP-1 (see comprehensive list in Appendix I) (Zalba et al., 2001). H₂O₂ is thought to inactivate phosphatases through oxidation of the cysteine active site. It is also considered to activate protein kinases by cysteine oxidation, although the exact mechanism by which kinase activation by ROS occurs remains elusive (Rhee et al., 2003). H₂O₂ also produced from eNOS uncoupling can also subsequently interact with signal

transduction pathways (Heinzel et al., 1992; Pou et al., 1992; Vesquez-Vivar et al., 1998; Eyries et al., 2004). It has also been documented that under certain conditions H_2O_2 can stimulate the proliferation response via activation of the mitogen-activated protein kinase (MAPK) pathway (Ushio-Fukai et al., 1998). ROS thus has potential to stimulate growth of cells, assuming cells are able to defend sufficiently against the initial assault of excess ROS that could result in cell death (Ushio-Fukai et al., 1998).

1.3.3 Antioxidants

Nuclear factor-erythroid-2-related factor 2 (Nrf2) is a basic leucine zipper transcription factor and a key element in the transcriptional activation of genes encoding both enzymatic and non-enzymatic antioxidants in response to ROS. Nrf2 thus plays an essential role in the redox balance of the cell. Under normal physiological conditions, it forms an inactive cytoplasmic complex with a negative regulator Kelch-like ECH-associated protein 1 (Keap1) that is found in the actin cytoskeleton (Zhang et al., 2004; Zhang et al., 2005). Keap1 controls the subcellular localization and steady state levels of Nrf2 via its cysteine residues that act like redox “sensors”. Oxidation of these highly reactive cysteine residues under conditions of ROS results in dissociation of Nrf2 from Keap1 and subsequent nuclear translocation of Nrf2, where it then transactivates Antioxidant Response Element (ARE) – regulated genes (Lee & Surh, 2005; Egger et al., 2008). This occurs following its heterodimeric combination with other transcription factors such as small Maf protein, and binding to the 5'-upstream cis-acting regulatory sequence, referred to as the

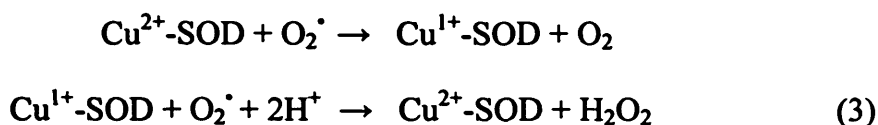
ARE, located in the promoter region of genes encoding various enzymatic and non-enzymatic antioxidant (Itoh et al., 1997). Stress responsive and cytoprotective enzymes induced by this mechanism are diverse, including SOD, CAT, GPX, TXN, NAD(P)H dehydrogenase, quinone 1 (NQO1), Glutathione S-transferase (GST), and heme oxygenase-1 (HO-1) (Chen & Kong, 2004; Motohashi & Yamamoto, 2004; Lee & Surh, 2005; Dinkova-Kostova & Talalay, 2008; Egger et al., 2008). Such enzymatic and non-enzymatic antioxidants can subsequently go on to quench ROS in the cell to limit its diverse, potentially adverse effects (Chen & Kong, 2004; Motohashi & Yamamoto, 2004; Lee & Surh, 2005; Dinkova-Kostova & Talalay, 2008; Egger et al., 2008).

1.3.3.1 Enzymatic Antioxidants

1.3.3.1.1 Superoxide Dismutase (SOD)

SOD is one of the most important intracellular enzymatic antioxidants and is the first line of defence induced against ROS. Although this enzyme had been isolated in as early as 1939, McCord and Fridovich were the first to discover its antioxidant activity and synthesised SOD in 1969. There are three forms of SOD in humans: cytosolic Cu/Zn-SOD, mitochondrial Mn-SOD, and extracellular SOD (EC-SOD) (Mates et al., 1999; Landis & Tower, 2005). More recently, a new class of SOD has been discovered in *Streptomyces* and cyanobacteria containing Nickel (Ni); however, Ni-SOD does not have any sequence homology to other SODs (Barondeau et al., 2004). All SODs belong to a family of metalloenzymes that catalyse dismutation reactions, where two

identical molecules have different fates, as one is oxidised and one is reduced (Mathews et al., 2000). SOD thus facilitates the formation of O_2 and the less reactive ROS H_2O_2 from the dismutation of the more reactive ROS O_2^{\cdot} , at a very high reaction rate (Figure 1.4) (McCord & Fridovich, 1969; Kirkman & Gaetani, 1984; de Hann, 2004). Below is a typical antioxidant reaction of Cu/Zn-SOD:

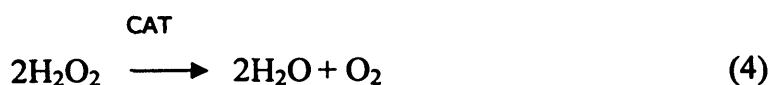


The H_2O_2 generated by total SOD (intracellular Cu/Zn-SOD and Mn-SOD) is then further catalysed into water by the further antioxidant enzymes CAT and GPX (see below, Kirkman & Gaetani, 1984; de Hann, 2004), thus decreasing excess ROS (Figure 1.4). MnSOD has received growing attention as a negative modulator of cellular apoptosis and as a survival factor for cancer cells by limiting cell death effects of ROS (Housset, 1987; Pani et al., 2004). Overexpression of MnSOD found in tumours (at even small amounts) can confer resistance to chemotherapy and prevent apoptosis (Housset, 1987; Pani et al., 2004). It has therefore been suggested that pharmacological inhibition of MnSOD could possibly be an effective strategy to selectively kill cancer cells and to circumvent their resistance to chemotherapy (Housset, 1987; Pani et al., 2004).

SOD is also of interest in the context of endocrine therapy; interestingly, a number of studies have shown that tamoxifen can have an effect on the intracellular redox state of the cell, acting as either a pro-oxidant or antioxidant depending on the microenvironment of the cell (Nuwaysir et al., 1998; Wei et al., 1998; Day et al., 1999). For example, tamoxifen can in some systems be activated into reactive electrophilic metabolites causing oxidative stress. However, tamoxifen can also protect against lipid peroxidation, and DNA damage by inducing phase I and II metabolising antioxidant enzymes (Nuwaysir et al., 1998; Wei et al., 1998). In 2000, Schiff and colleagues investigated growth of an *in vivo* model of tamoxifen resistance and began to explore its association with oxidative stress. They concluded that the antioxidant enzyme SOD, and also GST (see below), were significantly up regulated in TAMR cells compared to tamoxifen sensitive cells, where ROS activation of the AP-1 signalling pathway was also suggested to play a role in resistant growth (Schiff et al., 2000).

1.3.3.1.2 Catalase (CAT)

As stated above, the enzyme CAT efficiently promotes the conversion of H₂O₂ to water and O₂ (Valko et al., 2006), thus reducing ROS levels (figure 1.4).



The significant decrease in the ability of a variety of tumour types to detoxify H₂O₂ has in some instances been linked to a decrease in CAT levels (Valko et

al., 2006). However, tumour cells were also found to acquire resistance by up regulating their CAT activity when exposed to cisplatin *in vivo* (Spitz et al., 1993; Suematsu et al., 2002). Interestingly, this resulted in resistance of tumour cells to several therapies whose mechanism involves the induction of oxidative stress, including chemotherapeutics and radiotherapy (Housset, 1987; Szatrowski & Nathan, 1991; Spitz et al., 1993; Toyokuni S, et al., 1994).

1.3.3.1.3 *Glutathione Peroxidase (GPX)*

The GPX family of peroxidases compete with CAT to scavenge H₂O₂ as a substrate (figure 1.4). GPX is interesting in that it contains an unusual amino acid, *selenocysteine*, an analogue of cysteine (Mathews et al., 2000). There are two forms of the GPX enzyme, one of which is the selenium-independent GST, and the other selenium-dependent GPX (Mates et al., 1999). There are four different selenium-dependent GPXs, all of which add two electrons to peroxides forming selenoles (Se-OH) in order to reduce them (Mates et al., 1999; Valko et al., 2006). These selenoenzymes can therefore neutralise peroxides and prevent them from entering the Fenton reaction, thus depleting cellular ROS. GPX also works in conjunction with the non-enzymatic antioxidant glutathione (GSH) to reduce its substrate H₂O₂ in the following reaction referred to as the glutathione cycle:



GPX thus reduces peroxides to water whilst simultaneously oxidising GSH to GSSG (Valko et al., 2006). It remains elusive as to whether these antioxidant enzymes play any role in therapeutic resistant states.

1.3.3.2 Non-Enzymatic Antioxidants

1.3.3.2.1 Thiol Antioxidants – Glutathione (GSH) Network

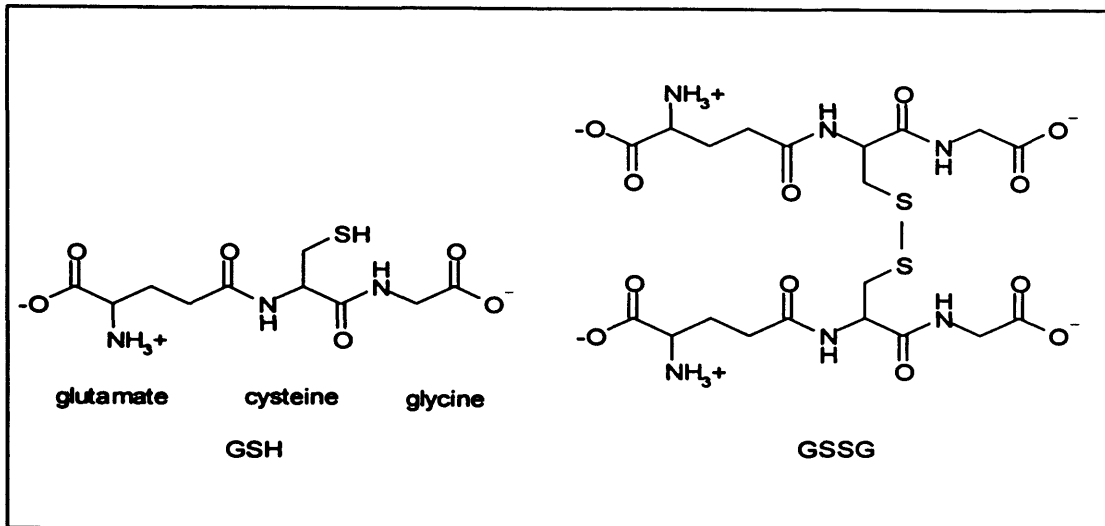
GSH is a multifunctional thiol antioxidant, and it is one of the most important of the non-enzymatic antioxidants. GSH is highly soluble and exists abundantly in the cytosol (1–11 mM), nuclei (3–15 mM), and mitochondria (5–11 mM) (Masella et al., 2005). GSH is able to regenerate further antioxidants (e.g. Vitamins C and E) and also acts as a cofactor for several detoxifying enzymes that can quench oxidative stress, including glutathione-S-transferase A4 (GSTA4), glutathione-S-transferase theta 2 (GSTT2), and (as described above) GPX family members. GSH can directly scavenge OH^\bullet and $^1\text{O}_2$ as well as detoxifying H_2O_2 by the catalytic effects of GPX (Masella et al., 2005), and is able to acquire resistance to chemotherapy through detoxification pathways involving a further enzymatic antioxidant NQO1 (Cheng et al., 2009).

Tumour cells have again been reported to be able to acquire resistance to chemotherapeutics and radiotherapy by up regulating their GSH activity levels, which in turn increases cellular GST and GPX enzyme levels (Housset, 1987; Szatrowski & Nathan, 1991; Spitz et al., 1993; Toyokuni S, et al., 1994; Suematsu et al., 2002). This is reported to be achieved by the ability of GSH to replenish other such antioxidants at the protein level, thus resulting in the

restoration of their function. This process is termed an “antioxidant network” (Sies et al., 2005). The capacity for one antioxidant to regenerate another is due to the redox potential of the [Redox/Ox] couple (Valko et al., 2006). Two molecules of GSH comprise the reduced form of a major thiol-disulphite redox “buffer” that once oxidised forms glutathione disulphite (GSSG) (Figure 1.7). The GSH capacity to regenerate other antioxidants is reliant on the redox state of this 2GSH/GSSG couple (Jones et al., 2000; Masella et al., 2005). Nuclear GSH also maintains the redox state of critical protein sulphhydryls that are necessary for DNA repair and gene expression. ROS can lead to rapid modification of protein sulphhydryls (protein-SH), where one electron oxidation can yield thiyl radicals (protein-S[•]), and two electron oxidation can yield sulphenic acid (protein-OSH) (Ji et al., 1999). In the absence of GSH, further oxidation of protein sulphhydryls by ROS would lead to the formation of other irreversible oxidised forms including sulphinic (protein-SO₂H), and sulphonic (protein-SO₃H) acids therefore leading to cell death by DNA damage (Ji et al., 1999).

However, GSH reacts with the ROS-promoted thiyl radicals and sulphenic acid to form S-glutathiolated proteins (protein-SSG) that are further reduced in the glutathione cycle (Equation 5) by glutathione reductase (GLRX) and small antioxidant proteins such as thioredoxin in order to restore protein sulphhydryls (protein-SH) and thus maintain cell viability (Ji et al., 1999).

Figure 1.7 Structures of reduced (GSH) and oxidised (GSSG) glutathione.



GSH homeostasis has been linked to a number of disease states including breast cancer (Townsend 2003). Depletion of GSH is known to facilitate apoptosis, whereas elevated levels of GSH have been shown to promote cell survival (Anderson et al., 1999; Hammond et al., 2001). Interestingly, Craig Jordan's team have shown that their endocrine resistant cell line, MCF-7:2A, had elevated levels of GSH (Lewis-Wambi et al., 2009). This promoted survival against oestradiol-induced apoptosis. However with the aid of L-Buthionine sulfoximine (BSO), a synthetic GSH biosynthesis inhibitor, oestradiol-induced apoptosis sensitivity was regained linking GSH clearly with endocrine resistant growth in this model (Lewis-Wambi et al., 2009).

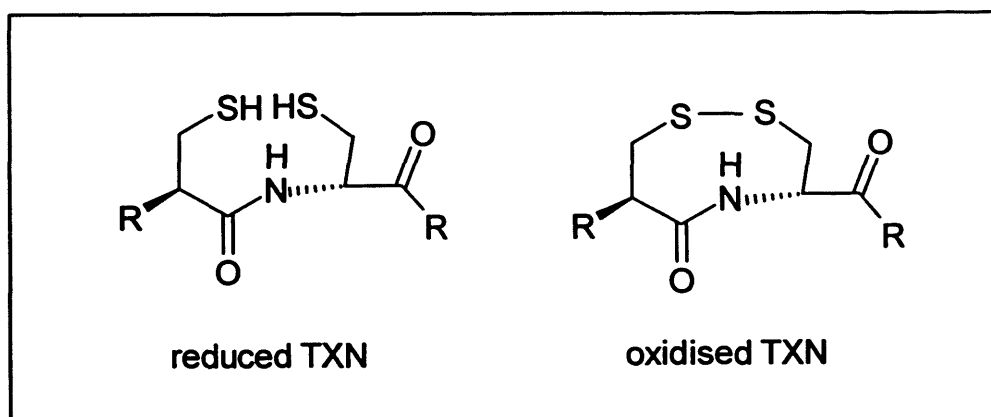
1.3.3.2 Thiol Antioxidants – Thioredoxin (TXN)

TXN is a 12kDa disulphide-containing redox protein, having two redox active cysteine residues within a conserved active site (Cys–Gly–Pro–Cys) (Nakanura et al., 1997). In its reduced form, TXN contains two adjacent –SH groups that once oxidised through redox reactions with proteins are converted to disulphide units (Figure 1.8) as follows:

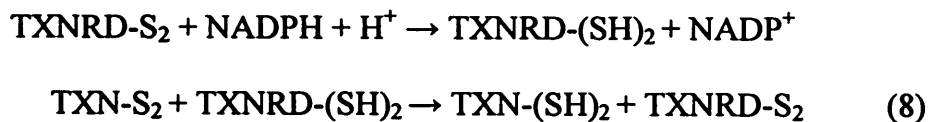


TXN can therefore quench the oxidative effects of ROS at the protein level.

Figure 1.8 Reduced and oxidised TXN



TXN is restored to its reduced antioxidant form by the catalysis of thioredoxin reductase (TXNRD). The source of electrons in this TXN-replenishing reaction is NADPH.



Significant experimental and clinical evidence exists connecting TXN to cancer, indicating elevated levels of TXN occur in some forms of cancer such as cervical carcinoma, hepatoma, gastric tumours, colorectal and lung carcinomas (Sinha et al., 1998; Grogan et al., 2000; Raffel et al., 2003; Hedley et al., 2004; Ding et al., 2004; Csiki et al., 2006). Overexpression of TXN has been shown to defend cells from pro-oxidant induced apoptosis and thus promotes cell survival as well as a growth advantage to tumours (such as in colorectal and gastric carcinoma) (Grogan et al., 2000; Raffel et al., 2003). It has also again been suggested that an increase in TXN expression in human tumours may cause resistance to radiotherapy and to chemotherapeutics that induce ROS, such as doxorubicin, cisplatin, mitomycin C, and etoposide (Yokomizo et al., 1995; Sinha et al., 1998; Grogan et al., 2000; Hedley et al., 2004; Ahmadi et al., 2006). Interestingly, Kim and colleagues have reported elevated levels of TXN and PRDX1 (see below) in their acquired tamoxifen resistant cells in comparison to control MCF7 cells. They also related this increased antioxidant expression to Nrf2/ARE regulation of growth of these particular resistant cells (Kim et al., 2008).

1.3.3.2.3 Peroxiredoxins (PRDX) and their interplay with TXN

PRDX are a novel group of 25k Da peroxidases containing high antioxidant efficiency for peroxides. The mammalian PRDX family has six distinct members, PRDX1-6, which are located in various subcellular locations, such as peroxisomes and mitochondria, where oxidative stress is most evident (Noh et al., 2001; Karihtala et al., 2003). The non-enzymatic antioxidant TXN acts as an electron donor to PRDX, further replenishing its reducing ability for peroxides. Thus the redox cycles of TXN and PRDX again form a further antioxidant network (Kang et al., 1998; Seo et al., 2000). Karihtala and colleagues have found that the expression of PRDX3, 4, and 5 are increased in breast malignancy, suggesting the induction of PRDX can occur in response to increased production of reactive oxygen species in proliferative carcinoma tissue (Ksrihtala et al., 2003).

In addition, PRDX2 is involved in the cellular response to ionizing radiation, where it functions to reduce intracellular ROS levels. Interestingly increases in PRDX2 resulted in increased resistance of MCF-7 cells to ionizing radiation (Wang et al., 2005). A further interesting study comes from Kato and colleagues (2005) whereby nearly 50% of patients in a study of 70 patients with primary breast cancer or locally recurrent breast cancer (tumor size ≥ 3 cm) treated with the chemotherapeutic agent docetaxel failed to respond to chemotherapy (Iwao-Koizumi et al., 2005). Kato's group performed gene expression profiling of breast cancer samples to see if a signature could be determined that was predictive of a patients' response/failure to docetaxel.

Interestingly, they discovered elevated expression of genes controlling the cellular redox environment, including PRDX1, TXN and also GST. Overexpression of these genes was also able to protect MCF-7 cells from docetaxel-induced cell death, suggesting an important role for PRDX/TXN and GSH networks in docetaxel resistance (Iwao-Koizumi et al., 2005). These results further highlight that a molecular mechanism of chemotherapeutic resistance can involve elevation of antioxidant genes.

1.4 Hypothesis and Aims

While there is substantial evidence for a contribution in chemotherapy / radiotherapy resistance, and some tentative tamoxifen resistance data as described above, it remains largely unexplored as to whether endocrine or anti-EGFR agent resistance is associated with changes in redox balance, whereby pro-oxidants might play a role in regulating cell growth and death, and in turn whether alterations in antioxidants might actively contribute to cell survival and as such resistant growth. The initial phase of the investigation for the first time therefore aimed to monitor any increased expression in key antioxidants in these diverse acquired resistant states *in vitro*.

These studies examining whether key components that can underlie redox balance are altered in acquired resistance, and hence might potentially contribute to growth regulation of this state, will employ a panel of *in vitro* human breast cancer models previously-derived in the Tenovus Centre. These cells have acquired resistance either to (i) the anti-oestrogens tamoxifen (TAMR cells) or

faslodex (FASR cells), (ii) to severe oestrogen deprivation (X-MCF cells); or (iii) to tamoxifen and subsequently the EGFR inhibitor gefitinib (NEW DUBS), where these cells will be compared with their endocrine responsive parental cell line w/t MCF7.

The proposed exploration of antioxidants will be achieved through Microarray analysis and PCR studies of gene expression, as well as through biochemical monitoring of total antioxidant capacity, examining if increases are a feature of these acquired resistant models and if any changes identified span multiple forms of acquired resistance. Further studies will address if the antioxidants are oestrogen-regulated and influenced by initial treatment with antioestrogens in endocrine responsive cells, or if any changes observed occur only at the time of resistant growth. In addition, the relationship of antioxidants to EGFR signalling, a known growth promoting pathway for tamoxifen resistant models, will be examined in the resistant cells. These various studies of antioxidants will be paralleled by further studies of the redox balance in resistance by monitoring ROS level within the acquired resistant models, as well as during treatment with antihormones or EGFR pathway inhibition.

If deregulation of antioxidants/ROS is encountered in the acquired endocrine or anti-EGFR resistant cells, the following will be performed to further ascertain growth relevance of the alterations in redox balance to resistant cells:

- In the case of elevated levels of antioxidants apparent in the resistant models, the impact of inhibitors of the antioxidants of interest will be examined, where possible, using a pharmacological approach.
- In the case of deregulated ROS, pro-oxidant level will be manipulated to see how further increases impact on resistant cells, addressing if this excess is able to overcome the level of antioxidants present and hence can be growth inhibitory to resistant cells.

It is hoped that this approach will, for the first time, detail if changes in redox balance (including antioxidants) contribute to acquired resistance to diverse endocrine agents and also anti-EGFR inhibition in breast cancer, and thus that its manipulation could potentially provide new therapeutic avenues to treat these various undesirable states.

Chapter 2 – Methodology

2.1 Cell Culture studies

2.1.1 Materials

2.1.1.1 Cell culture reagents and Plasticware

Plasticware including T-25 flasks, T-75 flasks and 96 well plates were purchased from Nunc, Roskilde, Denmark, and were supplied by Fisher Scientific UK Ltd., Loughborough, Leicestershire, UK. All other components required for cell culture including: RPMI 1640 and phenol-red-free RPMI 1640 media, antibiotics (penicillin/streptomycin), Fungizone, L-glutamine and Foetal calf serum (FCS) were obtained from Invitrogen Ltd., Paisley, Scotland, UK., unless otherwise stated. Activated Charcoal and Tris HCL were purchased from Sigma-Aldrich Company Ltd, Poole, Dorset UK. Isoton® II azide free balanced electrolyte solution (containing sodium chloride at 7.9g, disodium hydrogen orthophosphate at 1.9g., Ethyl diamine tetraacetic acid (EDTA) disodium salt at 0.4g., sodium dihydrogen orthophosphate at 0.2g. and sodium fluoride at 0.3g.) was purchased from Beckman Coulter Ltd, High Wycombe, UK. Eppendorf tubes were purchased from Eppendorf, Hamburg, Germany. Micro-centrifuge tubes (0.5ml and 1.5ml) were purchased from Elkay Laboratory Products, Basingstoke UK. Bijou tubes were purchased from Bibby Sterilin Ltd., Stone, UK. Sterile, disposable serological pipettes (5ml, 10ml, and 25ml), Falcon tubes (50ml), Coulter Counter lids and caps were purchased from Sarstedt AG and Co., Nümbrecht, Germany.

2.1.1.2 Cell lines, anti-oestrogens, signal transduction inhibitors, and drugs impacting on oxidative stress

The wild type (w/t) MCF-7 human breast cancer cell line was originally obtained from AstraZeneca Pharmaceuticals, Cheshire, UK. The SERM 4-hydroxy-tamoxifen (4-OH-TAM, which is used clinically), referred to as tamoxifen in this investigation, was purchased from Sigma-Aldrich Company Ltd, Poole, Dorset UK. The pure antioestrogen faslodex, the EGFR Tyrosine Kinase Inhibitor (TKI) gefitinib, and the Src kinase inhibitor AZD0530 were obtained as gifts from AstraZeneca Pharmaceuticals, Cheshire, UK. The oxidative stress-inducer Menadione-Sodium-Bisulfite (MSB), a selective inhibitor of GSH synthesis Buthionine Sulphoximine (BSO), the PI3K-inhibitor Wortmannin (WORT), the NFκB inhibitor Parthenolide (PARTH) and the MEK inhibitor U0126 were again obtained from Sigma-Aldrich Company Ltd, Poole, Dorset UK.

2.1.1.3 Reagents used for MTT growth assays

The 3-(4,5-Dimethylthiazol-2-yl)-2,5-diphenyltetrazolium bromide (MTT) assay kit, Phosphate Buffer Solution (PBS) and Triton X-100 used for the detection of cellular growth response to different treatments in this study were purchased from Sigma-Aldrich Company Ltd, Poole, Dorset UK.

2.1.1.4 Reagents used for TAC analysis

Total Antioxidant Assay kits was purchased from Sigma-Aldrich Company Ltd, Poole, Dorset UK. The antioxidant assay kit contained 30ml of 10x concentrated Assay Buffer, 20ml Stop solution, 2 x 1mg Myoglobin stock from horse heart, 2 x 1mg 6-Hydroxy-2,5,7,8-tetramethylchromane-2-carboxylic acid (Trolox), 4 x 10mg tablets of 2,2'-azino-bis(3-ethylbenzthiazoline-6-sulfonic acid) (ABTS), 4 x phosphate-citrate Buffer tablets at pH 5 and 1ml of H₂O₂ (3%) solution. The kit was sufficient for 200 assays in 96 well plates.

2.1.1.5 Reagents and plasticware used for ROS detection

All reagents for ROS detection analysis including the stock solutions of 2'-7'-dihydrodichlorofluorescein diacetate (H₂DCFDA) fluorescent dye, and delivery agent Dimethyl Sulfoxide (DMSO) were again purchased from Sigma-Aldrich Company Ltd, Poole, Dorset UK unless otherwise stated. The ROS-inducing internal control, H₂O₂, and Trypsin used for lysing cells in the assay were also purchased from Sigma-Aldrich Company Ltd, Poole, Dorset UK. Due to light sensitivity of the fluorescent dye, flat-bottomed black 96 well plates were purchased from Invitrogen Ltd., Paisley, Scotland, UK.

2.1.1.6 Reagents and glassware used for Ki67 immuno staining

All reagents for Ki67 proliferation marker immunostaining (including acetone for cell fixation, TESPA (3-Aminopropyltriethoxysilane), Methyl green, PBS, DPX and ethanol) were purchased from Sigma-Aldrich Company Ltd, Poole, Dorset UK unless otherwise stated. The Ki67 Mouse primary antibody, Goat

anti-Mouse Immunoglobulins secondary antibody, Mouse tertiary peroxidase antiperoxidase (PAP) reagent and 3,3' Diaminobenzidine (DAB) chromogen were purchased from DakoCytometrics, Carpinteria, California, USA. All glassware including coverslips and glass slides were purchased from Nunc, Roskilde, Denmark, and were supplied by Fisher Scientific UK Ltd., Loughborough, Leicestershire, UK.

2.1.1.7 Reagents used in apoptosis analysis

The ApoAlert mitochondrial membrane sensor kit (MMS) was purchased from Clontech Laboratories UK Ltd., Basingstoke, UK. The kit comprised Incubation Buffer, and five vials of MitoSensor reagent. All glassware were again purchased from Nunc, Roskilde, Denmark, and were supplied by Fisher Scientific UK Ltd., Loughborough, Leicestershire, UK.

2.1.2 Methodology

2.1.2.1 Development of acquired resistant breast cancer cell models

In this thesis, the wild type (w/t) MCF7 breast cancer cell line was used as the endocrine responsive control for comparison with acquired tamoxifen resistant (TAMR) and faslodex resistant (FASR) models, cells with acquired resistance to severe oestrogen (and growth factor) deprivation (X-MCF), and cells with acquired tamoxifen and gefitinib resistance (NEW DUBS). These models were developed prior to this project in the Tenovus Centre for Cancer Research Cell

Culture Unit by continuous drug exposure of the wtMCF7 cells *in vitro*. In brief, to establish the TAMR or FASR cells, w/t MCF7 cells were maintained in their experimental medium (comprising Phenol red-free RPMI with 5% charcoal-stripped fetal calf serum (csFCS – see Appendix II for charcoal-stripping procedure), penicillin (10iU/ml), streptomycin (10µg/ml), fungizone [2.5µg/ml] and 4mM Glutamine) supplemented with 4-OH Tamoxifen or Faslodex respectively at 10^{-7} M. For derivation of X-MCF cells, experimental medium was supplemented with 5% serum which had again been charcoal-stripped of steroids and also heat-inactivated at 65°C for 30 minutes (“X”-medium). After an initial inhibition of cell growth of approximately 12 weeks duration in the presence of Tamoxifen, Faslodex, or X-containing medium, cells became able to proliferate in the presence of these treatments indicating emergence of acquired resistance.

Cells were subsequently always used for experiments at passage numbers 13-18 for w/t MCF7 cells, 37- 52 for TAMR cells, 89-100 for FASR cells, and 66-67 for X-MCF cells once the TCCR unit had determined the resistant phenotypes had become stable. The acquired TAMR cells were subsequently treated with 1µM of the EGFR-TKI gefitinib (10^{-6} M in experimental medium, maintaining 10^{-7} M tamoxifen) for 6 months until resistance to this additional targeted therapy had been acquired. The resultant model (NEWDUBS) was subsequently used once stable over passage numbers 39-51 for this thesis.

2.1.2.2 Maintenance of w/t MCF7 and acquired resistant breast cancer cell models

w/t MCF7 breast cancer cells were routinely maintained in phenol red-containing RPMI 1640 media supplemented with 5% foetal calf serum (FCS), penicillin-streptomycin (10iU/ml – 100µg/ml), and fungizone (2.5µg/ml) in either T-25 or T-75 flasks depending on the density of cells required. The TAMR, FASR, X-MCF and NEW DUBS breast cancer cell lines were routinely maintained in their respective experimental medium i.e. TAMR / FASR / NEWDUBS: phenol-red free RPMI media, supplemented with 5% charcoal stripped steroid-depleted FCS, penicillin-streptomycin (10iU/ml – 100µg/ml), fungizone (2.5µg/ml) and glutamine (4mM) with 10^{-7} M tamoxifen, faslodex or tamoxifen plus 10^{-6} M gefitinib respectively; X-MCF were maintained in X medium.

The media was replenished on cells in culture every 4 days and passaging was performed every 7 days once cells were in log phase (i.e. ~70% confluency). To passage, cells were washed three times with PBS and were detached from the bottom of the flasks by incubating with Trypsin/EDTA solution (0.05%/0.02% w/v) at 37°C for 3-4min. The resultant cell suspension was centrifuged at 1000rpm for 5 minutes, discarding the supernatant, and the remaining cell pellet was resuspended in the appropriate medium in fresh flasks using a split ratio of 1:10. All cells were maintained at 37°C in a 5% CO₂ humidified Sanyo MCO-17AIC incubator purchased from Sanyo E&E

Europe BV, Loughborough, UK., and all reagents for cell culture were pre-warmed to 37°C before use.

2.1.2.3 Coulter Counting Growth experiment in responsive and acquired resistant cell lines

w/t MCF7cell, TAMR cells, FASR cells, X-MCF cells and NEW DUBS cells from a T75 flasks were passaged as described in section 2.1.2.2. Cell suspensions were diluted to 4×10^4 cells/ml and were seeded in 24 well plates (1ml/well). All cell models were incubated for 24 hours prior to experimentation in their respective experimental media (phenol red-free RPMI supplemented with 5% csFCS, penicillin-streptomycin (10iU/ml – 100µg/ml), fungizone (2.5µg/ml) and glutamine (4mM) with 10^{-7} M tamoxifen, faslodex or tamoxifen plus 10^{-6} M gefitinib respectively; X-MCF were maintained in X medium), the medium was replenished every 3-4 days. All cell lines were grown over 0 – 11 days, counting wells at days 1, 4, 6, 8 and 11 using a Beckman Coulter Counter Multisizer II. To record the number of cells per well, the medium was initially removed and replaced with 1ml of trypsin solution and incubated at 37°C for 3-5 minutes. Using a 5ml syringe with a G5/8 0.5 X 16 needle, the detached cells were pipetted up and down twice to encourage a single-cell suspension for accurate analysis of cell number. 1ml Isoton solution was then added to the well and the solution was again pipette up and down twice before being drawn into the syringe. This procedure was repeated twice to give a total volume of 4ml. The cell suspensions were subsequently transferred to a counting pot containing 6ml of Isoton giving a

final volume of 10ml. The numbers of cells in each pot were determined in duplicate using the Coulter™ Multisizer II set to count the number of cells in 500µl. Pots were counted twice and duplicate counts for every cell line were averaged and multiplied by the dilution factor of 20 to give the average number of cells per well. The experiment was performed three times with significance calculated using a student T-test at day 8 compared to the control parental cells (w/t MCF7) ± Standard Deviation (SD) with $p < 0.05$ considered significant.

2.1.2.4 MTT assay to evaluate basal growth of acquired resistant versus responsive cells and in the presence of tyrosine kinase inhibitors (TKI), signal transduction inhibitors (STIs), Antioxidant inhibitor (BSO), or oxidative stress inducer Menadione (MSB)

For MTT growth studies, cell lines were seeded out into 96 well plates at a density of approximately 7000 cells per well for w/t MCF7 cells, TAMR, FASR, X-MCF or NEW DUBS, subsequently leaving the cells to attach to the flask for 24 hours prior to experimentation. To initially seed out cells, T25 or T75 flask preparations (depending on number of cells required for multiple experimental runs) of the resistant or responsive cell lines at 70% confluency were trypsinised and centrifuged as described in section 2.1.2.2. The subsequent pellet was then resuspended in 10ml Phenol red-free RPMI with 5% csFCS.

To ensure equal cell density for each experiment, cells were then counted and diluted appropriately prior to plating into the 96 well plate. To count, 100µl of

this suspension was added to 10 ml of Isoton and the cell number counted twice using a Beckman Coulter counter multisizer II (from Beckman Coulter Ltd, High Wycombe, UK). Calculation of average cell density for each cell preparation could then be made from these counts so that the correct cell number could then be seeded per well for growth studies. For all MTT assays, all resistant cells were subsequently grown in their respective experimental media as described in 2.1.2.2, while w/t MCF7 cells were grown in phenol-red free, RPMI medium containing 5% csFCS, penicillin-streptomycin (10iU/ml – 100µg/ml), fungizone (2.5µg/ml) and glutamine (4mM). Cell growth was examined under these untreated (basal conditions) or when exposed to different treatments added to the media at varying concentrations, as detailed in Table 2.1. Drug concentrations known to be selective for the target and also growth inhibitory in further breast cancer models were employed and prepared from a stock concentration (made up in ultrapure distilled water in the case of MSB, and Ethanol for all other treatments). Literature search enabled determination of the optimal dose range for treatment with tamoxifen, faslodex, gefitinib (Gee et al., 2003), AZD0503, wortmannin, PARTH, U0126 (Knowlden et al., 2003; Jordan et al., 2004; Hiscox et al., 2006), the antioxidant inhibitor BSO (Lewis-Wambi et al., 2009) and the ROS inducer Menadione-Sodium-Bisulfite (MSB; Noto et al., 1989; Nutter et al., 1991; Sun et al., 1997). Cells were incubated with/without these various treatments at 37°C in a 5% CO₂ humidified incubator for 7 days, replenishing media after 4 days. The medium was then removed and the MTT assay performed within the plates. MTT results were obtained in replicates of 8 for each cell line/treatment.

For the MTT assay, 8.75mg MTT solution was added to 3.5ml phenol-red free RPMI medium (without serum, penicillin-streptomycin, fungizone or glutamine). This mixture was then filter sterilised through a 0.2µm Supor membrane VacuCap 60 filter unit (from Gellman Laboratory Pall, Ann Arbour, USA), and diluted 1:5 to produce a final concentration of 0.5mg/ml. 3.2ml of this stock solution was added to 12.8ml stripped serum RPMI to give 16ml of working solution at 0.5mg/ml, 150µl of which was added to each well in the various growth study plates. The plate was incubated at 37°C in a 5% CO₂ humidified incubator for 4 hours. During this time, the MTT was metabolised by mitochondrial dehydrogenase enzymes to produce insoluble purple formazan crystals. After removing the MTT solution, the cells were lysed using 100µl Triton X-100 (10% in PBS) and left at 4°C overnight. The following morning, the plates were allowed to reach room temperature and were then gently tapped to mix the solution within the wells, being careful that no bubbles were produced. Absorbance of the solution was then read at 540nm using an ELISA plate reader (from Biotron diagnostics Inc. California USA.), and optical density was plotted on a bar graph with higher optical density associated with more formazan crystals formed during growth. Experiments were repeated three times and statistical analysis was carried out using Student T-test ± SD (p value considered significant <0.05). The half maximal growth inhibitory concentrations (IC₅₀), if required, were calculated for treatments by obtaining 50% of the maximum effect.

Table 2.1 Summary of experimental technique and drug concentrations used to examine particular cell models in the thesis.

Drug and Concentration	Experimental technique					Cell model					
	TAC	ROS	MTT	Ki 67	ApoAlert	w/t	MCF7	TAMR	FASR	X-MCF	NEW DUBS
Tamoxifen (10 ⁻⁷ M)	✓	✓				✓					
Faslodex (10 ⁻⁷ M)	✓	✓				✓					
Gefitinib (10 ⁻⁹ M)	✓	✓	✓	✓	✓			✓			
AZD0503 (1 μ M)	✓	✓	✓					✓			
Wortmanin (100nM)	✓	✓	✓					✓			
PARTH (3 μ M)	✓	✓	✓					✓			
U0126 (10 μ M)	✓	✓	✓					✓			
BSO (100 μ M)	✓		✓					✓			
BSO (100 μ M) + Gefitinib (10 ⁻⁹ M)	✓		✓					✓			
MSB (2-18 μ M)		✓	✓			✓	✓	✓	✓	✓	✓

2.1.2.5 TAC analysis

Using a commercial antioxidant assay kit (Sigma) the resistant breast cancer models were assessed for total antioxidant capacity (TAC) in relation to the parental endocrine responsive breast cancer cell line w/t MCF7 again under basal conditions and following manipulation with antihormones, the EGFR TKI, STIs and BSO as in Table 2.1. A water-soluble vitamin E analogue, Trolox, was used as an antioxidant assay internal control (Kalinich et al., 1997). Preparation of all working solutions for TAC analysis from the Total Antioxidant kit was carried out using ultrapure water prepared in the Welsh School of Pharmacy. The concentrated TAC Assay kit Buffer was diluted 1x for use and the kit Myoglobin was reconstituted from a Stock Solution by addition of 285µl ultrapure water, subsequently diluting 100-fold with the 1x Assay Buffer to give a Myoglobin Working Solution. The Trolox working solution (1.5mM) for TAC assay standard curve construction also required reconstitution of kit Trolox in 2.67ml of 1x TAC Assay Buffer. One 2,2'-azino-bis(3-ethylbenzthiazoline-6-sulfonic acid) (ABTS) tablet and one Phosphate-Citrate Buffer tablet from the kit were mixed well with 100ml ultrapure water to obtain an ABTS Substrate working solution for the assay.

The principle of the antioxidant assay is that oxidation of the ABTS substrate produces a radical cation $ABTS^{•+}$, which is a soluble green colour chromogen that can be detected spectrophotometrically at 405 nm. Antioxidants naturally occurring within the cell suppress the production of the radical cation $ABTS^{•+}$ in a concentration dependent manner, and the colour intensity decreases

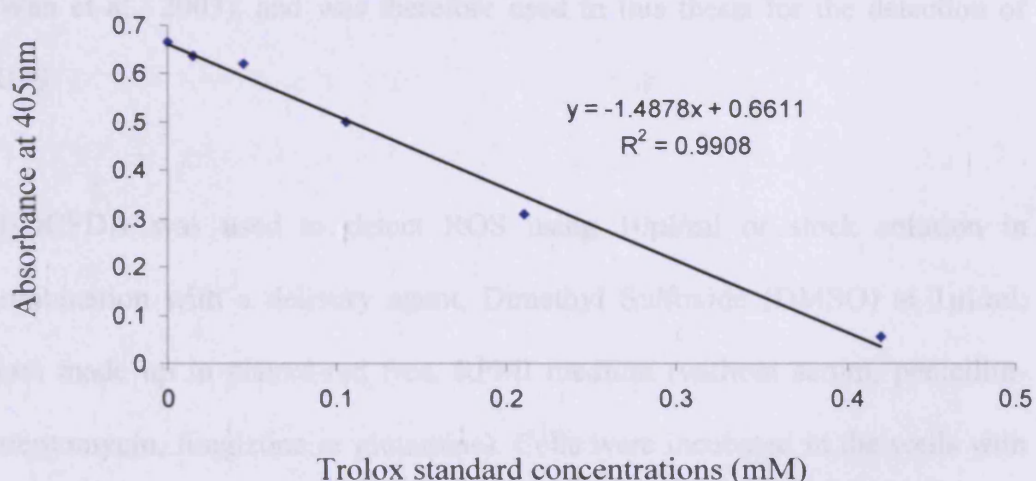
proportionally to the level of antioxidants present. By combining with ABTS Substrate working solution (150 μ l) containing H₂O₂ (25 μ l of a 3% solution), Myoglobin working solution (20 μ l), and 1x Assay kit buffer (500 μ l), increasing volumes of the 1.5mM Trolox antioxidant standard were used to create a standard curve (concentrations in the standard ranging 0-0.42mM). Antioxidant concentration (mM) of the test breast cancer models could then be calculated using equation (a) in Figure 2.1(a) which uses the linear regression of the Trolox standard curve obtained also as shown in Figure 2.1(b). To perform the assay on the test cell lines, these were seeded down at an optimised 10,000 cells per well of a 96 well plate in preparation for the experiment, and allowed to grow for 24hours, 7days and 10days (changing media at day 4) before being measured for TAC. Assays were performed in duplicates. As for the Trolox internal control, ABTS Substrate Working Solution was prepared by adding 25 μ l of 3% H₂O₂ solution to 10ml ABTS stock solution, 150 μ l of which was added to 10 μ l of Trolox standard and 20 μ l Myoglobin Working Solution in the 96 well plate. 150 μ l ABTS Substrate Working Solution and 20 μ l Myoglobin Working Solution was again added to the cell lines in each of the wells in the 96 well plates. Plates were incubated for 5min before the reaction was stopped using 100 μ l kit Stop Solution and final absorbance was read at 405nm using a plate reader. Absorbance values were used to subsequently calculate approximate antioxidant capacity for each cell model. Experiments were repeated three times with data plotted on a bar graph and statistical analysis was carried out using Student T-test \pm SD (p value considered significant <0.05), as demonstrated by Rice-Evans, 2000.

Figure 2.1 Determining Total Antioxidant Capacity (TAC) of test samples

(a) Calculation for determining TAC of a test sample:

$$X \text{ (mM)} = \frac{y(A_{405}) - \text{Intercept}}{\text{Slope}}$$

(b) Example of Trolox Standard Curve obtained in this study:



Total Antioxidant capacity of the test samples (e.g. resistant model versus w/t MCF7 cells) was calculated using equation (a) as shown above, obtained from the linear regression of the Trolox standard curve (see example b achieved in this thesis in Figure 2.1 above). X (mM) refers to the antioxidant concentration in mM, calculated relative to the Trolox internal control. y(A₄₀₅) is the average absorbance of the test sample at 405nm. Intercept is the intercept of the Y axis by the standard curve shown here as 0.6611 in Figure 2.1 (b), and the Slope refers to the slope of the standard curve, a negative value shown here as -1.4878 in Figure 2.1(b). The standard curve was duplicated for accuracy and the experiment was repeated three times with duplicates again for each sample for accuracy. Final data was represented in a bar graph with statistical analysis using a Student T-test ± SD.

2.1.2.6 ROS detection

Cells for ROS experimentation according to Table 2.1 were seeded down as for TAC at i.e. 10,000 cells per well of a 96 well plate in preparation for the experiment, allowing the cells to grow for 24 hours, 7 days and 10 days and subsequently measuring total ROS. In this assay a cell-permeable non-fluorescent probe 2'-7'-dihydrodichlorofluorescein diacetate (H₂DCFDA) is de-esterified intracellularly and becomes the highly fluorescent 2',7'-dichlorofluorescein (DCF) dye upon oxidation. H₂DCFDA thus provides a sensitive and rapid quantitation of ROS in response to oxidative metabolism (Wan et al., 2003), and was therefore used in this thesis for the detection of ROS.

H₂DCFDA was used to detect ROS using 10µl/ml of stock solution in combination with a delivery agent, Dimethyl Sulfoxide (DMSO) at 1µl/ml, both made up in phenol-red free, RPMI medium (without serum, penicillin-streptomycin, fungizone or glutamine). Cells were incubated in the wells with 150µl dye (i.e. H₂DCFDA and DMSO) for 30 minutes at 37°C followed by draining off their media. The ROS detection assay also required further wells prepared from the various cell models under control conditions but treated with 1mM H₂O₂ (from a 0.03% stock solution) for 10 minutes as an internal positive control for oxidative stress in the assay. In addition, wells treated with DMSO alone at 1µl/ml of stock solution in phenol-red free, RPMI medium without serum, penicillin-streptomycin, fungizone or glutamine were used as a negative assay control. Following incubation with dye, all cells were lysed using 100µl

Trypsin (0.05%) and transferred to black 96 well plates in which the intensity of fluorescence was measured from 8 wells for each model (per treatment/per time point) at 420nm excitation and 580nm emission using a FlouoroStar absorbance reader (from BMG LabTech, Aylesbury, UK). The FlouoroStar compared the “gain” (highest reading from each 96 well plate) of each experimental design against its replicates in order to produce comparable results. Results were taken for each cell model and treatment in triplicate. Mean absorbance readings were presented in a bar graph with statistical analysis using a Student T-test \pm SD (p value considered significant <0.05).

2.1.2.7 Ki67 immunostaining for proliferation

The Ki67 proliferation marker detects all cells in cell cycle, while resting cells (in GO) remain unstained (Gerdes et al., 1983). w/t MCF7 cells and TAMR cells were seeded down at 1×10^6 cells onto TESPA coated glass coverslips (22x22mm) and grown to log phase (7 days) before evaluation of proliferation under basal conditions in their respective experimental media. Treatment of TAMR cells with 10^{-6} M gefitinib for 7days was also examined in parallel versus the untreated TAMR cells. Cells growing on the coverslips were fixed using acetone for 10 minutes at room temperature and then allowed to air-dry for 30 minutes. A single wash of the coverslips was carried out using PBS (pH 7.2, 0.01M) for 5 minutes, before a blocking step with 10% normal goat serum prepared in PBS for 10 minutes. Excess blocking reagent was then wiped off before the addition of Dako Ki67 monoclonal primary antibody (80mg/L) at 1/100 in PBS for 45 minutes. Negative control coverslips omitted the primary

antibody step, were incubated with the PBS carrier for 45 minutes. All coverslips were then washed three times for 4 minutes using PBS before the application of the secondary antibody, Dako Goat anti-Mouse Immunoglobulins. This was applied at 1/25 prepared in PBS for 30 minutes and then washed three times using PBS for 4 minutes. A Tertiary reagent, Dako Mouse PAP was then added at 1/250 in PBS for 30 minutes and again washed three times for 4 minutes using PBS. The chromagen Dako DAB chromogen (1 drop DAB to 1ml Substrate Buffer as provided by manufacturer) was then applied for 8 minutes followed by three washes for 4 minutes using distilled water. Coverslip preparations were then counterstained using 0.5% methyl green (aqueous) for 5 minutes followed by two 2 minute washes with distilled water, dehydration through graded ethanols, and then mounting on glass slides using DPX mountant when dry. Assessment of staining was carried out on an Olympus BH-2 microscope, where cells were counted in 10 square fields for positive (brown) or negative (blue/green) staining and given an average percentage positivity score. Representative photographs of staining were also taken using an Olympus DP12 digital camera (X40 magnification).

2.1.2.8 ApoAlert assay (MMS) for apoptosis

The ApoAlert mitochondrial membrane sensor kit (MMS) uses a Mitosensor reagent to detect cells in early apoptosis. MitoSensor reagent forms red fluorescent mitochondrial aggregates in non-apoptotic cells, however in early apoptosis MitoSensor remains in a monomeric green fluorescent cytoplasmic form due to altered mitochondrial membrane permeability (Green & Reed

1998; Gee et al., 2003). Apoptosis is therefore evaluated by the percentage of green fluorescent cells. The MMS kit comprised an Incubation Buffer (100ml), and five vials (20 μ l) of MitoSensor reagent (5mg/ml).

w/t MCF7 and TAMR cells were seeded at 1×10^6 onto TESPA-coated glass coverslips and grown to log phase (7 days) in their experimental media before analysis of apoptosis. Treatment with 10^{-6} M gefitinib was also examined in parallel versus the untreated TAMR cells. Assays also included an internal positive control comprising w/t MCF-7 grown for 7 days and then exposed to UV light for 20 minutes followed by a 4 hour incubation period at 37°C prior to assay. Each coverslip was then washed with 1ml of phenol-red free, RPMI medium (without serum, penicillin-streptomycin, fungizone or glutamine) that was pre-warmed to 37°C. MitoSensor assay solution was then prepared immediately prior to use by addition of 1 μ l stock Mitosensor reagent per 1ml of kit Incubation Buffer to give a final Mitosensor concentration of 5 μ g/ml. 1ml of this MitoSensor solution was then added to every coverslip and incubated for 20 minutes at 37°C in a 5% CO₂ incubator, foil-covering the coverslips to protect the Mitosensor from light. Subsequently the MitoSensor solution was removed and the coverslip gently rinsed with 1ml of serum-free media (pre-warmed to 37°C) and viewed immediately under a fluorescence microscope at x40 magnification. The average apoptotic cell percentage for each coverslip was estimated by counting, green-stained cells (versus red cells) over nine fields per coverslip.

2.2 Affymetrix microarray analysis

2.2.1 Materials

2.2.1.1 Cell culture reagents and plasticware for microarrays

All plasticware and reagents employed for the initial generation of experimental material from the wtMCF-7 cells and the acquired resistant, TAMR, FASR, MCF-7X and NEWDUBS models for microarraying were as described above in section 2.1.1.1. Lysis of cell preparations for RNA preparation used TRI-Reagent from Sigma-Aldrich Company Ltd, Poole, Dorset UK.

2.2.1.2 RNA purification kits

Deoxyribonuclease 1 was purchased from Sigma-Aldrich Company Ltd, Poole, Dorset UK. RNeasy columns for RNA cleanup and the RNeasy mini kit were purchased from Qiagen House Fleming Way, Crawley, West Sussex, UK. Chloroform and isopropanol were purchased from Sigma-Aldrich Company Ltd, Poole, Dorset UK, and agarose gel was purchased from Bionline Ltd. London UK.

2.2.2 Methodology

Initial RNA extraction, and Microarray preparation from w/t MCF7, TAMR, FASR, X-MCF and NEW DUBS cells and the subsequent expression database construction for triplicate preparations of each of these cell lines was

performed prior to the commencement of this thesis by Mr. RA McClelland (Tenovus Centre for Cancer Research) and by the Affymetrix-approved commercial microarray facility Central Biotechnology Services (Wales College of Medicine, Cardiff University). The methodology that was employed for these steps is briefly provided for clarity in sections 2.2.2.1 and 2.2.2.2. Since this thesis focussed around performing subsequent analysis of the antioxidant gene probe sets represented within this expression database, this analysis is provided in detail in the subsequent sections 2.2.2.3 onwards.

2.2.2.1 RNA extraction from cell lines

RNA was initially isolated from triplicate experimental cultures of w/t MCF7, TAMR, FASR and NEW DUBS cells (maintained in their respective experimental medium and containing 10^{-7} M tamoxifen, faslodex, or 10^{-7} M tamoxifen with 10^{-6} M gefitinib for TAMR, FASR and NEW DUBS respectively). Cells were seeded at 1×10^6 cells/80-cm² flask and harvested during log phase growth at day 7 (with a media change at day 4). Equivalent preparations were made for X-MCF cells maintained in X medium. Further preparations were made from w/t MCF7 cells harvested at day 10 in their experimental medium supplemented throughout with oestradiol (10^{-9} M), in the absence of oestradiol, or in the presence of the antihormones tamoxifen or faslodex (at 10^{-7} M). All cell preparations were then lysed in situ in the presence of phenol-based TriReagent, scraped into 1.5 ml microcentrifuge tubes and stored at -80°C overnight. Total RNA was isolated according to the TriReagent kit protocol, including chloroform extraction and isopropanol

precipitation of RNA which produced a precipitation of a pink protein layer, a cloudy DNA layer and a clear RNA supernatant that was removed, washed using 75% ethanol and re-dissolved in RNase free water. This was quantified at 260nm and purity assessed by analysis of the spectrophotometric ratio of 260/280nm to give acceptable optical density levels of >1.7 using UV spectrophotometry (using a UV Transilluminator from Alpha Innotech Corp. California, USA). Assessment of RNA integrity was then made by horizontal 2% agarose gel electrophoresis followed by DNase1 treatment (for 30minutes at 37°C) of RNA to ensure absence of genomic DNA, and subsequent RNA clean-up using RNeasy Mini Columns. RNA samples were eluted in sterile RNase free water and then re-quantified, with RNA integrity again determined by spectrophotometry and electrophoresis.

2.2.2.2 Hybridisation to Affymetrix Chips and expression database construction for expression studies in the cell lines

RNA samples at >1µg/µl were transferred on dry ice to the specialist Cardiff University Central Biotechnology Services (CBS) Microarray facility for initial Agilent RNA chip analysis to check suitability of the RNA for subsequent Affymetrix U133A GeneChip hybridisation analyses. All samples satisfied CBS quality control parameters, and so the triplicate RNA samples from each cell line were then used to generate biotinylated cRNA which was then hybridised to cDNA oligonucleotides on Affymetrix Genechips, using one Affymetrix HG U133A Genechip for each sample. This microarray encompasses probes representing 22800 genes as well as array controls.

Hybridised arrays were then scanned and fluorescence data output per probeset generated using Microarray Suite 5.0 (MAS5.0) software (Affymetrix, UK). This software interprets the laser-generated intensity scores for each probe, subtracts non-specific signal obtained from parallel single-band mismatch controls for each, and unifies and reports the expression signal for each “probe set” by combining the n=11-14 individual values as a single “probe set” value. A “probe set” for each individual RNA species thus represents the data from a set of different oligonucleotides (often 11-14, overlapping / adjacent) spanning a region towards the poly A terminals of the RNA of interest. MAS 5.0 also statistically produces a likely expression call of present (P), absent (A), or marginal (M) based on specific/non-specific signal ratios.

Data files detailing the Affymetrix HG-U133A GeneChip-determined expression levels of individual RNA species in each sample were then recorded on CD-ROM and returned in an Excel file format to the Tenovus Centre to enable comparative analysis across the various cell models. The triplicate expression data for each cell line were uploaded into the online software package GeneSifter™ (www.genesifter.net), creating an expression database encompassing each cell line to perform microarray analysis. The data were then normalised and log transformed within the software, creating “projects” (see below) for comparative analysis of gene expression across groups of particular cell models, in this instance ultimately allowing interrogation of expression of individual oxidative stress-related genes.

2.2.2.3 Creating new projects for expression analysis

Once logged on to GeneSifter, the online Homepage displayed a control panel by which existing projects could be analysed or inventoried, or new projects could be created (Figure 2.2). For this thesis, the first new project created in GeneSifter was to analyse expression in wtMCF-7 cells versus the resistant models TAMR, FASR, X-MCF or NEW DUBS. This was achieved by clicking on the ‘create new: project’ option in the control panel (Figure 2.2) on the left of the homepage screen, and the U133A:HG-U133A array option was then selected (Figure 2.3) as this was the microarray chip format used in this investigation. The conditions of this array were subsequently displayed in the ‘common conditions’ text box (Figure 2.3), and it was then possible to ‘continue’ on to page 2 of 3 for ‘create new: project’.

Figure 2.2 GeneSifter Homepage at <http://gs41.genesifter.net/users/>

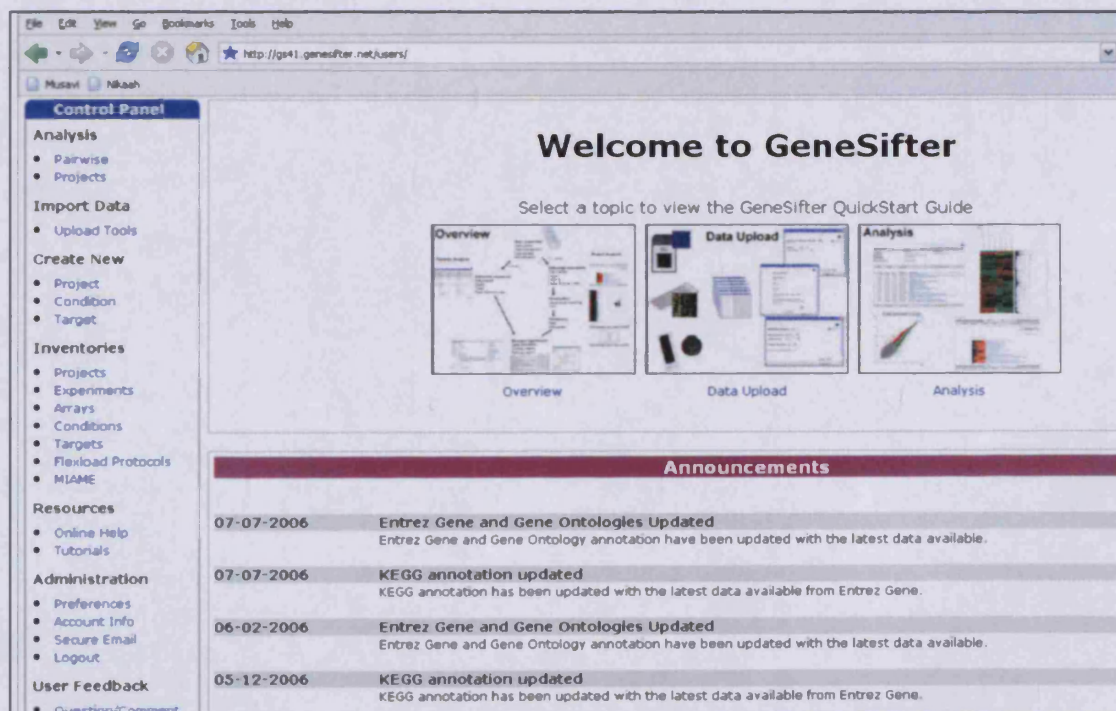
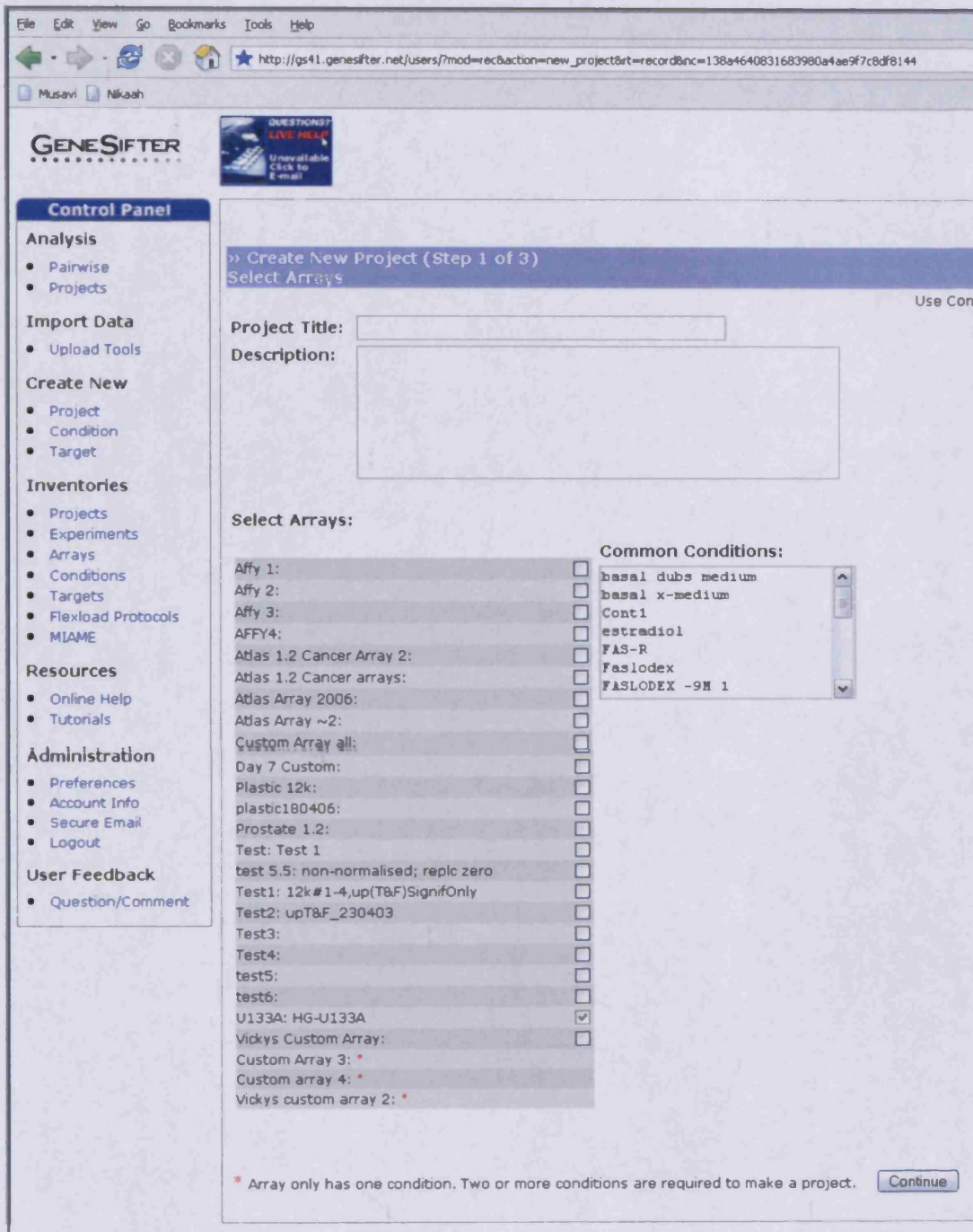


Figure 2.3 Creating a new project in GeneSifter, page 1 of 3.



Subsequent to creating a new project, a group name describing the cell model used was designated in the description text box on page 2 (Figure 2.4: “w/t vs.resistant models”). As recommended in Genesifter, median normalization of the U133A array data was chosen using the ‘All Median’ option (Figure 2.4), and data log transformed prior to choosing the experimental conditions for comparative analysis. The first cell line chosen is automatically treated as control, which for these studies was the w/t MCF7 cell line, for comparison with the resistant models TAMR, FASR, X-MCF, or NEW DUBS (referred to as NEW TAMR/TKIR in the database). Once the desired conditions were chosen, it was possible to ‘create group’ (Figure 2.4), and go into the final page of “create new project” (Figure 2.5) where all experimental replicates were selected for each condition, thus allowing new project creation to be completed ready for analysis (Figure 2.5). Other projects created included exploring if antioxidant genes were hormone/antihormone regulated, where w/t MCF7 cells were run in GeneSifter as the control alongside oestradiol treated w/t MCF7 cells (+E2, 10^{-9} M), tamoxifen treated w/t MCF7 cells (+TAM, 10^{-7} M), or faslodex treated w/t MCF7 cells (+FAS, 10^{-7} M) (10days treatment).

Figure 2.4 Creating a new project in GeneSifter, page 2 of 3.

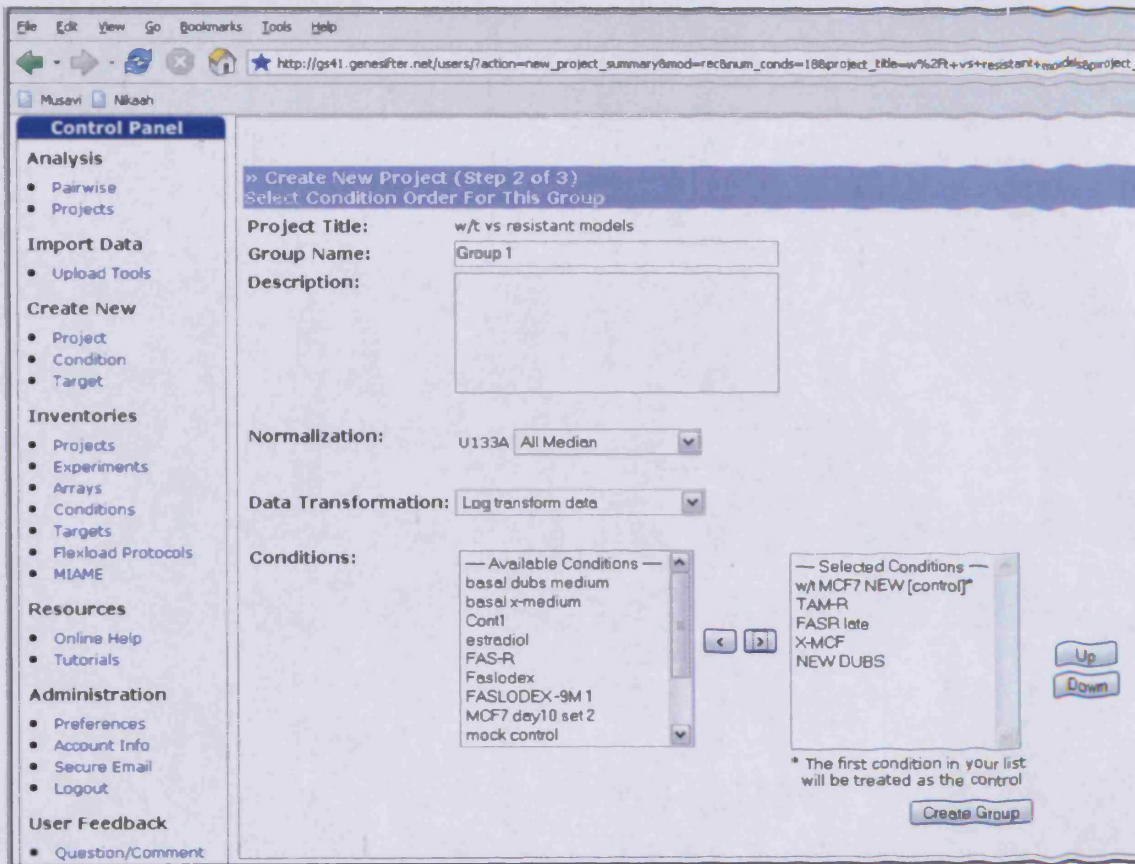
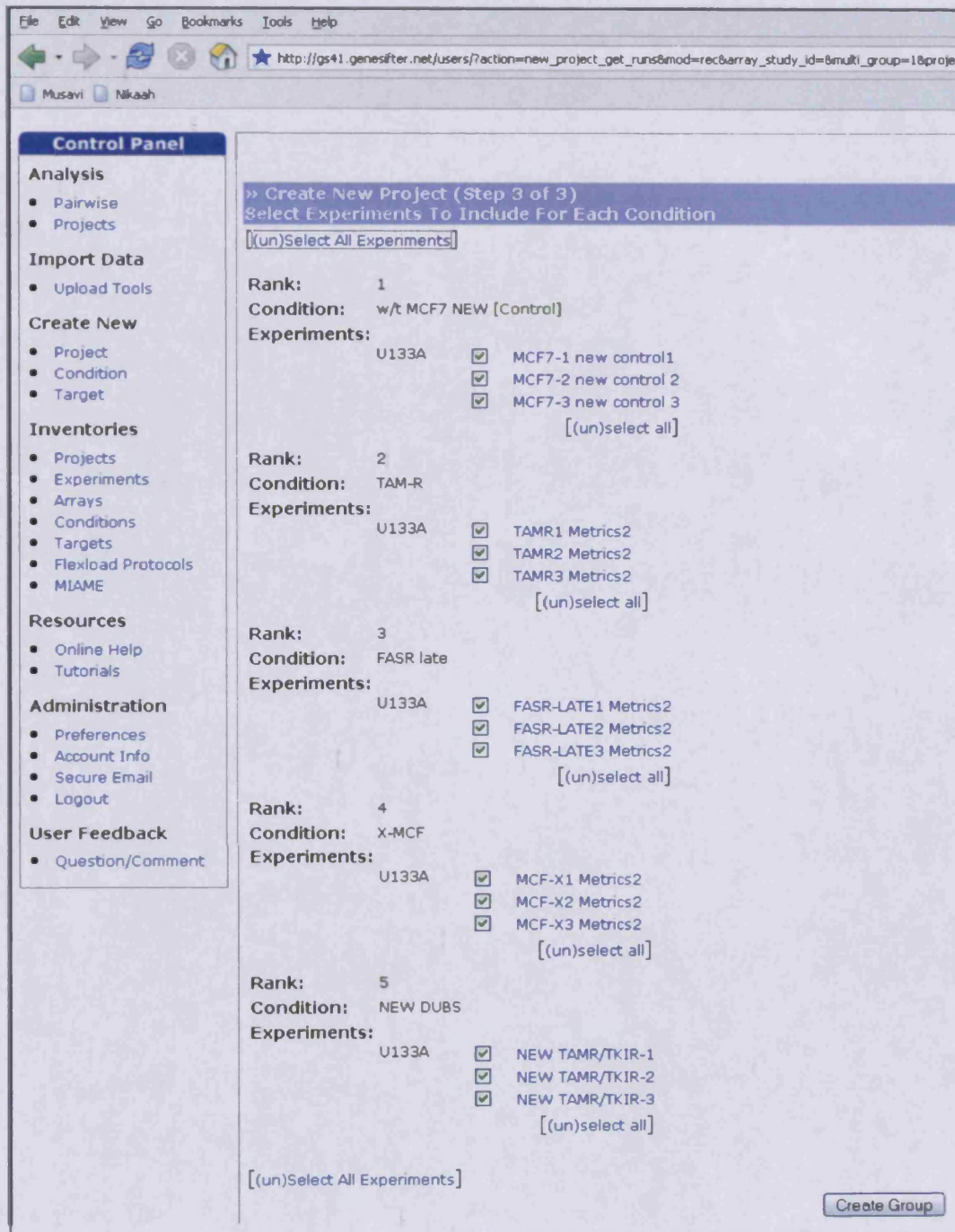


Figure 2.5 Creating a new project in GeneSifter, page 3 of 3.



2.2.2.4 Initial interrogation of gene of known expression profile (quality control step)

The expression profile of the oestrogen/ER-regulated gene pS2 (Affymetrix probe no. 205009_at), a gene of known expression in the responsive and resistant models and during oestrogen/antihormone manipulation (Henry et al., 1991; Hutcheson et al., 2003; Staka et al., 2005), was then interrogated to initially check the quality of the arrayed samples, ensuring the expression database was likely to subsequently permit robust interrogation of genes of unknown expression profile (in this instance, antioxidant genes).

2.2.2.5 Interrogation of antioxidant gene expression profile

A set of 39 antioxidant genes were chosen (through extensive literature searches using references from Medline: <http://www.ncbi.nlm.nih.gov/pubmed/> and using the GeneCards® online database, a database of genomic, proteomic, transcriptomic, genetic and functional information on all known human genes), as listed in Results Table 3.1, to interrogate expression across the responsive and resistant models.

Their gene names were also individually entered into the web-based computer programme GeneCards® (<http://genecards.org/index.shtml>) in order to obtain the Affymetrix probe set ID number(s) for each of the genes under investigation. Initially 200 oxidative stress related genes were found and probe set numbers obtained for each gene were listed in an Excel worksheet, along with the gene name, aliases, reported function, and gene accession number.

However this thesis focussed on Antioxidant genes (n=39, Table 3.1) and in order to analyse these genes, the ‘analysis: projects’ option on the GeneSifter homepage was selected (Figure 2.2). The project of interest for analysis (e.g. resistant and responsive cells) was opened and its group information checked (Figure 2.6). As shown in Figure 2.6, this new project could then be used to analyse the desired genes via the ‘Analyze this project’ option and their Affymetrix probe set ID numbers.

To analyze the project (containing triplicate experimental arms) for antioxidant gene expression (Figure 2.7), Affymetrix probe set ID numbers for each of the oxidative stress related genes were placed in the identifiers box (*). If statistical analysis was required to compare two (or more) experimental arms in the group (e.g. Student t-test or ANOVA), these were selected in the “statistics” box in Figure 2.7. A search was then initiated and resultant heatmap diagram of relative gene expression produced, choosing to sort the results by relative expression (and significance). A sample Heatmap of a selection of antioxidant genes up regulated (red – representing at least 2 fold increase) and down regulated (green – representing at least 2 fold decrease) in TAMR or FASR cells versus w/t MCF7 cells (Black – for control) is shown in Figure 2.8. If statistical analysis was again required to compare two (or more) experimental arms in the group (e.g. Student t-test or ANOVA), these were selected in the “statistics” box in Figure 2.8. Each gene represented by a line on the resultant heatmap diagram had hyperlinks to information regarding that antioxidant gene and also the option to click for a graphical display of the mean

log intensity values (+/- SEM) profile for that gene across the analysed samples (Figure 2.9). The log intensity data were accompanied by likely absent (no or low expression), marginal or present (high expression) calls for the gene at the mRNA level for each replicate. Results of the statistical analyses, if selected, were also displayed enabling the identification of significant gene expression changes (Figure 2.8).

Of the 39 antioxidant genes investigated, 23 gene showed evidence of up-regulation across at least two forms of resistance and 15 genes were ANOVA significant and of potential interest for PCR verification. The strongest overall ontological and expression profiles (Results Tables 3.2 and 3.3), were designated by their present call at the RNA level, above described ontological selection, and heatmap significant patterns in resistance. Of the strong profiles chosen, 11 antioxidant genes were thus chosen for analysis by PCR.

2.2.2.6 Multiple probe analysis for antioxidant genes (quality control)

Of the 39 antioxidant genes investigated by project analysis, some (e.g. the antioxidant gene UDP glycosyltransferase 1 family polypeptide A6 [UGT1A6]) had up to 5 Affymetrix probe set representations on the array so that there was a total of 61 Affymetrix probe IDs representing the 39 genes under test. Using Genesifter, all probes for significant differentially expressed genes were examined to investigate if the multiple probes exhibited reproducible expression profiles using heatmaps. In the absence of known splice variants for these genes, such a finding would further re-enforce

confidence in the use of GeneSifter as a tool for robustly analysing expression data derived from Affymetrix HG-U133A chips (see Results section 3.2, Figure 3.8).

Figure 2.6 Details of Project selected in GeneSifter for expression analysis

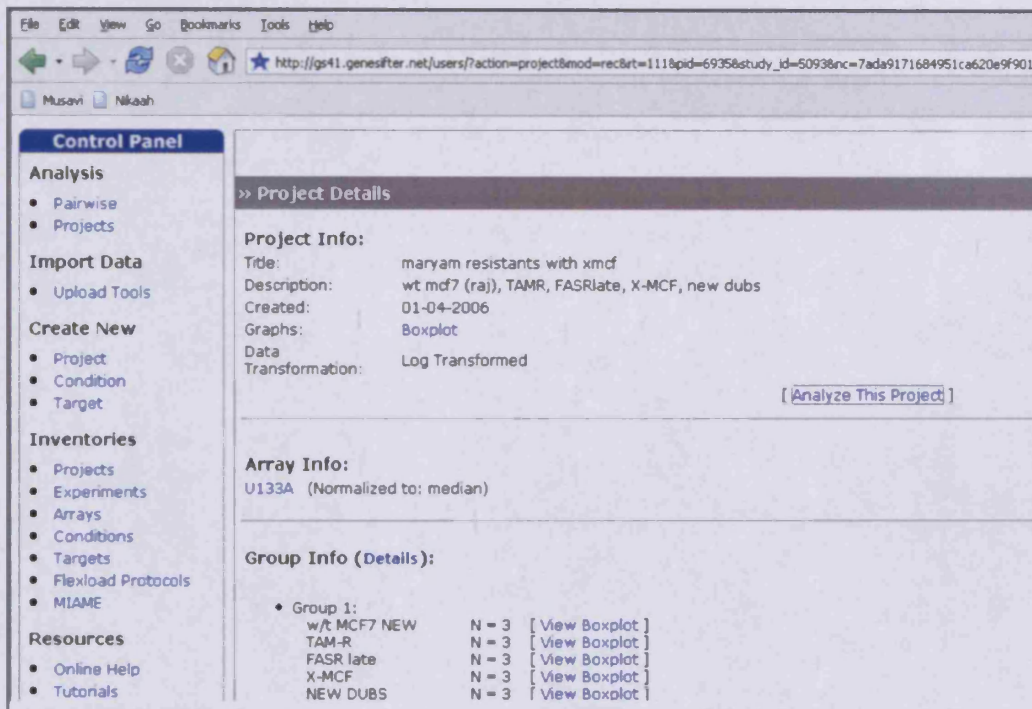


Figure 2.7 Expression analysis of genes of interest (using Affymetrix Probeset IDs entered in box *) in selected project

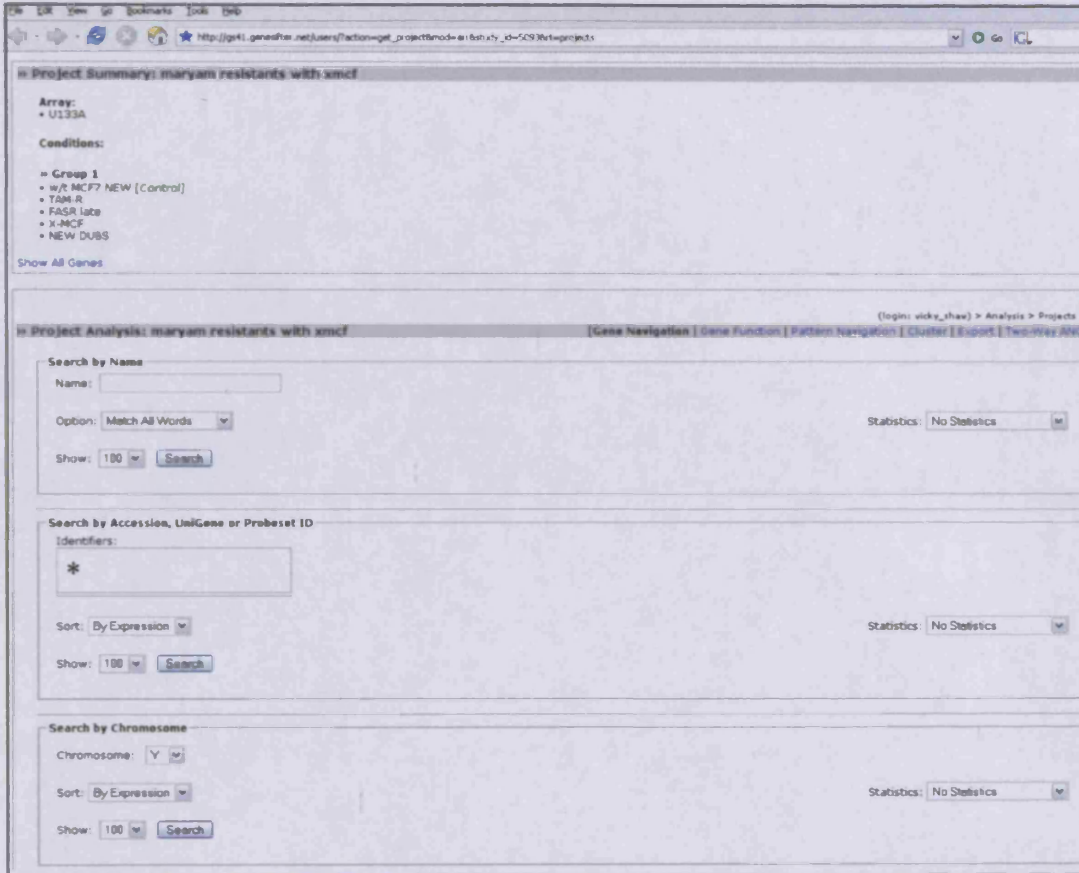


Figure 2.8 Resultant Heatmap of a selection of antioxidant genes

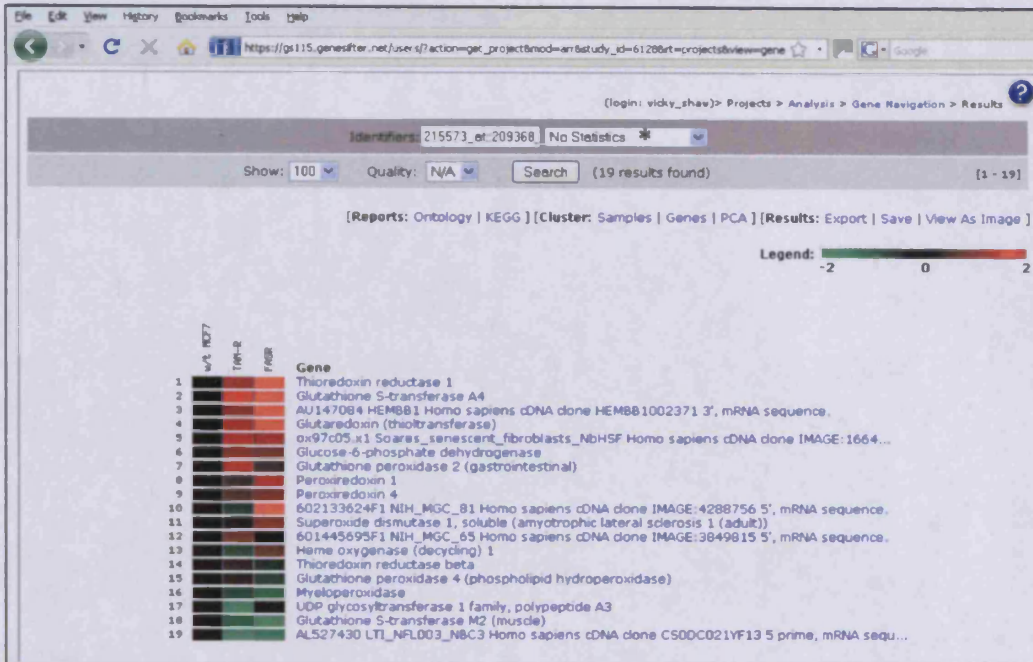
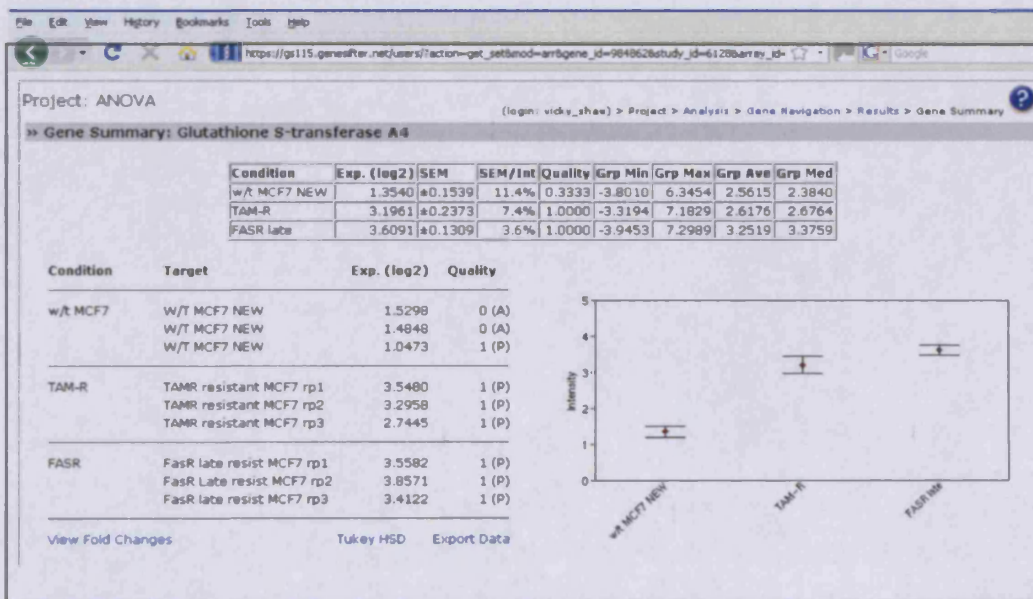


Figure 2.9 Intensity profile for each antioxidant gene from Heatmap



Log intensity profile for antioxidant gene GSTA4 is shown as an example where this gene is generally called absent (A) in w/t MCF7 cell preparations but significantly present (P) in TAMR and FASR cells.

2.3 RT-PCR studies of selected antioxidant gene expression

2.3.1 Materials

2.3.1.1 Cell culture reagents and plasticware for PCR studies

All plasticware and reagents employed for the initial generation of experimental material and RNA extraction from the w/t MCF7 cells and the acquired resistant, TAMR, FASR, MCF-7X and NEWDUBS models for PCR was as described above in section 2.2.

2.3.1.2 Enzymes and inhibitors

The enzyme Taq DNA polymerase, MMLV-Reverse Transcriptase, the RNasin[™] RNase inhibitor and dNTP mix was purchased from Invitrogen Ltd., Paisley, Scotland UK. Random hexamer oligonucleotide mix was purchased from Promega UK, Southampton, UK.

2.3.1.3 PCR reagents

All chemicals and buffers used in this RT-PCR investigation were purchased from Sigma-Aldrich Company Ltd, Poole, Dorset UK, unless otherwise stated. Dithiothreitol (DTT) and 10 x concentration of PCR buffer used in reverse transcription (RT) and the further polymerase chain reaction (PCR) reactions were purchased from Invitrogen Ltd., Paisley, Scotland UK. Molecular biology grade multipurpose agarose used for PCR gel electrophoresis was obtained from Bioline Ltd, Humber Road, London, UK. Standard size (range of 100bp

to 1000bp) DNA molecular weight marker (Hyperladder IV 100-Lanes) used to estimate nucleic acid was obtained from Bioline Ltd, Humber Road, London, UK. Large molecular weight β -actin Primers (380bp) were purchased from MWG Biotech AG, Anzinger Str.7, D-85560 Ebersberg, Germany. All other PCR primers used in this thesis were synthesised by Invitrogen Ltd., Paisley, Scotland UK.

2.3.1.4 Equipment

The PTC-100TM Programmable thermal controller (PCR machine) was purchased from MJ Research Global Medical Instrumentation, Inc., Bunker Lake Boulevard, Ramsey, Minnesota U.S.A. The microcentrifuge was purchased from Heraeus instruments, Inc., South Plainfield, NJ. The BioRad Power Pac p1000 and BioRad gel electrophoresis tank were purchased from BioRad Laboratories Ltd, Hemel Hempstead, Hertfordshire, UK. PCR products were photographed using an AlphaDigiDoc® RT Olympus camera, and images were obtained and analysed using the Alpha DigiDocTM computer software, all purchased from Alpha Innotech Corporation, Merced St., San Leandro, U.S.A.

2.3.2 Methodology

w/t MCF7, TAMR and FASR cells were seeded and cultured to log phase for RNA preparation as in section 2.2.2.1 in their respective experimental media. w/t MCF7 RNA preparations treated with oestradiol (10^{-9} M), tamoxifen (10^{-7} M), or faslodex (10^{-7} M) for 10days, and TAMR cells treated with gefitinib

(10^{-6} M) for 7days were also prepared following the same RNA preparation procedure as in section 2.2.2.1.

2.3.2.1 Polymerase Chain Reaction (PCR)

PCR is an *in vitro* method of nucleic acid synthesis by which a particular segment of deoxyribonucleic acid (DNA) can be specifically replicated for evaluation. This technique has become an increasingly useful tool in molecular biology for its inherent speed, simplicity, specificity, and sensitivity. Due to this sensitivity, all components of the PCR reaction are required to be ribonucleic acid (RNA) and DNase free, as any traces of such nucleases in the PCR reaction mixture would result in degradation of the RNA or DNA templates. All reagents for this technique were therefore prepared in RNA/DNase-free solutions. All plasticware and tips used was autoclaved before use in the PCR procedure. As skin is a major potential contaminant, gloves were worn at all time when handling any equipment or performing the experiment.

2.3.2.1.1 Reverse transcription (RT) of cDNA templates

PCR is used to amplify messenger RNA (mRNA) using the retroviral enzyme reverse transcriptase. mRNA sequences are transcribed by the enzyme into double stranded complimentary DNA (cDNA), a more stable form, in first strand cDNA synthesis. First strand cDNA was accomplished in this thesis using the method described by O'Brian et al., (1991). A typical RT reaction was performed in a total volume of 20 μ l in 10 x PCR buffer (10mM Tris-HCl

pH 8.3, 50mM KCl, 1.5mM MgCl₂ 0.001% w/v gelatine), and the reaction mixture comprised the following reagents made up in a 0.5ml microcentrifuge tube on ice:

Total RNA* (1µg/µl)	1µl
dNTP mix (0.625mM each of dCTP, dATP, dGTP, & dTTP)	5µl
Random hexamer oligonucleotide mix (100µM)	2µl
DTT (0.1M)	2µl
10x concentration of PCR buffer	<u>2µl</u>
Sterile nuclease free water to a final volume of	20µl

*Total RNA was from the various cell preparations generated as described in section 2.1.2.1

In order to check for contamination, a “minus RNA” sample was also included as a negative RT control. A denaturation step at 95°C for 5 minutes in a PTC-100™ Programmable Thermal Controller was initially performed in order to break up any aggregates or secondary RNA structures that could inhibit subsequent primer annealing. The reaction mixture was then rapidly cooled on ice for another 5 minutes followed by a pulse spin in a microfuge to collect the solution, and then placed back on ice. 10 Weiss units (1µl) of MMLV-Reverse Transcriptase and 25 Weiss units (0.5µl) of RNasin™ RNase inhibitor were added to the reaction. The PTC-100™ Programmable Thermal Controller was then used to perform the RT reaction using the following parameters:

incubation at room temperature for 10 minutes to facilitate primer annealing; heating to 42°C for 42 minutes as the RT extension time; and subsequent denaturing of samples at 95°C for 5 minutes that terminated the reaction by separating cDNA/RNA hybrids and inactivating the reverse transcriptase. The cDNA templates resulting from RT were rapidly cooled on ice for an additional 5 minutes and were either used immediately for PCR, or stored at -20°C until required.

2.3.2.1.2 Oligonucleotide primer design and PCR amplification from cDNA

The oligonucleotide primer pairs (Table 2.3) used for the PCR were designed manually from DNA sequences for the antioxidant genes of interest (master sequences were provided by Clontech®) using the web based package Primer3 (Rozen & Skaletsky, 2000), following the general guidelines listed in Table 2.2. 20µM primer stock solution was then prepared in nuclease free water for use in subsequent PCR reactions. Annealing conditions used subsequently for all primers was 60 seconds at 55°C, using variable cycle numbers following optimisation (to generate a robust, non-saturated, specific signal) as shown in Table 2.3. The cycle number to begin optimisation was chosen according to the likely abundance of the 11 antioxidant genes of interest subsequent to microarray analysis that generated expression call within the cell lines. The genes/sequences examined with product sizes, are presented in Table 2.3, including B-actin controls, and also pS2 primers for normalisation and quality control purposes respectively.

Table 2.2 General guidelines used for PCR Primer design

Parameter	General Guidelines
Length:	18–30 nucleotides
G/C content:	40–60%
Conc.:	0.1–0.5 μ M (0.2 μ M)
T_m :	Similar melting temperature (T_m) for both primer pairs $T_m = 2^\circ\text{C} \times (\text{A}+\text{T}) + 4^\circ\text{C} \times (\text{G}+\text{C})$ (Suggs et al., 1981)
Sequences:	Avoid a run of 3 or more G or C bases at the 3'-terminal as it may stabilise non-specific annealing of the primer, and avoid a T at the 3' end as it is more prone to mis-priming than other nucleotides (Kwok et al., 1990). Avoid mismatches between the 3' end and the target sequence, as well as avoiding complimentary sequences within and between primers that would reduce primer dimer formation (Sommer & Tautz, 1989; Kwok et al., 1990).

Table 2.3 Primer Sequences, expected product size and PCR cycle number

Primer	Sequences	Product Size	Optimised Cycle number
5' β -actin	5'-GGA GCA ATG ATC TTG ATC TT-3'	204bp	27
3' β -actin	5'-CCT TCC TGG GCA TGG AGT CCT-3'		
5' β -actin	5'-CTA CGT CGC CCT GGA CTT CGA GC-3'	380bp	27
3' β -actin	5'-GAT GGA GCC GCC GAT CCA CAC GG-3'		
5' pS2	5'-CATGGAGAACAAGGTGATCTG-3'	380bp	24
3' pS2	5'-CAGAAGCGTGTCTGAGGTGTC-3'		
5' CAT	5'-AGC TTA GCG TTC ATC CGT G-3'	220bp	30
3' CAT	5'-TCC AAT CAT CCG TCA AAA C-3'		
5' GLRX	5'-AAC GGT GCC TCG AGT CTT T-3'	180bp	36
3' GLRX	5'-CTT GGT GTA GGG GGC T-3'		
5' GPX2	5'-CAA GCG CCT CCT TAA AGT T-3'	380bp	30
3' GPX2	5'-GAG GGT TGG GAG AGG AAA A-3'		
5' GSTA4	5'-TCC GTG AGA TGG GTT TTA G-3'	200bp	30
3' GSTA4	5'-TGC CAA AGA GAT TGT GCT T-3'		
5' NQO1	5'-TTA CTA TGG GAT GGG GTC C-3'	250bp	24
3' NQO1	5'-TCT CCC ATT TTT CAG GCA A-3'		

Chapter 2 – Methodology

5' SOD1	5'-CGATGTGTCTATTGAAGATTCTGTG-3'	180bp	24
3' SOD1	5'-ACAGCTAGCAGGATAACAGATGAGT-3'		
5' PRDX1	5'-CAA CTG CCA AGT GAT TGG TG-3'	220bp	27
3' PRDX1	5'-TGA TCT GCC GAA GAA TAC CC-3'		
5' PRDX6	5'-CGT GTG GTG TTT GTT TTT GG-3'	350bp	24
3' PRDX6	5'-CTG ACA TCC TCT GGC TCA CA-3'		
5' TXN	5'-CTG CTT TTC AGG AAG CCT TG-3'	250bp	27
3' TXN	5'-ACC CAC CTT TTG TCC CTT CT-3'		
5' TXNRD1	5'-GGT CAC ACA AAG CTT C-3'	200bp	27
3' TXNRD1	5'-TCA GGG CCG TTC ATT T-3'		
5' TXNRD2	5'-AGCTTCAGGACAGAAAAGTCAAGTA-3'	200bp	27
3' TXNRD2	5'-GTCATCACTTGTGATTCCATATTCC-3'		

The PCR procedure carried out in this investigation was adopted from that developed for use in breast cancer cells by Knowlden et al., (1997). PCR for each gene was performed on cDNA templates, in the first instance using β -actin (204bp) primers to initially verify the recovery and check for any degradation of the RNA, as well as to verify sample-to-sample uniformity under RT-PCR conditions. For each PCR reaction 0.5 μ l of template DNA (i.e. 0.5 μ l of RT product) was added to the following reagents on ice in a 0.5ml microcentrifuge tube:

10x concentration of PCR buffer	2.5 μ l
dNTP mix (2.5mM stock)	2.0 μ l
5' Primer (20 μ M stock)	0.625 μ l
3' Primer (20 μ M stock)	0.625 μ l
Taq DNA polymerase (5 Weiss units/ μ l)	<u>0.2μl</u>
Sterile nuclease free water to a final volume of	25 μ l

A “minus cDNA” sample was also incubated as a negative PCR control. Assembled reactions were all amplified in a PTC-100TM Programmable thermal controller, the standard thermal cycling conditions of which are tabulated in Table 2.4. The optimised cycle number was varied according to the gene of interest (see Table 2.3) at the “Remaining Cycles” step in Table 2.4.

Table 2.4 Standard thermal cycling conditions for PCR

Cycle	Cycle conditions
Initial Cycle:	Cycle number 1
• Denaturation	2 minutes at 95°C
• Annealing	1 minutes at 55°C
• Extension	10 minutes at 72°C
Remaining Cycles:	Cycle number 24–36
• Denaturation	30 seconds at 94°C
• Annealing	1 minute at 55°C
• Extension	1 minute at 72°C
Final Cycle:	Cycle number 1
• Denaturation	1 minute at 94°C
• Annealing	1 minute at 55°C
• Extension	10 minutes at 60°C

2.3.2.1.3 *Visualisation of PCR Products*

Following PCR, the PCR products were analysed by size separation using 2% agarose gel electrophoresis and visualised using ethidium bromide (EtBr) staining of agarose gels under ultra violet (UV) light illumination. The β -actin product was also added to the appropriate wells for each gene sample to allow normalisation.

In order to prepare the 2% agarose gel, 2g of molecular biology grade multipurpose agarose was added to 100ml of 1 x Tris acetate buffer pH 8.3 (TAE) (made as a 50 x concentration stock using 242g/L Trizma® base, 57.1ml/L glacial acetic acid and 18.2g/L disodium salt EDTA). TAE containing the agarose was brought to the boil using a microwave oven, and left to cool before addition of 1 μ l of EtBr (5mg/ml stock) to the gel. The gel was then poured into a gel casting tray with the appropriate well former (20 μ l comb spaces) inserted at the top end. The gel was allowed to polymerise for at least 40 minutes on a flat surface before use. Once set, the gel was placed in a BIORAD electrophoresis tank filled with 1 x TAE. Samples were loaded using RNA loading buffer (containing 6g sucrose and 10ml distilled water filtered through a 0.2 μ M filter), loading each well with 3 μ l loading buffer, 3 μ l β -actin PCR product, and 11.5 μ l gene Primer PCR product, alongside a standard size molecular weight marker (Hyperladder IV 100-Lanes). The products on the gel were set to run at 70 volts for 40 minutes.

The PCR products were then visualised under UV and photographed using an AlphaDigiDoc® RT Olympus camera, and images obtained and analysed using Alpha DigiDoc™ computer software. Intensity of each band was estimated by the Alpha DigiDoc™ computer software, which normalised to β -actin signal. Results obtained were subsequently standardised to the control preparation for the experiment (e.g. in treated w/t MCF7 cells) and plotted onto a graph. Error bars were added according to standard deviation and statistical significance was measured using a two tailed Student T-test (p value considered significant <0.05).

Chapter 3 – Results

Antioxidants and Oxidative stress in Resistant and Responsive Breast Cancer Cells

3.1 Total Antioxidant Capacity (TAC) measured in ER+ Tamoxifen resistant versus Endocrine responsive MCF-7 breast cancer cells, and further antihormone and anti-EGFR resistant models

Recent literature indicates that an excess of antioxidants may be detrimental to the effectiveness of some chemotherapeutics in cancer which rely on the induction of ROS as part of their antitumour mechanism. As such, antioxidants released subsequent to chemotherapeutic-induced ROS can inevitably confer therapeutic resistance. Interestingly, blockade of such antioxidants can in turn enforce chemotherapeutic response (Spitz et al., 1993). The relationship between antioxidants and response and failure with antihormones remains largely unknown in breast cancer. Equally it remains unexplored in the context of growth factor inhibitor resistance, for example anti-erbB inhibitors (such as the anti-EGFR agent gefitinib) that are under evaluation in patients with breast cancer who have failed on endocrine therapy. Measurement of TAC in our antihormone resistant (and gefitinib resistant) breast cancer models could thus provide important biological information as to whether increased antioxidants may play a role in resistance to these various targeted therapies. In turn this could begin to determine if antioxidants may have relevance as a new therapeutic target to limit resistance.

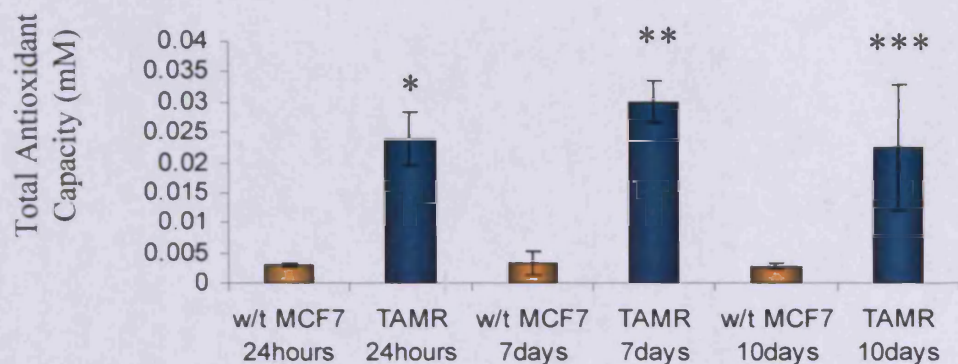
Basal measurement of TAC was first undertaken using an Antioxidant assay kit following 24 hours seeding down of tamoxifen resistant versus responsive

Chapter 3 – Results

cells. There was an elevated level of basal TAC within the TAMR cells, with a significant 12 fold increase in TAC ($p=0.005$) in comparison to the parental w/t MCF-7 models (Figure 3.1). Approximately 10 fold difference was maintained throughout the subsequent growth of these cell models for both 7 and 10 days with significantly increased TAC levels ($p=0.001$ and $p=0.0005$ respectively) versus w/t MCF7 cells (Figure 3.1).

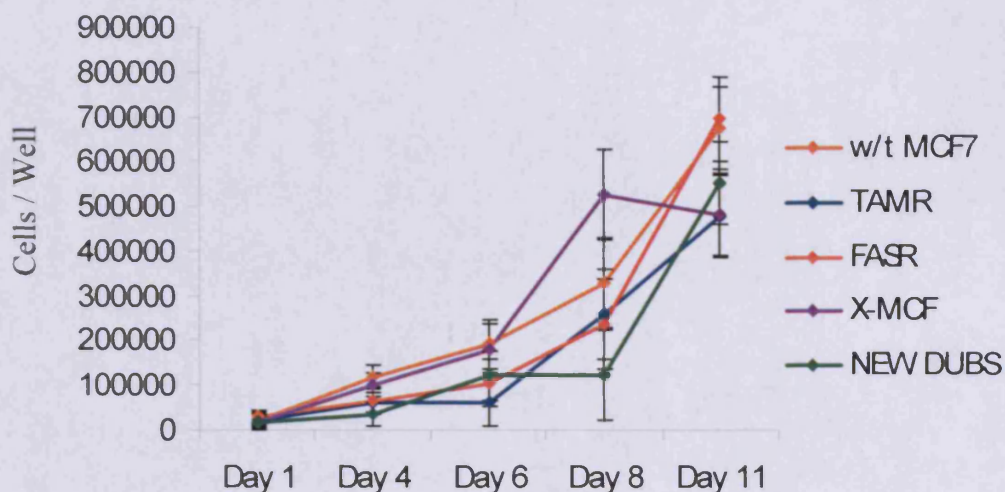
With the observation that significantly increased levels of TAC appeared to exist in the therapeutic resistant breast cancer model TAMR in comparison to the w/t MCF-7, it was explored whether this relationship extended to other antihormone resistant cells and also to the acquired tamoxifen and EGFR inhibitor resistant breast cancer model. These comprised the Faslodex resistant FASR cells, oestrogen deprivation resistant X-MCF cells and the tamoxifen and gefitinib resistant NEW DUBS model. Growth curve analysis of these models in their experimental media was performed in parallel in order to confirm that any increase in TAC detected in the various resistant models was not a result of increased proliferative capacity in the resistant cells (Figure 3.2). There was no significant difference in growth rate in any of the resistant models TAMR, FASR, X-MCF or NEW DUBS cells versus untreated w/t MCF7 cells (Figure 3.2).

Figure 3.1 Total Antioxidant Capacity examination of TAMR resistant model versus w/t MCF-7 cell line at 24 hours, 7 days and 10 days



Basal TAC levels in TAMR and w/t MCF-7 cells were measured using the Total Antioxidant Assay Kit from Sigma-Aldrich Company Ltd. The antioxidant assay measures the oxidation of the ABTS substrate to ABTS^{•+} which is a soluble green colour chromogen that can be detected spectrophotometrically at 405nm. Antioxidants naturally occurring within the cell suppress this reaction in a concentration dependent manner, with the colour intensity decreasing proportionally to the increased levels of antioxidants present. TAMR cells were tested against the parental MCF-7 cell line at 24 hours, 7 days and 10 days and were significant by Student T-test compared to the parental cells with * $p=0.005$, ** $p=0.001$, *** $p=0.0005$ respectively. These data represent a typical example of $n=3$ experiments \pm SD.

Figure 3.2 Growth curve for resistant models TAMR, FASR, X-MCF and NEW DUBS versus w/t MCF-7 cells



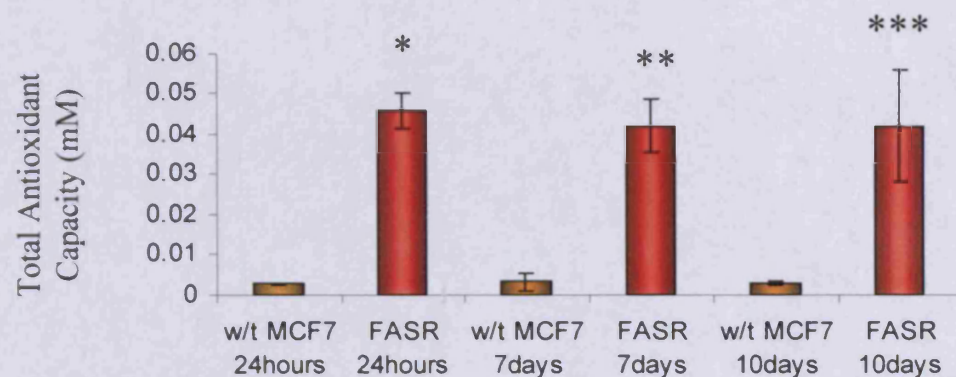
Cell models w/t MCF-7, TAMR, FASR, X-MCF, and NEW DUBS were grown in phenol red-free RPMI supplemented with 5% csFCS, penicillin/streptomycin (10iU/ml – 100µg/ml), fungizone (2.5100µg/ml), and glutamine (4mM) over 0-11days, counting wells at days 1,4,6,8 and 11 using a Beckman Coulter Counter Multisizer II. Cells were initially seeded at an equivalent density (4×10^4 cells/well) on 24 Well Corning Co-star plates. Significance was calculated using Student T-test (on day 8) compared to the control parental cells (w/t MCF7) with TAMR at $p=0.321$, FASR at $p=0.987$, X-MCF at $p=0.0558$ and NEW DUBS at $p=0.067$. These data represent a typical example of an experiment performed three times \pm SD.



Chapter 3 – Results

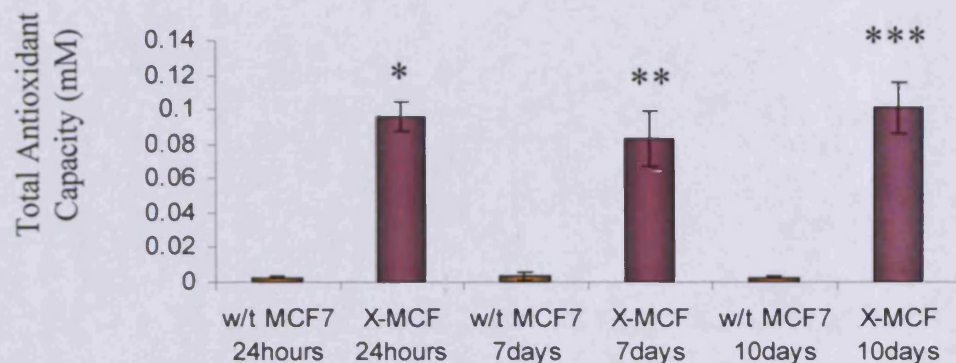
There was again, however, an increase in TAC in the FASR versus the w/t MCF-7 model. Indeed, the elevated level of TAC appeared even greater in FASR models, with differences of up to 22 fold increase shown at 24 hours and 21 fold increase at 7 and 10 days in comparison to the w/t MCF-7 ($p=0.0003$, $p=0.0006$ and $p=0.0005$ respectively) (Figure 3.3). In oestrogen deprived X-MCF cells, an even more prominent elevation of TAC was present with 50 fold difference shown in X-MCF models versus the w/t MCF-7 model by day 10 ($p=0.0006$) (Figure 3.4). This was again similar to the 24 hour and 7 day level, which gave a 48 fold and 40 fold increase respectively compared to the w/t MCF-7 models ($p=0.003$ and $p=0.01$ respectively) (Figure 3.4). When detection of TAC was extended to the tamoxifen and anti-EGFR inhibitor resistant model NEW DUBS, again significant upregulation of TAC was apparent (Figure 3.5). Thus there were significantly elevated levels of TAC present at 24 hours, 7 days and 10 days, which were at 14 fold, 11 fold, and 16 fold difference in comparison to the w/t MCF-7 model ($p=0.007$, $p=0.03$ and $p=0.0006$ respectively) (Figure 3.5).

Figure 3.3 Total Antioxidant Capacity examination of FASR resistant model versus w/t MCF-7 cell line at 24 hours, 7 days and 10 days.



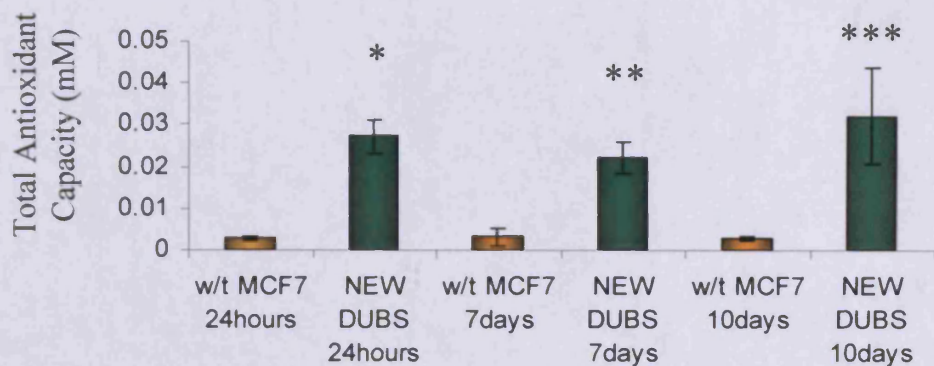
Basal TAC levels in FASR and w/t MCF-7 cells were measured using the Total Antioxidant Assay Kit from Sigma-Aldrich Company Ltd. FASR cells were tested against the parental MCF-7 cell line at 24 hours, 7 days and 10 days and were significant by student T-test compared to the parental cells with * $p=0.0003$, ** $p=0.006$, *** $p=0.0005$ respectively. These data represent a typical example of $n=3$ experiments \pm SD.

Figure 3.4 Total Antioxidant Capacity examination of X-MCF resistant model versus w/t MCF-7 cell line at 24 hours, 7 days and 10 days.



Basal TAC levels in X-MCF and w/t MCF-7 cells were measured using the Total Antioxidant Assay Kit from Sigma-Aldrich Company Ltd. X-MCF cells were tested against the parental MCF-7 cell line at 24 hours, 7 days and 10 days and were significant by student T-test compared to the parental cells with * $p=0.003$, ** $p=0.01$, *** $p=0.0006$ respectively. These data represent a typical example of $n=3$ experiments \pm SD.

Figure 3.5 Total Antioxidant Capacity examination of NEW DUBS resistant model versus w/t MCF-7 cell line at 24 hours, 7 days and 10 days.



Basal TAC levels in NEW DUBS and w/t MCF-7 cells were measured using the Total Antioxidant Assay Kit from Sigma-Aldrich Company Ltd. NEW DUBS cells were tested against the parental MCF-7 cell line at 24 hours, 7 days and 10 days and were significant by student T-test compared to the parental cells with * $p=0.007$, ** $p=0.03$, *** $p=0.0006$ respectively. These data represent a typical example of $n=3$ experiments \pm SD.

3.2 Affymetrix Microarray mRNA profiling to determine Antioxidant gene expression in antihormone resistance

Given that TAC increased in all the acquired resistant cell models, mRNA profiling of antioxidant (and other oxidative stress-related) genes was performed using Affymetrix HG-U133A microarray data available for these models. The web-based microarray data analysis software Genesifter™ was used to analyse and compare the expression data for the antioxidant genes derived from triplicate Affymetrix HG-U133A chips for each cell model. The project created for this investigation in GeneSifter was that of w/t MCF-7 cells as a control versus the various resistant cell lines i.e. TAMR, FASR, X-MCF, and NEW DUBS. For confidence in array performance prior to the antioxidant expression interrogation, the trefoil factor 1 (breast cancer, oestrogen-inducible sequence) or pS2 gene was initially profiled using heatmapping in GeneSifter to see if it exhibited the expression pattern already known for such models (Henry et al., 1991; Hutcheson et al., 2003; Staka et al., 2005) (Figure 3.6). On the heatmaps, green represented down regulated genes versus the w/t MCF-7 model, and red represented up regulation of the gene versus the w/t MCF-7 model, where black indicates no change. As expected, expression of the gene was down regulated in TAMR and FASR models versus w/t MCF-7 cells. Equally pS2 was up regulated in X-MCF and NEW DUBS models where there are known to be high levels of this ER regulated gene. These findings give confidence of the arrayed sample performance for subsequent antioxidant gene interrogation.

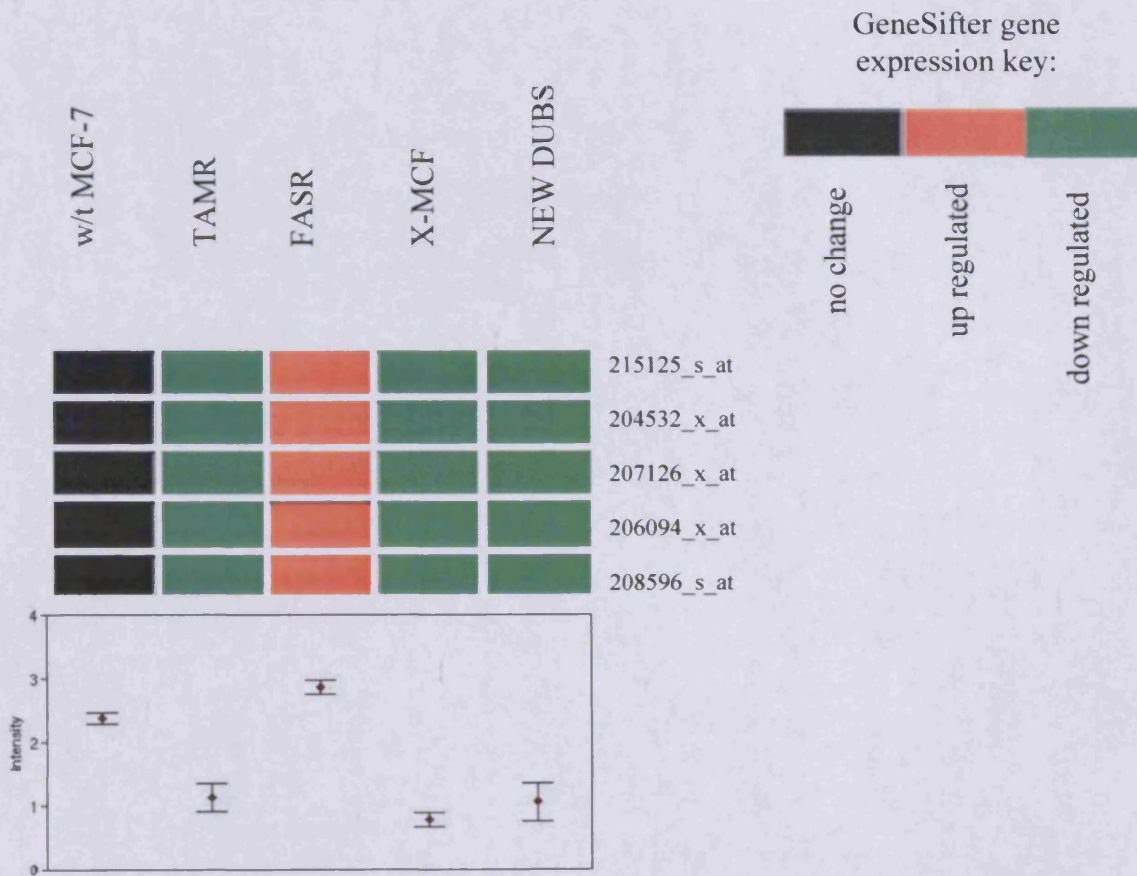
Figure 3.6 Trefoil Factor 1 or pS2 gene (Affymetrix probe no. 205009_at) expression heatmap profile from GeneSifter across acquired resistant versus responsive breast cancer models



3.2.1 GeneSifter analysis of antioxidant gene expression on the arrays

Initially through extensive literature search, 200 oxidative stress related genes were identified for study, 39 of which were antioxidant genes, comprising n=61 Affymetrix probes in total. Of note, analysis of individual genes and their multiple probes confirmed that multiple probes in general exhibited the same trend of expression across the cell models. For example, it was revealed that the multiple probes exhibited highly comparable expression profiles for the antioxidant gene UDP glycosyltransferase 1 family, polypeptide A6 (UGT1A6) (Figure 3.7a). The intensity of the colour red on the heatmaps indicated approximately the increase in expression of the gene for each model, where bright red indicated high expression and a dark red/brown shade was indicative of a more modest increase in expression versus the MCF-7 model (in black). The five probes of this gene exhibited down regulation in three resistant models and up regulation in the FASR cells only versus the w/t MCF-7 model, with small error bars from the triplicate results for each probe's log intensity plot (Figure 3.7b). This finding gave confidence in individual antioxidant probe profiles revealed by Genesifter, and thus in its potential usefulness as a tool for analysing expression data derived from Affymetrix HG-U133A chips for antioxidant genes.

Figure 3.7a GeneSifter heatmaps showing mRNA profiles for the multiple probes of the antioxidant gene UGT1A6 across acquired resistant versus responsive cell lines



(b) Log intensity profile of expression as shown by GeneSifter™ for representative probe no. 215125_s_at (mean +/- SEM) for gene UGT1A6

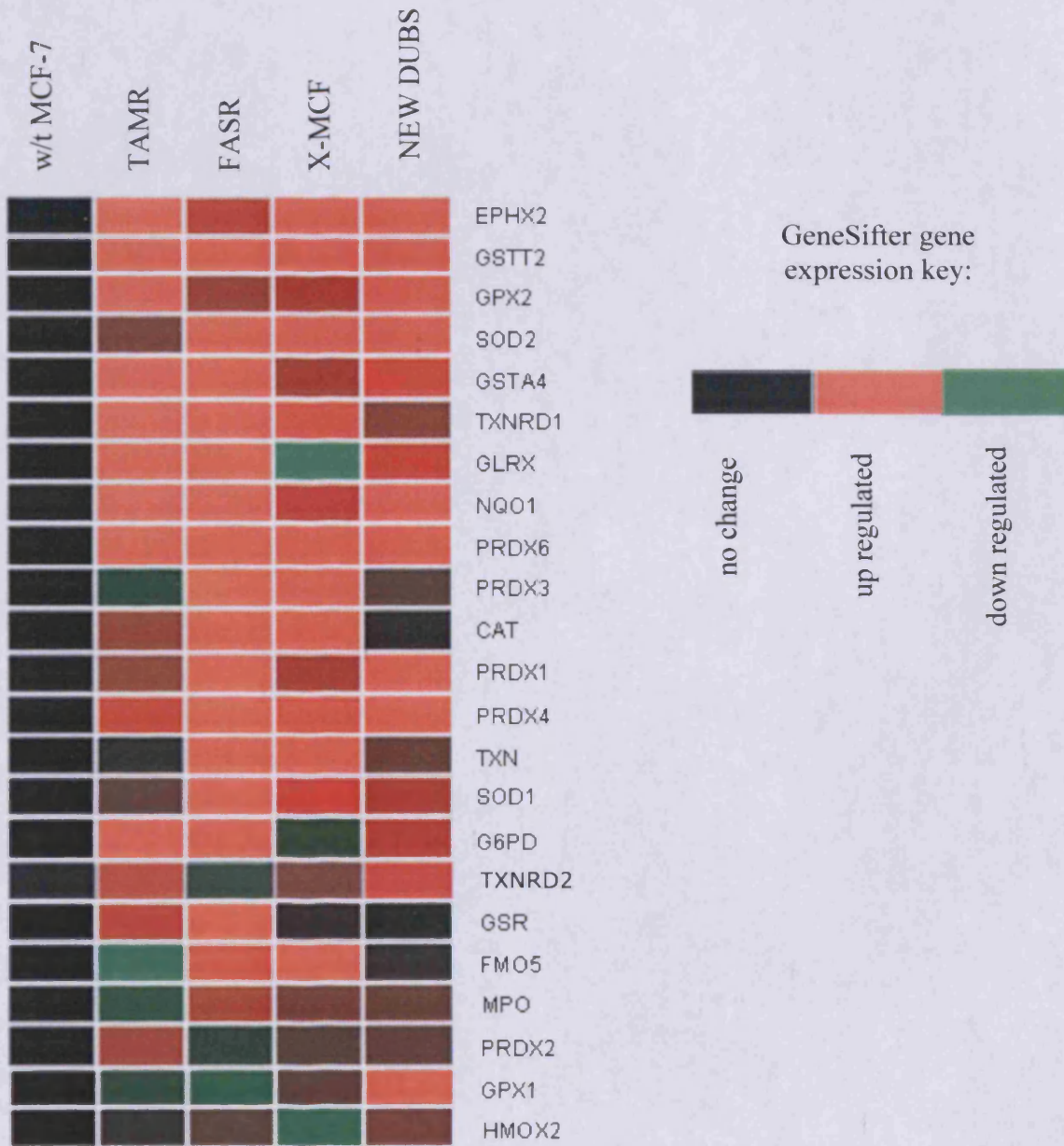
3.2.2 GeneSifter analysis of antioxidant gene category

As indicated above, of the 200 oxidative stress related genes originally collected, 39 genes were antioxidants that could potentially defend against pro-oxidant assaults on the cell. These 39 antioxidant genes which could have a potential role in contributing to therapeutic resistant growth are displayed in Table 3.1. In order to subsequently begin to find if any of these antioxidant genes are up regulated in two or more forms of resistance, GeneSifter heatmap profiles were initially examined across all the acquired endocrine and anti-EGFR resistant cell lines to monitor for any associated trends, examining for increases in resistant models TAMR, FASR, X-MCF, and NEW DUBS versus w/t MCF-7 cells. Of these 39 antioxidant genes, 59% (n=23 genes) showed up regulation to some degree in at least two forms of resistance in comparison to the w/t MCF-7 and their typical probe profiles are displayed in Figure 3.8. It was subsequently explored using statistical testing if any of these up regulated antioxidant genes were significantly-induced in the endocrine and anti-EGFR resistant models versus w/t MCF-7 cells. Testing using ANOVA across the cell lines showed that 15 of the antioxidant genes showed evidence of significant ($p < 0.05$) up regulation, and for these that the up regulation spanned at least two forms of resistance. Of these antioxidant genes, 9 displayed upregulation shared across all forms of antihormone and anti-EGFR resistance (Figure 3.9), with 6 antioxidant genes displaying upregulation in two or three forms of resistance (Figure 3.9). These GeneSifter profile findings are further clarified in the Venn diagram for the various models in Figure 3.10.

Table 3.1 Antioxidant genes (n=39) examined using GeneSifter

Alias	Name
AFAR3	Aldehyde reductase 3
CAT	Catalase
EPHX2	Epoxide hydrolase 2, cytoplasmic
EPX	Eosinophil peroxidase
FMO1	Flavin containing monooxygenase 1
FMO5	Flavin containing monooxygenase 5
G6PD	Glucose-6-phosphate dehydrogenase
GPX1	Glutathione peroxidase 1
GPX2	Glutathione peroxidase 2 (gastrointestinal)
GPX3	Glutathione peroxidase 3 (plasma)
GPX4	Glutathione peroxidase 4 (phospholipid hydroperoxidase)
GRX	Glutaredoxin (thioltransferase)
GSR	Glutathione reductase
GST2	Glutathione S-transferase A2
GSTA4	Glutathione S-transferase A4
GSTM1	Glutathione S-transferase M1
GSTM3	Glutathione S-transferase M3 (Brain)
GSTT2	Glutathione S-transferase theta 2
HMOX1	Heme oxygenase (decycling) 1
HMOX2	Heme oxygenase (decycling) 2
LPO	Lactoperoxidase
MGST1	Microsomal glutathione S-transferase 1
MPO	Myeloperoxidase
NQO1	NAD(P)H dehydrogenase, quinone 1
PON1	Paraoxonase 1
PRDX1	peroxiredoxin 1
PRDX2	peroxiredoxin 2
PRDX3	peroxiredoxin 3
PRDX4	peroxiredoxin 4
PRDX5	peroxiredoxin 5
PRDX6	peroxiredoxin 6
SOD1	Superoxide dismutase 1, soluble
SOD2	Superoxide dismutase 2, mitochondrial
SOD3	Superoxide dismutase 3, extracellular
TXN	Thioredoxin
TXN2	Thioredoxin 2
TXNRD1	Thioredoxin reductase 1
TXNRD2	Thioredoxin reductase 2
UGT1A6	UDP glucuronosyltransferase 1 family, peptide A6

Figure 3.8 GeneSifter heatmaps displaying mRNA expression profiles for 23 genes showing upregulation in at least 2 acquired resistant model versus w/t MCF-7 cells.



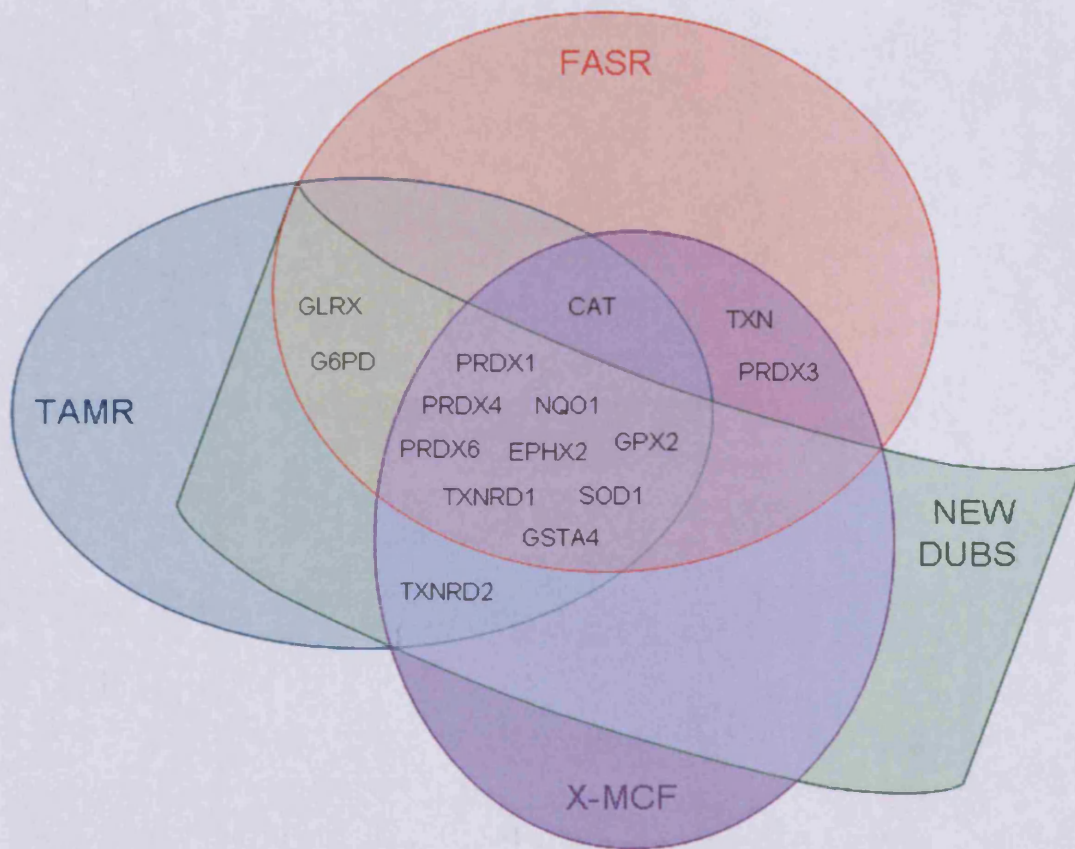
GeneSifter heatmap expression profiles were derived from Affymetrix HG-U133A chips for each cell model (from triplicate preparations). Of the 39 antioxidant genes, these 23 genes showed visual evidence on the heatmaps of up regulation (different shades of red/brown) in at least 2 resistant models versus w/t MCF-7 cells.

Figure 3.9 GeneSifter profile analysis for antioxidant genes with a significant increase in expression (ANOVA $p < 0.05$) in the resistant cell lines versus the w/t MCF-7 model (n=15)



Heatmaps were derived from Affymetrix HG-U133A chips for each cell model in triplicate using GeneSifter for these genes that were ANOVA significant. 9 genes show a trend of upregulation (different shades of red) across all resistant models, shown in yellow. The remaining 6 genes are shared by two or more forms of resistance versus the w/t MCF-7 model, shown in orange.

Figure 3.10 Venn diagram of patterns of up regulated antioxidant gene changes shared across multiple resistant models (ANOVA $p < 0.05$)



This four-way Venn diagram was designed to show the ANOVA significant upregulated antioxidant genes for each resistant model. Where resistant models overlap, the antioxidant genes were shared across those forms of resistance.

Chapter 3 – Results

Of the 15 antioxidant genes that showed evidence of up-regulation across at least two forms of resistant models, the 9 genes shared by all forms of resistance were PRDX6, PRDX1, PRDX4, NQO1, EPHX2, GPX2, GSTA4, TXNRD1, and SOD1 (Figure 3.9 and 3.10). In addition, GLRX, and G6PD were upregulated in TAMR cells, FASR cells, and NEW DUBS models. CAT is upregulated in TAMR cells, FASR cells, and X-MCF models. TXN and PRDX3 antioxidant genes are upregulated in FASR and X-MCF models, and the antioxidant gene TXNRD2 is upregulated in TAMR cells, NEW DUBS and X-MCF models (Figure 3.9 and 3.10). Although there were also genes that were upregulated specific to individual forms of resistance, they are not the main focus of this thesis since they are unlikely to contribute to a generic resistance mechanism, and are therefore not displayed in Figures 3.9 and 3.10.

Along with expression increases in multiple forms of resistance, to select the final resistant antioxidant gene-set for further investigation by PCR verification priority was also given to genes that were linked together in specific pathways. This included the antioxidant networks of the PRDX family that regulates intracellular H_2O_2 , and TXN, TXNRD1, TXNRD2 that can react with oxygen free radicals and help to replenish depleted PRDX that can be inactivated upon over-oxidation by H_2O_2 (GeneCards™). Not all genes of the PRDX family were chosen as two were considered to suffice to examine if there was a trend of involvement for this pathway. Both PRDX1 and PRDX4 were very similar in expression profile, therefore only PRDX1 was chosen for further analysis. PRDX6 was upregulated significantly (T-test $p < 0.05$) across all resistant

Chapter 3 – Results

models, and was therefore chosen above PRDX3 that was induced in only two forms of resistance and only T-test significantly up regulated in FASR cells.

Montano et al. had previously reported that anti-oestrogens could activate NQO1 that can protect cells against the toxic and tumour promoting effects of carcinogens in early onset of disease (Montano et al., 2005). NQO1 was of interest since it would be of value to see if this protection also extended to promotion of growth in multiple resistant states. GLRX, GSTA4 and GPX2 are all glutathione dependant antioxidant genes, although each have their own unique redox function within the cell. With the availability of a glutathione inhibitor, buthionine sulfoximine (BSO), all these genes in the glutathione network were thus deemed important for further verification by PCR to try to determine if there is an importance of glutathione in resistance. SOD1 and CAT are also high priority for verification by PCR since they not only conveyed a strong profile but also comprise a common first line defence against ROS, whereby SOD1 destroys intracellular free radicals and CAT protects against toxic effects of the peroxides formed within the cell. EPHX2 mainly targets xenobiotics and G6PD plays a more important role in the pentose phosphate pathways and therefore were deemed ontologically of less interest at this stage of the investigation in the context of progression to antioxidant verification at the mRNA level.

The 15 shared antioxidant genes of potential interest for PCR verification were also further analysed using GeneSifter software capabilities and also intensity

Chapter 3 – Results

profiles, along with literature searches (including available inhibitors for further future study), in order to compile comprehensive data for each “shared” gene as presented in Table 3.2, and for genes up regulated in two or three forms of resistance in Table 3.3. Along with intensity profiles, GeneSifter also reported likely mRNA expression level for each gene from the Affymetrix data. These “present” (high expression), “absent” (low/no expression) and “marginal” calls indicated relative expression abundance. Individual models in which the increase of expression reached levels that were also T-test significant versus w/t MCF-7 cells ($p < 0.05$), across triplicate cell preparations for each model were also noted. In addition, it was noted by examination of the w/t MCF7 Affymetrix database that some of the genes were also induced early by 10 day tamoxifen and/or faslodex treatment, while others were potentially unique to acquired resistance (Table 3.2 and 3.3)

The strongest overall ontological and expression profiles in Tables 3.2 and 3.3, were designated by their present call at the RNA level, above described antioxidant pathway and ontological selection, and heatmap significant patterns in resistance. 11 antioxidant genes were thus chosen for analysis by PCR with a strong overall profile.

Table 3.2 ANOVA Significant antioxidant genes (n=9) with expression profiles upregulated in all resistant models

Gene name	Call at mRNA level	T-test Significance	Antihormonal up-regulation in w/t MCF7 cells	Drugs to target mechanistic link	Ontological and Drug Reference	Overall Strong profile
PRDX1	Present	FASR X-MCF NEW DUBS	Anti-hormone induced	AW464	Wells et al., 2003; Berry et al., 2005	✓
PRDX4	Present	FASR X-MCF NEW DUBS	Anti-hormone induced	AW464	Wells et al., 2003; Berry et al., 2005	
PRDX6	Present	All models	Specific to resistance	AW464	Wells et al., 2003; Berry et al., 2005	✓
NQO1	Present	TAMR FASR NEW DUBS	Anti-hormone induced	dicoumarol	Lien et al., 2008	✓
EPHX2	Absent	X-MCF NEW DUBS	Anti-hormone induced	AUDA	Motoki et al., 2008	
TXNRD1	Present	TAMR FASR	TAM and FAS anti-hormone induced	PX-916	Powis et al., 2006	✓
GPX2	Mixed present & Absent	TAMR NEW DUBS	Specific to resistance	BSO	Lewis-Wambi et al., 2009	✓
SOD1	Present	FASR X-MCF	Anti-hormone induced	Disulfiram (DSF)	Marikovskiy et al., 2003	✓
GSTA4	Present	TAMR FASR NEW DUBS	TAM and FAS anti-hormone induced	BSO	Lewis-Wambi et al., 2009	✓

Table 3.3 ANOVA significant antioxidant genes (n=6) with expression profiles upregulated in two or three forms of resistance

Gene name	Call at mRNA level	T-test Significance	Antihormonal up-regulation in w/t MCF7 cells	Drugs to target mechanistic link	Ontological and Drug Reference	Overall Strong profile
GLRX	Mixed present & absent	TAMR FASR	FAS anti-hormone induced	BSO	Lewis-Wambi et al., 2009	✓
G6PD	Present	TAMR only	Specific to resistance	DHEA	Okouchi et al., 2005	
CAT	Mixed present & Absent	FASR X-MCF	Specific to resistance	Copper sulfate, 3-amino-1,2,4-triazole	Margollash & Novogradsky, 1958	✓
TXN	Present	FASR X-MCF	Specific to resistance	AW464	Wells et al., 2003; Berry et al., 2005	✓
PRDX3	Present	FASR only	Specific to resistance	AW464	Wells et al., 2003; Berry et al., 2005	
TXNRD2	Present	TAMR NEW DUBS	Specific to resistance	1-Chloro-2,4-dinitrobenzene	Arnér et al., 1995	✓

3.3 PCR Verification studies for the 11 induced Antioxidant genes increased in resistance

The 11 antioxidant genes PRDX1, PRDX6, TXN, TXNRD1, TXNRD2, GPX2, GSTA4, GLRX, NQO1, SOD1, and CAT were chosen for verification by PCR in triplicate mRNA preparations from resistant cells, focusing on TAMR and FASR cells, versus the parental w/t MCF-7 model. An RNA free sample was also run as a negative control and this always failed to give a spurious signal. Densitometric results obtained for each model were subsequently normalised to β actin expression, and presented graphically in relation to the w/t MCF7 model. Statistical analysis was performed for each resistant model against the w/t MCF7 model using a Student's paired t-Test. Again for confidence in PCR and the mRNA samples, the trefoil factor 1 (pS2) gene was first examined in these mRNA samples to see if it exhibited the expression change that would be expected (Figure 3.11), where the additional use of 10 day oestradiol (E_2 (10-9M)) – treated w/t MCF7 cell mRNA samples confirmed this is behaving as an E_2 – regulated gene in this system. As in Affymetrix, small but significantly detectable decreases were shown in TAMR and FASR respectively versus w/t MCF7 cells, with the expected significant E_2 increase in expression.

The following genes were readily detectable, in keeping with the “present” call by Affymetrix (Tables 3.2 and 3.3): (i) GSTA4 – The antioxidant gene GSTA4 was shown by microarray gene analysis profiling to be up regulated across all forms of resistance, with particular significance (by t-Test) in TAMR

Chapter 3 – Results

and FASR cells (Figure 3.12). PCR verified this, with over a 50% significant increase in mRNA expression achieved in the TAMR model ($p = 0.012$), and FASR models ($p = 0.047$) versus the w/t MCF7 model (Figure 3.12). (ii) TXNRD1 – the antioxidant gene TXNRD1 had been shown by gene analysis profiling to be up regulated across all forms of resistance, again with particular significance (by t-Test) in TAMR and FASR cells. Again, PCR verified these increases in TAMR and FASR cells increasing approximately 80% in both models ($p = 0.028$ and $p = 0.033$ respectively, Figure 3.13). (iii) NQO1 – the antioxidant gene NQO1 had also been shown by gene analysis profiling to be a resistant gene significantly up regulated in both TAMR and FASR models (Figure 3.14). However, mRNA analysis by PCR was only able to confirm a significant (t-Test) elevation of NQO1 expression in TAMR cells with a substantial (over 100%) increase in expression versus w/t MCF7 cells ($p = 0.02$) (Figure 3.14).

(iv) GLRX – equating with its mixed present and absent call at mRNA level using Affymetrix, GLRX required a higher PCR cycle number of 36. Affymetrix analysis for GLRX also showed higher expression levels of this resistant gene particularly in TAMR and FASR models. PCR analysis verified these gene changes, with over 50% increase shown in the TAMR model ($p=0.006$) and over 80% increase in GLRX shown in the FASR model ($p=0.037$) versus w/t MCF7 cells (Figure 3.15).

(v) CAT – Again like GLRX, equating with its mixed present and absent call at mRNA level using Affymetrix, CAT required a higher PCR cycle number of 30 cycles. The antioxidant gene CAT had again been shown by gene analysis profiling to be up regulated in all endocrine resistant models with particular significance in the FASR model (Figure 3.16). mRNA analysis by PCR was able to detect a small yet significant (t-Test) increase in CAT expression of 20% in TAMR models ($p=0.049$) and over 40% increase in FASR models ($p=0.016$) consistent with the Affymetrix profile obtained for that gene (Figure 3.16).

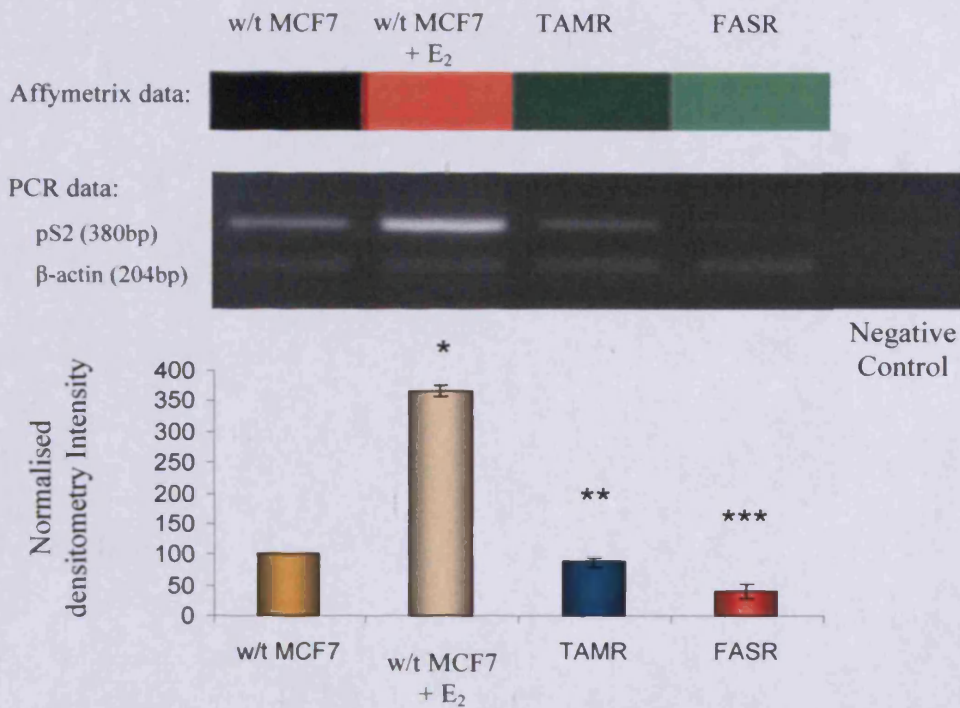
(vi) TXN – This gene was more easily detectable, in agreement with the present call by Affymetrix using 27 cycles for PCR. TXN was shown by Genesifter log intensity profiles to be a resistance gene significantly (by t-Test) up regulated in FASR (and in X-MCF model not displayed here). PCR analysis of mRNA expression was able to reveal significant increase in FASR expression by 80% ($p=0.028$), and also suggested this could extend to TAMR cells with over 70% increase ($p=0.015$) in comparison to w/t MCF7 control (Figure 3.17).

(vii) TXNRD2 was a resistant gene giving a present call equating with a lower cycle number of 27 cycles. It was shown to be slightly upregulated in TAMR models but down regulated in FASR model (in contrast to other resistant models) by Affymetrix gene analysis. This profile was verified by PCR, with a

50% increase in TAMR models ($p=0.042$) and over 30% decrease in FASR cells ($p=0.042$) versus w/t MCF7 cells (Figure 3.18).

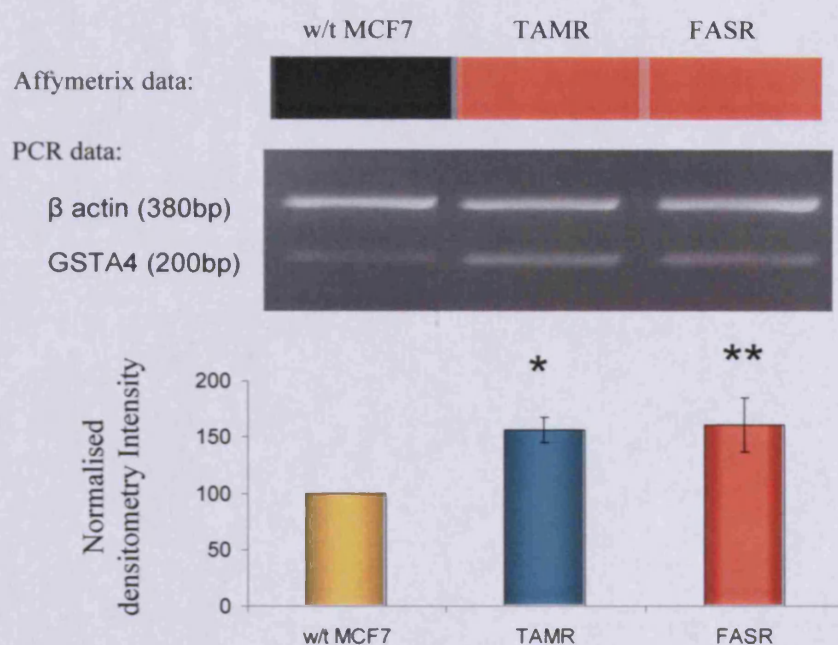
(viii) GPX2 had been shown by gene analysis profiling to be up regulated to some degree in all resistant models, with particular significance in the TAMR model (Figure 3.19). However, with a mixed present and absent call at mRNA level and thus 30 PCR cycles required, mRNA analysis by PCR was only able to detect the significant (t-Test) increase in the TAMR model with over 300% up regulation compared to the w/t MCF7 model ($p=0.0009$), and no significant increase in FASR cells (Figure 3.19). Although the remaining SOD1, PRDX1 and PRDX6 called present and showed upregulation by Affymetrix gene analysis in the resistant models, PCR results detected expression but failed to verify the increases in antioxidant genes' mRNA expression in both TAMR and FASR models versus w/t MCF7 cells (Figures 3.20). There was thus some evidence of upregulation in resistance by both Affymetrix and PCR for 8 out of the 11 genes, with GSTA4, TXNRD1, GLRX, CAT, and TXN proving to be “shared” genes upregulated in both TAMR and FASR cells.

Figure 3.11 Verification of PCR samples (versus Affymetrix heatmap data) for TAMR and FASR samples versus the w/t MCF7 model (and oestradiol treated w/t MCF7 cells) by monitoring the Trefoil Factor 1 gene (pS2)



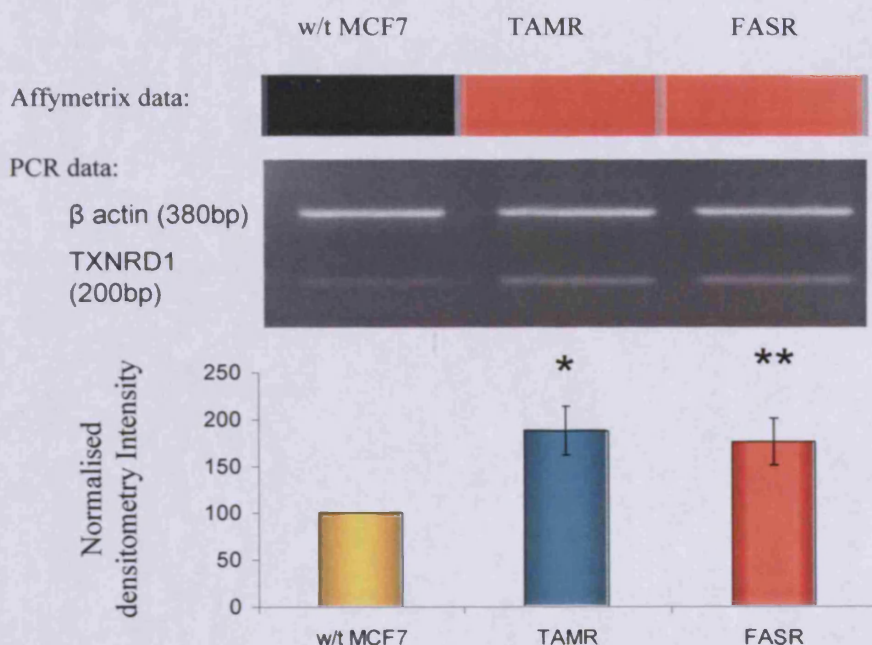
Affymetrix profile data were obtained using GeneSifter heatmaps for w/t MCF7 cells treated with 10^{-9} M E₂, TAMR and FASR models versus w/t MCF7 cells for pS2. These intensity changes were verified by PCR analysis and the mean expression \pm SD are displayed in a histogram as shown above. Normalised PCR densitometry results were represented relative to 100% for w/t MCF7 cells for the E₂ treatment, TAMR and FASR cells and these were statistically significant using a Student T-test (* $p=0.004$, ** $p=0.022$, and *** $p=0.015$ respectively) using triplicate preparations versus untreated w/t MCF7 cells. The same analysis approach was carried out in resistant models versus w/t MCF7 cells for all antioxidant genes in the following Figures (3.12 – 3.20)

Figure 3.12 PCR profile for GSTA4 gene (versus Affymetrix heatmap data) in TAMR and FASR cell lines versus w/t MCF-7 cells



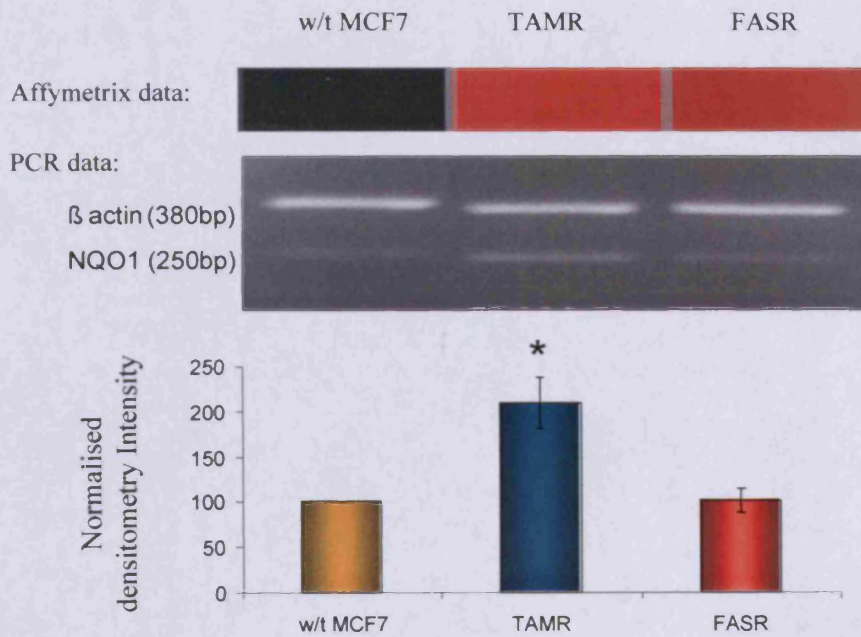
Affymetrix profile data were obtained using GeneSifter heatmaps for TAMR and FASR models versus w/t MCF7 (day 7) cells for GSTA4. These expression changes were verified by PCR analysis and the mean \pm SD are displayed in a histogram as shown above. Normalised PCR densitometry results were represented relative to 100% for w/t MCF7 cells for TAMR and FASR cells and these were statistically significant using a Student T-test (* $p=0.012$ and ** $p=0.047$ respectively) using triplicate preparations.

Figure 3.13 PCR profile for TXNRD1 gene (versus Affymetrix heatmap data) in TAMR and FASR cell lines versus w/t MCF-7 cells



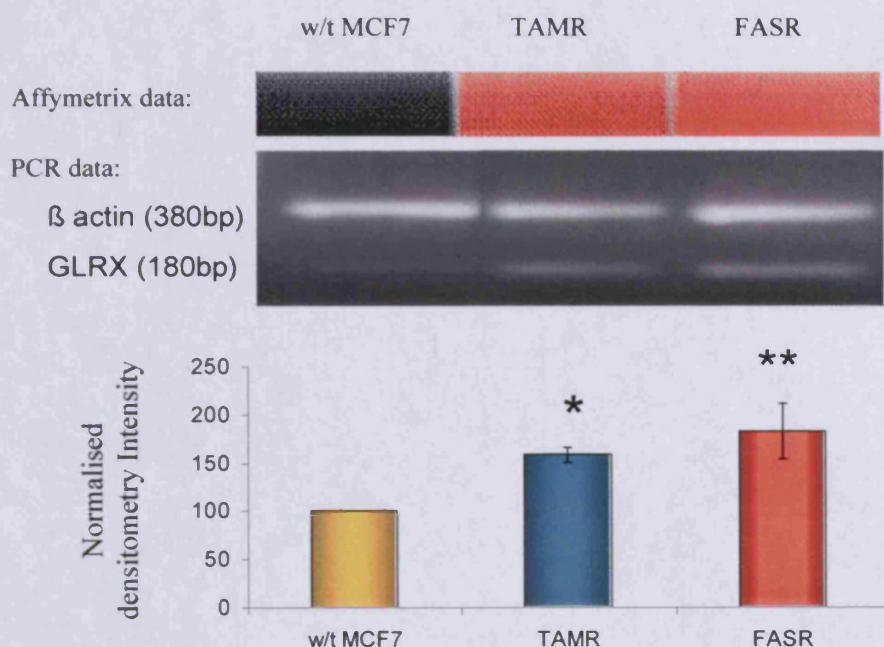
Affymetrix profile data were obtained using GeneSifter heatmaps for TAMR and FASR models versus w/t MCF7 (day 7) cells for TXNRD1. These expression changes were verified by PCR analysis and the mean \pm SD are displayed in a histogram as shown above. Normalised PCR densitometry results were represented relative to 100% for w/t MCF7 cells for TAMR and FASR cells and these were statistically significant using a Student T-test (* $p=0.028$ and ** $p=0.033$ respectively) using triplicate preparations.

Figure 3.14 PCR profile for NQO1 (versus Affymetrix heatmap data) in TAMR and FASR cell lines versus w/t MCF-7 cells



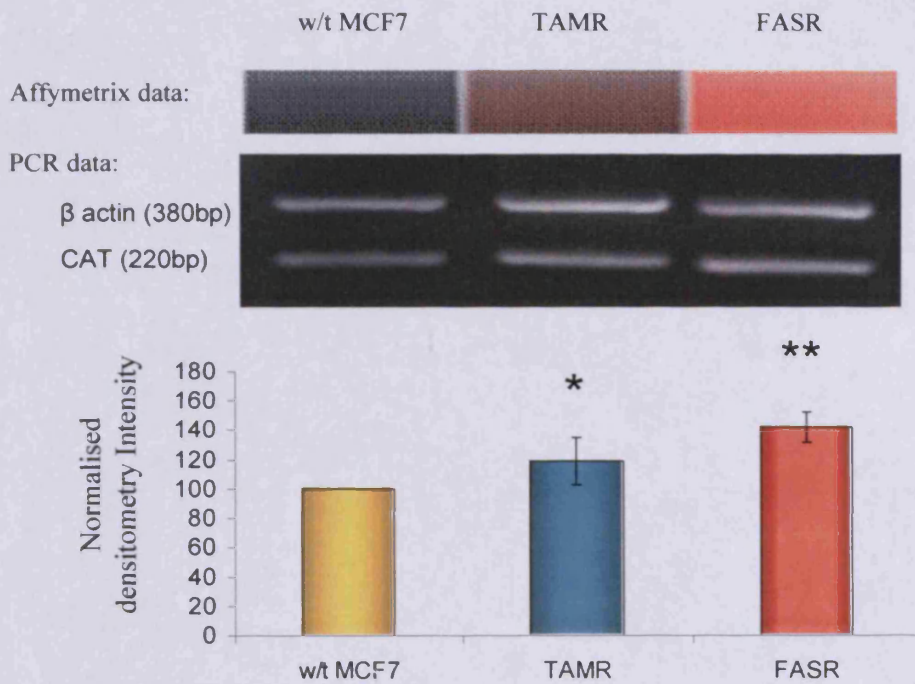
Affymetrix profile data were obtained using GeneSifter heatmaps for TAMR and FASR models versus w/t MCF7 (day 7) cells for NQO1. These expression changes were verified by PCR analysis and the mean \pm SD are displayed in a histogram as shown above. Normalised PCR densitometry results were represented relative to 100% for w/t MCF7 cells for TAMR and FASR cells and only TAMR cells were statistically significant using a Student T-test (* $p=0.02$) using triplicate preparations.

Figure 3.15 PCR profile for GLRX gene (versus Affymetrix heatmap data) in TAMR and FASR cell lines versus w/t MCF-7 cells



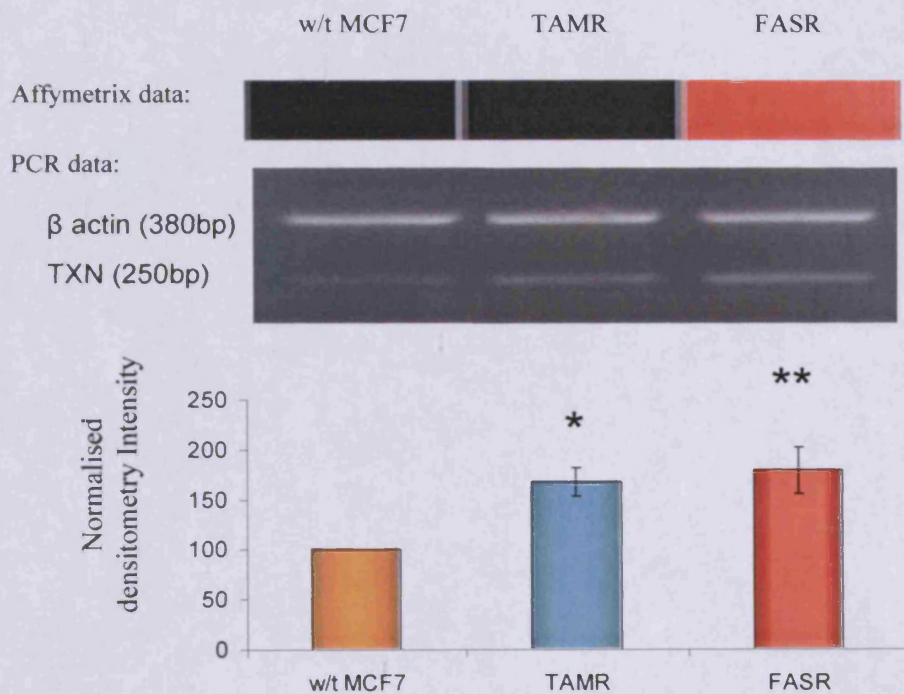
Affymetrix profile data were obtained using GeneSifter heatmaps for TAMR and FASR models versus w/t MCF7 (day 7) cells for GLRX. These expression changes were verified by PCR analysis and the mean \pm SD are displayed in a histogram as shown above. Normalised PCR densitometry results were represented relative to 100% for w/t MCF7 cells for TAMR and FASR cells and these were statistically significant using a Student T-test (* $p=0.006$ and ** $p=0.037$ respectively) using triplicate preparations.

Figure 3.16 PCR profile for CAT gene (versus Affymetrix heatmap data) in TAMR and FASR cell lines versus w/t MCF-7 cells



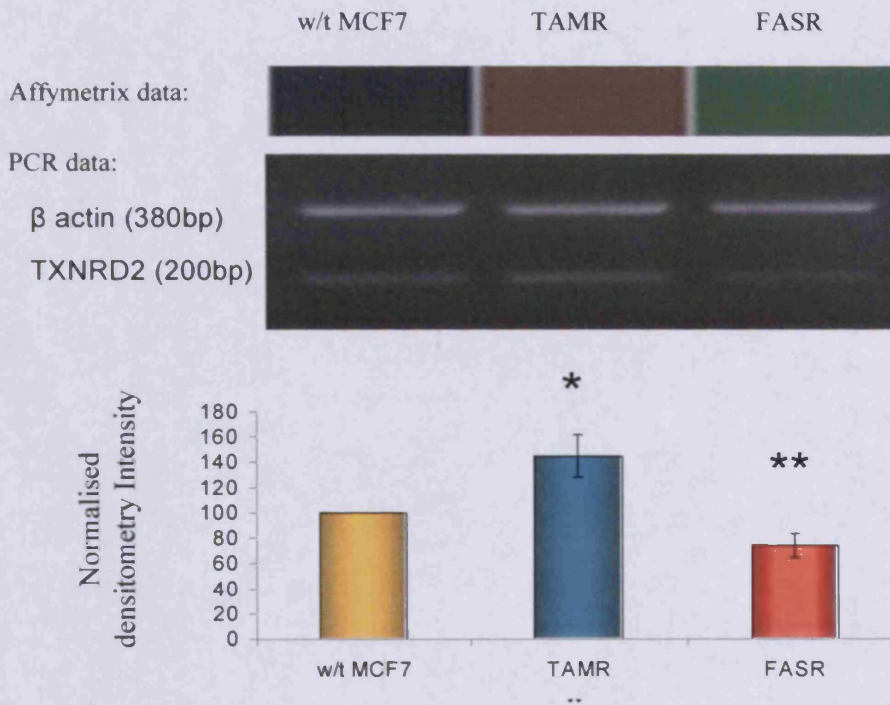
Affymetrix profile data were obtained using GeneSifter heatmaps for TAMR and FASR models versus w/t MCF7 (day 7) cells for CAT. These expression changes were verified by PCR analysis and the mean \pm SD are displayed in a histogram as shown above. Normalised PCR densitometry results were represented relative to 100% for w/t MCF7 cells for TAMR and FASR cells and these were statistically significant using a Student T-test (* $p=0.049$ and ** $p=0.016$ respectively) using triplicate preparations.

Figure 3.17 PCR profile for TXN gene (versus Affymetrix heatmap data) in TAMR and FASR cell lines versus w/t MCF-7 cells



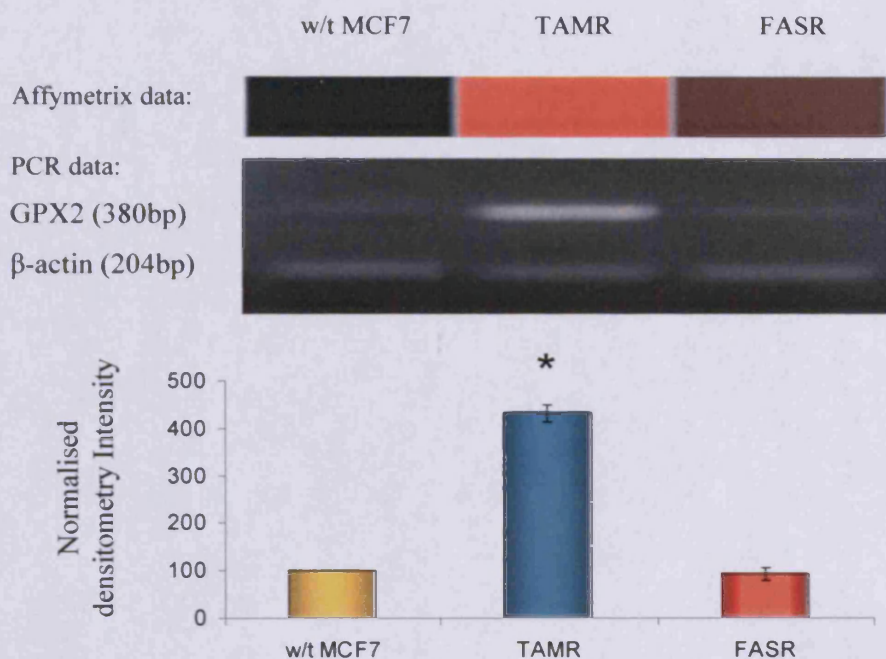
Affymetrix profile data were obtained using GeneSifter heatmaps for TAMR and FASR models versus w/t MCF7 (day 7) cells for TXN. These expression changes were verified by PCR analysis and the mean \pm SD are displayed in a histogram as shown above. Normalised PCR densitometry results were represented relative to 100% for w/t MCF7 cells for TAMR and FASR cells and these were statistically significant using a Student T-test (* $p=0.015$ and ** $p=0.028$ respectively) using triplicate preparations.

Figure 3.18 PCR profile for TXNRD2 gene (versus Affymetrix heatmap data) in TAMR and FASR cell lines versus w/t MCF-7 cells



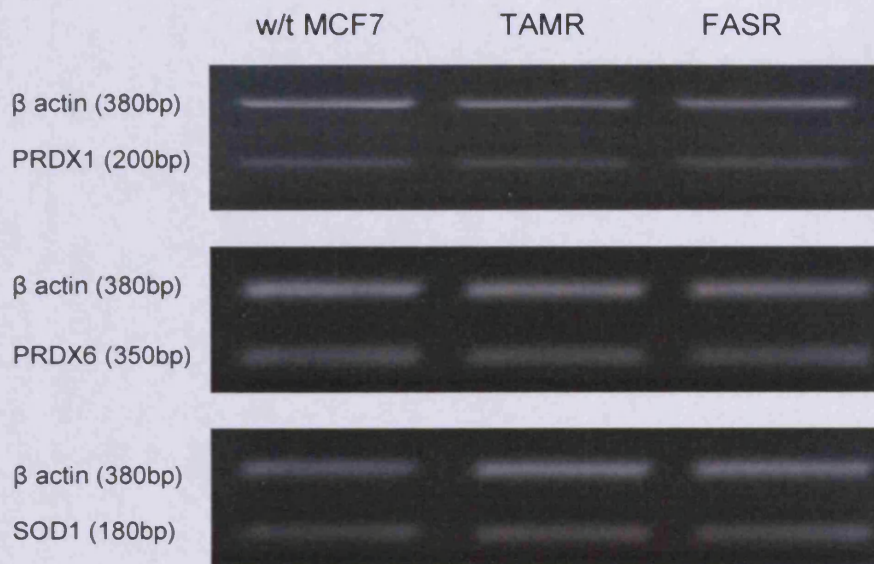
Affymetrix profile data were obtained using GeneSifter heatmaps for TAMR and FASR models versus w/t MCF7 (day 7) cells for TXNRD2. These expression changes were verified by PCR analysis and the mean \pm SD are displayed in a histogram as shown above. Normalised PCR densitometry results were represented relative to 100% for w/t MCF7 cells for TAMR and FASR cells and these were statistically significant using a Student T-test (* $p=0.042$ and ** $p=0.042$ respectively) using triplicate preparations, TAMR expression increasing and FASR expression decreasing respectively.

Figure 3.19 PCR profile for GPX2 gene (versus Affymetrix heatmap data) in TAMR and FASR cell lines versus w/t MCF-7 cells



Affymetrix profile data were obtained using GeneSifter heatmaps for TAMR and FASR models versus w/t MCF7 (day 7) cells for GPX2. These expression changes were verified by PCR analysis and the mean \pm SD are displayed in a histogram as shown above. Normalised PCR densitometry results were represented relative to 100% for w/t MCF7 cells for TAMR and FASR cells and these were only statistically significant in TAMR cells using a Student T-test (* $p=0.0009$) using triplicate preparations.

Figure 3.20 PCR profile for PRDX1, PRDX6, and SOD1 genes in TAMR and FASR cell lines versus w/t MCF-7 cells



PCR expression profiles were obtained for TAMR and FASR models versus w/t MCF7 (day 7) cells for PRDX1, PRDX6, and SOD1 genes. Results were not statistically significant in TAMR and FASR cells using a student T-test ($p > 0.05$) using triplicate preparations.

3.4 TAC and Antioxidant gene expression during initial treatment of w/t MCF7 cells with anti-hormonal agents

Total antioxidant capacity had been shown earlier in the project to be elevated significantly in all the anti-hormone and anti-EGFR resistant models versus the w/t MCF7 cell line. Gene profiling analysis by Affymetrix also revealed significant upregulation of 15 genes across at least two forms of resistance versus w/t MCF7 cells with 9 potentially spanning all resistant states. In total 11 antioxidant genes were chosen for their strong profiles and potential role in the antioxidant pathways, and these underwent verification studies at the mRNA level using RT-PCR on the TAMR and FASR versus w/tMCF7 cells. Of these, 11 antioxidant genes, 8 showed significant upregulation in at least one of the antihormone resistant breast cancer models with 5 spanning both states. However, a question arises as to whether the increase occurring in the verified antioxidant genes and TAC actually begins early in w/t MCF-7 cells during their treatment with endocrine agents such as tamoxifen (TAM) or faslodex (FAS), or if such increases are a feature only associated with the resistant state.

In order to address this, TAC analysis of triplicate w/t MCF7 cell preparations were treated with the growth inhibitory dose of 0.1 μ M tamoxifen or faslodex. TAC measurement was performed after 10 days anti-hormone treatment to ensure cells are undergoing a growth inhibitory response and to allow comparison with further available Affymetrix, day 10 expression data, and

Chapter 3 – Results

subsequently PCR. Results showed an elevated level of TAC in w/t MCF7 cells in the presence of tamoxifen ($p=0.008$) and in the presence of faslodex ($p=0.001$) versus untreated control w/t MCF7 cells (Figure 3.21). Levels achieved approximated 0.022mM and 0.042mM for TAMR and FASR cells respectively at 10 days (Figures 3.1 and 3.3). Thus, the elevated TAC appeared to be instigated early during initial exposure to endocrine agents.

The 11 selected antioxidant genes were then explored during 10-day anti-hormone treatment of w/t MCF7 cells with tamoxifen or faslodex by PCR analysis. The untreated parental w/t MCF-7 model and w/t MCF-7 treated with 10^{-9} M oestradiol (E_2) were used as controls to run against w/t MCF7 cells treated with the anti-hormonal agents to learn more about the ER regulation of these genes. To initially check the quality of the mRNA samples and for confidence in PCR performance, the pS2 gene was again examined using the mRNA samples +/- anti-hormone treatment to see if the expected expression change was observed (Henry et al., 1991). An RNA free sample was also included as a negative control (Figure 3.22). As expected, PCR analysis of the oestrogen regulated pS2 gene revealed it was significantly upregulated in w/t MCF7 cells treated with E_2 , and significantly decreased in the presence of tamoxifen and particularly faslodex treatment versus untreated w/t MCF7 cells, indicating the samples were representative of behaviour of w/t MCF7 cells during endocrine response (Figure 3.22), and thus appropriate to examine antioxidant genes during this phase.

Chapter 3 – Results

The 11 antioxidant genes were not E₂ induced versus w/t MCF7 cells. Thus, PCR results showed no significant changes for the antioxidant genes for E₂ treated w/t MCF7 cells versus control w/t MCF7 cells also with an acceptable mRNA free negative control shown for all (Figure 3.23). However in contrast, there was evidence of gene regulation by the growth inhibitory antihormones tamoxifen and/or faslodex in w/t MCF7 cells as had been observed by Affymetrix (referring to Table 3.2), whereby 8 of the 11 Antioxidant genes PRDX6, NQO1, TXNRD1, GPX2, GSTA4, GLRX, TXN, and TXNRD2 all correlate at the PCR level with the Affymetrix day 10 profiles. Only CAT, SOD1, and PRDX1 did not correlate.

Thus, the antioxidant gene GSTA4 was upregulated in both the presence of tamoxifen by over 80% (p=0.033) and faslodex by approximately 140% (p=0.026) compared to E₂ treated w/t MCF7 cells (Figure 3.24), equating with Affymetrix findings (Table 3.2), where (as shown in Figure 3.12) this antihormone induced increase was subsequently retained by PCR in both the resistant TAMR and FASR cells versus w/t MCF7 cells.

TXNRD1 also had a similar profile to GSTA4 as it was again upregulated in w/t MCF7 cells treated with tamoxifen (by over 80%, p=0.027) and faslodex (by 145%, p=0.034) (Figure 3.25) again equating with Affymetrix profiles (Table 3.2) and again with increases retained within resistance by PCR (Figure 3.13). NQO1 was also upregulated in w/t MCF7 cells treated with tamoxifen (by 65%, p=0.015) or faslodex (by over 100%, p=0.003) as shown in Figure

3.26, equating with Affymetrix profiles (Table 3.2), although this upregulation was only subsequently retained in the TAMR model by PCR (Figure 3.14).

Although both antioxidant genes GLRX and CAT were upregulated in both resistant models TAMR and FASR by PCR (Figures 3.15 and 3.16), they were only significantly upregulated by 10 day faslodex treatment and not by tamoxifen in w/t MCF7 cells (Figures 3.27 and 3.28 respectively). GLRX was upregulated by faslodex by over 100% ($p=0.036$) (Figure 3.27), and CAT by over 140% ($p=0.016$) (Figure 3.28). The GLRX profile thus equated with Affymetrix findings, although some discrepancies are with CAT (Table 3.3).

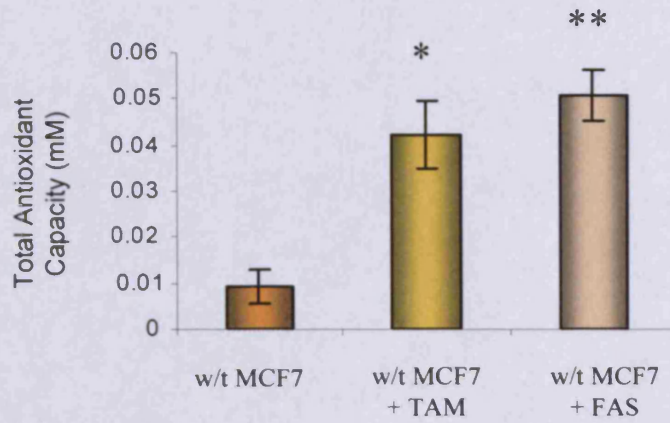
Despite a lack of E_2 induction, GPX2 was found to be significantly down regulated in w/t MCF7 cells in the presence of either tamoxifen or faslodex suggesting this may be a classically ER regulated gene (contrasting all other antioxidant genes examined). Thus w/t MCF7 cells treated with tamoxifen showed approximately 50% reduction ($p=0.00074$) in GPX2 expression, and a 100% reduction ($p=0.0017$) in the presence of faslodex treated (Figure 3.29). Lack of upregulation during treatment equates with the Affymetrix profile (Table 3.2), but was clearly different to the increase that subsequently appeared to arise later in TAMR cells as verified by PCR (Figure 3.19).

Finally, the antioxidant genes TXN, TXNRD2, PRDX6, PRDX1 and SOD1 were found to not be significantly changed in expression by 10 days tamoxifen or faslodex treatment in w/t MCF7 cells versus E_2 treated w/t MCF7 cells

Chapter 3 – Results

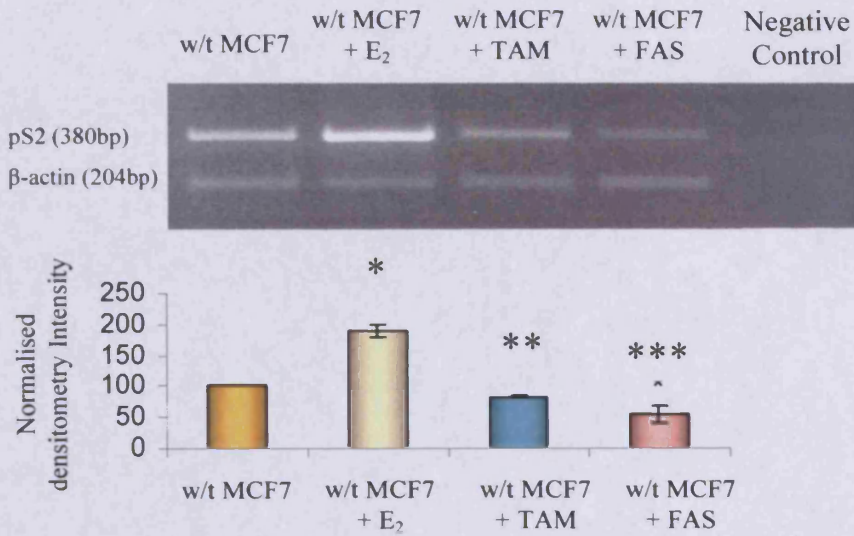
(Figures 3.30 – 3.34 respectively). Any changes displayed during treatment did not reach significance, equating with Affymetrix data for TXN, TXNRD2, and PRDX6 (Tables 3.2 and 3.3) that were confirmed by Affymetrix expression profiling as specific to resistance and subsequently PCR verified for TXN and TXNRD2 only (Figures 3.17 and 3.18), PRDX1 and SOD1 showed no regulation at PCR level in response (Figures 3.33 and 3.34 respectively) or resistance (Figure 3.20).

Figure 3.21 TAC analysis of w/t MCF7 cells treated with 10^{-7} M Tamoxifen or Faslodex for 10 days



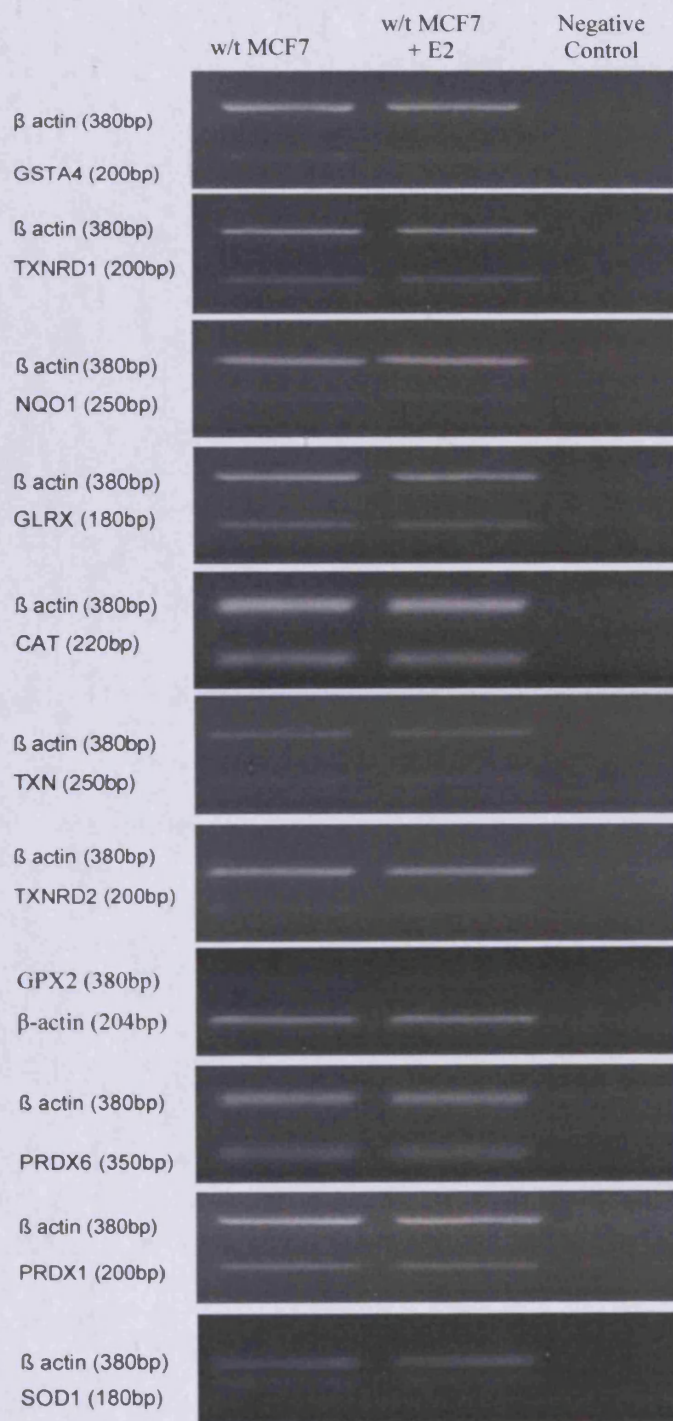
TAC levels were measured using the Total Antioxidant Assay Kit from Sigma-Aldrich Company Ltd. TAC for w/t MCF-7 cells treated with 10^{-7} M Tamoxifen (TAM) or Faslodex (FAS) for 10 days was significant by Student T-test compared to the parental cells (* $p=0.042$, ** $p=0.005$ respectively). These data represent a typical example of an experiment performed three times \pm SD.

Figure 3.22 pS2 gene verification of PCR samples for the w/t MCF-7 model treated with 10^{-9} M E_2 , 10^{-7} M Tamoxifen or Faslodex for 10 days



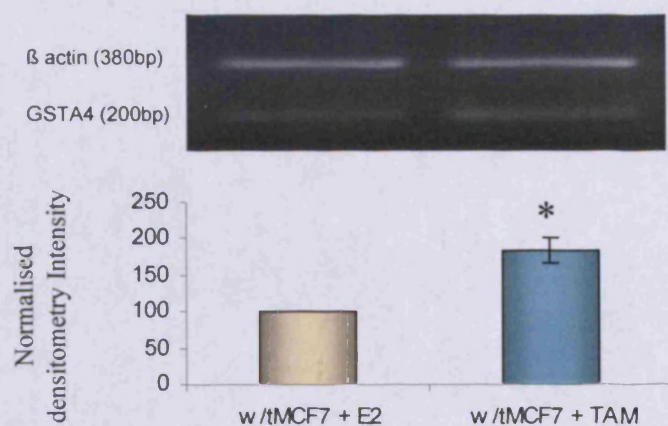
pS2 PCR expression results were obtained from a densitometer and normalised to readings obtained for β actin in triplicate. Statistical analysis was performed for each model against the w/t MCF-7 model using a Student's paired t-Test \pm SD (* $p=0.004$, ** $p=0.004$, and *** $p=0.027$).

Figure 3.23 Effect of 10 day E₂ treatment of w/t MCF7 cells on antioxidant gene expression

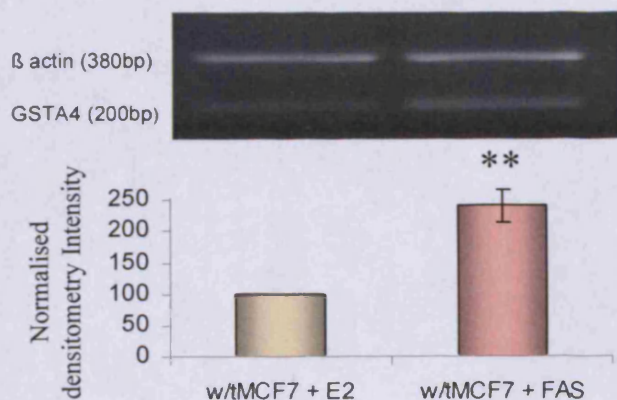


PCR analysis of the 11 antioxidant genes for 10⁻⁹M E₂ treated w/t MCF7 cells versus control w/t MCF7 cells, together with β actin. Negative control comprises loading buffer only.

Figure 3.24 a) The effect of treatment with 10 day Tamoxifen versus E₂ treatment of w/t MCF7 cells on GSTA4 gene expression

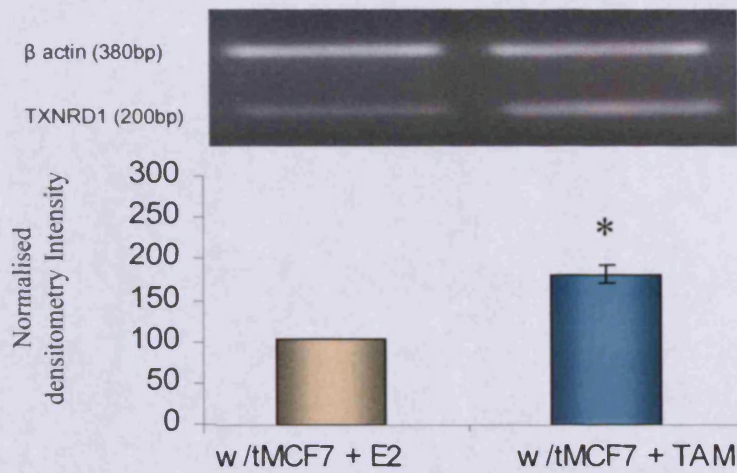


b) The effect of treatment with 10 day Faslodex versus E₂ treatment of w/t MCF7 cells on GSTA4 gene expression

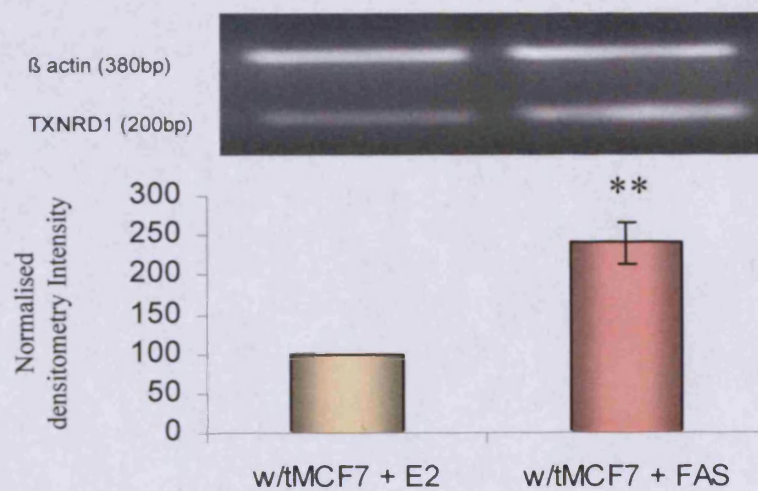


a & b) PCR for GSTA4 gene expression following treatment with 10^{-7} M Tamoxifen or Faslodex (*p = 0.033 and **p = 0.026 respectively) compared to treatment of w/t MCF7 cells with 10^{-9} M E₂. Results are from triplicate preparations and were statistically compared using the Student T-test \pm SD.

Figure 3.25 a) The effect of treatment with 10 day Tamoxifen versus E₂ treatment of w/t MCF7 cells on TXNRD1 gene expression

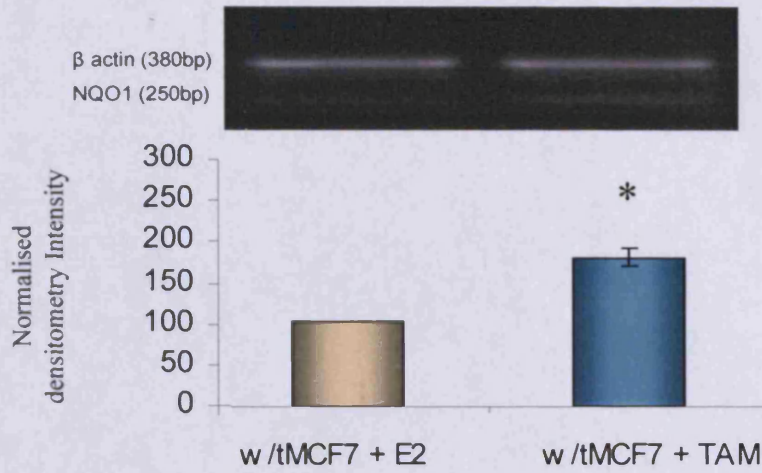


b) The effect of treatment with 10 day Faslodex versus E₂ treatment of w/t MCF7 cells on TXNRD1 gene expression

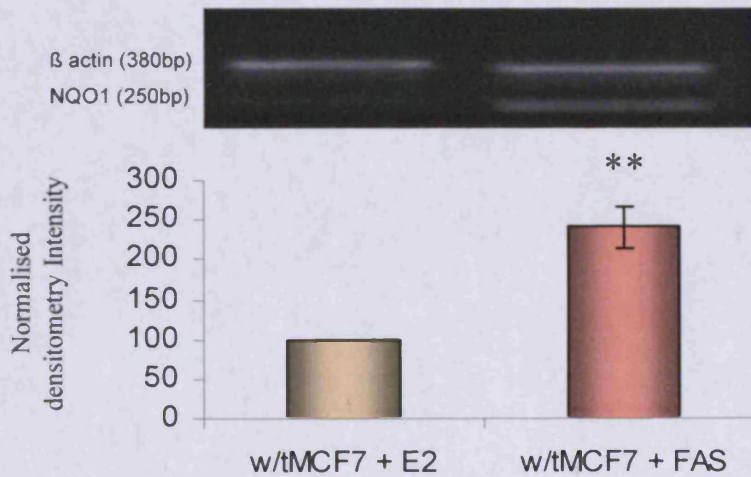


a & b) PCR analysis for TXNRD1 gene expression following treatment with 10⁻⁷M Tamoxifen or Faslodex (*p = 0.027 and **p = 0.034 respectively) compared to treatment of w/t MCF7 cells with 10⁻⁹M E₂. Results are from triplicate preparations and were statistically compared using the Student T-test ± SD.

Figure 3.26 a) The effect of treatment with 10 day Tamoxifen versus E₂ treatment of w/t MCF7 cells on NQO1 gene expression

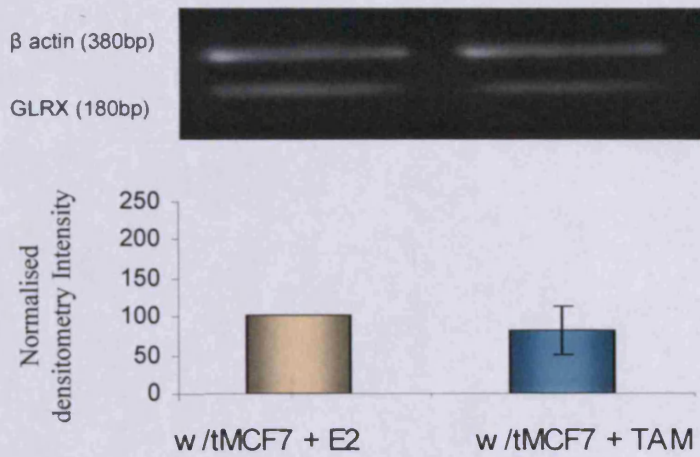


b) the effect of treatment with Faslodex versus E₂ treatment of w/t MCF7 cells on NQO1 gene expression

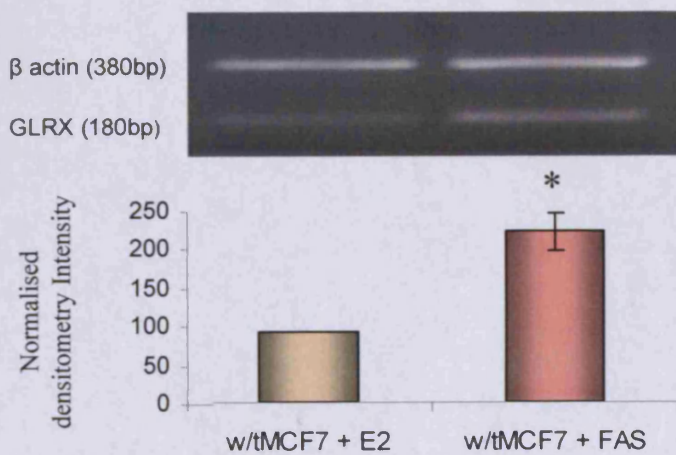


a & b) PCR analysis for NQO1 gene expression following treatment with 10⁻⁷M Tamoxifen or Faslodex (*p = 0.015 and **p = 0.003 respectively) compared to treatment of w/t MCF7 cells with 10⁻⁹M E₂. Results are from triplicate preparations and were statistically compared using the Student T-test ± SD.

Figure 3.27 a) The effect of treatment with 10 day Tamoxifen versus E₂ treatment of w/t MCF7 cells on GLRX gene expression

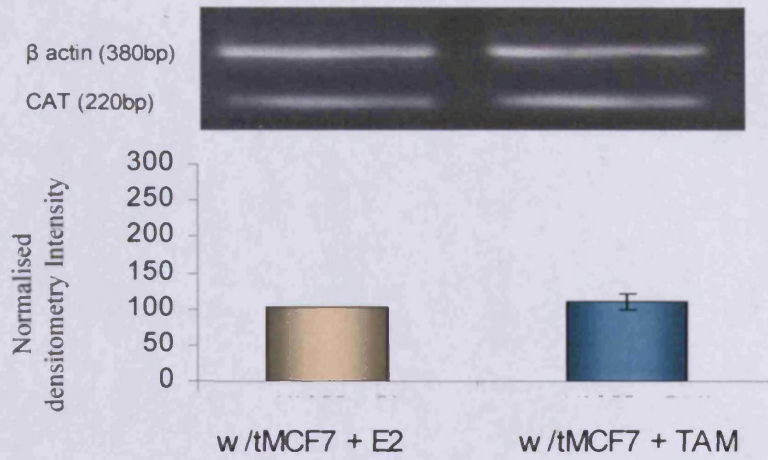


b) The effect of treatment with 10 day Faslodex versus E₂ treatment of w/t MCF7 cells on GLRX gene expression

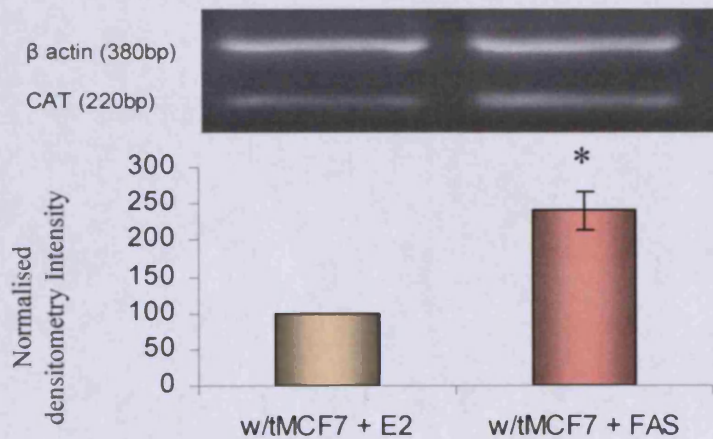


a & b) PCR analysis for GLRX gene expression following treatment with 10⁻⁷M Tamoxifen or Faslodex (p = 0.57 and *p = 0.036 respectively) compared to treatment of w/t MCF7 cells with 10⁻⁹M E₂. Results are from triplicate preparations and were statistically compared using the Student T-test ± SD.

Figure 3.28 a) The effect of treatment with 10 day Tamoxifen versus E₂ treatment of w/t MCF7 cells on CAT gene expression

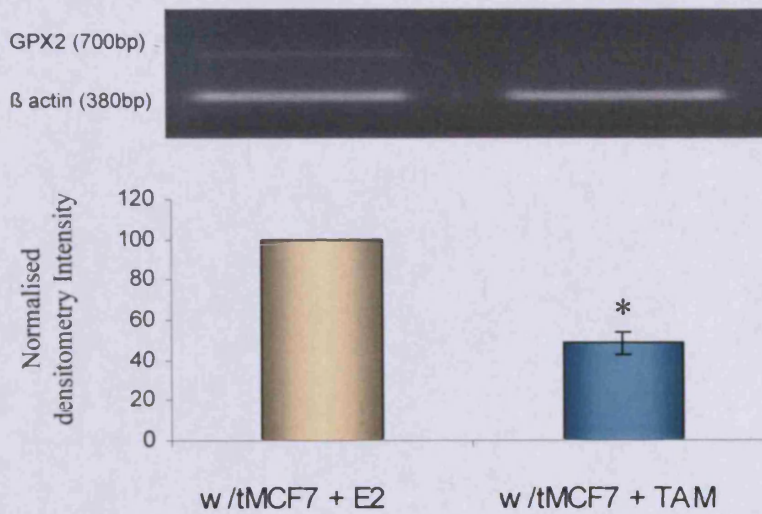


b) The effect of treatment with 10 day Faslodex versus E₂ treatment of w/t MCF7 cells on CAT gene expression

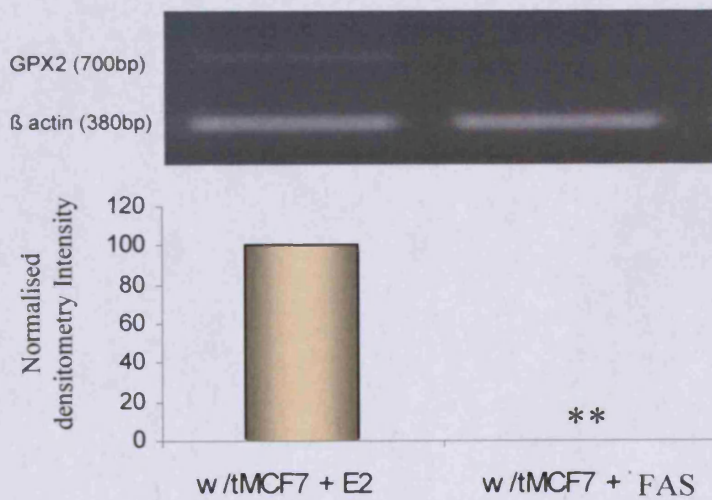


a & b) PCR analysis for CAT gene expression following treatment with 10⁻⁷M Tamoxifen or Faslodex (p = 0.26 and *p = 0.016 respectively) compared to treatment of w/t MCF7 cells with 10⁻⁹M E₂. Results are from triplicate preparations and were statistically compared using the Student T-test ± SD.

Figure 3.29 a) The effect of treatment with 10 day Tamoxifen versus E₂ treatment of w/t MCF7 cells on GPX2 gene expression

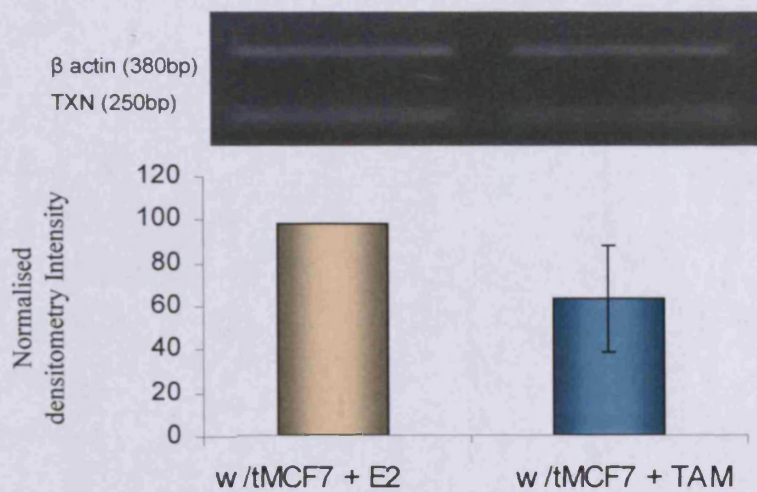


b) The effect of treatment with 10 day Faslodex versus E₂ treatment of w/t MCF7 cells on GPX2 gene expression

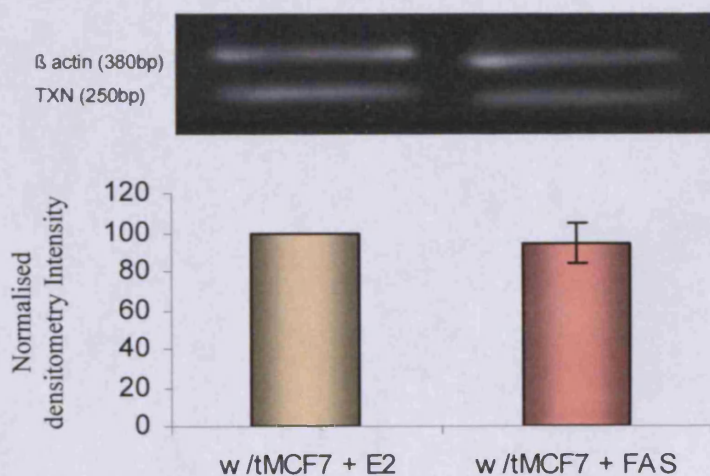


a & b) PCR analysis for GPX2 gene expression following treatment with 10⁻⁷M Tamoxifen or Faslodex (*p = 0.00074 and **p = 0.0017 respectively) compared to treatment of w/t MCF7 cells with 10⁻⁹M E₂. Results are from triplicate preparations and were statistically compared using the Student T-test ± SD.

Figure 3.30 a) The effect of treatment with 10 day Tamoxifen versus E₂ treatment of w/t MCF7 cells on TXN gene expression

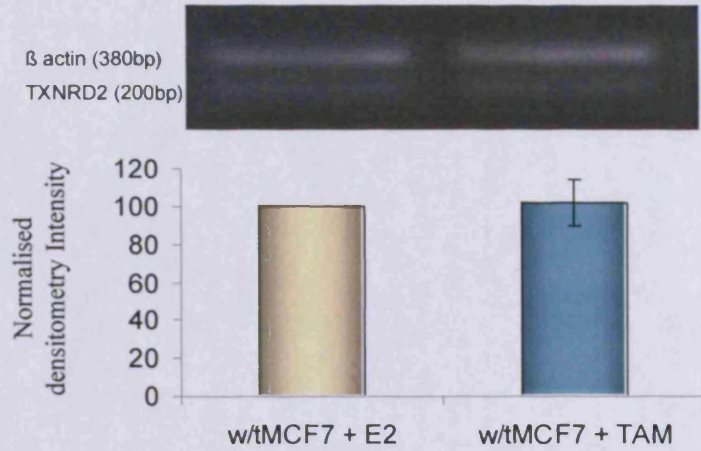


b) The effect of treatment with 10 day Faslodex versus E₂ treatment of w/t MCF7 cells on TXN gene expression

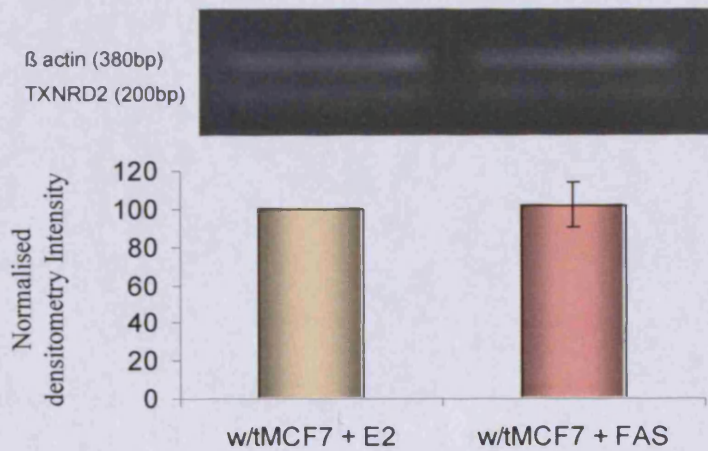


a & b) PCR analysis for TXN gene expression following treatment with 10⁻⁷M Tamoxifen or Faslodex (p = 0.134 and p = 0.118 respectively) compared to treatment of w/t MCF7 cells with 10⁻⁹M E₂. Results are from triplicate preparations and were statistically compared using the Student T-test ± SD.

Figure 3.31 a) The effect of treatment with 10 day Tamoxifen versus E₂ treatment of w/t MCF7 cells on TXNRD2 gene expression

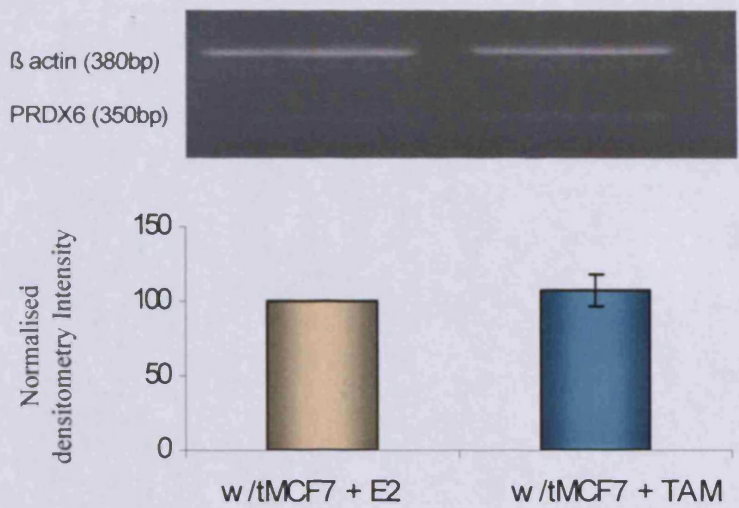


b) The effect of treatment with 10 day Faslodex versus E₂ treatment of w/t MCF7 cells on TXNRD2 gene expression

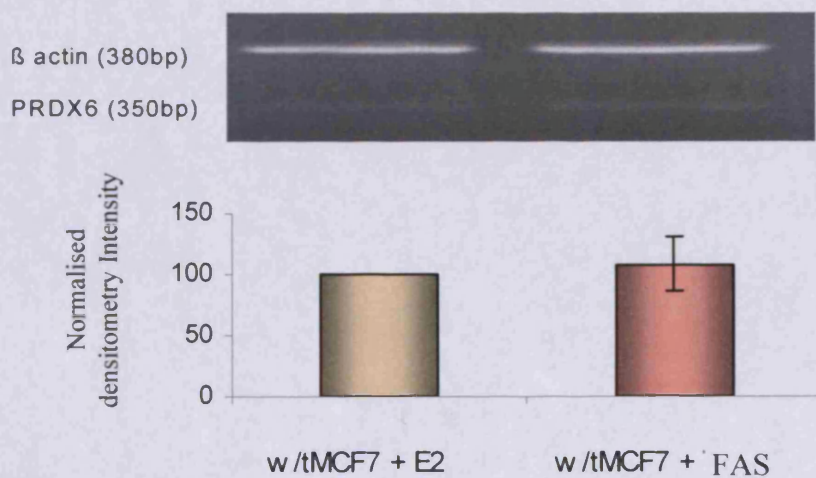


a & b) PCR analysis for TXNRD2 gene expression following treated with 10⁻⁷M Tamoxifen or Faslodex (p = 0.253 and p = 0.249 respectively) compared to treatment of w/t MCF7 cells with 10⁻⁹M E₂. Results are from triplicate preparations and statistically significant using the Student T-test ± SD.

Figure 3.32 a) The effect of treatment with 10 day Tamoxifen versus E₂ treatment of w/t MCF7 cells on PRDX6 gene expression

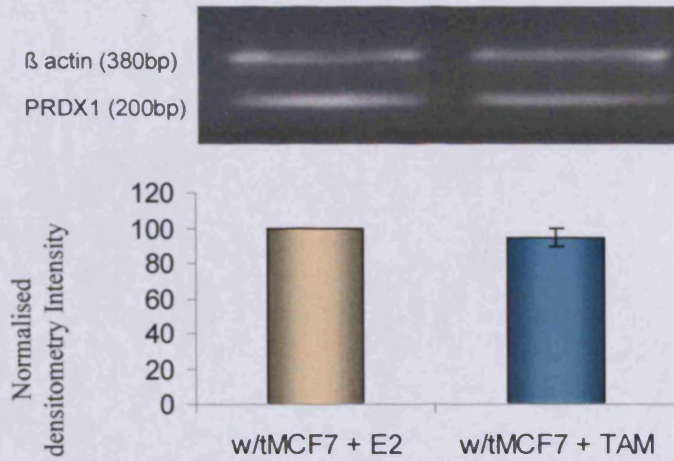


b) The effect of treatment with 10 day Faslodex versus E₂ treatment of w/t MCF7 cells on PRDX6 gene expression

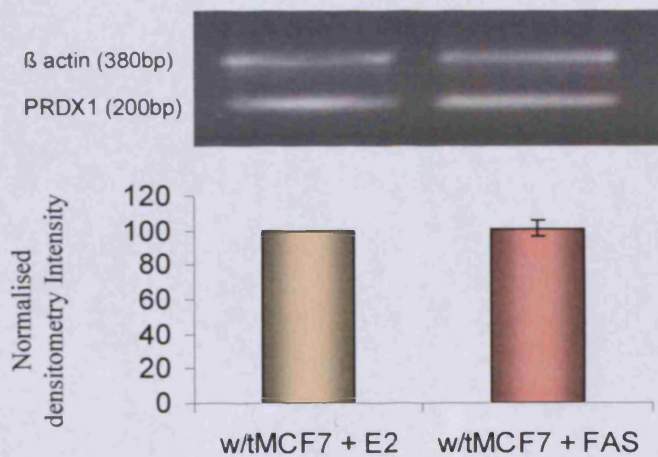


a & b) PCR analysis for PRDX6 gene expression following treatment with 10⁻⁷M Tamoxifen or Faslodex (p = 0.836 and p = 0.852 respectively) compared to treatment of w/t MCF7 cells with 10⁻⁹M E₂. Results are from triplicate preparations and were statistically compared using the Student T-test ± SD.

Figure 3.33 a) The effect of treatment with 10 day Tamoxifen versus E₂ treatment of w/t MCF7 cells on PRDX1 gene expression

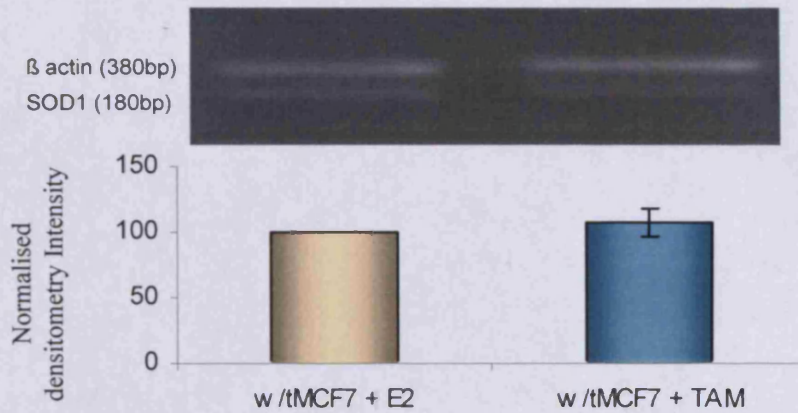


b) The effect of treatment with 10 day Faslodex versus E₂ treatment of w/t MCF7 cells on PRDX1 gene expression

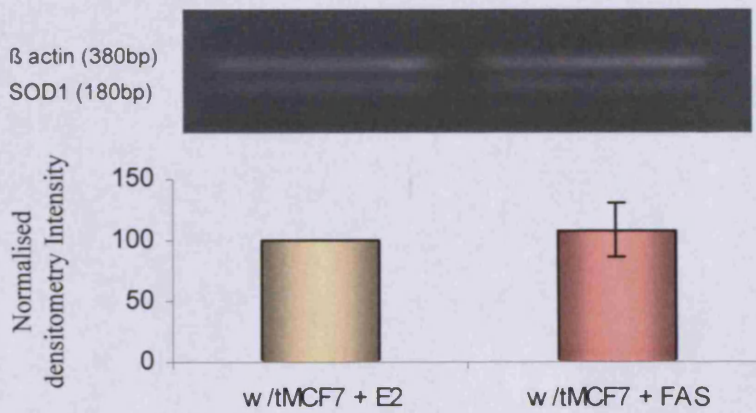


a & b) PCR analysis for PRDX1 gene expression following treatment with 10⁻⁷M Tamoxifen or Faslodex (p = 0.177 and p = 0.595 respectively) compared to treatment of w/t MCF7 cells with 10⁻⁹M E₂. Results are from triplicate preparations and were statistically compared using the Student T-test ± SD.

Figure 3.34 a) The effect of treatment with 10 day Tamoxifen versus E₂ treatment of w/t MCF7 cells on SOD1 gene expression



b) The effect of treatment with 10 day Faslodex versus E₂ treatment of w/t MCF7 cells on SOD1 gene expression



a & b) PCR analysis for SOD1 gene expression following treatment with 10⁻⁷M Tamoxifen or Faslodex (p = 0.064 and p = 0.274 respectively) compared to treatment of w/t MCF7 cells with 10⁻⁹M E₂. Results are from triplicate preparations and were statistically compared using the Student T-test ± SD.

3.5 Impact of EGFR inhibitor Gefitinib on antioxidant gene expression in TAMR cells

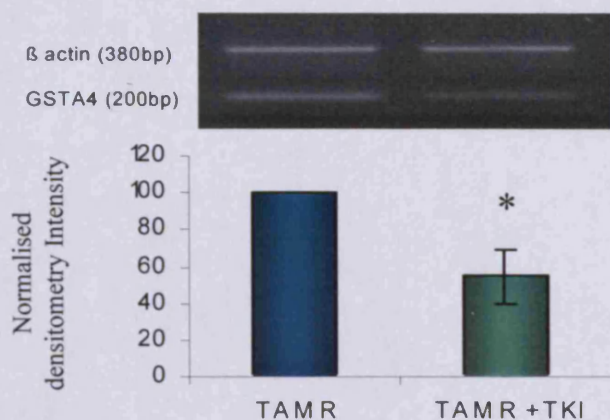
Colleagues at the Tenovus Centre for Cancer Research and further groups, have previously linked increased EGFR signalling to acquired TAM resistance *in vitro* and this pathway can be deregulated in further resistant cell models, including some cell lines resistant to faslodex (McClelland et al., 2001; Knowlden et al., 2003; Gee et al., 2003; Hiscox et al., 2004; Jones et al., 2004; Gee et al., 2005; Jones et al., 2005;). Thus in the TAMR model, targeting of EGFR using a selective Tyrosine Kinase Inhibitor (TKI), gefitinib, at 1 μ M had been shown to promote approximately 60% inhibition of TAMR models, illustrating that EGFR signalling is dominant in their growth (Knowlden et al., 2003). It was thus investigated here whether the 11 antioxidant genes, that also could be growth-relevant, were regulated by EGFR in TAMR cells by monitoring the genes by PCR in mRNA samples prepared from TAMR cells +/- 1 μ M TKI treatment for 7 days.

Of the genes that had been shown to be increased in TAMR by PCR, the antioxidant genes GSTA4, TXNRD1, NQO1, GLRX, CAT, TXN, and TXNRD2 were all downregulated in the presence of TKI treatment. GSTA4 was inhibited in TAMR cells treated with TKI by over 40% (p=0.041) (Figure 3.35), TXNRD1 was inhibited by over 90% (p=0.002) (Figure 3.36), NQO1 was inhibited by over 50% (p=0.006) (Figure 3.37), GLRX was inhibited by approximately 20% (p=0.005) (Figure 3.38), CAT was inhibited by

Chapter 3 – Results

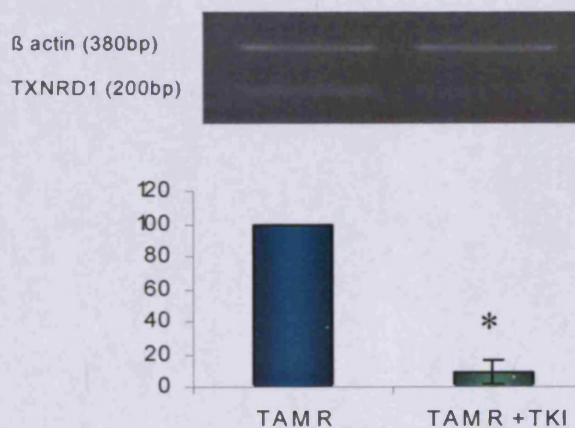
approximately 45% ($p=0.014$) (Figure 3.39), TXN was inhibited by approximately 40% ($p=0.005$) (Figure 3.40), and TXNRD2 was inhibited by approximately 45% ($p=0.02$) (Figure 3.41) compared to the untreated control TAMR cells. In contrast, the gene GPX2 was shown to be further upregulated in the presence of the TKI gefitinib by over 130% ($p=0.005$) compared to the untreated TAMR cells (Figure 3.42). Antioxidant genes that were not confirmed by PCR as increased in resistance, PRDDX6 and SOD1, were also not regulated by TKI treatment (Figures 3.43 and 3.44 respectively), although PRDX1 was again slightly decreased by 10% ($p=0.001$) compared to untreated TAMR cells (Figure 3.45). Table 3.4 represents this PCR information in summary form, alongside the expression of these 11 antioxidant genes in the resistant models TAMR and FASR and whether they are induced by antihormone treatments tamoxifen and faslodex at the PCR level.

Figure 3.35 Impact of gefitinib on GSTA4 gene expression in TAMR cells



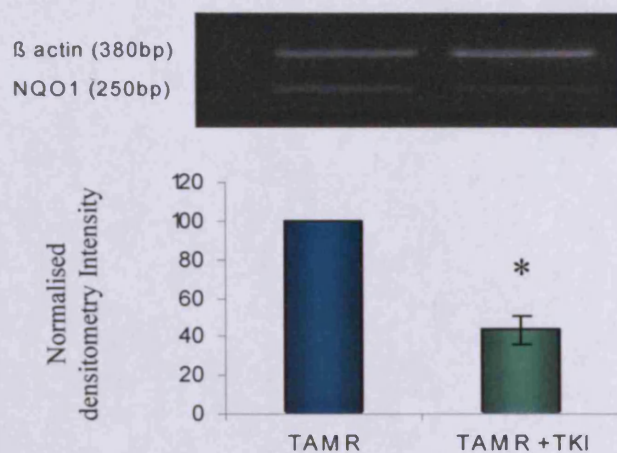
PCR analysis was performed and the specific mRNA band measured for intensity by a densitometer, normalised to β actin, and presented as TAMR + $1\mu\text{M}$ TKI (gefitinib, 7 days) compared to untreated TAMR which was normalised to 100%. Experiments were performed three times and statistical analysis was carried out using a Student T-test \pm SD (* $p=0.041$). The same experimental design was carried out for all antioxidant genes examined in TAMR +/- TKI over Figures 3.36 – 3.45.

Figure 3.36 Impact of gefitinib on TXNRD1 gene expression in TAMR cells



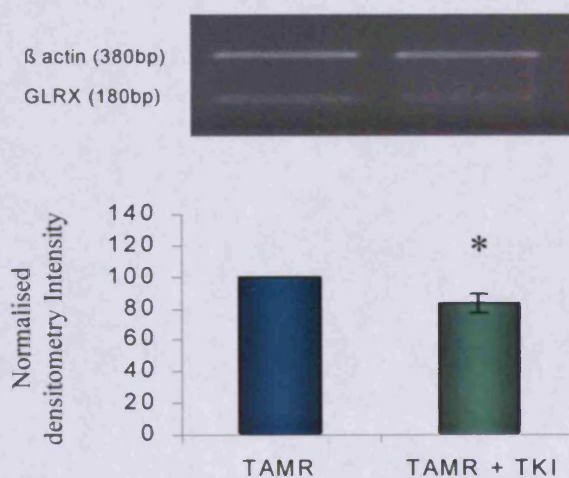
Experiments were performed three times and statistical analysis was carried out using a Student T-test \pm SD (* $p=0.002$).

Figure 3.37 Impact of gefitinib on NQO1 gene expression in TAMR cells



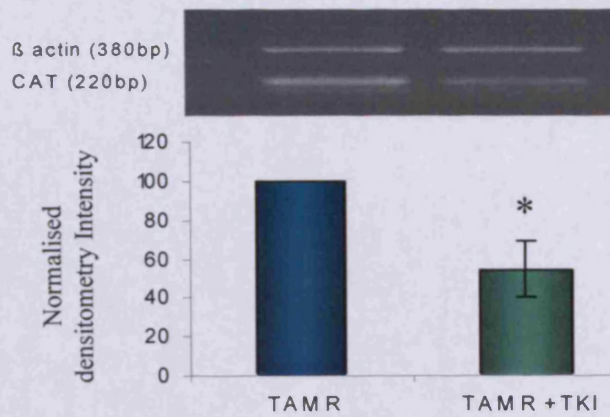
Experiments were performed three times and statistical analysis was carried out using a Student T-test \pm SD (* $p=0.006$).

Figure 3.38 Impact of gefitinib on GLRX gene expression in TAMR cells



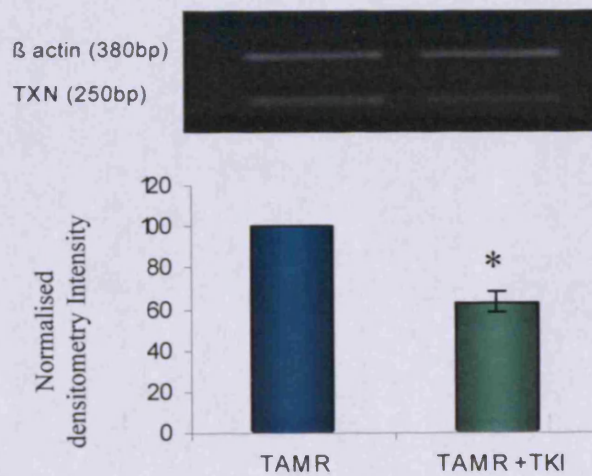
Experiments were performed three times and statistical analysis was carried out using a Student T-test \pm SD (* $p=0.005$).

Figure 3.39 Impact of gefitinib on CAT gene expression in TAMR cells



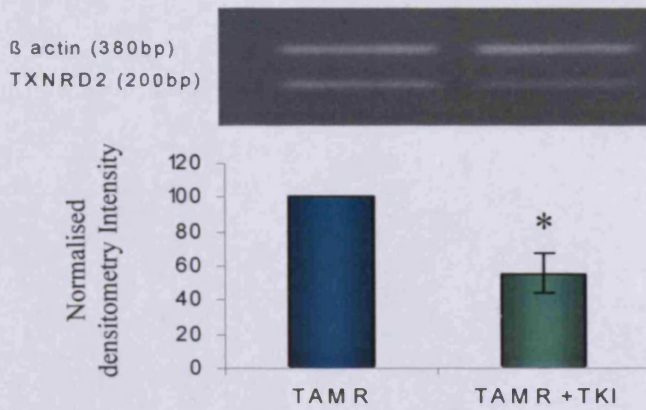
Experiments were performed three times and statistical analysis was carried out using a Student T-test \pm SD (* $p=0.014$).

Figure 3.40 Impact of gefitinib on TXN gene expression in TAMR cells



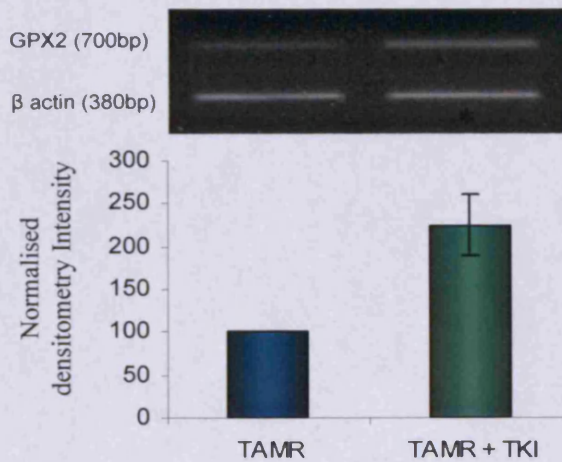
Experiments were performed three times and statistical analysis was carried out using a Student T-test \pm SD (* $p=0.005$).

Figure 3.41 Impact of gefitinib on TXNRD2 gene expression in TAMR cells



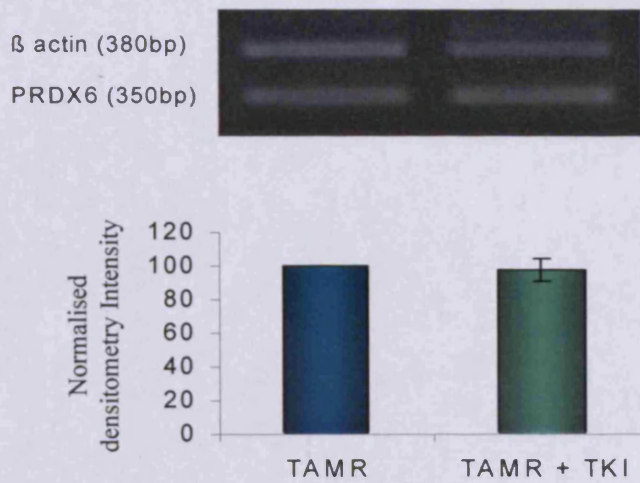
Experiments were performed three times and statistical analysis was carried out using a Student T-test \pm SD (* $p=0.02$).

Figure 3.42 Impact of gefitinib on GPX2 gene expression in TAMR cells



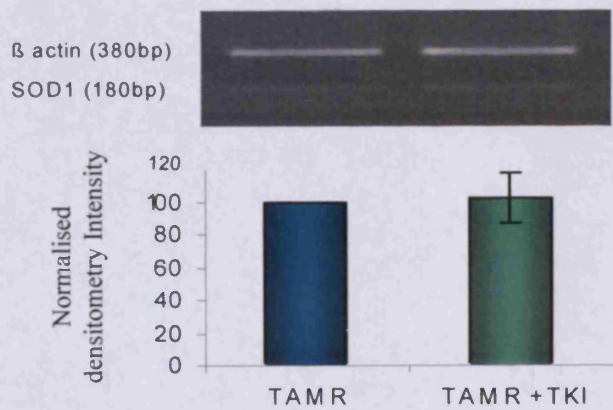
Experiments were performed three times and statistical analysis was carried out using a Student T-test \pm SD (* $p=0.005$).

Figure 3.43 Impact of gefitinib on PRDX6 gene expression in TAMR cells



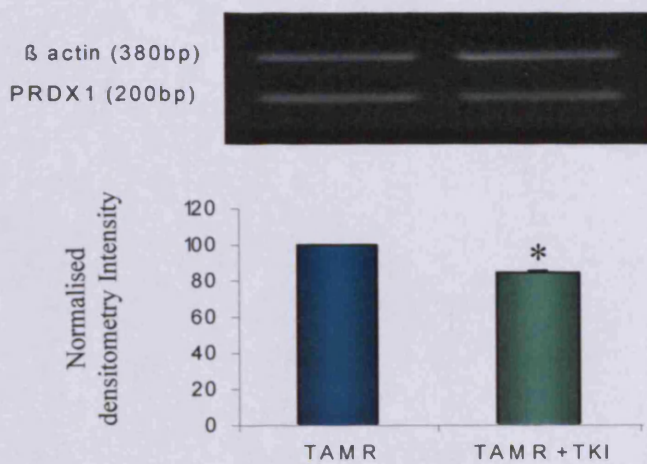
Experiments were performed three times and statistical analysis was carried out using a Student T-test \pm SD ($p=0.08$).

Figure 3.44 Impact of gefitinib on SOD1 gene expression in TAMR cells



Experiments were performed three times and statistical analysis was carried out using a Student T-test \pm SD ($p=0.09$).

Figure 3.45 Impact of gefitinib on PRDX1 gene expression in TAMR cells



Experiments were performed three times and statistical analysis was carried out using a Student T-test \pm SD ($p=0.001$).

Table 3.4 Summary of PCR results for 11 antioxidant genes in resistant models, as well as their regulation by antihormones in w/t MCF7 cells and by anti-EGFR TKI treatment in TAMR cells

Gene name	Upregulated in TAMR cells	Upregulated in FASR cells	TAM Induced	FAS Induced	TKI Supressed
GSTA4	✓	✓	✓	✓	✓
TXNRD1	✓	✓	✓	✓	✓
NQO1	✓	X	✓	✓	✓
GLRX	✓	✓	X	✓	✓
CAT	✓	✓	X	✓	✓
TXN	✓	✓	X	X	✓
TXNRD2	✓	*	X	X	✓
GPX2	✓	X	**	**	***
PRDX6	X	X	X	X	X
PRDX1	X	X	X	X	✓
SOD1	X	X	X	X	X

*TXNRD2 is suppressed in FASR cells. **GPX2 is suppressed in Tamoxifen or Faslodex treated w/t MCF7 cells, and unlike the other antioxidant genes
 ***GPX2 is further TKI induced in TAMR cells.

3.6 Impact of EGFR inhibitor gefitinib and further growth factor signalling inhibitors on TAC in TAMR cells

The PCR findings indicated a number of the antioxidant genes that increased in TAMR cells were positively regulated at the expression level by the EGFR pathway and thus inhibited by EGFR TKI gefitinib at 7 days. To further explore the relationship between EGFR and antioxidant regulation in TAMR cells, the growth and TAC levels in the TAMR cell line with and without TKI treatment for 24 hours, 7 days and 10 days were investigated, compensating for TKI growth inhibitory effect. Thus, MTT growth analysis of TAMR cells with TKI treatment revealed approximately 30% growth inhibition after 24 hours ($p=0.008$), approximately 60% inhibition after 7 days and 50% inhibition after 10 days ($p=0.042$ and $p=0.017$ respectively) as shown in Figure 3.46. There was an 18 fold drop in total antioxidant capacity in TAMR cells with TKI treatment after 24 hours (Figure 3.47a). Surprisingly, however by 7 and 10 days there was a further increase in the level of TAC in TAMR cells with TKI treatment by 9 fold ($p = 0.0148$) and 4 fold ($p = 0.007$) respectively (Figure 3.47b and c), contrasting the decrease seen with this agent for most antioxidant genes here investigated by PCR (Figures 3.35 – 3.45), and implying TAC may be driven by EGFR independent mechanisms.

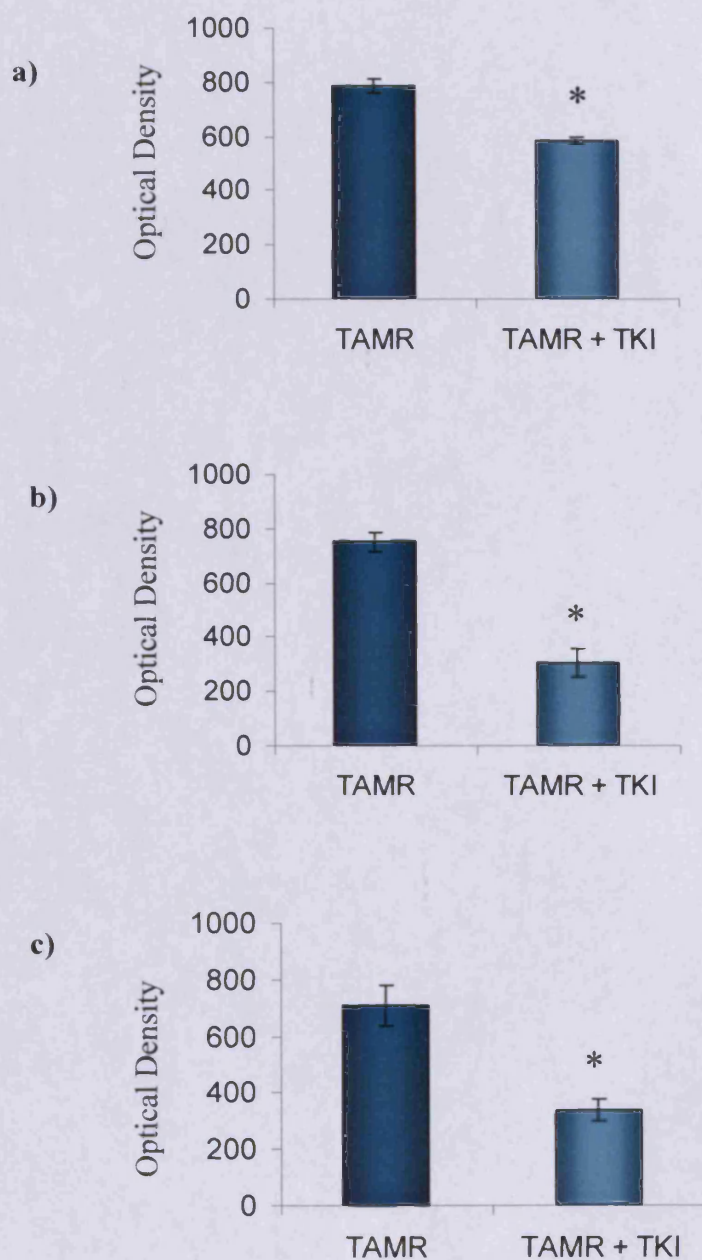
In order to further investigate TAC regulation by other growth factor pathway signalling elements in TAMR cells, the impact of further signal transduction inhibitors were examined after 7 days treatment. TAMR cells were monitored

Chapter 3 – Results

for growth impact during treatment with 1 μ M TKI (gefitinib), a Src inhibitor AZD0530 at 1 μ M, a PI3K inhibitor Wortmannin (WORT) at 100nM, an NF κ B pathway inhibitor Parthenolide (PARTH) at 3 μ M and a MEK 1/2 inhibitor U0126 at 10 μ M (Figure 3.47). As indicated in the Methods, dosages were chosen from the group's previous studies monitoring pathway targeting and growth impact of these various compounds. MTT assay results showed that the inhibitors gefitinib, AZD, PARTH and U0126 all were partially inhibitory of growth of TAMR cells (Figure 3.48). TAMR cells treated with 1 μ M gefitinib for 7 days showed the 60% inhibition, TAMR cells treated with 1 μ M AZD0530 or 10 μ M U0126 showed over 70% inhibition ($p=0.0212$ and $p=0.005$ respectively), and treatment with 3 μ M PARTH showed approximately 50% inhibition ($p=0.0183$). Treatment with 100nM WORT showed no change in growth ($p=0.88$, Figure 3.48).

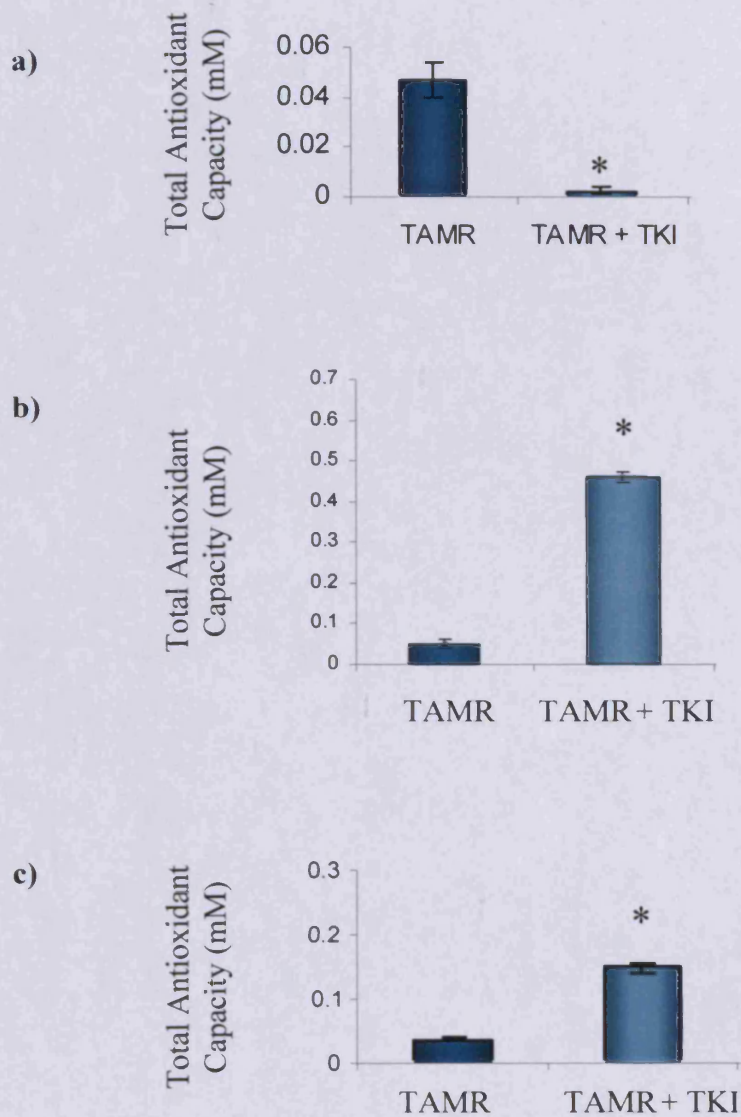
Parallel TAC analysis results with these inhibitors (compensated for cell number decreases obtained in the MTT analysis) (Figure 3.49) again revealed significant increases in TAC levels after 7 days. Thus, TAMR cells treated with 1 μ M GEF for 7 days showed a 6 fold increase in TAC ($p=0.003$), TAMR cells treated with 1 μ M AZD0530 showed a 7.4 fold increase ($p=0.005$), treatment with 3 μ M PARTH showed a 4 fold increase ($p=0.013$) and treatment with 10 μ M U0126 showed a 2 fold increase ($p = 0.01$). There was no significant change in TAC level in response to 100nM WORT ($p=0.06$).

Figure 3.46 MTT growth analysis of TAMR cells treated with the TKI gefitinib for 24 hours, 7 days or 10 days



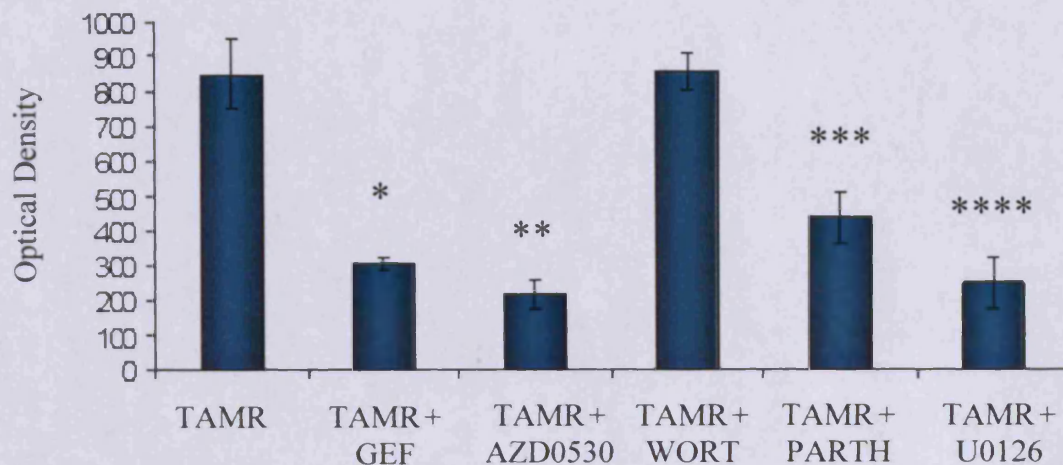
MTT analysis of growth for TAMR cells treated with/without 1 μ M TKI gefitinib for (a) 24 hours ($p=0.008$) (b) 7 days ($p=0.042$), or (c) 10 days ($p=0.017$). All results are representative of an experiment performed three times and statistical analysis was carried using a Student T-test \pm SD.

Figure 3.47 Total antioxidant capacity of TAMR cells treated with the TKI gefitinib for 24 hours, 7 days and 10 days



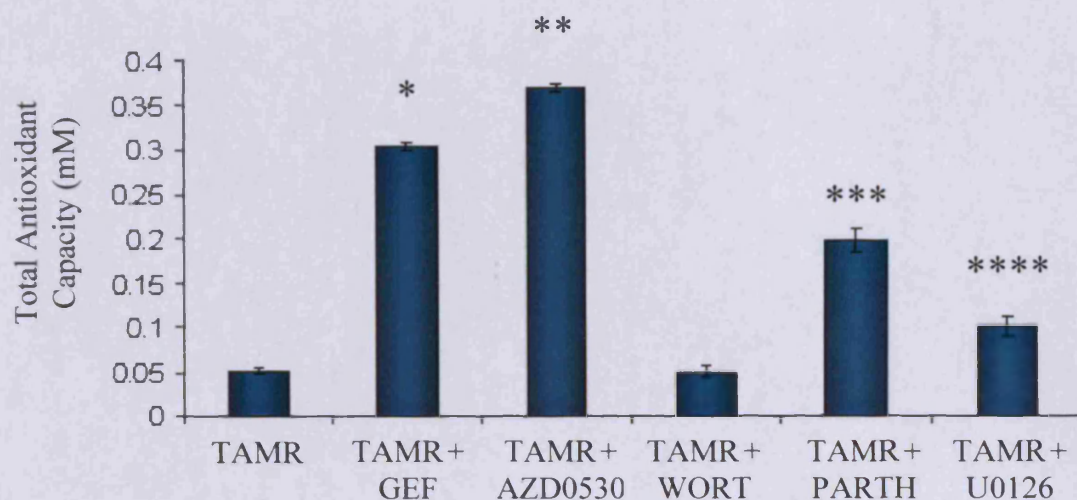
TAMR cells treated with/without 1 μ M TKI gefitinib for (a) 24 hours ($p=0.0068$) (b) 7 days ($p=0.0148$), or (c) 10 days ($p=0.007$). These data are presented after compensation for the TKI growth inhibitory effects shown in Figure 3.46(a, b and c). All results are representative of an experiment performed three times and statistical analysis was carried using a Student T-test \pm SD.

Figure 3.48 MTT growth analysis of TAMR cells treated with gefitinib, AZD0530, wortmannin, parthenolide, or U0126 for 7 days



TAMR cells were treated with/without 1 μ M GEF (* p =0.0171), 1 μ M AZD0530 (** p =0.0212), 100nM WORT (p =0.88), 3 μ M PARTH (** p =0.018) or 10 μ M U0126 (**** p =0.005) for 7 days. Cells were exposed to the MTT reagent for 4hours, and refrigerated overnight in Triton X-100. Absorbances were read the following day using a plate reader at 570nm from multiple wells. Statistical analysis was carried out using a Student T-test \pm SD versus untreated TAMR cells, and results shown are representative of n =3 experiments.

Figure 3.49 TAC analysis of TAMR cells treated with growth factor signalling inhibitors gefinitib, AZD0530, wortmannin, parthenolide, or U0126 for 7 days



TAMR cells were treated with/without 1 μ M GEF (* p =0.003), 1 μ M AZD0530 (** p =0.005), 100nM WORT (p =0.06), 3 μ M PARTH (** p =0.013) or 10 μ M U0126 (**** p =0.01) for 7 days. TAC analysis was carried out as described in the Sigma-Aldrich kit protocol. These data are presented after compensation for the growth inhibitory effects shown in Figure 3.48. Results are representative of $n=3$ experiments and statistical analysis was carried using a Student T-test \pm SD versus untreated TAMR cells.

3.7 Impact of glutathione (GSH) pathway depletion using BSO +/- EGFR blockade in TAMR cells

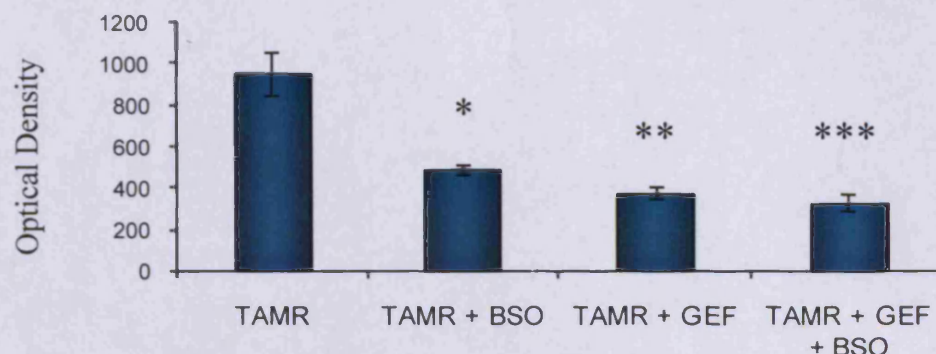
It has been shown here that the tyrosine kinase inhibitor gefitinib can inhibit TAMR cell growth by approximately 60% inhibition. However, in parallel with this anti-tumour effect, TAMR cells showed an increased level of TAC that may feasibly be contributing to cell survival in the presence of TKI, subsequently maintained at high levels into resistance (NEW DUBS). Of the 11 antioxidant genes examined, only GPX2 was upregulated (complementing the TAC data) in the presence of gefitinib at 7 days. The glutathione (GSH)/GPX system is reported to be essential for maintaining the redox balance and defending against elevated levels of oxidative stress, where cells may develop a conditional GSH-dependent GPX reduction system that confers stronger resistance against oxidative challenge (Fu et al., 2007). GSH is a naturally occurring tripeptide whose reducing properties enable it to play a central role in antioxidant pathways. GSH is essential for the survival of many cell systems and its depletion by the GSH biosynthesis inhibitor BSO has been proven to lead to cell death and highly sensitise tumor cells to apoptosis induced by chemotherapy and in an endocrine resistant model to pro-apoptotic effects of E₂ (Lewis-Wambi et al., 2009).

To further examine the role of GSH/GPX in TAMR cells, including during TKI treatment, experiments were performed in TAMR cells with BSO, and with BSO in combination with gefitinib. 100µM BSO was able to significantly

Chapter 3 – Results

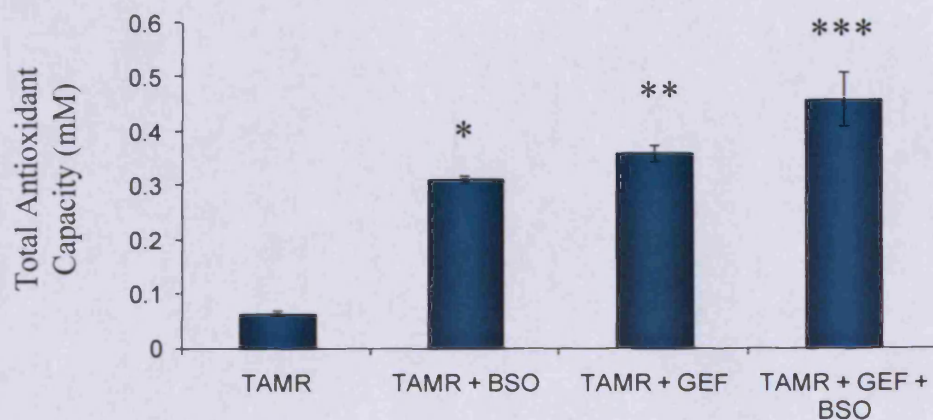
inhibit TAMR growth by 48% ($p=0.001$) (Figure 3.50). TAMR treated with GEF + BSO gave an inhibition of 66% ($p=0.0005$), with 60% for GEF alone ($p=0.0006$) (Figure 3.50). However, there was no significant increase in inhibition of the combination treatment versus GEF alone at 7 days. Parallel TAC analysis in TAMR cells again demonstrated that treatment with $1\mu\text{M}$ GEF for 7 days increased total antioxidant capacity. Surprisingly, treatment of TAMR cells with the glutathione antioxidant inhibitor BSO ($100\mu\text{M}$) for 7 days showed a 5 fold increase in TAC in TAMR ($p=0.0009$) (Figure 3.51). Combination treatment of GEF + BSO showed a higher increase of 8 fold in TAC ($p=0.0001$ versus untreated TAMR) that was also more significantly increased versus GEF alone ($p=0.03$) (Figure 3.51).

Figure 3.50 MTT analysis of TAMR cells monitoring impact of BSO, gefitinib, and combined treatment at 7 days



MTT analysis was carried out for TAMR cells treated with 100 μ M BSO (* p =0.001), 1 μ M GEF (** p =0.0006), or combination treatment (** p =0.0005) for 7 days. Results are from triplicate preparations and statistical testing was carried out using a Student T-test \pm SD versus untreated TAMR cells.

Figure 3.51 TAC analysis of TAMR cells following treatment with BSO, gefitinib or gefitinib + BSO for 7 days



TAC analysis was carried out for TAMR cells treated with 100 μ M BSO (p =0.0009), 1 μ M GEF (p = 0.0009), or combination treatment (p =0.0001) for 7 days. These data are presented after compensation for the growth inhibitory effects for shown in Figure 3.50. Results are from triplicate preparations and statistical testing was carried out using a Student T-test \pm SD versus untreated TAMR cells.

3.8 Oxidative stress (ROS) measured in TAMR cells versus w/t MCF-7 cells

Antioxidant levels in acquired endocrine or anti-EGFR resistant models have been shown here to be elevated in comparison to untreated endocrine responsive w/t MCF7. However it remains elusive as to whether these antioxidants are upregulated in response to elevated levels of ROS, or are independent of this in resistant models. In order to more fully understand the redox balance in the resistant models, total oxidative stress was measured in each of these models in relation to the endocrine responsive cells over a 24hour to 10 day time course using a ROS fluorescence assay (H₂DCFDA).

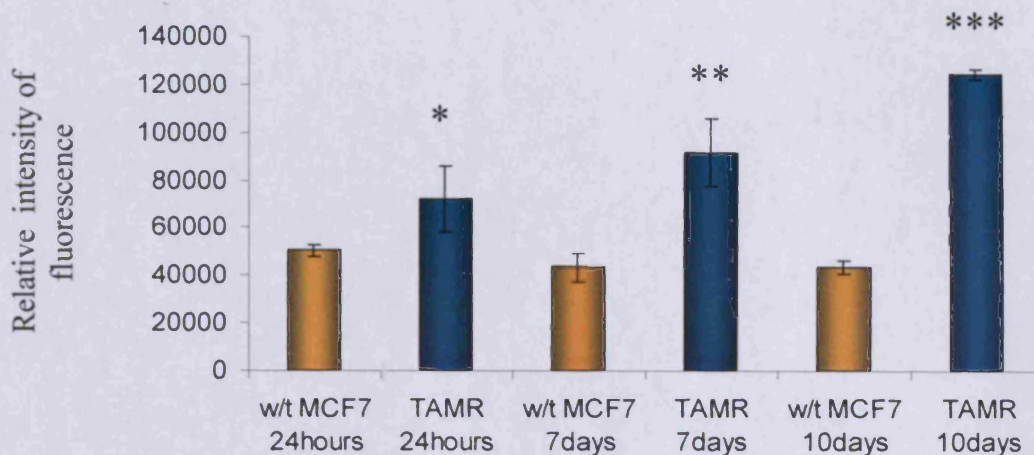
ROS measurements taken 24hours after seeding allowed monitoring of the basal levels of ROS that existed within the various cell lines before they entered exponential growth. Results showed significantly elevated levels of basal ROS existed within TAMR cells (65% increase, $p=0.034$) compared to the parental w/t MCF-7 model (Figure 3.52). After 7 days growth there was an even greater increase (110% increase, $p=0.036$) with ROS levels further increasing to 190% ($p=0.01$) in TAMR cells compared to the w/t MCF-7 cells by 10 days (Figure 3.52).

Along with previous growth curve data (Figure 3.2), in order to address if ROS was paralleled by any changes in cell proliferation or cell survival in the TAMR versus w/t MCF7 cells, staining for the Ki67 protein and an ApoAlert

Chapter 3 – Results

kit were employed respectively at day 7. TAMR cells were 100% positive for Ki67 versus 80% positive in w/t MCF7 models, while apoptosis was 7% versus 11% respectively (Figure 3.53). Thus the increased ROS (and associated increased TAC) was paralleled by very modestly increased cell proliferative capacity and cell survival in TAMR cells versus w/t MCF7 cells at day 7 (a time that both cell lines are in log phase growth). Although this does not appear to translate out into a significant increase in overall growth profile in TAMR versus w/t MCF7 cells (Figure 3.2), equivalent growth rates to untreated w/t MCF7 had clearly been acquired by the TAMR cells despite the elevated ROS.

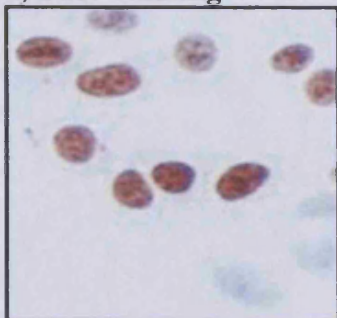
Figure 3.52 H₂DCFDA fluorescent examination of ROS levels in TAMR cells at 24 hours, 7 days, and 10 days in comparison to the w/t MCF7 cell line



ROS analysis using H₂DCFDA fluorescent dye was carried out for TAMR cells at 24hours (*p=0.034), 7 days (**p=0.036), and 10 days (***p = 0.01) versus the w/t MCF7 model. Results are of triplicate preparations and statistical analysis was by Student T-test ± SD.

Figure 3.53 Ki 67 staining and ApoAlert MMS staining to identify level of proliferation and apoptosis respectively in w/t MCF-7 cell line versus TAMR cells at 7 days.

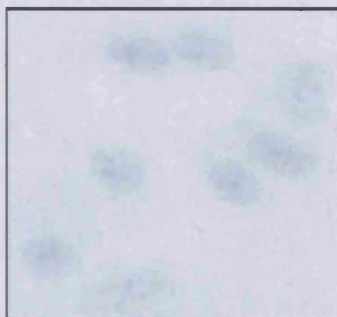
a) Ki67 staining



w/t MCF7: 80% Ki67+

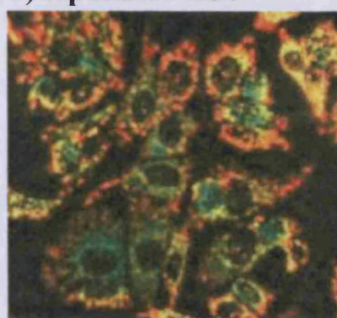


TAMR: 100% Ki67+

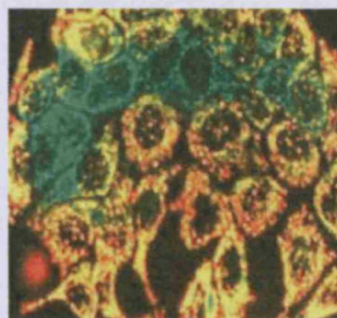


-ve Control: MCF7

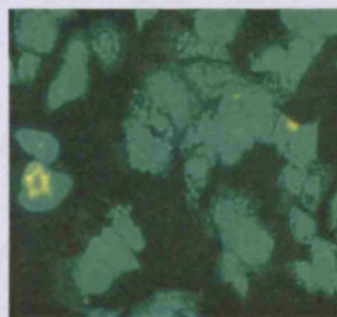
b) ApoAlert KIT



w/t MCF7: 11% apoptosis



TAMR: 7% apoptosis



+ve Control: MCF7 +UV 100% apoptosis

Ki67 immunostaining and ApoAlert MMS assays were carried out in accordance to the manufacturers' protocol for detection of proliferation and apoptosis respectively. For Ki67 staining (a), the brown signal represents cells in proliferation (versus blue/green counterstain of non-proliferating cells) and the absence of a secondary antibody was used as a negative control. In the ApoAlert assay (b), green signal represents cells undergoing early apoptosis with exposure to UV being used as a positive control (representative of n=3 experiments, X40 magnification).

3.9 ROS measurements in other acquired resistant models versus w/t MCF7 cells

Total ROS was also examined using the H₂DCFDA assay in the further resistant breast cancer models FASR, X-MCF and NEW DUBS versus the w/t MCF7 breast cancer model.

3.9.1 ROS measurement in FASR cells versus w/tMCF7

ROS measurements for FASR following 24hours after seeding and after 7 days growth again showed significant increases in ROS levels at 135% and 140% (p=0.0021 and p=0.023 respectively) compared to parental w/t MCF-7 models, with ROS after 10 days also substantially elevated versus w/t MCF7 cells (175%, p=0.025) (Figure 3.54).

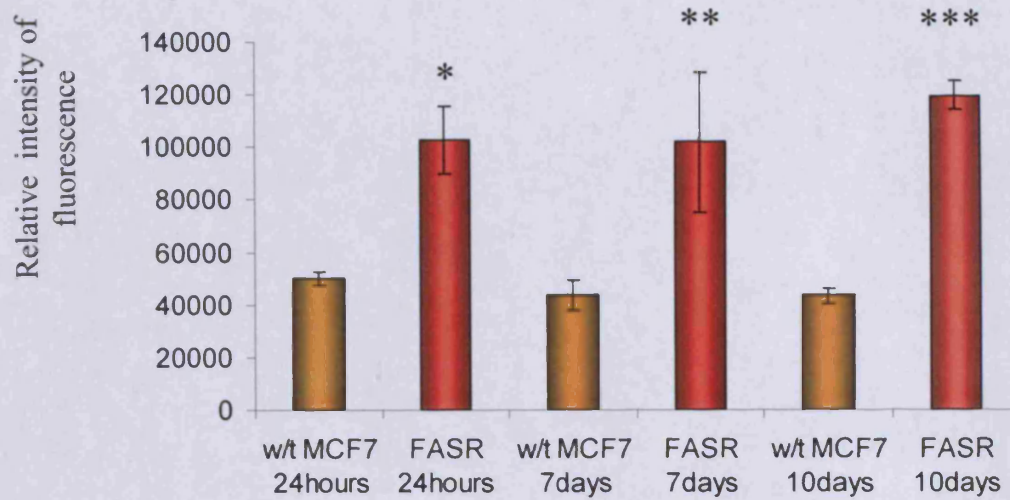
3.9.2 ROS measurement in X-MCF cells versus w/tMCF7

ROS measurements taken from the oestrogen deprived resistant cell line X-MCF showed the greatest increase in ROS elevation versus w/t MCF7. Following 24hours after seeding, X-MCF cells showed a significant 160% increase (p=0.0008) in ROS levels compared to the parental w/t MCF-7 models (Figure 3.55). At 7 days for the X-MCF model, ROS increase was 170% (p=0.022) and 190% (p=0.0023) after 10 days (Figure 3.55).

3.9.3 ROS measurement in NEW DUBS cells versus w/tMCF7

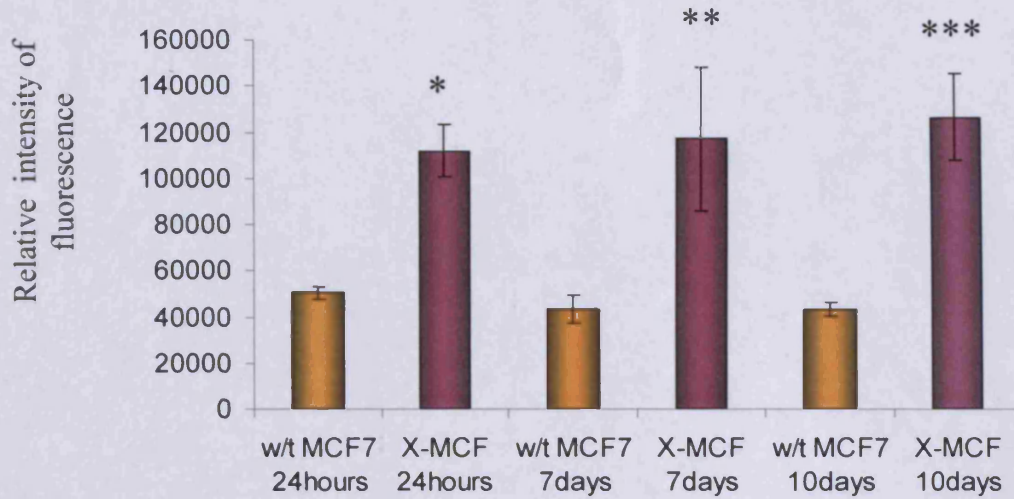
There was a 110% increase of ROS ($p=0.019$) after 24hours compared to the parental w/t MCF-7 model (Figure 3.56). Results after 7 days for the NEW DUBS model again showed an increase in ROS levels compared to the w/t MCF-7 cells at 150% ($p=0.036$) (Figure 3.56). At 10 days there was a more prominent increase in ROS at 170% ($p=0.009$) (Figure 3.56).

Figure 3.54 H₂DCFDA fluorescent analysis of ROS in FASR cells at 24 hours, 7 days, and 10 days in comparison to the w/t MCF7 cell line



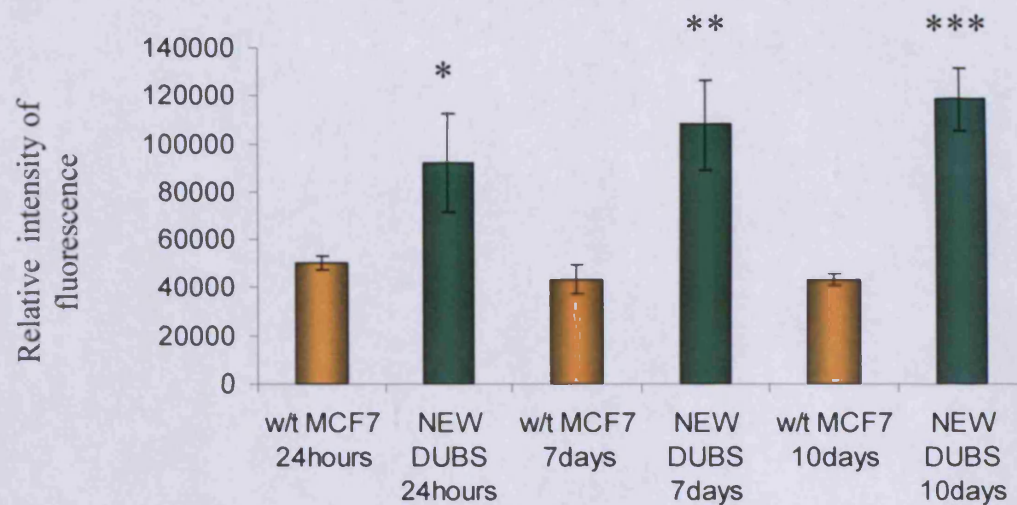
ROS analysis using H₂DCFDA fluorescent dye was carried out for FASR cells at 24 hours (*p=0.0021), 7 days (**p=0.023), and 10 days (***p=0.025) versus the w/t MCF7 model. Results are of triplicate preparations and statistical analysis was by Student T-test ± SD.

Figure 3.55 H₂DCFDA fluorescent analysis of ROS in X-MCF cells at 24 hours, 7 days and 10 days in comparison to the w/t MCF7 cell line



ROS analysis using H₂DCFDA fluorescent dye was carried out for X-MCF cells at 24 hours (*p=0.0008), 7 days (**p=0.022), and 10 days (***p=0.0023) versus the w/t MCF7 model. Results are of triplicate preparations and statistical analysis was by Student T-test \pm SD.

Figure 3.56 H₂DCFDA fluorescent analysis of ROS in NEW DUBS cells at 24 hours, 7 days, and 10 days in comparison to w/t MCF7 cells

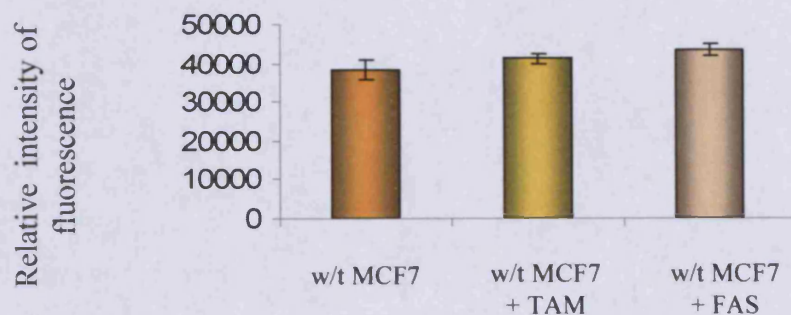


ROS analysis using H₂DCFDA fluorescent dye was carried out for NEW DUBS cells at 24hours (*p=0.019), 7 days (**p=0.036), and 10 days (**p=0.009) versus the w/t MCF7 model. Results are of triplicate preparations and statistical analysis was by Student T-test ± SD.

3.10 Examination of ROS in w/t MCF7 cells during initial treatment with antihormonal agents

Since total ROS was elevated significantly in all acquired resistant models versus the w/t MCF7 cell line, as for TAC the project again investigated whether these increases begin early in w/t MCF-7 cells during initial treatment (10 day) with the endocrine agents tamoxifen or faslodex (10^{-7} M). Results showed no change in ROS levels in w/t MCF7 cells in the presence of tamoxifen ($p=0.949$) or faslodex ($p=0.961$) (Figure 3.57).

Figure 3.57 H₂DCFDA fluorescent examination of ROS in w/t MCF-7 cells treated with tamoxifen or faslodex for 10 days



w/t MCF7 models in Phenol free RPMI medium with 5% charcoal-stripped serum were treated with $0.1\mu\text{M}$ tamoxifen or $0.1\mu\text{M}$ faslodex. ROS analysis using H₂DCFDA fluorescent dye was carried out after 10 days, comparing with untreated w/t MCF7 cells ($p=0.949$ and $p=0.961$ respectively). Results were of triplicate preparations and statistical analysis was by Student T-test \pm SD.

3.11 Impact of Inhibitors of growth factor signalling pathways on ROS level in TAMR cells

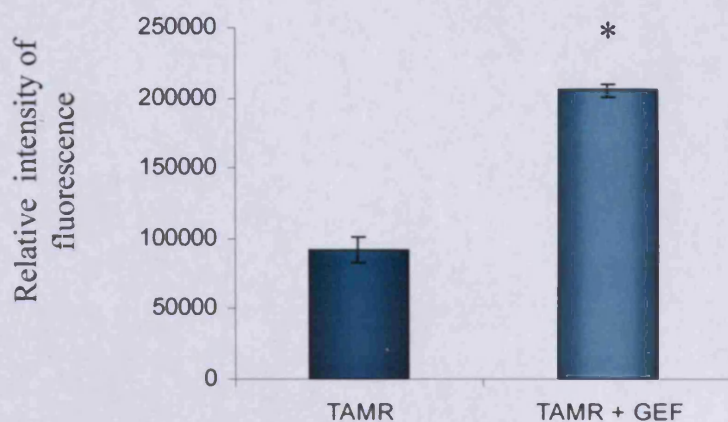
To again explore regulation of the elevated ROS in TAMR cells by EGFR and further growth factor signalling pathways, we investigated ROS levels in the TAMR cell line with/without treatment with the EGFR TKI gefitinib over 24 hours, 7 days and 10 days. There was an increase in ROS of approximately 2 fold at 24hours ($p = 0.0008$) (Figure 3.58) and 10 days (2 fold, $p=0.001$) (Figure 3.60) and 4 fold at 7 days with gefitinib ($p=0.0009$) (Figure 3.59). A further experiment was prepared to compare impact of 1 μ M TKI (gefitinib) and the further STIs Src inhibitor AZD0530 (AZD) at 1 μ M, PI3K inhibitor Wortmanin (WORT) at 100nM, NF κ B inhibitor Parthenolide (PARTH) at 3 μ M or a MEK 1/2 inhibitor U0126 at 10 μ M in TAMR cells, measuring ROS at 7 days and again compensating for the various growth inhibitory effects seen with these agents as in Figure 3.48. Gefitinib, AZD0530, PARTH and U0126 all increased ROS in TAMR cells, with over a 3-4 fold increase with such treatments ($p=0.038$, $p=0.0036$, $p=0.0005$, and $p=0.0005$ respectively) (Figure 3.61). Treatment with WORT showed no change in ROS level ($p=0.425$).

In addition to the overall growth data with MTT (Figure 3.48), Ki67 staining and the ApoAlert kit was again used to monitor level of proliferation and apoptosis respectively, in parallel with ROS, in TAMR cells during treatment with the EGFR-TKI gefitinib (1 μ M) at 7 days (Figure 3.62). As shown in Figures 3.62a, there was 60% reduction in proliferation in TAMR cells treated

Chapter 3 – Results

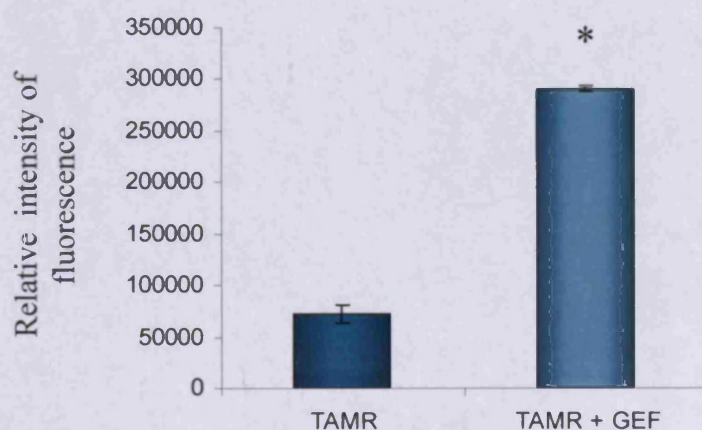
with GEF, and a 10% increase in early apoptosis (Figure 3.62b), equating with the significant growth inhibition (Figure 3.48) but contrasting the increase in ROS induced by this agent.

Figure 3.58 Impact of gefitinib on ROS level in TAMR cells at 24 hours



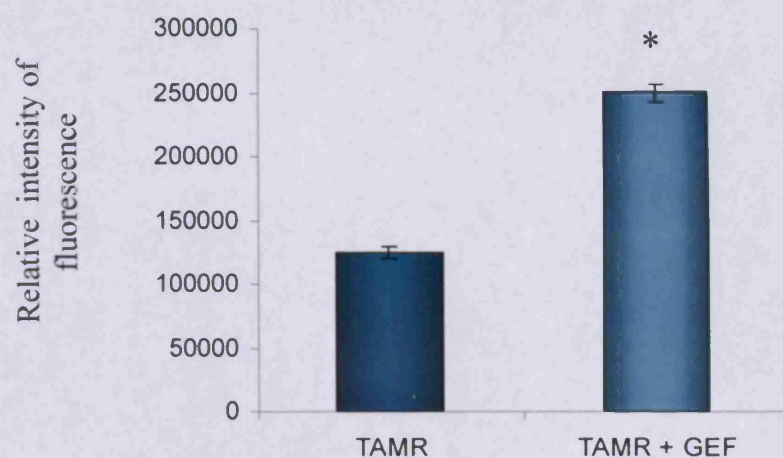
ROS analysis using H₂DCFDA fluorescent dye was carried out in TAMR cells treated with/without the EGFR TKI 1 μ M GEF for 24hours (p=0.0008). Results were for triplicate preparations and statistical analysis was by Student T-test \pm SD. These data are compensated for cell number from MTT data shown in Figure 3.46.

Figure 3.59 Impact of gefitinib on ROS level in TAMR cells at 7 days



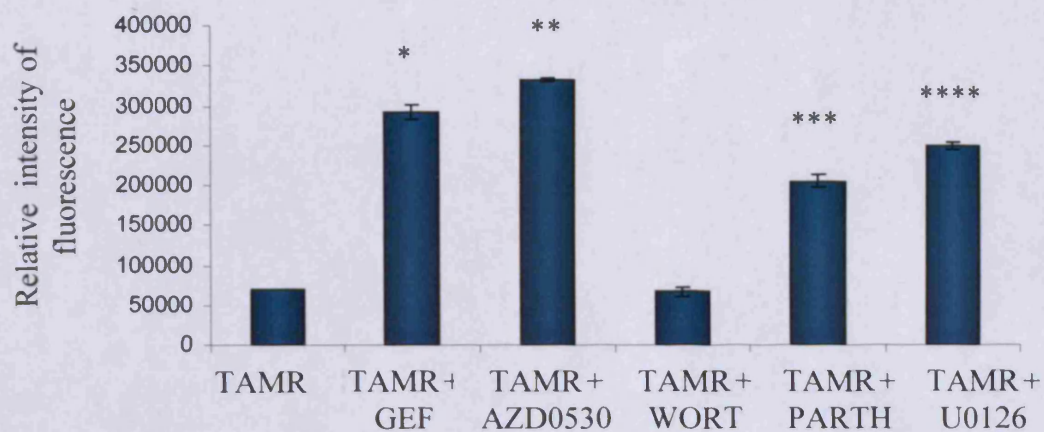
ROS analysis using H₂DCFDA fluorescent dye was carried out in TAMR cells treated with/without the EGFR TKI 1 μ M GEF for 7 days (p=0.0009). Results were for triplicate preparations and statistical analysis was by Student T-test \pm SD. These data are compensated for cell number from MTT data shown in Figure 3.46.

Figure 3.60 Impact of gefitinib on ROS level in TAMR cells at 10 days



ROS analysis using H₂DCFDA fluorescent dye was carried out in TAMR cells treated with/without the EGFR TKI 1 μ M GEF at 10 days ($p=0.001$). Results were for triplicate preparations and statistical analysis was by Student T-test \pm SD. These data are compensated for cell number from MTT data shown in Figure 3.46.

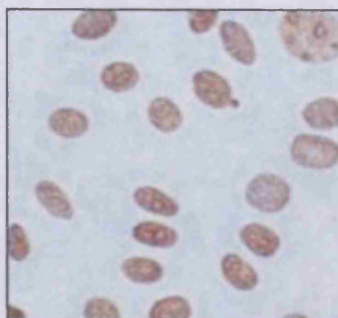
Figure 3.61 Impact of growth factor signalling inhibitors on ROS in TAMR cells at 7 days



ROS analysis using H2DCFDA fluorescent dye was carried out in TAMR cells treated with/without 1 μ M GEF (p=0.038), 1 μ M AZD0530 (p=0.0036), 100nM WORT (p=0.425), 3 μ M PARTH (p=0.0005), or 10 μ M U0126 (p = 0.0005) at 7 days. Results were for triplicate preparations and statistical analysis was by Student T-test \pm SD versus untreated TAMR cells. These data are compensated for cell number from MTT data shown in Figure 3.48.

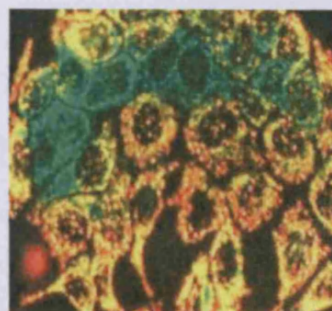
Figure 3.62 Ki 67 and ApoAlert MMS Staining of TAMR cells during treatment with gefitinib

a) Ki67 staining

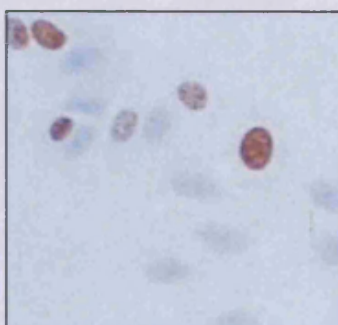


TAMR:100% Ki67+

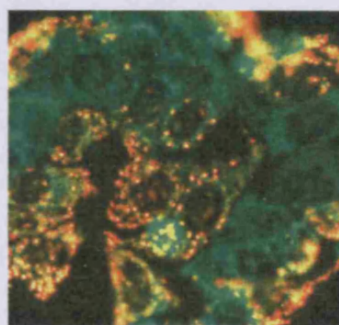
b) ApoAlert KIT



TAMR: 7% apoptosis



TAMR + TKI 1uM: 40% Ki67+



TAMR + TKI 1uM: 17% apoptosis

Ki67 and ApoAlert MMS assays were carried out in accordance to the manufacturer's protocol for detection of proliferation and apoptosis respectively. For Ki67 staining (a), the brown signal represents cells proliferating, and the absence of a secondary antibody was used as a negative control. In the ApoAlert assay (b), a green signal represents cells undergoing early apoptosis, with exposure to UV being used as a positive control. Results are representative of n=3 experiments, X40 magnification.

3.12 TAMR growth sensitivity to excess oxidative stress

With significantly increased levels of ROS in the acquired resistant models versus the w/t MCF7 cell line, but also with further increased ROS in gefitinib treated TAMR cells under growth inhibitory conditions, it remained to be explored if induction of more substantial levels of oxidative stress could be growth inhibitory in resistant models versus responsive cells. The oxidative stress inducing agent Menadione (MSB) was used for this investigation, as it is reported to work similarly to H₂O₂ in promoting ROS but is easier to manipulate experimentally (Noto et al., 1989). MSB is reported to promote substantial ROS within cell, and the μ M dose range used was chosen for use in TAMR (versus w/t MCF7 cells) by extensive literature search (Noto et al., 1989; Nutter et al., 1991; Sun et al., 1997).

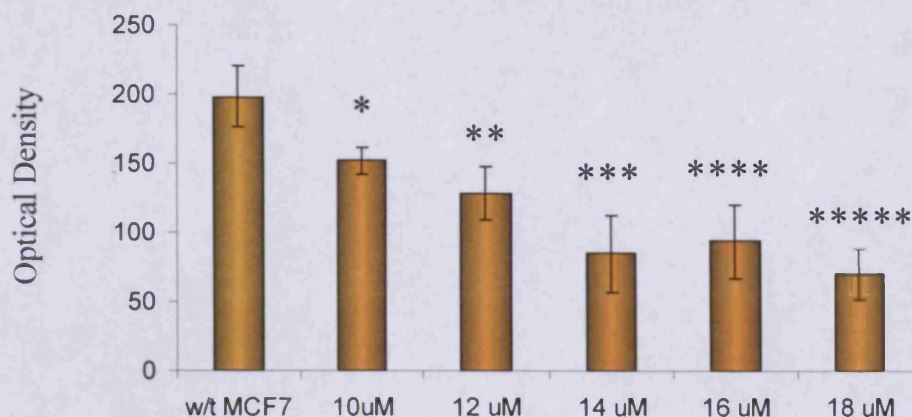
MTT analysis of w/t MCF7 cells treated with different doses of MSB for 7 days showed a dose dependent decrease in growth with increased exposure to MSB (Figure 3.63). There was a 23% significant reduction in growth at 10 μ M MSB ($p=0.02$), with a calculated IC₅₀ (50% growth inhibitory concentration) of 15.4 μ M (Figure 3.63). The greatest reduction in w/t MCF7 growth (64%, $p=0.001$) was achieved with the highest MSB concentration examined at 18 μ M. In TAMR cells there was also a reduction in cell growth at 7 days by MSB at 10 μ M, but this was more substantial than in w/t MCF7 cells (Figure 3.64). Indeed, the IC₅₀ was reached at this concentration ($p=0.002$), suggesting

Chapter 3 – Results

increased sensitivity to this oxidative stress inducer in the acquired resistant versus w/t MCF7 cells.

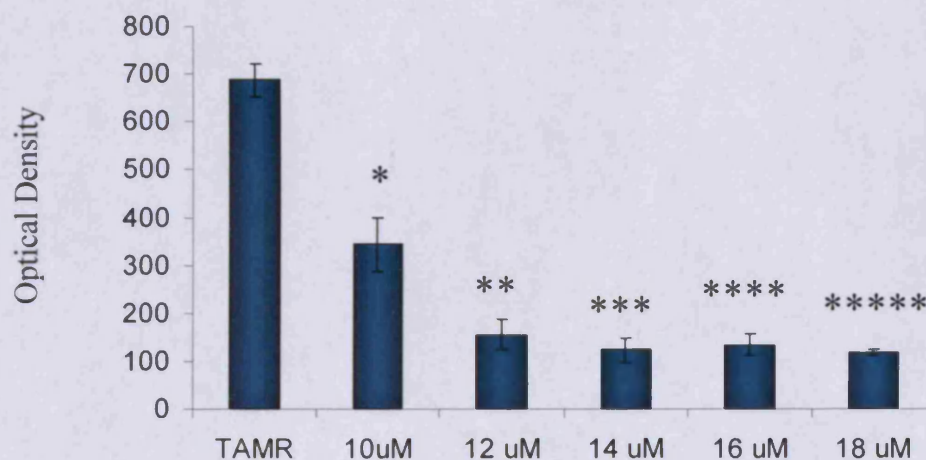
Parallel ROS measurements for w/t MCF7 cells and TAMR cells treated with/without 10 μ M MSB were subsequently taken after 7 days treatment. Basal ROS levels in TAMR cells were 2.7 fold higher than in w/t MCF7 cells, as previously observed in the project. MSB increased ROS levels in w/t MCF7 cells by 3.9 fold ($p=0.005$) and by 2.9 fold in TAMR cells at 10 μ M MSB ($p=0.036$) (Figure 3.65), reaching substantially higher levels in the TAMR than w/t MCF7 cells in the presence of this agent.

Figure 3.63 MTT analysis of w/t MCF7 cells treated with MSB for 7 days



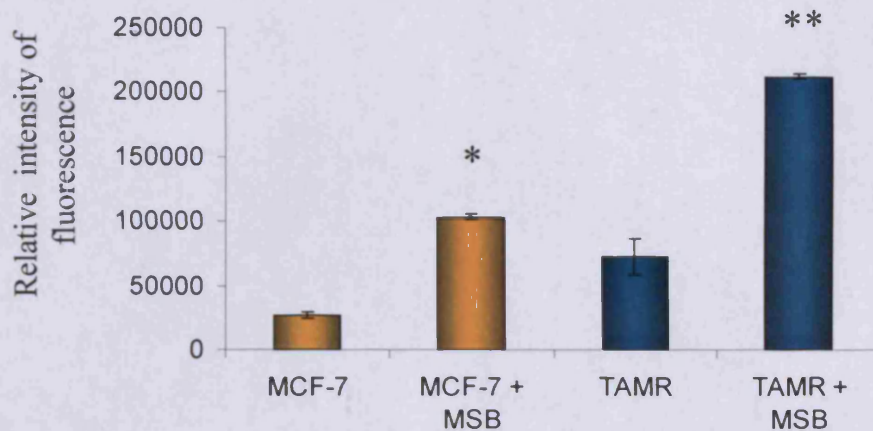
MTT analysis was carried out for w/t MCF7 cells treated with 10 μ M (*p=0.02), 12 μ M (**p=0.01), 14 μ M (**p=0.003), 16 μ M (****p=0.004) or 18 μ M (*****p= 0.001) MSB for 7 days. Results were for triplicate preparations and statistical analysis was by Student T-test \pm SD versus untreated w/t MCF7 cells.

Figure 3.64 MTT analysis of TAMR cells treated with MSB for 7 days



MTT analysis was carried out for TAMR cells treated with 10 μ M (*p=0.006), 12 μ M (**p=0.003), 14 μ M (**p=0.001), 16 μ M (****p=0.005) or 18 μ M (*****p= 0.002) MSB for 7 days. Results were for triplicate preparations and statistical analysis was by Student T-test \pm SD versus untreated TAMR cells.

Figure 3.65 ROS analysis of TAMR cells versus w/t MCF7 cells treated with and without 10 μ M MSB



ROS analysis using H₂DCFDA fluorescent dye was carried out in w/t MCF7 cells and TAMR cells treated with and without 10 μ M MSB (*p=0.005, and **p=0.036 respectively) for 7 days. Results for cell models were compensated for growth inhibitory effect of 10 μ M MSB in Figures 3.63 and 3.64 and for triplicate preparations with statistical analysis by Student T-test \pm SD versus the respective untreated models.

3.13 Growth sensitivity of further acquired resistant models to excess oxidative stress

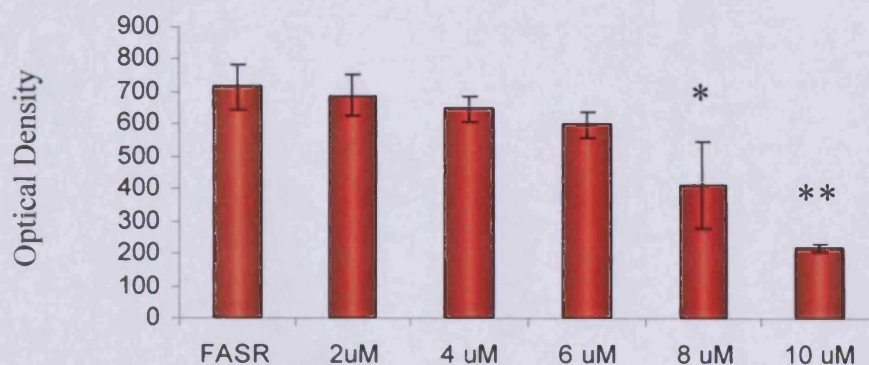
Monitoring of growth sensitivity to excess oxidative stress induced by MSB was also examined in the further acquired endocrine or anti-EGFR resistant models FASR, X-MCF and NEW DUBS. Initial MTT analysis of FASR, X-MCF and NEW DUBS models with doses above 10 μ M MSB revealed such concentrations were markedly inhibitory in these resistant models, thus the impact of lower doses of 2 μ M, 4 μ M, 6 μ M, 8 μ M and 10 μ M MSB was explored over 7 days in these models. Results showed that FASR, X-MCF and NEW DUBS were all highly sensitive to MSB in a dose dependent manner. FASR models were significantly growth inhibited from 8 μ M MSB ($p=0.017$) with an IC_{50} of 8.3 μ M (Figure 3.66). X-MCF cells exhibited a greater sensitivity to growth inhibition by MSB, significantly inhibited from 2 μ M MSB ($p=0.02$) with an IC_{50} of 7.3 μ M (Figure 3.67). NEW DUBS approximated to TAMR cells in their sensitivity to MSB significantly inhibited from 8 μ M ($p=0.022$) with an IC_{50} of 9.3 μ M (Figure 3.68). All the resistant models thus had an IC_{50} of 10 μ M MSB or below, and thus significantly increased sensitivity to this agent versus w/t MCF7 cells.

ROS measurements for w/t MCF7 cells versus the resistant models FASR, X-MCF and NEW DUBS treated with or without growth inhibitory 10 μ M MSB were also made at 7 days (Figure 3.69). Basal ROS levels in all these resistant models were again increased versus w/t MCF7 cells, as seen earlier in this

Chapter 3 – Results

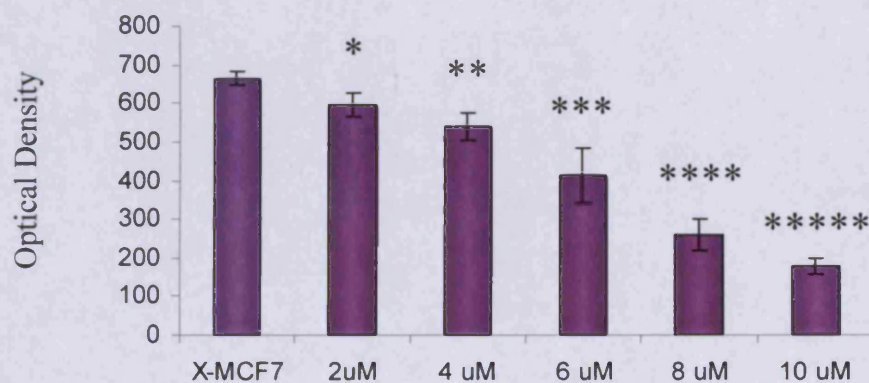
project. FASR cells treated with 10 μ M MSB displayed a 2.5 fold increase in ROS ($p=0.023$). X-MCF cells treated with MSB showed a 3 fold increase in ROS ($p=0.022$), and NEW DUBS with MSB displayed a 2.1 fold increase ($p=0.036$) compared to their respective untreated controls (Figure 3.69). In all resistant models, although showing approximately similar/lower fold induction in ROS with MSB than w/t MCF7 cells, the resistant cells all displayed substantially higher overall ROS levels than their w/t MCF7 counterpart after MSB treatment, which may underlie the more effective growth inhibitory effects seen with this compound in the resistant cells if a threshold for tolerable oxidative stress has been reached in the various acquired resistant cell lines. Of note, therefore, we were successful in promoting cell death in all acquired resistant models by manipulation of redox balance through use of the oxidative stress inducer MSB.

Figure 3.66 MTT analysis of FASR cells treated with MSB for 7 days



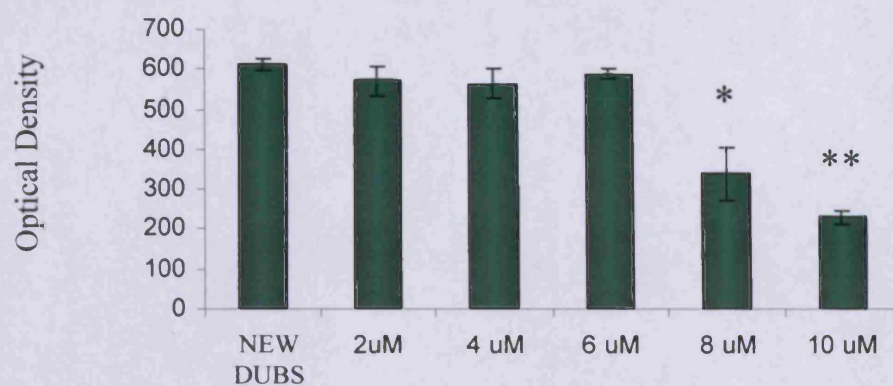
MTT analysis was carried out for FASR cells treated with MSB at 2 μ M ($p=0.351$), 4 μ M ($p=0.132$), 6 μ M ($p=0.113$), 8 μ M (* $p=0.017$) and 10 μ M (** $p=0.011$) for 7 days. Results for cell models were from triplicate preparations with statistical analysis by Student T-test \pm SD versus untreated FASR cells.

Figure 3.67 MTT analysis of X-MCF cells treated with MSB for 7 days



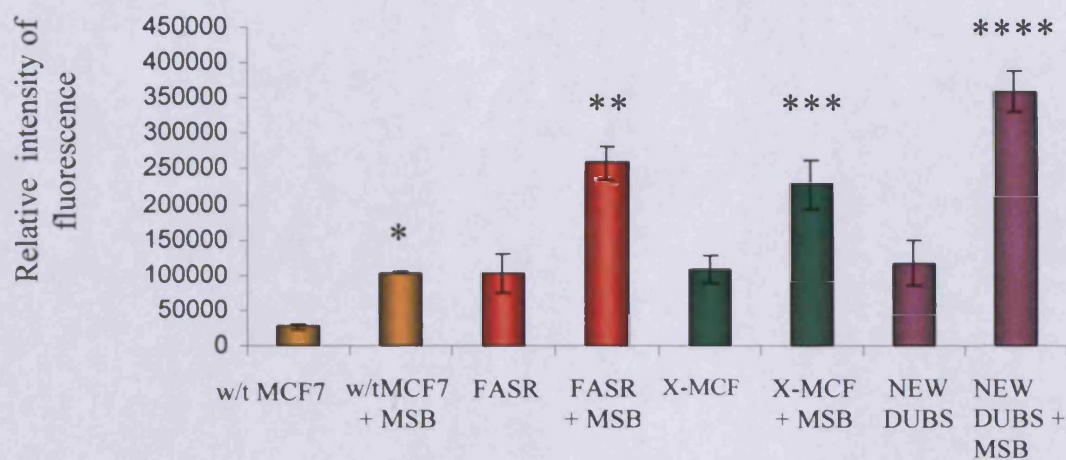
MTT analysis was carried out for X-MCF7 cells treated with MSB at 2 μ M (* $p=0.022$), 4 μ M (** $p=0.004$), 6 μ M (** $p=0.01$), 8 μ M (**** $p=0.0006$) and 10 μ M (***** $p=0.003$) for 7 days. Results for cell models were from triplicate preparations with statistical analysis by Student T-test \pm SD versus untreated X-MCF cells.

Figure 3.68 MTT analysis of NEW DUBS cells treated with MSB for 7 days



MTT analysis was carried out for NEW DUBS treated with MSB at 2 μ M ($p=0.314$), 4 μ M ($p=0.164$), 6 μ M ($p=0.137$), 8 μ M (* $p=0.022$) and 10 μ M (** $p=0.002$) for 7 days. Results for cell models were from triplicate preparations with statistical analysis by Student T-test \pm SD versus untreated NEW DUBS cells.

Figure 3.69 ROS examination in acquired resistant models versus w/t MCF7 cells treated with/without 10µM MSB for 7 days



ROS levels were measured using the H₂DCFDA fluorescent dye in w/t MCF7 cells (+MSB, *p=0.046) versus FASR (+MSB, **p=0.023), X-MCF (+MSB, ***p=0.022) and NEW DUBS (+MSB, ****p=0.036) with/without 10µM MSB for 7 days. Results for cell models were compensated for any growth inhibitory effects of 10µM MSB as in Figures 3.66 – 3.68. Results for cell models were also from triplicate preparations with statistical analysis by Student T-test ± SD versus each cell line's respective untreated control.

Chapter 4 – Discussion

4.1 Discussion & future studies

Chemotherapy and radiotherapy can induce ROS as part of their growth inhibitory mechanism, but it is understood that subsequent induction of antioxidants can ultimately promote development of chemotherapy or radiotherapy resistance in tumour cells (Housset, 1987; Szatrowski & Nathan, 1991; Spitz et al., 1993; Toyokuni S, et al., 1994; Pani et al., 2004; La Torre et al., 1997; Kim et al., 2008). However it remains unexplored as to whether the acquisition of endocrine or anti-EGFR agent resistance is similarly associated with changes in redox balance, where alterations in antioxidants might again actively contribute to such resistant growth. Treating such resistance to targeted therapies remains an area of unmet clinical need in breast cancer since this state can confer a poorer patient outlook (Schiff et al., 2001); hence research in this area is important since it may reveal means of improving in treatment or even preventing resistance, and thereby confer better patient prognosis. This thesis therefore tested the hypothesis that there is an altered antioxidant state, and changes in oxidative stress in acquired resistance, using the various Tenovus acquired resistant breast cancer cell models *in vitro* including cell lines resistant to anti-oestrogen therapy (TAMR, FASR) (Knowlden *et al.*, 2003), severe oestrogen deprivation (X-MCF) (Staka et al., 2005) or the anti-EGFR agent gefitinib (NEW DUBS) (Jones et al., 2004), versus the endocrine responsive parental cell line w/t MCF7. This approach may reveal a new biology of resistance and thus potentially new therapeutic approaches, perhaps which could be extended to multiple resistant states if common changes in redox balance are encountered.

Chapter 4 – Discussion

The above models are reported to mirror the relapse that commonly occurs during treatment of clinical breast cancer, in that they emerged following an initial response period, with the resultant resistant cells having re-instated their proliferation and in some instances having gained invasive behaviour (Hiscox et al., 2004). In keeping with this concept, growth curve analysis of the TAMR, FASR, X-MCF and NEW DUBS models in this thesis was equivalent to untreated w/t MCF7 cells. These data showed the models had indeed become resistant to therapy, in that their growth was re-instated despite the presence of the respective treatment regime, giving confidence that the cells under test were truly reflective of the acquired resistant state in the thesis. The growth data also implied that any differences shown subsequently in redox balance (i.e. in TAC or ROS production) were unlikely to be merely due to a grossly-elevated growth rate in resistant cells, which would make any redox data difficult to interpret, but was likely to be an inherent feature of these cells. Moreover, any changes in redox balance that were subsequently encountered in resistant cells clearly were not giving an overall adverse impact on acquired resistant growth rate. Indeed, there was a small increase in proliferation and cell survival detected in TAMR resistant cells versus the responsive w/t MCF7 cells using ApoAlert MMS and Ki67 staining respectively.

Schiff, and Osborne had previously shown that resistance in their TAMR cell line was associated with increased oxidative stress and also an increase in the antioxidants SOD and GST (Osborne et al., 1991; Schiff et al., 2000), while

Chapter 4 – Discussion

Besada and colleagues (2006) more recently noted using proteomics that their tamoxifen resistant model was also associated with altered oxidative stress processes (amongst changes in other processes such as the mitochondrial respiratory chain, apoptosis, signal transduction, and DNA and protein synthesis machinery). Given these limited tamoxifen resistance data and previous findings linking antioxidants to chemotherapy resistance (Szatrowski & Nathan, 1991; Spitz et al., 1993; Toyokuni S, et al., 1994), the initial phase of this investigation therefore aimed to examine if there was an increase in total antioxidant capacity, and also antioxidant gene expression, not only in the Tenovus antihormone resistant TAMR cells but importantly extending such studies to further resistant models spanning endocrine strategies and an EGFR inhibitor.

TAC was found to be significantly increased in TAMR cells versus w/t MCF7 cells from the basal level measured at 24hours through to 7 and 10days. Of note, the further resistant models FASR, X-MCF, and NEW DUBS all displayed a similar trend of significantly upregulated TAC at these timepoints in comparison to w/t MCF7 cells. It is possible therefore that this elevated level of TAC could be an important feature of acquired resistance that is shared by multiple resistant states. Global oxidative stress-related gene expression, and within this antioxidant enzyme gene expression analysis, was also undertaken using an Affymetrix microarray database of the various cell lines. The web-based technology GeneSifter was used, with careful initial pS2 verification of samples and Affymetrix performance, as well as monitoring of

Chapter 4 – Discussion

multiple probes (using the UGT1A6 antioxidant gene as an example). This gave confidence in the individual gene expression profile changes exhibited. The system proved to have considerable power as a tool for analysing expression data derived from Affymetrix HG-U133A chips for oxidative stress related genes.

200 oxidative stress related genes were compiled of which 39 genes were antioxidants that could potentially defend against pro-oxidant assault on the cell, comprising n=61 Affymetrix probes. Antioxidants exhibited large increases in expression, with 59% of these probes up regulated versus w/t MCF7 cells (n=23/39 genes) that in some instances, spanned multiple forms of resistance. This was further supportive of the concept that prominent increases in antioxidant capacity occur in such resistant cells that may potentially be important in promoting cell survival and therapeutic resistance (Housset, 1987; Szatrowski & Nathan, 1991; Osborne et al., 1991; Spitz et al., 1993; Toyokuni S, et al., 1994; Pani et al., 2004). With elevated levels of antioxidant genes occurring within all four resistant cell lines, it is possible that oxidative stress is a common feature associated with endocrine resistant and anti-EGFR resistant breast cancer cells. These antioxidant gene changes may feasibly contribute to the increased TAC detected in the resistant models.

Subsequent statistical analyses by ANOVA ($p \leq 0.05$) identified that 15 significant antioxidant gene expression changes occurred across the endocrine and anti-EGFR resistant models TAMR, FASR, X-MCF and NEW DUBS

versus the w/t MCF7 model. This testing showed that all 15 of the antioxidant genes had upregulation spanning at least two forms of resistant models, confirming that significant gene expression changes related to oxidative stress could be detected that occurred across all endocrine and anti-EGFR resistant models. 9 of the antioxidant genes showed evidence of up-regulation across all 4 endocrine and anti growth factor resistant models, whilst 6 antioxidant genes were up regulated in 2 or 3 forms of resistance. Ontological and literature searches using GeneCards and Entrez PubMed revealed that of the 9 “generic” shared antioxidant genes, the vast majority had previously been implicated in protecting cells against intracellular oxidative stress promoted by H₂O₂ (Spitz et al., 1993; Suematsu et al., 2002), O₂[•] (Kirkman & Gaetani, 1984; de Hann, 2004) and other ROS, thus potentially preventing against oxidative DNA damage (Dizdaroglu et al., 2002) and cell membrane damage by lipid peroxidation (Biemond et al., 1986). As these events could be detrimental to the cell, sometimes resulting in death if significant oxidative stress is unchecked, it may be that resistant cells have adapted to using antioxidants as a cell survival mechanism in the presence of therapy-induced oxidative stress, where an increase in antioxidants may thus be an advantage to emergence of such resistant growth as previously described for chemotherapy (Szatrowski & Nathan, 1991; Spitz et al., 1993; Toyokuni S, et al., 1994).

The 9 genes increased in all forms of antihormone and anti-EGFR resistance included: (a) Genes within the PRDX/TXN antioxidant network i.e. PRDX6, PRDX1 and PRDX4, three members of the peroxiredoxin (PRDX) family that

regulate intracellular H_2O_2 , short chain organic fatty acids and phospholipid hydroperoxides, protecting cells against injury to the cell membrane and associated signal transduction pathways leading to apoptosis (Kang et al., 1998; Seo et al., 2000; Noh et al., 2001; Karihtala et al., 2003). In addition, TXNRD1 was induced, an antioxidant that can react with oxygen free radicals and helps to replenish depleted PRDX if the latter is inactivated upon over-oxidation by H_2O_2 (Arnér et al., 1995; Powis et al., 2006); (b) Genes involved in the glutathione cycle i.e. GPX2 that also regulates intracellular H_2O_2 and GSTA4 that defends the cell against lipid peroxidation by-products such as 4-hydroxynonenal (4-HNE) (Yang et al., 2003); (c) SOD1 (Cu/Zn-SOD) that destroys free radicals such as $O_2 \cdot$ that in excess can be toxic to biological systems, NQO1, a gene involved in the detoxification pathway, and EPHX2 that degrades potentially toxic epoxides (McCord & Fridovich, 1969; Kirkman & Gaetani, 1984; de Hann, 2004; Cheng et al., 2009).

The 6 antioxidant genes that were shared by at least two forms of resistance versus the w/t MCF-7 model comprised: (a) PRDX3, another member of the PRDX family and hence potentially again within the PRDX/TXN network that can be involved in redox regulation of the cell, protecting radical-sensitive enzymes from oxidative damage by a radical-generating system (Kang et al., 1998; Seo et al., 2000; Noh et al., 2001; Karihtala et al., 2003), as well as TXN that participates in various redox reactions through the reversible oxidation of its active centre dithiol sites and TXNRD2, that like TXNRD1 reacts with oxygen free radicals and helps replenish depleted PRDX that can be inactivated

by over-oxidation with H₂O₂; (b) a further glutathione mechanism-related gene, GLRX, shared by TAMR, FASR and NEW DUBS that as a member of the glutathione cycle reduces low molecular weight proteins (Ji et al., 1999; Valko et al., 2006) and (c) CAT, that protects against the toxic effects of peroxide and G6PD which is involved in the pentose phosphate pathway and is the main producer of NADPH reducing power (Valko et al., 2006).

Given the potential role in cell survival in multiple forms of resistance and according to their strong profiles (with present call at mRNA level and ontology taken into consideration), 11 of the 15 antioxidant genes up regulated in at least two forms of resistance were prioritised for subsequent verification by PCR. The 11 antioxidant genes were the glutathione-related genes GSTA4, GLRX, GPX2; the PRDX/TXN related genes TXNRD1, TXN, TXNRD2, PRDX1 and PRDX6; as well as SOD1, CAT and NQO1 in TAMR and FASR cells versus the parental w/t MCF7 model. It was found that there was some evidence of upregulation in resistance by both Affymetrix and PCR for 8 of these 11 genes, and that these genes again encompassed at least two potential antioxidant networks (TXN/PRDX; glutathione cycle). These antioxidant networks could feasibly contribute to the elevated TAC in resistant cells, and potentially to cell survival and acquired resistant growth. As such, this could even indicate that such antioxidants might comprise potential new targets for resistance, in some instances spanning resistant states.

Chapter 4 – Discussion

Among these, the antioxidant gene GSTA4 was up regulated across all forms of resistance by gene analysis profiling with particular significance (by t-Test) in TAMR and FASR cells, and was similarly shown to be significantly up regulated in both TAMR and FASR models by over 50% at the mRNA level by PCR. This finding is in agreement with the data of Schiff and colleagues who discovered statistically significantly increased GST (twofold; $p=0.004$) activity in their TAMR models, using an antioxidant enzyme assay kit (Schiff et al., 2000), although this thesis was able to also show that GSTA4 gene upregulation extended at the mRNA level to FASR cells. In agreement with the mixed present and absent call at mRNA level using Affymetrix, the gene GLRX required a high cycle numbers of 36 for PCR indicating minimal expression of this gene, albeit increased in resistant cells. Affymetrix analysis for GLRX had showed up regulation in all endocrine resistant models with particular significance in TAMR and FASR and PCR analysis again verified these gene changes, with over 50% and 80% increases for GLRX in TAMR and FASR models respectively. Finally, GPX2 shown to be predominantly upregulated in TAMR models by Affymetrix gene analysis, was verified by PCR with over a 300% increase in the TAMR model. In total, these various gene changes further indicate that the glutathione cycle may be important in such resistant states.

Potentially part of a PRDX/TXN antioxidant network within resistant cells, the antioxidant gene TXNRD1 has been shown by gene analysis profiling here to be up regulated across all forms of resistance, again with particular significance

(by t-Test) in the TAMR and FASR models. In agreement, PCR verified significant increases in both TAMR and FASR cells by approximately 80%. TXNRD2 was also shown to be up regulated predominantly in TAMR models by Affymetrix gene analysis and this was verified by PCR with a significant 50% increase in the TAMR model. The potential importance of this network to the resistant states was further verified by PCR for TXN (whose reducing ability of TXN can be replenished by TXNRD1; Valko et al., 2006). This gene was shown by Genesifter log intensity profiles to be significantly (by t-Test) up regulated in FASR cells and PCR analysis of mRNA expression verified significant increases in FASR cells by 80%, as well as a 70% increase in expression in TAMR cells in comparison to the w/t MCF-7 control. Significant experimental and clinical evidence exists suggesting elevated levels of TXN occur in some forms of cancer such as cervical carcinoma, hepatoma, gastric tumours, colorectal and lung carcinomas (Sinha et al., 1998; Grogan et al., 2000; Raffel et al., 2003; Hedley et al., 2004; Ding et al., 2004; Csiki et al., 2006).

Overexpression of TXN has also been shown to defend cells against pro-oxidant induced apoptosis and thus can promote cell survival as well as conferring a growth advantage to tumours (Grogan et al., 2000; Raffel et al., 2003). Kim and colleagues (2008) have also previously found significantly elevated levels of TXN in tamoxifen resistant cells in comparison to control MCF7 cells, where they were able to relate increased antioxidant expression to an NF-E2-related factor2 (Nrf2)/ARE mechanism. A further gene potentially

Chapter 4 – Discussion

in this network, PRDX1, was also increased in the Kim et al. (2008) study; although PRDX1 and also PRDX6 showed upregulation by Affymetrix gene analysis in the present project in all resistant models, PCR failed to verify such increases in the TAMR and FASR models versus w/t MCF7 cells. Nevertheless, these latter antioxidants were still detected in all cells and may thus still be relevant within this network to such cells.

The antioxidant gene NQO1 had also been shown by gene analysis profiling in the project to be a resistant gene significantly up regulated in both TAMR and FASR models. However, mRNA analysis by PCR was only able to confirm a significant elevation of NQO1 expression in TAMR cells, with a substantial (over 100%) increase in expression versus w/t MCF7 cells, data suggesting this antioxidant may be important in the tamoxifen resistant state rather than spanning other endocrine resistant states. In this regard, interestingly Sripathy and colleagues (2008) have found that in the presence of the novel protein hPMC2, ER beta is recruited as a coactivator complex to mediate transcriptional upregulation of NQO1 in order to protect breast cancer cells against oxidative DNA damage by tamoxifen. This project suggests continued exposure to tamoxifen is also associated with the upregulation of NQO1 which may contribute to cell survival and therefore resistance. Further studies have shown association of NQO1 with the formation of breast cancer and also resistance to chemotherapeutics (Ross et al., 2001; Menzel et al., 2004; Fagerholm et al., 2008),

In agreement with the mixed present and absent call at mRNA level using Affymetrix, CAT required a high cycle numbers of 30 respectively for PCR. Affymetrix analysis for CAT showed up regulation in all endocrine resistant models with particular significance in the FASR model. PCR analysis verified some gene changes, with 20% increase in expression shown in TAMR models and over 40% increase in the FASR model. Previous literature has shown that CAT, alongside GSH, GPX and GST, TXN and PRDX1, and also SOD, is an antioxidant also upregulated following chemotherapy-induced oxidative stress, in some instances promoting resistance (Iwao-Koizumi et al., 2005; Sharma et al., 2007). Exogenous addition of CAT has also been shown to be able to overcome growth inhibition by oxidative stress in ER+ breast cancer cells (Noto et al., 1989).

SOD1 also showed some induction in all resistant models by Affymetrix analysis, but PCR failed to verify this change although of note this gene was again readily expressed in all cells, and coupled with the observation of Schiff and colleagues (2000) showing increases in this gene in their resistant model does not rule out a role for this antioxidant enzyme in resistance. Schiff and colleagues (2000) found significantly elevated levels of SOD in TAMR cells, but this was using an assay kit specifically for SOD activity at the protein level, and it may be that TAMR cells have elevated levels of this enzyme active in their cytoplasm independent of mRNA expression.

Chapter 4 – Discussion

It has previously been found that tamoxifen treatment was associated with increases in certain antioxidants such as NQO1 (Sripathy et al., 2008), where Schiff and colleagues (2000) had argued that initial tamoxifen treatment was again an effective inducer of antioxidant enzymes in responsive cells. Therefore, it was important in this thesis to ascertain whether the antioxidant genes increases actually began earlier within w/t MCF7 cells during their treatment with, and response to, tamoxifen or faslodex, or if the antioxidant increases observed in this project were specifically associated with resistant states. Tamoxifen or faslodex treated w/t MCF7 cells (using inhibitory doses of 0.1 μ M for 10days) were thus tested for total antioxidant capacity. In agreement with the findings from Sripathy and colleagues (2008), results here showed significantly elevated levels of TAC in w/t MCF7 cells in the presence of tamoxifen treatment ($p=0.008$) and that there was also increases in the presence of faslodex ($p=0.001$) versus untreated control w/t MCF7 cells.

After sample verification (again by monitoring the pS2 gene), the expression of the 11 selected antioxidant genes were similarly explored during anti-hormone treatment with tamoxifen or faslodex, by PCR analysis, additionally examining oestrogen impact on expression to determine if the genes might be classically oestrogen regulated. Of the 11 antioxidant genes analysed, none proved to be E₂-induced in this study versus w/t MCF7 cells, indicating that *in vitro* oestrogen/ER signalling was unlikely to be required for their expression. GPX2 was the only antioxidant gene found to be significantly (T-test $p\leq 0.05$) down regulated in w/t MCF7 cells treated with tamoxifen (50% reduction) or

Chapter 4 – Discussion

faslodex (100% reduction), but was again not classically E2-regulated. Interestingly, however, there was more substantial evidence of increases in expression during treatment with tamoxifen and/or faslodex for genes potentially within the glutathione network (GSTA4, GLRX), as well as TXNRD1 from the PRDX/TXN network, and also NQO1 and CAT, in keeping with a lack of classical E2/ER regulation. TXN and TXNRD2, PRDX6, PRDX1 and SOD1 were not tamoxifen or faslodex regulated by PCR in w/t MCF7 cells. Thus, GSTA4 and TXNRD1 were T-test significantly ($p \leq 0.05$) upregulated in the presence of tamoxifen by over 80% and with faslodex by over 140% (compared to E₂ treated w/t MCF7 cells) equating with Affymetrix findings, with increases subsequently retained within resistance by PCR.

NQO1 was also upregulated in w/t MCF7 cells treated with Tamoxifen by over 60% (equating with the data from Sripathy et al., 2008), and also with initial faslodex treatment by over 100%, where this upregulation was subsequently retained only in the TAMR resistant model. Both the antioxidant genes GLRX and CAT were also T-test significantly ($p \leq 0.05$) upregulated in faslodex treated w/t MCF7 cells by over approximately 100% and 140% respectively, subsequently maintained in the FASR model. The GLRX profile again equated with the Affymetrix data, although some discrepancy arose for the CAT gene since this appeared to be specific to resistance according to Affymetrix analysis but this was clearly shown by PCR not to be the case. This discrepancy may feasibly be due to differences in probe/primer performance in Affymetrix versus PCR analysis of CAT mRNA, or even possibly that the PCR primers

detect an altered form of CAT that the Affymetrix studies do not consider (as explained on the official Affymetrix website). While both genes were found to be upregulated in TAMR cells, they were not regulated by early tamoxifen treatment suggesting that longer treatment of the MCF-7 cells with this antihormone might be needed for instigation of this inductive event (in relation to more rapid induction achieved with faslodex which is established as a more potent antioestrogen (Wakeling et al., 1991; Osborne et al., 1995; Dowsett et al., 2005; Nicholson & Johnson, 2005)).

As stated above, the antioxidant genes examined do not appear to be classically E2/ER regulated *in vitro* but 5 of these genes (GSTA4, GLRX, TXNRD1, NQO1 and CAT) were clearly antihormone-induced in the thesis. While Schiff and colleague (2000) suggested that their tamoxifen-induced oxidative stress mechanism was ER regulated, and NQO1 has been reported to be tamoxifen regulated via ER-dependent ARE activation (Montano M et al., 1997, 1998), Kim et al. (2008) reported that the tamoxifen-induced oxidative-stress-related events they observed were ER independent. They found basal phosphorylation of extracellular signal-regulated kinase (ERK) and p38 kinase increased in TAMR cells and that inhibition of ERK significantly decreased the activity of minimal ARE protein expression in TAMR cells, with no effect of E₂ or faslodex on ARE events. Thus it appeared to be the ERK pathway, and not oestrogen receptor signalling, involved in the up-regulation of Nrf2/ARE in their TAMR cells. The mechanism of induction of antioxidants by antihormones thus clearly remains controversial. Indeed, relatively little is

Chapter 4 – Discussion

known about how antihormones can induce (and in turn how oestrogen down regulates) gene transcription (Frasor et al., 2003). This is despite microarray analysis having found that E₂ reduces the expression of a significantly large proportion of the genome, with 70% of all the genes regulated by E₂ treatment of MCF7 cells down regulated and many of these reversed by antihormones (Frasor et al., 2003; Deroo et al., 2004).

Interestingly, while some antihormone-induced genes are growth suppressive, surprisingly the antihormone induced elements reported to date include known growth-promoting genes such as EGFR and HER2, whose induction permits cell survival during antihormone treatment and can subsequently be prominent drivers of antihormone resistant growth (Gee et al., 2003). It is thus possible that early induction of antioxidant genes/networks (e.g. glutathione; PRDX/TXN; and also NQO1 and CAT) and potentially parallel TAC increases during antihormone treatment of w/t MCF7 cells might also serve to allow residual cell survival and could limit growth inhibitory response during the rigours of early antihormone treatment, as has been noted with chemotherapy and radiotherapy (Yokomizo et al., 1995; Sinha et al., 1998; Gorgan et al., 2000; Hedley et al., 2004; Ahmadi et al., 2006; Cheng, et al., 2009). Such increases could help support a residual cell population for emergence of resistance, alongside (and potentially interactive with) the induced EGFR during tamoxifen treatment and subsequently into resistance (Gee et al., 2003; Knowlden et al., 2003). Interestingly, since some antioxidant genes such as CAT (and also SOD) are also upregulated by other agents such as histamines

(Medina et al., 2007), and several antioxidant genes again such as CAT and genes in the glutathione cycle including GST (as well as GSH and GPX) and PRDX/TXN networks (e.g. TXN, PRDX1) can also be upregulated following chemotherapy (Iwao-Koizumi et al., 2005; Sharma et al., 2007), it is possible that induction of some antioxidant genes/networks and parallel increased TAC may even comprise a generic stress response mechanism used to survive multiple adverse agents, including antihormonal measures.

The observed antihormone induction of antioxidants may imply that, in addition to their potential targeting value in resistance, such antioxidants co-targeted alongside antihormones could have some therapeutic value during the endocrine responsive phase of the disease to prevent emergence of resistance, as has been noted for combination anti-EGFR/antihormone treatment (Gee et al., 2003). Any antioxidant genes (e.g. GPX2; also TXN and TXNRD2) that were found by PCR and Affymetrix analysis not to be induced by tamoxifen or faslodex treatment in this thesis but only increased once resistance is acquired may of course also potentially become growth-contributory once resistance is established. Of note, all antioxidant genes shown to be elevated in resistance could also potentially be interactive with any known mitogenic contributory pathways in this state, notably EGFR signalling in TAMR cells (Knowlden et al., 2003). Increased EGFR signalling has not only been previously linked to acquired tamoxifen resistance *in vitro* but has also been reported to be deregulated in further acquired resistant cell models, including some FASR lines (Gee et al., 2003; Hiscox et al., 2004; Jones et al.,

2004; Gee et al., 2005; Jones et al., 2005; Knowlden et al., 2003; McClelland et al., 2001).

To examine if the 11 antioxidant genes had any potential interplay with EGFR in resistance, the impact of the EGFR inhibitor Gefitinib was investigated on antioxidant gene expression in parallel with growth studies in TAMR cells, using a dosage known to selectively target the activity of this receptor in such cells (1 μ M; Knowlden et al., 2003). Expression of the antioxidant genes was monitored by PCR in mRNA samples prepared from TAMR cells +/- gefitinib for 7days. Moreover, growth impact of additional signal transduction inhibitors (STIs) known to target further elements in EGFR signalling and further pathways linked to tamoxifen resistance was examined (e.g. MAPK signalling using U0126 [Knowlden et al., 2003; Britton et al., 2006] wortmannin to target PI3K signalling (Jordan et al., 2004), c-Src activity using AZD0530 (Hiscox et al., 2006). and signalling of a downstream nuclear transcription factor (Nf κ B) with parthenolide (Zhou et al., 2005)). MTT analysis of these different signal transduction pathway inhibitors in TAMR cells confirmed substantial growth inhibition with gefitinib, AZD0530, Parthenolide and U0126, although no change was demonstrated with wortmannin in this study.

Further exploration of the gefitinib response using Ki 67 staining and ApoAlert MMS assays showed that there was also a 60% decrease in proliferation in TAMR treated with GEF but only modestly-

increased apoptosis. These data confirm the relevance of such signalling to TAMR growth and were generally in keeping with previous data obtained for this model (Knowlden et al., 2003; Hiscox et al., 2006) as well as the emerging importance of such signalling in clinical tamoxifen resistance (Gee et al., 2005).

Of the 11 antioxidant genes further analysed by PCR for response to gefitinib in TAMR cells, elements representing the glutathione and also PRDX/TXN networks (i.e., the antioxidant genes GSTA4, GLRX, TXNRD1 TXNRD2 and, TXN), as well as NQO1 and CAT, all showed T-test significant ($p \leq 0.05$) downregulation, to a greater or lesser extent, in the presence of the growth-inhibitory dose of gefitinib implying these antioxidants are all positively regulated by EGFR signalling in TAMR cells. Thus, GSTA4 was inhibited in TAMR cells treated with TKI by over 40%, GLRX by approximately 20%, TXNRD1 by over 90%, TXN by approximately 40%, TXNRD2 by approximately 45%, NQO1 by over 55% and CAT by approximately 45% compared to the untreated TAMR cells. In addition, while PRDX6 and SOD1 were not regulated by TKI treatment ruling out their involvement in such signal transduction pathways, the expression of PRDX1 detected in TAMR cells was also very slightly decreased by 10% with gefitinib suggesting partial EGFR regulation. In accordance with the findings linking EGFR to redox balance in further cell types reported by Duval and colleagues (2002), who showed that enhanced cellular antioxidant defences against mitochondrial oxidative stress can occur through EGFR-dependent activation of antioxidant genes (in their

studies exemplified by GPX), it appears that 8 of the 11 antioxidant genes require stimulation by EGFR in the TAMR cells, where the subsequent inhibition of this tyrosine kinase has therefore resulted in their downregulation.

Thus, most of these antioxidant genes do appear to interplay with EGFR in TAMR cells, where it is known that EGFR can be activated by pro-oxidants such as H₂O₂ (King et al., 1989; Knebel et al., 1996; Rao, 1996) resulting in the upregulation of antioxidants (Duval et al., 2002; Kim et al., 2008). Interestingly, Kim and colleagues (2008) showed increased expression of Nrf2/ARE-dependent anti-oxidant proteins in their tamoxifen resistant breast cancer cells and they showed that tamoxifen induced oxidative stress activated MAPK signalling and subsequently increased Nrf2 levels to increase ARE activity and antioxidant gene expression (Kim et al., 2008). Induction of stress responsive and cytoprotective enzymes encoded by their mechanism included SOD, CAT, GPX, TXN, NQO1 and GST in their TAMR cells. Since tamoxifen resistance could be partially reversed by Nrf2 siRNA, this Nrf2 mechanism contributed to TAMR cell growth. Results of the present investigation could link in further specific antioxidant genes downstream and also EGFR upstream if this Nrf2 mechanism were to be apparent within our own TAMR cells. In this regard, EGFR has previously been shown to regulate MAPK activity in these cells (Knowlden et al. 2003) and interestingly Nrf2 expression has also been shown through a preliminary heatmap analysis to increase, as reported by Kim and colleagues (2008), in the resistant cells studied in the present project (Dr Gee, personal communication).

The gefitinib data suggest the antioxidant genes could feasibly be an important part of the EGFR signalling mechanism in TAMR cells, driven by EGFR to potentially promote cell survival. The value of these antioxidant genes as targets therefore remains possible if they are indeed growth contributory; however, whether their individual targeting would further improve on EGFR blockade alone in TAMR cells (given that the TKI gefitinib reduces their expression to some degree here) is difficult to predict. Since some of the antioxidant genes appear to be EGFR regulated, it is also possible that the increases detected for these antioxidant genes during antihormone response in w/t MCF7 cells could again be a consequence of an antihormone-induced oxidative stress mechanism involving increases in EGFR that could subsequently maintain cell survival during early treatment (Gee et al., 2003).

While the antioxidant gene findings are certainly interesting, it was important in the thesis to consolidate further the concept that interplay might occur between EGFR signalling and the antioxidants in the TAMR cells beyond the mRNA expression level. To do this, the impact of the EGFR inhibitor gefitinib and further growth factor signalling inhibitors on TAC in TAMR cells was also investigated in the project. Paradoxically, there appeared to be no parallel relationship between TAC and the EGFR mitogenic pathway in TAMR cells. Thus, TAC levels for TAMR cells treated with the TKI, while at 24hours significantly down regulated, were surprisingly further up regulated by 7days and remained elevated at 10days. There was thus a difference between most of

the antioxidant genes examined at the mRNA level at 7 days and the TAC findings in the thesis with the TKI. In explanation, it is possible that the antioxidant gene mRNA expression measured is not reflective of TAC. In the future, antioxidants should thus also be measured at the protein level (e.g. using Western blotting) in the breast cancer resistant models versus the parental w/t MCF7 cell line to account for their potential replenishment and recycling in order to identify if these antioxidants contribute to TAC. Pharmacological challenge of any of the induced antioxidant genes /networks using antioxidant inhibitors listed in Tables 3.2 and 3.3, or molecular knockdown using SiRNA, could further explore if these are contributory to TAC and resistant growth. However, altered levels of non-enzymatic antioxidants as well as enzymatic antioxidants have also been related to changes in signal pathways and are evident in many human cancers (McEligot et al., 2005). Therefore it may be that certain non-enzymatic antioxidants (which can include lipoic acid, Vitamins C, E, carotenoids, natural flavonoids, and melatonin) that have not been accounted for in this investigation may actually be playing a crucial role in making up the cellular TAC analysed in TAMR cells (Mates et al., 1999; McCall & Frie, 1999; Mathews et al., 2000).

Therefore it may be that despite the expression deregulation of antioxidants revealed in this investigation, perhaps these particular antioxidant genes really are independent from the TAC increases noted in TAMR cells. Thus, in contrast to most of the antioxidant gene data, TAC was not convincingly positively EGFR (or associated kinase) regulated in our TAMR model. Indeed

it was actually further stimulated during growth inhibition by the EGFR inhibitor. Only one antioxidant gene examined here, GPX2 (a glutathione cycle component) was, like TAC, induced further by TKI and so may be contributory in some way not only to the increased TAC detected in the TAMR cells but also subsequently to the further increased TAC during gefitinib treatment. Thus, the GPX2 gene was shown to be T-test significantly ($p \leq 0.05$) upregulated in the presence of the TKI gefitinib by over 130% compared to the untreated TAMR cells. However, TAC (and potentially any contributory GPX2) in TAMR cells does appear to be driven by EGFR-independent mechanisms, contrasting the majority of the particular antioxidant gene expression we studied.

In this regard, the TAC in TAMR cells also does not appear to be positively regulated by Src or MAPK as TAC analysis of further signal transduction inhibitors in TAMR also showed significant upregulation with AZD0530 or U0126. Martin and colleagues (2008) recently discovered that parthenolide possesses free radical scavenging activity against a wide range of reactive oxygen species *in vitro* with greater activity than Vitamin C. They also found that parthenolide attenuated the formation of UV-induced hydrogen peroxide and *In vivo*, reduced UV-induced DNA damage and apoptosis (Martin et al., 2008). Given this apparent inherent antioxidant capacity, therefore, the TAC increase associated with parthenolide in TAMR cells here may not actually be a reliable indication of independence of antioxidant capacity from NfκB in

such cells, and so future studies examining alternative means of manipulating NfκB, in parallel with TAC measurement, remain needed.

While probably not EGFR driven, TAC could potentially interplay with IGF1R signalling in TAMR cells. Indeed, further growth factor receptors such as the IGF1R and other members of the ErbB family have previously been linked with oxidative stress (Khan EM, et al., 2006). Moreover, Knowlden and colleagues have shown that IGF1R/Insulin receptor substrate-1 (IRS1) signalling is also strongly promoted by treatment with gefitinib (Knowlden et al., 2008). The present investigation has also shown up regulated TAC in NEW DUBS cells at 24hours, 7days, and 10days compared to w/t MCF7 cells, potentially equating with the prominent IGF1R signalling also described for these acquired resistant cells (Jones et al., 2004). However, TAC was also high in this investigation in cell lines where EGFR and IGF1R signalling are already known to not be prominent, for example in the FASR and X-MCF lines (Staka et al., 2005). Therefore the TAC induction could also be driven by other as yet unknown signalling mechanisms in resistant cells, or the TKI/STI observations could even be further supportive of the concept that TAC increases comprise a generic stress-induced mechanism launched to anti-tumour agents, as a mechanism of residual cell survival during substantial growth inhibition. IGF1R and further potential signalling mechanisms contributing to TAC could be investigated by future relevant STI challenge. There thus appears to be induction of TAC during growth inhibition by antihormone treatments in endocrine responsive breast cancer cells, with these increases retained into the

acquired antihormone resistant models (perhaps contributing to cell survival and growth in these states), with TAC then induced further by growth inhibitory secondary agents in TAMR cells (e.g. TKI and other STIs) to again allow residual cell survival, permitting and maintaining subsequent resistance (as in NEW DUBS cells).

If TAC is indeed involved in cell survival and growth, these findings could indicate that full blockade of the induced TAC might treat resistance and could potentially improve response in TAMR cells when targeted alongside gefitinib. In these regards, the investigation has provided a preliminary exploration of BSO +/- gefitinib in TAMR, using BSO to potentially target the glutathione inducer of GPX2 (Lewis-Wambi et al., 2009) which could be contributing to TKI-induced TAC. Interestingly, Lewis-Wambi and colleagues have recently identified and characterised a novel resistant subclone of w/t MCF7 cells, MCF-7:2A. This group's studies suggest endocrine resistant cells can be inhibited by higher oestrogen dosages, but interestingly this cell line only undergoes dramatic increase in apoptosis (7-fold) in the presence of combined treatment of E2 plus BSO, rather than with E2 alone, suggesting the antioxidant target of BSO (potentially the elevated glutathione measured in these cells) may be contributing to cell survival in this model. Their microarray analysis revealed upregulation of the GPX2 antioxidant gene by 40-fold in MCF-7:2A cells compared to hormone-responsive MCF-7 cells, where BSO almost completely inhibited this increase (Lewis-Wambi et al., 2009).

Of note, the GSH/GPX system has been reported in other systems to be able to defend against elevated levels of oxidative stress to promote cell survival (Fu et al., 2007). While not being able to further add to the gefitinib effect, MTT analysis promisingly revealed a significant decrease in TAMR growth in the present study with 100uM BSO. This simplistically would suggest that BSO targeting of a deregulated glutathione antioxidant pathway could, as in the Lewis-Wambi studies, have potential value in treating resistance. However, TAC analysis in this thesis (not examined in the Lewis-Wambi study) paradoxically showed significant increases in TAC during BSO treatment, implying any growth inhibitory effect of this dosage of BSO was likely to be non-specific since the “target” antioxidant capacity was not depleted. This agent may thus again simply be promoting a stress response and thus increasing TAC during its growth inhibition of TAMR cells. Further study of the role of the relationship between GPX2 and TAC needs to be performed in the future, perhaps using a GPX2 siRNA approach.

Unfortunately, the data with gefitinib in the TAMR cells also indicate targeting of the further antioxidant genes that are increased in resistance is unlikely to deplete TAC and thereby any associated cell survival. However, recent studies from Kim and colleagues (2008) have shown that blocking Nrf2, a key regulator of ARE-mediated transcription and hence potentially of multiple antioxidant expression in their own TAMR model, is able to restore tamoxifen growth inhibition in TAMR cells (Kim et al., 2008). This implies global depletion of ARE activity (and thus presumably many of the cell's

antioxidants), if achievable and tolerable, might provide one strategy to target the increased TAC and thus deplete growth in cells resistant to endocrine (or other targeted) agents. ARE signalling and its regulation should thus be examined within our TAMR cells, both in relation to regulation of their elevated TAC and their growth in the future.

In addition to monitoring TAC and antioxidant enzymes, this thesis also monitored changes in Redox status (ROS level) as a further indicator of the level of oxidative stress in the various acquired resistant models and during antihormone or gefitinib response. In keeping with the concept that resistance to targeted therapies is associated with an increased oxidative stress and (based on existing chemotherapy data and previous tamoxifen resistance findings from Schiff et al. [2000] and Kim et al., [2008]) that a signalling/ARE mechanism may promote increases in antioxidant capacity to maintain growth and cell survival in the resistant state, ROS levels were found to be increased in all the acquired resistant models versus w/t MCF7 cells. Thus, there was a consistently increased level of ROS in TAMR cells versus w/t MCF7 reaching a 190% increase ($p=0.01$) after 10 days culture. Unique to this investigation ROS was shown to also be up regulated in FASR, X-MCF and NEW DUBS resistant models in a similar manner to TAMR cells with at least 100% increase versus w/t MCF7 cells (T-test $p\leq 0.05$). Along with the observations of increased antioxidants, the ROS data confirm that cells that have acquired resistance to targeted therapies are commonly experiencing increased oxidative stress. While Kim and colleagues (2008) reported significantly decreased

intracellular peroxide production alongside increased antioxidants in their TAMR cells (contradicting the findings of this investigation of increased ROS alongside increased antioxidants and presumably reflecting considerable ROS buffering by the antioxidants in their model), Schiff et al. (2000) also reported an increase in oxidative stress in their TAMR model which is in agreement with this project.

However, the modestly elevated ROS detected observed does not appear to be promoting substantial cell death in the TAMR cells and other resistant models (as demonstrated by the growth data findings previously described). The parallel elevated TAC may indeed, therefore, be helping to maintain cell survival in the face of their increased oxidative stress. Antioxidants at relatively low concentrations are able to compete with oxidizable substrates, thus significantly delaying or inhibiting their oxidation and thus preventing extreme levels of ROS being reached in cells that would promote cell death (Halliwell & Gutteridge, 1989). Moreover, it should be remembered there is also literature to indicate modest redox is also capable of triggering other signalling mechanisms that could potentially directly contribute to resistant growth: for example redox is known to be able to induce AP-1, EGFR signalling and diverse kinase activation (King et al., 1989; Knebel et al., 1996; Rao, 1996; Schiff et al., 2000; Kim et al., 2008). Future studies could explore if there is any ROS cross talk, for example, with EGFR phosphorylation status in the resistant cells. For a table of all signalling pathway genes that have been associated with increased oxidative stress, as compiled from literature and the

web based GeneCards® database in this thesis, the reader is referred to Appendix 1. Many of such elements are at increased activation in TAMR cells (e.g. EGFR, MAPKs; Knowlden et al., 2003) and so it is feasible that the modestly-increased ROS levels detected in the resistant models may be contributing to the triggering of such signalling and thereby resistant growth.

An increase in ROS was not detected during short term (up to 10 days) tamoxifen or faslodex antihormone treatment in w/t MCF7 cells in this investigation, where such cells consistently had low ROS levels. Some studies have previously described that tamoxifen is capable of causing oxidative stress and thereby apoptosis in certain contexts, including in T-leukaemic Jurkat and ovarian A2780 cancer cells (Nuwaysir et al., 1998; Wei et al., 1998; Day et al., 1999; Ferlini et al., 1999; Peralta et al., 2006)). For example, TAM could be activated into reactive electrophilic metabolites. However, it also launches mechanisms to protect against oxidative lipid and DNA damage by inducing phase I and II metabolising enzymes (Nuwaysir et al., 1998; Wei et al., 1998). Perhaps any initial ROS induced by antihormones (that could be detrimental to cell survival) was rapidly buffered in the endocrine responsive, ER+ w/t MCF7 cell context by the readily-detectable anti-hormone induced TAC, limiting cell death effects with these agents. Interestingly, although antihormones are known to promote anti-proliferative effects (Dowsett et al., 2005; Lacey et al., 2005; Nicholson & Johnson, 2005), all such agents to date exert only small pro-apoptotic effects, in keeping with their known induction of EGFR/ErbB2

survival signalling (Gee et al., 2003). Such antihormone-induced cell survival mechanisms may extend to increased TAC.

Given that EGFR signalling has been shown in some systems to be able to promote oxidative stress (Rao, 1996) and that EGFR is known to be increased in the TAMR cells (Knowlden et al., 2003) it was important to examine the relationship between EGFR and ROS within TAMR cells by treating them with gefitinib. However, this agent showed at least a 2fold significant (T-test, $p \leq 0.05$) further up regulation in ROS at 24hours, 7 and 10days, suggesting there is actually no positive regulation of ROS within TAMR cells by EGFR. This appears to extend to the additional STIs examined in the thesis (including the MAPK signalling inhibitor). However, it does confirm earlier findings by Mimeault and colleagues (2005) and Kishida and colleagues (2005) that gefitinib promotes ROS in prostate and gastric cancer cells respectively.

TAMR cells also showed a similar significant up regulation of ROS with AZD0530, Parthenolide and U0126 (although no change was again observed for Wortmanin as in the MTT and TAC analysis). These inhibitor data in TAMR cells appear to indicate that it is unlikely EGFR-related signalling is promoting their oxidative stress, although this does not preclude increased oxidative stress impacting on EGFR activity in the resistant cells, an aspect which warrants future study.

The gefitinib- and other STI-induced ROS in TAMR cells occurred alongside these agents promoting significant anti-proliferative effects and growth inhibition. The detectable drug-induced oxidative stress in TAMR cells may in some way contribute to these anti-tumour effects. However, this oxidative stress mechanism encompassed a substantial TAC response in TAMR cells. This could potentially defend against excessive ROS and limit STI pro-apoptotic effects, enabling residual cell survival in the presence of drug. In agreement with this concept, there was only a modest detectable apoptotic effect of gefitinib in the TAMR cells; indeed, the action of such STIs used as single agents has to date largely been reported to be cytostatic in cancer.

Halliwell (2006) stated that modestly increased ROS is tolerable and not pro-apoptotic in some cancer cells, where this ROS is held at tolerable, beneficial levels by the triggered antioxidant response (Halliwell & Cross, 1992). However, Halliwell also suggested that if it were possible to reach excessive ROS levels in cancer cells, this may be sufficient to overcome the antioxidant buffering mechanism and be able to promote marked cell death and more substantial antitumour effects (Halliwell, 2006). Since this could have therapeutic implications, this concept has been addressed in this thesis in the acquired resistant models using the agent menadione (MSB) whose antitumour effects have been under investigation since 1947 (Michell et al., 1947; Mitchell et al., 1948; Su et al., 1991). Thor and colleagues (1982) showed that alongside the production of H_2O_2 , menadione generates O_2^\bullet and semiquinone radicals through redox cycling of the quinone. A mechanism where MSB promotes

Chapter 4 – Discussion

excess oxidative stress is also supported by Nutter et al., (1991), who detected MSB-induced oxidative stress with increased DNA strand breaks due to OH^\bullet in MCF-7 cells. Noto and colleagues (1989) demonstrated that MSB at $\sim 14\mu\text{g/ml}$ was also able to produce a 50% inhibition of breast cancer (MCF-7) cell growth. This was suppressed by the addition of exogenous catalase, suggesting the excessive production of H_2O_2 and thus oxidative stress was responsible for this growth inhibition (Noto et al., 1989; Nutter et al., 1991).

Interestingly, induction of excess ROS using the agent MSB in this project proved to be highly growth inhibitory not only in w/t MCF7 but also in TAMR cells and the other acquired resistant models. Of note, the resistant models (which as stated above all had a higher basal ROS level) had an increase in sensitivity to the anti-tumour effect of this agent versus the endocrine responsive cells. Thus, MTT for w/t MCF7 cells treated with MSB showed a dose dependent decrease in growth with a calculated IC_{50} of $15.4\mu\text{M}$, similar to that reported by Noto et al. (1989). TAMR cells also showed a similar dose dependent decrease, although they proved more highly sensitive, with a lower calculated IC_{50} of $10\mu\text{M}$ for MSB. High sensitivity to MSB was also shown in FASR, X-MCF and NEWDUBS via MTT analysis, again with considerably lower calculated IC_{50} values versus w/t MCF7 cells of $8.3\mu\text{M}$, $7.3\mu\text{M}$, and $9.3\mu\text{M}$ respectively. There were increased ROS levels in w/t MCF7 cells, TAMR and all the additional resistant cells treated with MSB, confirming that MSB induces substantial ROS within these various models. However, higher ROS levels were achieved with MSB in the resistant models versus the w/t

Chapter 4 – Discussion

MCF7 cells. In accordance with Halliwell's concept (2006), perhaps by induction of these more extreme ROS levels in the various resistant models using MSB, the TAC that may be contributing to their cell survival basally is overpowered, allowing oxidative stress-driven cell death in resistant models. Future consolidation of this concept (and its relation to DNA damage and lipid peroxidation) will be required.

4.2 Summary of potential redox mechanism in acquired resistant breast cancer cells and therapeutic implications:

From the *in vitro* data amassed in this project spanning multiple models and the diverse methodological approaches employed, it seems that oxidative stress commonly increases in cells that have been exposed long-term and become resistant to various endocrine and other targeted therapies, observations that extend published tamoxifen and chemotherapy data (Figure 4.1a). This modest change in redox may or may not activate pro-proliferative signalling in the acquired resistant cells; however, the altered redox does not appear to adversely impact on growth rate of the various resistant cells or to be associated with high levels of cell death as measured in these cells. Any potentially adverse (pro-apoptotic) effects of increased oxidative stress could feasibly be being prevented by the marked increased antioxidant capacity that this thesis has also detected in all of the acquired resistant cells models. This event may thus, as in the chemotherapy resistance scenario, be preventing excessive increases in oxidative stress, promoting cell survival and thereby contributing to acquired resistant growth with multiple targeted therapies (Figure 4.1a).

Interestingly, examination of short-term treatment with multiple antihormones in endocrine responsive cells in the thesis also indicated that TAC (and

expression of some antioxidant genes) commonly begins to be induced during early treatment. However, given that ROS increases are not detected in parallel, this antioxidant capacity may be overcoming any modest initial ROS induction by treatment. Again, the antioxidant increase could be feasibly contributing to cell survival, limiting apoptosis (alongside an established role for antihormone-induced EGFR/HER2 signalling) during early treatment of endocrine responsive cells.

Further targeted therapy with STIs in the established acquired resistant cells (such as gefitinib, AZD0530, Parthenolide or U0126 in TAMR) induced additional ROS increases (that could perhaps be contributory to their anti-tumour effect). This implies that ROS is not EGFR promoted in TAMR cells, (although these data do not preclude ROS impacting on EGFR signalling as part of the growth regulation in such cells). Importantly, however, such treatment also further increased antioxidant capacity. This event may again be maintaining residual cell survival and hence limiting maximal STI pro-apoptotic effect.

The thesis also determined that there was increased expression of several antioxidant genes in the acquired resistant cells (including those potentially within PRDX/TXN and glutathione networks), in some instances again spanning multiple resistant states. These could potentially have contributed to the increased antioxidant capacity increases within resistant cells. However, the studies examining impact of gefitinib and other STIs in TAMR cells indicated

Chapter 4 – Discussion

that their total antioxidant capacity, unlike expression of most of these antioxidant genes, was not EGFR/kinase signalling regulated suggesting that TAC is dissociated from such gene expression in the resistant cells. Thus, further genes and signalling mechanisms may drive the increased antioxidant capacity in resistant cells. Data in the thesis initially suggested a potential contributor could be the GPX2 antioxidant gene; however, this remains to be consolidated since application of an agent (BSO) to target its potential glutathione mechanism proved equivocal.

With regards to the therapeutic implications of these findings, this thesis has suggested that targeting of the identified antioxidant genes increased in resistance may not in general be useful in decreasing TAC (as based on the gefitinib findings), although as stated above further manipulation of GPX2/glutathione is worthy of further investigation. However, given available literature, global depletion of TAC, if achievable, could perhaps be useful to block cell survival in acquired resistance (and alongside antihormones improve initial response), potentially extending to multiple acquired resistant states (Figure 4.1b). Equally, however, since the resistant cells have a higher basal ROS than their endocrine responsive counterpart, this thesis importantly has also been able to show that they may be particularly sensitive to treatment with agents which induce more excessive oxidative stress, presumably exceeding the buffering capacity of the antioxidant capacity in such cells to promote cell death events. Indeed, one such agent (MSB) was substantially growth inhibitory in resistant cells, extending to the multiple acquired resistant states

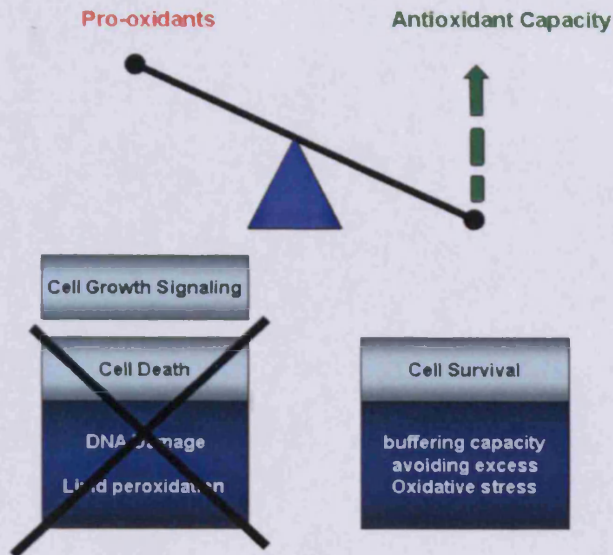
Chapter 4 – Discussion

(Figure 4.1b). The findings in the thesis may thus have therapeutic implications for acquired resistance to various targeted therapies (and potentially some selectivity, since it was observed that the endocrine responsive cells were less sensitive to ROS manipulation). In turn, Beck and colleagues (2009) established that Menadione induced oxidative stress should affect cancer cells such as w/t MCF7 cells to a greater extent than normal cells, and therefore this differential sensitivity could feasibly have clinical applications (Beck et al., 2009).

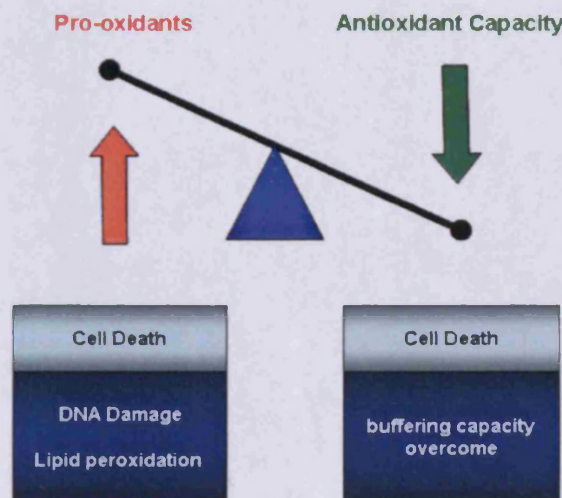
The novel findings in this thesis with Menadione that suggest such strategies may have relevance in treating acquired resistant states join those increasing from other groups who are proposing this may be a useful tool in breast cancer therapy. Thus, Akiyoshi and colleagues (2009) have very recently found that Menadione caused mitochondrial dysfunction, including a disappearance of mitochondrial membrane potential, and that this mitochondrial damage was induced by Menadione-induced ROS with subsequent activation of caspase 7 and 9 in MCF-7 cells (Akiyoshi et al., 2009). They demonstrated that Menadione-induced apoptosis (at a calculated IC_{50} of $14.2\mu\text{M}$) was selectively initiated by the mitochondria related pathway and suggested that it may be a potential growth inhibitory breast cancer treatment (Akiyoshi et al., 2009).

Figure 4.1

a) Model of the redox balance in acquired resistant breast cancer cells *in vitro*



b) Potential growth inhibition strategies for acquired resistance based on redox findings *in vitro*



Pro-oxidant activation of cell growth signalling may enable resistant breast cancer cells to grow. In response, antioxidants levels may be increased to buffer any excess oxidative stress that may cause cell death, therefore promoting cell survival (a). Potential growth inhibitory strategies that promote cell death in these resistant models may therefore include induction of pro-oxidants, such as by MSB as demonstrated in this thesis, or inhibition of Total Antioxidant Capacity either pharmacologically or by SiRNA (b).

Chapter 4 – Discussion

It should be remembered that the relationship between oxidative stress and breast cancer growth is complex, as is the feasibility of using agents influencing redox, given that manipulation of oxidative stress could potentially exert effects on normal tissues (Valko et al., 2006). There remains much still to be done, therefore, to consolidate the relevance of antioxidants as therapeutic targets in endocrine and anti EGFR resistant breast cancer, or promotion of excessive oxidative stress in such cells. However, the findings and resultant concepts emerging from this thesis are exciting when considering potential treatments for acquired resistance to endocrine agents as well as other targeted therapies that are clearly worthy of future exploration given that new therapies remain much needed for these adverse states.

Chapter 5 – References

References

- Acconcia F, Totta P, Ogawa S, Cardillo I, Inoue S, Leone S, Trentalance A, Muramatsu M, Marino M. Survival versus apoptotic 17beta-estradiol effect: role of ER alpha and ER beta activated non-genomic signaling. *J Cell Physiol.* 2005;**203**(1):193-201.
- Adams F. *Works by Hippocrates.* eBooks@Adelaide. 2004.
- Ahmadi R, Urig S, Hartmann M, Helmke BM, Koncarevic S, Allenberger B, Kienhoefer C, Neher M, Steiner HH, Unterberg A, Herold-Mende C, Becker K. Antiglioma activity of 2,2':6',2"-terpyridineplatinum(II) complexes in a rat model--effects on cellular redox metabolism. *Free Radic Biol Med.* 2006;**40**(5):763-78.
- Aibara S, Yamashita H, Mori E, Kato M, Morita Y. Isolation and characterization of five neutral isoenzymes of horseradish peroxidase. *J Biochem (Tokyo).* 1982;**92**(2):531-9.
- Akiyoshi T, Matzno S, Sakai M, Okamura N, Matsuyama K. The potential of vitamin K(3) as an anticancer agent against breast cancer that acts via the mitochondria-related apoptotic pathway. *Cancer Chemother Pharmacol.* 2009. [Epub ahead of print]
- Anderson CP, Tsai JM, Meek WE, Liu RM, Tang Y, Forman HJ, Reynolds CP. Depletion of glutathione by buthionine sulfoxine is cytotoxic for human neuroblastoma cell lines via apoptosis. *Exp Cell Res.* 1999;**246**:183-192.

Chapter 5 – References

- Anderson WF, Chen BE, Jatoi I, Rosenberg PS. Effects of Estrogen Receptor Expression and Histopathology on Annual Hazard Rates of Death from Breast Cancer. *Breast Cancer Res Treat.* 2006; [Epub ahead of print]
- Arnér ESJ, Björnstedt M, Holmgren A. 1-Chloro-2,4-dinitrobenzene Is an Irreversible Inhibitor of Human Thioredoxin Reductase. *The American Society for Biochemistry and Molecular Biology, Inc.* 1995;270 (8): 3479-3482
- Babior BM. NADPH oxidase: an update. *Blood.* 1999;93(5):1464-76.
- Bachert C, Hormann K, Mosges R, Rasp G, Riechelmann H, Muller R, Luckhaupt H, Stuck BA, Rudack C. An update on the diagnosis and treatment of sinusitis and nasal polyposis. *Allergy.* 2003;58(3):176-91.
- Barondeau DP, Kassmann CJ, Bruns CK, Tainer JA, Getzoff ED. Nickel superoxide dismutase structure and mechanism. *Biochemistry.* 2004;43(25):8038-47.
- Batandier C, Fontaine E, Keriél C, Leverve XM. Determination of mitochondrial reactive oxygen species: methodological aspects. *J Cell Mol Med.* 2002;6(2):175-87.
- Beck R, Verrax J, Dejeans N, Taper H, Calderon PB. Menadione reduction by pharmacological doses of ascorbate induces an oxidative stress that kills breast cancer cells. *Int J Toxicol.* 2009;28(1):33-42.
- Beckman JS, Beckman TW, Chen J, Marshall PA, Freeman BA. Apparent hydroxyl radical production by peroxynitrite: implications for endothelial injury from nitric oxide and superoxide. *Proc Natl Acad Sci USA.* 1990;87(4):1620-4.

Chapter 5 – References

Beliakoff J, Whitesell L. Hsp90: an emerging target for breast cancer therapy.

Anticancer Drugs. 2004;**15**(7):651-62.

Berry JM, Bradshaw TD, Fichtner I, Ren R, Schwalbe CH, Wells G, Chew EH,

Stevens MFG, Westwell AD. Quinols as novel therapeutic agents. 2.⁽¹⁾

4-(1-Arylsulfonylindol-2-yl)-4-hydroxycyclohexa-2,5-dien-1-ones and

related agents as potent and selective antitumor agents. *J Med Chem*.

2005;**48**(2):639-644.

Besada V, Diaz M, Becker M, Ramos Y, Castellanos-Serra L, Fichtner I.

Proteomics of xenografted human breast cancer indicates novel targets

related to tamoxifen resistance. *Proteomics*. 2006;**6**(3):1038-48.

Bianco NR, Perry G, Smith MA, Templeton DJ, Montano MM. Functional

implications of antiestrogen induction of quinone reductase: inhibition

of estrogen-induced deoxyribonucleic acid damage. *Mol Endocrinol*.

2003;**17**(7):1344-55.

Biamond P, Swaak AJ, Beindorff CM, Koster JF. Superoxide-dependent and

independent mechanisms of iron mobilization from ferritin by xanthine

oxidase. Implications for oxygen-free-radical-induced tissue destruction

during ischaemia and inflammation. *Biochem J*. 1986;**239**(1):169-73.

Blackburn RV, Spitz DR, Liu X, Galoforo SS, Sim JE, Ridnour LA, Chen JC,

Davis BH, Corry PM, Lee YJ. Metabolic oxidative stress activates

signal transduction and gene expression during glucose deprivation in

human tumor cells. *Free Radic Biol Med*. 1999;**26**(3-4):419-30.

Chapter 5 – References

- Boveris A, Chance B. The mitochondrial generation of hydrogen peroxide. General properties and effect of hyperbaric oxygen. *Biochem J.* 1973;134(3):707-16.
- Boveris A, Oshino N, Chance B. The cellular production of hydrogen peroxide. *Biochem J.* 1972;128(3):617-30.
- Bradshaw TD, Matthews CS, Cookson J, Chew EH, Shah M, Bailey K, Monks A, Harris E, Westwell AD, Wells G, Laughton CA, Stevens MFG. Elucidation of thioredoxin as a molecular target for antitumor quinols. *Cancer Res.* 2005;65:3911-3919.
- Brekelmans CT. Risk factors and risk reduction of breast and ovarian cancer. *Curr Opin Obstet Gynecol.* 2003;15(1):63-8.
- Britton DJ, Hutcheson IR, Knowlden JM, Barrow D, Giles M, McClelland RA, Gee JM, Nicholson RI. Bidirectional cross talk between ERalpha and EGFR signalling pathways regulates tamoxifen-resistant growth. *Breast Cancer Res Treat.* 2006;96(2):131-46.
- Brown GC, Borutaite V. Nitric oxide, mitochondria, and cell death. *IUBMB Life.* 2001;52(3-5):189-95.
- Brubacher JL, Bols NC. Chemically de-acetylated 2',7'-dichlorodihydrofluorescein diacetate as a probe of respiratory burst activity in mononuclear phagocytes. *J Immunol Methods.* 2001;251(1-2):81-91.
- Cai H, Harrison DG. Endothelial dysfunction in cardiovascular diseases: the role of oxidant stress. *Circ Res.* 2000;87(10):840-4.

Chapter 5 – References

- Calderon PB, Cadrobbi J, Marques C, Hong-Ngoc N, Jamison JM, Gilloteaux J, Summers JL, Taper HS. Potential therapeutic application of the association of vitamins C and K3 in cancer treatment. *Curr Med Chem.* 2002;**9(24)**:2271-85.
- Cebrian A, Pharoah PD, Ahmed S, Smith PL, Luccarini C, Luben R, Redman K, Munday H, Easton DF, Dunning AM, Ponder BA. Tagging single-nucleotide polymorphisms in antioxidant defense enzymes and susceptibility to breastcancer. *Cancer Res.* 2006;**66(2)**:1225-33.
- Chance B, Sies H, Boveris A. Hydroperoxide metabolism in mammalian organs. *Physiol Rev.* 1979;**59(3)**:527-605.
- Chen C, Kong AN. Dietary chemopreventive compounds and ARE/EpRE signalling. *Free Radical Biol Med.* 2004;**36**:1505-16
- Chen YR, Sturgeon BE, Gunther MR, Mason RP. Electron spin resonance investigation of the cyanide and azidyl radical formation by cytochrome c oxidase. *J Biol Chem.* 1999;**274(35)**:24611-6.
- Cheng L, Zhang X, Zhang M, Zhang P, Song Z, Ma Z, Cheng Y, Qu H.J
Characterization of chemopreventive agents from the dichloromethane extract of *Eurycorymbus cavaleriei* by liquid chromatography-ion trap mass spectrometry. *Chromatogr A.* 2009 Apr 16. [Epub ahead of print]
- Chlebowski RT, Col N, Winer EP, Collyar DE, Cummings SR, Vogel VG 3rd, Burstein HJ, Eisen A, Lipkus I, Pfister DG; American Society of Clinical Oncology Breast Cancer Technology Assessment Working Group. American Society of Clinical Oncology technology assessment of pharmacologic interventions for breast cancer risk

Chapter 5 – References

- reduction including tamoxifen, raloxifene, and aromatase inhibition. *J Clin Oncol.* 2002;**20(15)**:3328-43.
- Chew EH, Matthews CS, Zhang J, McCarroll AJ, Hagen T, Stevens MFG, Westwell AD, Bradshaw TD. Apoptosis-inducing antitumor quinols: Enhanced cytotoxicity in glutathione depleted cells and identification of putative cellular protein targets. [not published]
- Commoner B, Townsend J, Pake GE. Free radicals in biological materials. *Nature.* 1954;**174(4432)**:689–691.
- Cooke MS, Evans MD, Dizdaroglu M, Lunec J. Oxidative DNA damage: mechanisms, mutation, and disease. *FASEB J.* 2003;**17(10)**:1195-214.
- Csiki I, Yanagisawa K, Haruki N, Nadaf S, Morrow JD, Johnson DH, Carbone DP. Thioredoxin-1 modulates transcription of cyclooxygenase-2 via hypoxia inducible factor-1alpha in non-small cell lung cancer. *Cancer Res.* 2006;**66(1)**:143-50.
- Cui Y, Parra I, Zhang M, Hilsenbeck SG, Tsimelzon A, Furukawa T, Horii A, Zhang ZY, Nicholson RI, Fuqua SA. Elevated expression of mitogen activated protein kinase phosphatase 3 in breast tumors: a mechanism of tamoxifen resistance. *Cancer Res.* 2006;**66(11)**:5950-9.
- Cumming RC, Andon NL, Haynes PA, Park M, Fisher WH, Schubert D. Protein disulfide bond formation in the cytoplasm during oxidative stress. *J Biol Chem.* 2004;**279(21)**:21749-21758.
- Day BW, Tyurin VA, Tyurina YY, Liu M, Facey JA, Carta G, Kisin ER, Dubey RK, Kagan VE. Peroxidase-catalyzed pro- versus antioxidant

- effects of 4-hydroxytamoxifen: enzyme specificity and biochemical sequelae. *Chem Res Toxicol.* 1999;12(1):28-37.
- del Bello B, Paolicchi A, Comporti M, Pompella A, Maellaro E. Hydrogen peroxide produced during gamma-glutamyl transpeptidase activity is involved in prevention of apoptosis and maintenance of proliferation in U937 cells. *FASEB J.* 1999;13(1):69-79.
- de Hann JB. Fibroblasts derived from Gpx1 knockdown mice display senescent like features and are susceptible to H₂O₂-mediated cell death. *Free Radic Boil Med.* 2004;36:53-64.
- Deroo BJ, Hewitt SC, Peddada SD, Korach KS. Estradiol Regulates the thiredoxin antioxidant system in mouse uterus. *Endocrinology.* 2004;145(12):5485-5492
- Ding SJ, Li Y, Shao XX, Zhou H, Zeng R, Tang ZY, Xia QC. Proteome analysis of hepatocellular carcinoma cell strains, MHCC97-H and MHCC97-L, with different metastasis potentials. *Proteomics.* 2004;4(4):982-94.
- Dinkova-Kostova AT, Talalay P. Direct and indirect antioxidant properties of inducers of cytoprotective proteins. *Mol Nutr Food Res.* 2008;52:128-38.
- Dizdaroglu M, Jaruga P, Birincioglu M, Rodriguez H. Free radical-induced damage to DNA: mechanisms and measurement. *Free Radic Biol Med.* 2002;32(11):1102-15.
- Dobrzycka KM, Townson SM, Jiang S, Oesterreich S. Estrogen receptor corepressors – a role in human breast cancer? *Endo. Rel. Cancer.* 2003;10(4):517-536.

Douglas AS, Robinson SP, Hutchinson JD, Porter RW, Stewart A, Reid DM.

Carboxylation of osteocalcin in post-menopausal osteoporotic women following vitamin K and D supplementation. *Bone*. 1995;17(1):15-20.

Dowsett M, Nicholson RI, Pietras RJ. *Breast Cancer Res Treat*. Biological characteristics of the pure antiestrogen fulvestrant: overcoming endocrine resistance. *Breast Cancer Res Treat*. 2005;93 Suppl 1:S11-S18.

Droge W. Free radicals in the physiological control of cell function. *Physiol Rev*. 2002;82(1):47-95.

Duval C, Augé N, Frisach MF, Casteilla L, Salvayre R, Nègre-Salvayre A. *Biochem J*. Mitochondrial oxidative stress is modulated by oleic acid via an epidermal growth factor receptor-dependent activation of glutathione peroxidase. 2002;367(3):889-94.

Egglar AL, Gay KA, Mesecar AD. Molecular mechanisms of natural products in chemoprevention: induction of cytoprotective enzymes by Nrf2. *Mol Nutr Food Res*. 2008; 52:S84-94

Eyries M, Collins T, Khachigian LM. Modulation of growth factor gene expression in vascular cells by oxidative stress. *Endothelium*. 2004;11(2):133-9.

Fagerholm R, Hofstetter B, Tommiska J, Aaltonen K, Vrtel R, et al. NAD(P)H:quinine oxidoreductase 1 NQO1*2 genotype (P187S) is a strong prognostic and protective factor in breast cancer. *Nature Genetics*. 2008;40:844-853.

Chapter 5 – References

- Ferlini C, Scambia G, Marone M, Distefano M, Gaggini C, Ferrandina G, Fattorossi A, Isola G, Benedetti Panici P, Mancuso S. Tamoxifen induces oxidative stress and apoptosis in oestrogen receptor-negative human cancer cell lines. *Br J Cancer*. 1999;**79**(2):257-63.
- Filardo EJ, Quinn JA, Bland KI, Frackton AR. Estrogen induced activation of ERK-1 and ERK-2 requires the G-protein coupled receptor homolog, GRP30, and occurs via transactivation of the epidermal growth factor receptor through release of the HB-EGF. *Mol Endocrinol*. 2000;**14**:1649-1660.
- Fisher B, Costantino JP, Wickerham DL, Redmond CK, Kavanah M, Cronin WM, Vogel V, Robidoux A, Dimitrov N, Atkins J, Daly M, Wieand S, Tan-Chiu E, Ford L, Wolmark N. Tamoxifen for prevention of breast cancer: report of the National Surgical Adjuvant Breast and Bowel Project P-1 Study. *J Natl Cancer Inst*. 1998;**90**(18):1371-88.
- Flynn JM, Cammarata PR. Estradiol attenuates mitochondrial depolarization in polyol-stressed lens epithelial cells. *Mol Vis*. 2006;**12**:271-82.
- Frasor J, Danes JM, Komm B, Chang KC, Lyttle CR, Katzenellenbogen BS. Profiling of estrogen up and down regulated gene expression in human breast cancer cells: insight into gene networks and pathways underlying estrogenic control of proliferation and cell phenotype. *Endocrinology*. 2003;**144**:4562-4574.
- Fu RY, Chen J, Li Y. The Function of the Glutathione/Glutathione Peroxidase System in the Oxidative Stress Resistance Systems of Microbial Cells. *Chinese Journal of Biotechnology*. 2007;**23**(5):770-775

Chapter 5 – References

- Fujii T, Onohara N, Maruyama Y, Tanabe S, Kobayashi H, Fukutomi M, Nagamatsu Y, Nishihara N, Inoue R, Sumimoto H, Shibasaki F, Nagao T, Nishida M, Kurose H. α 12/13-mediated production of reactive oxygen species is critical for angiotensin receptor-induced NFAT activation in cardiac fibroblasts. *J Biol Chem*. 2005;**280**(24):23041-7.
- Fuqua SA, Schiff R, Parra I, Friedrichs WE, Su JL, McKee DD, Slentz-Kesler K, Moore LB, Willson TM, Moore JT. Expression of wild-type estrogen receptor beta and variant isoforms in human breast cancer. *Cancer Res*. 1999;**59**(21):5425-8.
- Fuqua SA, Schiff R, Parra I, Moore JT, Mohsin SK, Osborne CK, Clark GM, Allred DC. Estrogen receptor beta protein in human breast cancer: correlation with clinical tumor parameters. *Cancer Res*. 2003;**63**(10):2434-9.
- Furie B, & Furie BC. Molecular basis of vitamin K-dependent gamma carboxylation. *Blood*. 1990;**75**(9):1753-1762.
- Gee JM, Harper ME, Hutcheson IR, Madden TA, Barrow D, Knowlden JM, McClelland RA, Jordan N, Wakeling AE, Nicholson RI. The antiepidermal growth factor receptor agent gefitinib (ZD1839/Iressa) improves antihormone response and prevents development of resistance in breast cancer in vitro. *Endocrinology*. 2003;**144**(11):5105-17.
- Gee JM, Robertson JF, Gutteridge E, Ellis IO, Pinder SE, Rubini M, Nicholson RI. Epidermal growth factor receptor/HER2/insulin-like growth factor receptor signalling and oestrogen receptor activity in clinical breast cancer. *Endocr Relat Cancer*. 2005;**12** Suppl 1:S99-S111.

Chapter 5 – References

- Gerdes J, Schwab U, Lemke H, Stein H. Production of a mouse monoclonal antibody reactive with a human nuclear antigen associated with cell proliferation. *Int J Cancer*. 1983;**31(1)**:13-20.
- Gottardis MM, Jordan VC. Development of tamoxifen-stimulated growth of MCF-7 tumors in athymic mice after long-term antiestrogen administration. *Cancer Res*. 1988;**48(18)**:5183-7.
- Gougelet A, Bouclier C, Marsaud V, Maillard S, Mueller SO, Korach KS, Renoir JM. Estrogen receptor alpha and beta subtype expression and transactivation capacity are differentially affected by receptor-, hsp90- and immunophilin-ligands in human breast cancer cells. *J Steroid Biochem Mol Biol*. 2005;**94(1-3)**:71-81.
- Green S, Walter P, Kumar V, Krust A, Bornert JM, Argos P, Chambon P. Human oestrogen receptor cDNA: sequence, expression and homology to v-erb-A. *Nature*. 1986;**320(6058)**:134-9.
- Grdina DJ, Murley JS, Kataoka Y, Baker KL, Kunnavakkam R, Coleman MC, Spitz DR. Amifostine induces antioxidant enzymatic activities in normal tissues and a transplantable tumor that can affect radiation response. *Int J Radiat Oncol Biol Phys*. 2009;**1;73(3)**:886-96.
- Grogan TM, Fenoglio-Prieser C, Zeheb R, Bellamy W, Frutiger Y, Vela E, Stemmerman G, Macdonald J, Richter L, Gallegos A, Powis G. Thioredoxin, a putative oncogene product, is overexpressed in gastric carcinoma and associated with increased proliferation and increased cell survival. *Hum Pathol*. 2000;**31(4)**:475-81.

Chapter 5 – References

- Halliwell B. Reactive species and antioxidants. Redox biology is a fundamental theme of aerobic life. *Plant Physiol.* 2006;**141**(2):312-22.
- Halliwell B, Cross CE. Oxygen-derived species: their relation to human disease and environmental stress. *Environ Health Perspect.* 1994;**102**(10):5-12.
- Halliwell B, Gutteridge JMC. *Free Radicals in Biology and Medicine* (2nd ed). Oxford, UK: Clarendon, 1989.
- Hammond CL, Lee TK, Ballatori N. Novel roles for glutathione in gene expression, cell death, and membrane transport of organic solutes. *J Hepatol.* 2001;**34**:946-954.
- Harman D. Aging: a theory based on free radical and radiation chemistry. *J Gerontol.* 1956;**11**(3):298-300.
- Harman D. The aging process. *Proc Natl Acad Sci USA.* 1981;**78**(11):7124-7128.
- Hedley D, Pintilie M, Woo J, Nicklee T, Morrison A, Birle D, Fyles A, Milosevic M, Hill R. Up-regulation of the redox mediators thioredoxin and apurinic/apyrimidinic excision (APE)/Ref-1 in hypoxic microregions of invasive cervical carcinomas, mapped using multispectral, wide-field fluorescence image analysis. *Am J Pathol.* 2004;**164**(2):557-65.
- Heinzel B, John M, Klatt P, Bohme E, Mayer B. Ca²⁺/calmodulin-dependent formation of hydrogen peroxide by brain nitric oxide synthase. *Biochem J.* 1992;**281**(3):627-30.
- Henry JA, Piggott NH, Mallick UK, Nicholson S, Farndon JR, Westley BR, May FE. pNR-2/pS2 immunohistochemical staining in breast cancer:

Chapter 5 – References

- correlation with prognostic factors and endocrine response. *Br. J. Cancer*. 1991;**63**: 615-622.
- Hensley K, Robinson KA, Gabbita SP, Salsman S, Floyd RA. Reactive oxygen species, cell signaling, and cell injury. *Free Radic Biol Med*. 2000;**28**(10):1456-62.
- Herbst U, Toborek M, Kaiser S, Mattson MP, Hennig B. 4-Hydroxynonenal induces dysfunction and apoptosis of cultured endothelial cells. *J Cell Physiol*. 1999;**181**(2):295-303.
- Hiscox S, Morgan L, Barrow D, Dutkowskil C, Wakeling A, Nicholson RI. Tamoxifen resistance in breast cancer cells is accompanied by an enhanced motile and invasive phenotype: inhibition by gefitinib ('Iressa', ZD1839). *Clin Exp Metastasis*. 2004;**21**(3):201-12.
- Hiscox S, Morgan L, Green T, Nicholson RI. Src as a therapeutic target in anti hormone/anti-growth factor-resistant breast cancer. *Endocr Relat Cancer*. 2006;**13**(1):53-9.
- Housset B. Biochemical aspects of free radicals metabolism. *Bull Eur Physiopathol Respir*. 1987;**23**(4):287-90.
- Hutcheson IR, Knowlden JM, Madden TA, Barrow D, Gee JMW, Wakeling AE, Nicholson RI. Oestrogen receptor-mediated modulation of the EGFR/MAPK pathway in tamoxifen-resistant MCF-7 cells. *Breast Cancer Res Treat*. 2003;**81**(1):81-93.
- Iwao-Koizumi K, Matoba R, Ueno N, Kim SJ, Ando A, Miyoshi Y, Maeda E, Noguchi S, Kato K. Prediction of docetaxel response in human breast cancer by gene expression profiling. *J Clin Oncol*. 2005;**23**(3):422-31.

Chapter 5 – References

- Jensen EV & Jacobson HI. Basic guide to the mechanism of estrogen action. *Recent Progr. Hormone Res.* 1962;18:387-414.
- Ji Y, Akerboom TP, Sies H, Thomas JA. S-nitrosylation and S-glutathiolation of protein sulfhydryls by S-nitroso glutathione. *Arch Biochem Biophys.* 1999;362(1):67-78.
- Johnston SR. Clinical trials of intracellular signal transductions inhibitors for breast cancer--a strategy to overcome endocrine resistance. *Endocr Relat Cancer.* 2005;12(1):145-57.
- Jones DP, Carlson JL, Mody VC, Cai J, Lynn MJ, Sternberg P. Redox state of glutathione in human plasma. *Free Radic Biol Med.* 2000;28(4):625-35.
- Jones HE, Gee JM, Taylor KM, Barrow D, Williams HD, Rubini M, Nicholson RI. Development of strategies for the use of anti-growth factor treatments. *Endocr Relat Cancer.* 2005;12 Suppl 1:S173-82.
- Jones HE, Goddard L, Gee JM, Hiscox S, Rubini M, Barrow D, Knowlden JM, Williams S, Wakeling AE, Nicholson RI. Insulin-like growth factor-I receptor signalling and acquired resistance to gefitinib (ZD1839; Iressa) in human breast and prostate cancer cells. *Endocr Relat Cancer.* 2004;11(4):793-814.
- Jordan CV. Chemoprevention of breast cancer with selective oestrogen receptor modulators. *Nature.* 2007;7:46-53
- Jordan NJ, Gee JM, Barrow D, Wakeling AE, Nicholson RI. Increased Constitutive Activity of PKB/Akt in Tamoxifen Resistant Breast Cancer MCF-7 Cells. *Breast Cancer Res Treat.* 2004;87(2):167-80.

Chapter 5 – References

- Kalinich JF, Ramakrishnan N, McClain DE. The antioxidant Trolox enhances the oxidation of 2',7'-dichlorofluorescein to 2',7'-dichlorofluorescein. *Free Radic Res.* 1997;**26(1)**:37-47.
- Kang SW, Chae HZ, Seo MS, Kim K, Baines IC, Rhee SG. Mammalian peroxiredoxin isoforms can reduce hydrogen peroxide generated in response to growth factors and tumor necrosis factor-alpha. *J Biol Chem.* 1998;**273(11)**:6297-302.
- Karihtala P, Mantyniemi A, Kang SW, Kinnula VL, Soini Y. Peroxiredoxins in breast carcinoma. *Clin Cancer Res.* 2003;**9(9)**:3418-24.
- Kastrup EK, Kastrup EK, Burnham TH, Novak. KK, Schweain SL, Walsh JK, Polcyn SL, et al., eds. (eds). Respiratory inhalant products. In Drug Facts and Comparisons. *St. Louis, Facts and Comparisons.* 1998;1141-1163.
- Kato S, Endoh H, Masuhiro Y, Kitamoto T, Uchiyama S, Sasaki H, Masushige X, Gotoh Y, Nishida E, Kawashima H. Activation of the estrogen receptor through phosphorylation by mitogen-activated protein kinase. *Science.* 1995;**270**:1491-1494.
- Katzenellenbogen BS, Montano MM, Le Goff P, Schodin DJ, Kraus WL, Bhardwaj B, Fujimoto N. Antiestrogens: mechanisms and actions in target cells. *J Steroid Biochem Mol Biol.* 1995;**53(1-6)**:387-93.
- Khan EM, Heidinger JM, Levy M, Lisanti MP, Ravid T, Goldkorn T. EGF receptor exposed to oxidative stress undergoes Src-and caveolin-1 dependent perinuclear trafficking. *J Biol Chem.* 2006;**54**:674-78.

Chapter 5 – References

- Kim HJ, Cui X, Hilsenbeck SG, Lee AV. Progesterone receptor loss correlates with human epidermal growth factor receptor 2 overexpression in estrogen receptor-positive breast cancer. *Clin Cancer Res.* 2006;12(3 Pt 2):1013s-1018s.
- Kim SK, Yang JW, Kim MR, Roh SH, Kim HG, Lee KY, Jeong HG, Kang KW, Increased expression of Nrf2/ARE-dependent anti-oxidant proteins in tamoxifen-resistant breast cancer cells. *Free Radical Biology and Medicine.* 2008;45(4): 537-546
- King CR, Borrello I, Porter L, Comoglio P, Schlessinger J. Ligand independent tyrosine phosphorylation of EGF receptor and the erbB-2/neu proto oncogene product is induced by hyperosmotic shock. *Oncogene.* 1989;4(1):13-8.
- Kirkman HN, Gaetani GF. Catalase: a tetrameric enzyme with four tightly bound molecules of NADPH. *Proc Natl Acad Sci U S A.* 1984;81(14):4343-7.
- Kishida O, Miyazaki Y, Murayama Y, Ogasa M, Miyazaki T, Yamamoto T, Watabe K, Tsutsui S, Kiyohara T, Shimomura I, Shinomura Y. Gefitinib (Iressa, ZD1839) inhibits SN38-triggered EGF signals and IL 8 production in gastric cancer cells. *Cancer Chemother Pharmacol.* 2005;55(6):584-94.
- Klinge CM. Estrogen receptor interaction with co-activators and co-repressors. *Steroids.* 2000;65(5):227-51.
- Klinge CM. Estrogen receptor interaction with estrogen response elements. *Nucleic Acids Research.* 2001;29(14):2905-2919.

Chapter 5 – References

- Knebel A, Rahmsdorf HJ, Ullrich A, Herrlich P. Dephosphorylation of receptor tyrosine kinases as target of regulation by radiation, oxidants or alkylating agents. *EMBO J.* 1996;**15(19)**:5314-25.
- Knowlden JM, Gee JM, Bryant S, McClelland RA, Manning DL, Mansel R, Ellis IO, Blamey RW, Robertson JF, Nicholson RI. Use of reverse transcription-polymerase chain reaction methodology to detect estrogen-regulated gene expression in small breast cancer specimens. *Clin Cancer Res.* 1997;**3(11)**:2165-72.
- Knowlden JM, Hutcheson IR, Jones HE, Madden T, Gee JM, Harper ME, Barrow D, Wakeling AE, Nicholson RI. Elevated levels of epidermal growth factor receptor/c-erbB2 heterodimers mediate an autocrine growth regulatory pathway in tamoxifen-resistant MCF-7 cells. *Endocrinology.* 2003;**144(3)**:1032-44.
- Knowlden JM, Jones HE, Barrow D, Gee JM, Nicholson RI, Hutcheson IR. Insulin receptor substrate-1 involvement in epidermal growth factor receptor and insulin-like growth factor receptor signalling: implication for Gefitinib ('Iressa') response and resistance. *Breast Cancer Res Treat.* 2008;**111(1)**:79-91.
- Kohen R, Nyska A. Oxidation of biological systems: oxidative stress phenomena, antioxidants, redox reactions, and methods for their quantification. *Toxicol Pathol.* 2002;**30(6)**:620-50.
- Kopke R, Bielefeld E, Liu J, Zheng J, Jackson R, Henderson D, Coleman JK. Prevention of impulse noise-induced hearing loss with antioxidants.

Chapter 5 – References

- Acta Lacey JV Jr, Devesa SS, Brinton LA. Recent trends in breast cancer incidence and mortality. *Otolaryngol.* 2005;**125(3)**:235-43.
- Kuiper GG, Enmark E, Peltö-Huikko M, Nilsson S, Gustafsson JA. Cloning of a novel receptor expressed in rat prostate and ovary. *Proc. Natl Acad. Sci. USA.* 1996;**93**:5925-5930.
- Kuiper GG, Carlsson B, Grandien K, Enmark E, Haggblad J, Nilsson S, Gustafsson JA. Comparison of the ligand binding specificity and transcript tissue distribution of estrogen receptors alpha and beta. *Endocrinology.* 1997;**138(3)**:863-70.
- Kurdi M, Booz GW. Evidence that IL-6-type cytokine signaling in cardiomyocytes is inhibited by oxidative stress: parthenolide targets JAK1 activation by generating ROS. *J Cell Physiol.* 2007;**212(2)**:424-31.
- Kushner PJ, Agard DA, Greene GL, Scanlan TS, Shiau AK, Uht RM, Webb P. Estrogen receptor pathways to AP-1. *Steroid Biochem Molec Biol.* 2000;**74(50)**:311-317.
- Kwok S, Kellogg DE, McKinney N, Spasic D, Goda L, Levenson C, Sninsky JJ. Effects of primer-template mismatches on the polymerase chain reaction: human immunodeficiency virus type 1 model studies. *Nucleic Acids Res.* 1990;**18(4)**:999-1005.
- Lamson DW, Plaza, SM. The anticancer effects of vitamin K. *Altern Med Rev.* 2003;**8(3)**:303-18.
- Landis GN, Tower J. Superoxide dismutase evolution and life span regulation. *Mech Ageing Dev.* 2005;**126(3)**:365-79.

Chapter 5 – References

- La Torre F, Orlando A, Silipigni A, Giacobello T, Pergolizzi S, Aragona M. [Increase of oxygen free radicals and their derivatives in chemo- and radiation treated neoplasm patients]. *Minerva Med.* 1997;**88(4)**:121-6.
- Lee JS, Surh YJ. Nrf2 as novel molecular target for chemoprevention. *Cancer Lett.* 2005; **224**: 171-84.
- Lee MH, Hyun DH, Jenner P, Halliwell B. Effect of proteasome inhibition on cellular oxidative damage, antioxidant defences and nitric oxide production. *J Neurochem.* 2001;**78(1)**:32-41.
- Lee YJ, Galoforo SS, Berns CM, Chen JC, Davis BH, Sim JE, Corry PM, Spitz DR. Glucose deprivation-induced cytotoxicity and alterations in mitogen activated protein kinase activation are mediated by oxidative stress in multidrug-resistant human breast carcinoma cells. *J Biol Chem.* 1998;**273(9)**:5294-9.
- Legault-Poisson S, Jolivet J, Poisson R, Beretta-Piccoli M, Band PR. Tamoxifen induced tumor stimulation and withdrawal response. *Cancer Treat Rep.* 1979;**63(11-12)**:1839-41.
- Levin ER. Bidirectional signalling between the estrogen receptor and the epidermal growth factor receptor. *Mol Endocrinol.* 2003;**17(3)**:309-317
- Lewis-Wambi J, Kim H, Wambi C, Jordan VC. Glutathione depletion sensitizes hormone-independent human breast cancer cells to estrogen induced apoptosis. Fox Chase Cancer Center and University of Pennsylvania. U.S. Army Medical Research and Materiel Command under W81XWH-06-1-0590.2009;**2**:44

Chapter 5 – References

- Liehr JG. Is estradiol a genotoxic mutagenic carcinogen? *Endocr Rev* 2000;21:40–54.
- Lien YC, Kung HN, Lu KS, Jeng CJ, Chau YP. Involvement of endoplasmic reticulum stress and activation of MAP kinases in beta-lapachone induced human prostate cancer cell apoptosis. *Histol Histopathol.* 2008;23(11):1299-308.
- Liochev SI, Fridovich I. The Haber-Weiss cycle -- 70 years later: an alternative view. *Redox Rep.* 2002;7(1):55-7.
- Lipshutz RJ, Morris D, Chee M, Hubbell E, Kozal MJ, Shah N, Shen N, Yang R, Fodor SP. Using oligonucleotide probe arrays to access genetic diversity. *Biotechniques.* 1995;19(3):442-7.
- Liu Y, Adachi M, Zhao S, Hareyama M, Koong AC, Luo D, Rando TA, Imai K, Shinomura Y. Preventing oxidative stress: a new role for XBP1. *Cell Death Differ.* 2009;16(6):847-57.
- Lonard DM, & O'Malley BW. The expanding cosmos of nuclear receptor co-activators. *Cell.* 2006;125:411-414.
- Lønning PE. Cross-resistance to different aromatase inhibitors in breast cancer treatment. *Endocrine-Related Cancer.* 1999;6:251-257.
- Lønning PE, Kvinnsland S. Mechanisms of action of aminoglutethimide as endocrine therapy of breast cancer. *Drug.s* 1998;35:685-710.
- Loschen G, Azzi A, Richter C, Flohe L. Superoxide radicals as precursors of mitochondrial hydrogen peroxide. *FEBS Lett.* 1974;42(1):68-72.

Chapter 5 – References

- Losel RM, Falkenstein E, Feuring M, Schultz A, Tillmann HC, Rossol-Haseroth K, Wehling M. Non-genomic steroid action: Controversies, questions, and answers. *Physiol Rev.* 2003;**83**:965-1016.
- Madigan MP, Ziegler RG, Benichou J, Byrne C, Hoover RN. Proportion of Breast Cancer Cases in the United States Explained by Well-Established Risk Factors. *Journal of the National Cancer Institute.* 1995;**87**(22):1681-86.
- Margoliash E, Novogrodsky A. A study of the inhibition of Catalase by 3-amino 1,2,4-triazole. *J Biol Chem.* 1958;**68**:468-475.
- Marikovsky M, Ziv V, Nevo N, Harris-Cerruti C, Mahler O. J Immunol. Cu/Zn superoxide dismutase plays important role in immune response. *J Biol chem.* 2003;**170**(6):2993-3001.
- Marnett LJ. Lipid peroxidation-DNA damage by malondialdehyde. *Mutat Res.* 1999;**424**(1-2):83-95.
- Marnett LJ. Oxyradicals and DNA damage. *Carcinogenesis.* 2000;**21**(3):361-70.
- Martin K, Sur R, Liebel F, Tierney N, Lyte P, Garay M, Oddos T, Anthonavage M, Shapiro S, Southall M. Parthenolide-depleted Feverfew (*Tanacetum parthenium*) protects skin from UV irradiation and external aggression. *Arch Dermatol Res.* 2008;**300**(2):69-80.
- Martin LA, Farmer I, Johnston SR, Ali S, Marshall C, Dowsett M. Enhanced estrogen receptor (ER) alpha, ERBB2, and MAPK signal transduction pathways operate during the adaptation of MCF-7 cells to long term estrogen deprivation. *J Biol Chem.* 2003;**278**(33):30458-68.

Chapter 5 – References

- Martin MB, Franke TF, Stoica GE, Chambon P, Katzenellenbogen BS, Stoica BA, McLemore MS, Olivio SE, Stoica A. A role for Akt in mediating the estrogenic functions of epidermal growth factor and insulin like growth factor I. *Endocrinology*. 2000;141:4503-4511.
- Masuhiko Y, Mezaki Y, Sakari M, Takeyama K, Yoshida T, Inoue K, Yanagisawa J, Hanazawa S, O'malley BW, Kato S. Splicing potentiation by growth factor signals *via* estrogen receptor phosphorylation. *Proc Natl Acad Sci U S A*. 2005;102(23):8126-31.
- Mates JM, Perez-Gomez C, Nunez de Castro I. Antioxidant enzymes and human diseases. *Clin Biochem*. 1999;32(8):595-603.
- Mathews CK, van Hold KE, Ahern KG. *Biochemistry Third Edition*. Addison Wesley Longman. 2000;554-555.
- McCall MR, Frei B. Can antioxidant vitamins materially reduce oxidative damage in humans? *Free Radic Biol Med*. 1999;26(7-8):1034-53.
- McClelland RA, Barrow D, Madden TA, Dutkowski CM, Pamment J, Knowlden JM, Gee JM, Nicholson RI. Enhanced epidermal growth factor receptor signaling in MCF7 breast cancer cells after long-term culture in the presence of the pure antiestrogen ICI 182,780 (Faslodex). *Endocrinology*. 2001;142(7):2776-88.(a)
- McCord JM, Fridovich I. Superoxide dismutase. An enzymic function for erythrocyte hemocuprein (hemocuprein). *J Biol Chem*. 1969;244(22):6049-55.
- McEligot AJ, Yang S, Meyskens FL Jr. Redox regulation by intrinsic species and extrinsic nutrients in normal and cancer cells. *Annu Rev Nutr*. 2005;25:261-95.

Chapter 5 – References

- McKenna NJ, Lanz RB, O'Malley BW. Nuclear receptor Co-regulators: cellular and molecular biology. *Endocrine Reviews*. 1999;**20**:321-344
- Medina VA, Croci M, Mohamad NA, Massari N, Garbarino G, Cricco GP, Núñez MA, Martín GA, Crescenti EJ, Bergoc RM, Rivera ES. Mechanisms underlying the radioprotective effect of histamine on small intestine. *Int J Radiat Biol*. 2007;**83**(10):653-63.
- Menzel HJ, Sarmanova J, Soucek P, Berberich R, Grunewald K, Haun M, Kraft HG. *British Journal of Cancer*. 2004;**90**:1989-1994.
- Mimeault M, Jouy N, Depreux P, Hénichart JP. Synergistic antiproliferative and apoptotic effects induced by mixed epidermal growth factor receptor inhibitor ZD1839 and nitric oxide donor in human prostatic cancer cell lines. *Prostate*. 2005;**62**(2):187-99.
- Mitchell JS. Clinical trials of tetra-sodium 2-methyl-1: 4-naphthohydroquinone diphosphate, in conjugation with x-ray therapy. *Brit J Can*. 1948;**2**:351-359.
- Mitchell JS, Brinkley D, Haybittle JL. Clinical trials of radiosensitizers, including synkavit and oxygen inhaled at atmospheric pressure. *Acta Radiol Ter Phys Biol*. 1965;**3**:329-341.
- Mitchell JS, Simon-Reuss I. Combination of some effects of x-radiation and a synthetic vitamin K substitute. *Nature*. 1947;**160**:98-99.
- Montano MM, Bianco NR, Deng H, Wittmann BM, Chaplin LC, Katzenellenbogen BS. Estrogen receptor regulation of quinone reductase in breast cancer: implications for estrogen-induced breast

Chapter 5 – References

- tumor growth and therapeutic uses of tamoxifen. *Front Biosci.* 2005;**10**:1440-61.
- Motohashi H, Yamamoto M. Nrf2-Keap1 defines a physiologically important stress response mechanism. *Trends Mol Med.* 2004; **10**: 549-57.
- Motoki A, Merkel MJ, Packwood WH, Cao Z, Liu L, Iliff J, Alkayed NJ, Van Winkle DM. Soluble epoxide hydrolase inhibition and gene deletion are protective against myocardial ischemia-reperfusion injury in vivo. *Am J Physiol Heart Circ Physiol.* 2008;**295**(5):H2128-34.
- Mukherjee A, Westwell AD, Bradshaw TD, Stevens MF, Carmichael J, Martin SG. Cytotoxic and antiangiogenic activity of AW464 (NSC 706704), a novel thioredoxin inhibitor: an in vitro study. *Br J Cancer.* 2005;**92**(2):350-8.
- Murphy MJ Jr. Molecular Action and Clinical Relevance of Aromatase Inhibitors. *Oncologist.* 1998;**3**(2):129-130.
- Nakamura H, Nakamura K, Yodoi J. Redox regulation of cellular activation. *Annu Rev Immunol.* 1997;**15**:351-69.
- Nelson SK, Bose S, Rizeq M, McCord JM. Oxidative stress in organ preservation: a multifaceted approach to cardioplegia. *Biomed Pharmacother.* 2005;**59**(4):149-57.
- Nicholson RI, Hutcheson IR, Harper ME, Knowlden JM, Barrow D, McClelland RA, Jones HE, Wakeling AE, Gee JM. Modulation of epidermal growth factor receptor in endocrine-resistant, oestrogen receptor-positive breast cancer. *Endocr Relat Cancer.* 2001;**8**(3):175-82.

Chapter 5 – References

- Nicholson RI, Hutcheson IR, Knowlden JM, Jones HE, Harper ME, Jordan N, Hiscox SE, Barrow D, Gee JM. Nonendocrine pathways and endocrine resistance: observations with antiestrogens and signal transduction inhibitors in combination. *Clin Cancer Res.* 2004;**10(1 Pt 2)**:346S-54S.
- Nicholson RI, Johnston SR. Endocrine therapy--current benefits and limitations. *Breast Cancer Res Treat.* 2005;**93 Suppl 1**:S3-10.
- Nieminen AL, Byrne AM, Herman B, Lemasters JJ. Mitochondrial permeability transition in hepatocytes induced by t-BuOOH: NAD(P)H and reactive oxygen species. *Am J Physiol.* 1997;**272(4 Pt 1)**:C1286-94.
- Nishida M, Tanabe S, Maruyama Y, Mangmool S, Urayama K, Nagamatsu Y, Takagahara S, Turner JH, Kozasa T, Kobayashi H, Sato Y, Kawanishi T, Inoue R, Nagao T, Kurose H. G alpha 12/13- and reactive oxygen species-dependent activation of c-Jun NH2-terminal kinase and p38 mitogen-activated protein kinase by angiotensin receptor stimulation in rat neonatal cardiomyocytes. *J Biol Chem.* 2005;**280(18)**:18434-41.
- Ngo EO, Sun TP, Chang JY, Wang CC, Chi KH, Cheng AL, Nutter LM. Menadione induced DNA damage in a human tumor cell line. *Biochem Pharmacol.* 1991;**42(10)**:1961-8.
- Noh DY, Ahn SJ, Lee RA, Kim SW, Park IA, Chae HZ. Overexpression of peroxiredoxin in human breast cancer. *Anticancer Res.* 2001;**21(3B)**:2085-90.
- Noto V, Taper HS, Jiang YH, Janssens J, Bonte J, De Loecker W. Effects of sodium ascorbate (vitamin C) and 2-methyl-1,4-naphthoquinone (vitamin K3) treatment on human tumor cell growth in vitro. I.

Chapter 5 – References

- Synergism of combined vitamin C and K3 action. *Cancer*. 1989;**63**(5):901-6.
- Nutter LM, Ngo EO, Fisher GR, Gutierrez PL. DNA strand scission and free radical production in menadione-treated cells. Correlation with cytotoxicity and role of NADPH quinone acceptor oxidoreductase. *J Biol Chem*. 1992;**267**(4):2474-9.
- Nuwaysir EF, Dragan YP, McCague R, Martin P, Mann J, Jordan VC, Pitot HC. Structure-activity relationships for triphenylethylene antiestrogens on hepatic phase-I and phase-II enzyme expression. *Biochem Pharmacol*. 1998;**56**(3):321-7.
- Oberley TD, Oberley LW. Antioxidant enzyme levels in cancer. *Histol Histopathol*. 1997;**12**(2):525-35.
- O'Bryan JP, Frye RA, Cogswell PC, Neubauer A, Kitch B, Prokop C, Espinosa R 3rd, Le Beau MM, Earp HS, Liu ET. axl, a transforming gene isolated from primary human myeloid leukemia cells, encodes a novel receptor tyrosine kinase. *Mol Cell Biol*. 1991;**11**(10):5016-31.
- Okouchi M, Okayama N, Aw TY. Hyperglycemia potentiates carbonyl stress induced apoptosis in naïve PC-12 cells: relationship to cellular redox and activator protease factor-1 expression. *Curr Neurovasc Res*. 2005;**2**(5):375-86.
- Osborne CK, Coronado E, Allred DC, Wiebe V, DeGregorio M. Acquired tamoxifen resistance: correlation with reduced breast tumor levels of tamoxifen and isomerization of trans-4-hydroxytamoxifen. *J Natl Cancer Inst*. 1991;**83**(20):1477-82.

Chapter 5 – References

- Osborne CK, Coronado-Heinsohn EB, Hilsenbeck SG, McCue BL, Wakeling AE, McClelland RA, Manning DL, Nicholson RI. Comparison of the effects of a pure steroidal antiestrogen with those of tamoxifen in a model of human breast cancer. *J Natl Cancer Inst.* 1995;**87(10)**:746-50.
- Osborne CK, Fuqua SA. Mechanisms of tamoxifen resistance. *Breast Cancer Res Treat.* 1994;**32(1)**:49-55.
- Osborne CK, Jarman M, McCague R, Coronado EB, Hilsenbeck SG, Wakeling AE. The importance of tamoxifen metabolism in tamoxifen-stimulated breast tumor growth. *Cancer Chemother Pharmacol.* 1994;**34(2)**:89-95.
- Osborne CK, Schiff R. Estrogen-receptor biology: continuing progress and therapeutic implications. *J Clin Oncol.* 2005;**23(8)**:1616-1622
- Osborne CK, Wakeling A, Nicholson RI. Fulvestrant: an oestrogen receptor antagonist with a novel mechanism of action. *Br J Cancer.* 2004;**90 Suppl 1**:S2-6.
- Pahan K, Sheikh FG, Namboodiri AM, Singh I. N-acetyl cysteine inhibits induction of NO production by endotoxin or cytokine stimulated rat peritoneal macrophages, C6 glial cells and astrocytes. *Free Radic Biol Med.* 1998;**24(1)**:39-48.
- Pajak B, Gajkowska B, Orzechowski A. Molecular basis of parthenolide dependent proapoptotic activity in cancer cells. *Folia Histochem Cytobiol.* 2008;**46(2)**:129-35.

Chapter 5 – References

- Pani G, Colavitti R, Bedogni B, Fusco S, Ferraro D, Borrello S, Galeotti T. Mitochondrial superoxide dismutase: a promising target for new anticancer therapies. *Curr Med Chem.* 2004;**11(10)**:1299-308.
- Peralta EA, Viegas ML, Louis S, Engle DL, Dunnington GL. Effect of vitamin E on tamoxifen-treated breast cancer cells. *Surgery.* 2006;**140(4)**:607-14; discussion 614-5.
- Paruthiyil S, Parmar H, Kerekatte V, Cunha GR, Firestone GL, Leitman DC. Estrogen receptor beta inhibits human breast cancer cell proliferation and tumor formation by causing a G2 cell cycle arrest. *Cancer Res.* 2004;**64(1)**:423-8.
- Pease AC, Solas D, Sullivan EJ, Cronin MT, Holmes CP, Fodor SP. Light-generated oligonucleotide arrays for rapid DNA sequence analysis. *Proc Natl Acad Sci U S A.* 1994;**91(11)**:5022-6.
- Pela R, Calcagni AM, Subiaco S, Isidori P, Tubaldi A, Sanguinetti CM. N-acetylcysteine reduces the exacerbation rate in patients with moderate to severe COPD. *Respiration.* 1999;**66(6)**:495-500.
- Pinchuk I, Schnitzer E, Lichtenberg D. Kinetic analysis of copper-induced peroxidation of LDL. *Biochim Biophys Acta.* 1998;**1389(2)**:155-72.
- Platenik J, Stopka P, Vejrazka M, Stipek S. Quinolinic acid-iron(ii) complexes: slow autoxidation, but enhanced hydroxyl radical production in the fenton reaction. *Free Radic Res.* 2001;**34(5)**:445-59.
- Possel H, Noack H, Augustin W, Keilhoff G, Wolf G. 2,7-Dihydrodichlorofluorescein diacetate as a fluorescent marker for peroxynitrite formation. *FEBS Lett.* 1997;**416(2)**:175-8.

Chapter 5 – References

- Pou S, Pou WS, Bredt DS, Snyder SH, Rosen GM. Generation of superoxide by purified brain nitric oxide synthase. *J Biol Chem.* 1992;267(34):24173-6.
- Powis G, Wipf P, Lynch SM, Birmingham A, Kirkpatrick DL. Molecular pharmacology and antitumor activity of palmarumycin-based inhibitors of thioredoxin reductase. *Mol Cancer Ther.* 2006;5:630
- Pratt WB, Toft DO. Steroid receptor interactions with heat shock proteins and immunophilin chaperones. *Endocrine rev.* 1997;18:306-360
- Pryor WA. Oxy-radicals and related species: their formation, lifetimes, and reactions. *Annu Rev Physiol.* 1986;48:657-67.
- Rae TD, Schmidt PJ, Pufahl RA, Culotta VC, O'Halloran TV. Undetectable intracellular free copper: the requirement of a copper chaperone for superoxide dismutase. *Science.* 1999;284(5415):805-8.
- Raffel J, Bhattacharyya AK, Gallegos A, Cui H, Einspahr JG, Alberts DS, Powis G J. Increased expression of thioredoxin-1 in human colorectal cancer is associated with decreased patient survival. *Lab Clin Med.* 2003;142(1):46-51.
- Raisanen SR, Lehenkari P, Tasanen M, Rahkila P, Harkonen PL, Vaananen HK. Carbonic anhydrase III protects cells from hydrogen peroxide induced apoptosis. *FASEB J.* 1999;13(3):513-22.
- Rao GN. Hydrogen peroxide induces complex formation of SHC-Grb2-SOS with receptor tyrosine kinase and activates Ras and extracellular signal regulated protein kinases group of mitogen-activated protein kinases. *Oncogene.* 1996;13(4):713-9.

Chapter 5 – References

- Rao GS. Mode of entry of steroid and thyroid hormones into cell. *Mol Cell Endocrinol.* 1981;21:97-108
- Reid MB. Role of nitric oxide in skeletal muscle: synthesis, distribution and functional importance. *Acta Physiol Scand.* 1998;162(3):401-9.
- Rice-Evans CA. Measurement of Total Antioxidant capacity as a marker of antioxidant status in vivo; procedures and limitations. *Free Radical Res.* 2000;33:59-66.
- Ribeiro RC, Kushner PJ, Baxter JD. The nuclear hormone receptor gene superfamily. *Annu Rev Med.* 1995;46:443-53.
- Rhee J, Oishi K, Garey J, Kim E. Management of rash and other toxicities in patients treated with epidermal growth factor receptor-targeted agents. *Clin Colorectal Cancer.* 2005;5 Suppl 2:S101-6.
- Rhee SG, Chang TS, Bae YS, Lee SR, Kang SW. Cellular regulation by hydrogen peroxide. *J Am Soc Nephrol.* 2003;14:S211-5.
- Robertson JF. ICI 182,780 (Fulvestrant)- the first oestrogen receptor down regulator- current clinical data. *Br J Cancer.* 2001;5(2):11-14
- Robertson JF, Osborne CK, Howell A, Jones SE, Mauriac L, Ellis M, Kleeberg UR, Come SE, Vergote I, Gertler S, Buzdar A, Webster A, Morris C. Fulvestrant versus anastrozole for the treatment of advanced breast carcinoma in postmenopausal women – a prospective combined analysis of two multicenter trials. *Cancer.* 2003;98:229-238
- Roger P, Sahla ME, Makela S, Gustafsson JA, Baldet P, Rochefort H. Decreased expression of estrogen receptor beta protein in proliferative preinvasive mammary tumors. *Cancer Res.* 2001;61(6):2537-41.

Chapter 5 – References

- Ross D, Kepa JK, Winski SL, Beall HD, Anwar A, Siegel D. NAD(P)H:quinine oxidoreductase 1 (NQO1): Chemoprotection, bioactivation, gene regulation and genetic polymorphism. *Chemico Biological interactions*. 2001;**129(1-2)**:77-97.
- Rozen S, & Skaletsky HJ. Primer3 on the WWW for general users and for biologist programmers. In: Krawetz S, Misener S (eds) *Bioinformatics Methods and Protocols: Methods in Molecular Biology*. Humana Press, Totowa, NJ. 2000:365-386
- Source code available at <http://fokker.wi.mit.edu/primer3/>.
- Shaaban AM, O'Neill PA, Davies MP, Sibson R, West CR, Smith PH, Foster CS. Declining estrogen receptor-beta expression defines malignant progression of human breast neoplasia. *Am J Surg Pathol*. 2003;**27(12)**:1502-12.
- Sakai K, Matsumoto K, Nishikawa T, Suefuji M, Nakamaru K, Hirashima Y, Kawashima J, Shirotani T, Ichinose K, Brownlee M, Araki E. Mitochondrial reactive oxygen species reduce insulin secretion by pancreatic beta-cells. *Biochem Biophys Res Commun*. 2003;**300(1)**:216-22.
- Sanchez Ferrer A, Santema JS, Hilhorst R, Visser AJ. Fluorescence detection of enzymatically formed hydrogen peroxide in aqueous solution and in reversed micelles. *Anal Biochem*. 1990;**187(1)**:129-32.
- Santen RJ, Song RX, Zhang Z, Kumar R, Jeng MH, Masamura S, Yue W, Berstein L. Adaptive hypersensitivity to estrogen: mechanism for superiority of aromatase inhibitors over selective estrogen receptor

Chapter 5 – References

- modulators for breast cancer treatment and prevention. *Endocr Relat Cancer*. 2003;**10(2)**:111-30.
- Santen RJ, Song RX, Zhang Z, Yue W, Kumar R. Adaptive hypersensitivity to estrogen: mechanism for sequential responses to hormonal therapy in breast cancer. *Clin Cancer Res*. 2004;**10(1 Pt 2)**:337S-45S.
- Schaafsma A, Muskiet FA, Storm H, Hofstede GJ, Pakan I, Van der Veer E. Vitamin D(3) and vitamin K(1) supplementation of Dutch postmenopausal women with normal and low bone mineral densities: effects on serum 25 hydroxyvitamin D and carboxylated osteocalcin. *Eur J Clin Nutr*. 2000;**54(8)**:626-31.
- Schiff R, Reddy P, Ahotupa M, Coronado-Heinsohn E, Grim M, Hilsenbeck SG, Lawrence R, Deneke S, Herrera R, Chamness GC, Fuqua SA, Brown PH, Osborne CK. Oxidative stress and AP-1 activity in tamoxifen-resistant breast tumors in vivo. *J Natl Cancer Inst*. 2000;**92(23)**:1926-34.
- Schreck R, Rieber P, Baeuerle PA. Reactive oxygen intermediates as apparently widely used messengers in the activation of the NF-kappa B transcription factor and HIV-1. *EMBO J*. 1991;**10(8)**:2247-58.
- Seegers WH, & Bang NU. *Blood Clotting Enzymology*. New York, NY: Academic Press; 1967.
- Seo MS, Kang SW, Kim K, Baines IC, Lee TH, Rhee SG. Identification of a new type of mammalian peroxiredoxin that forms an intramolecular disulfide as a reaction intermediate. *J Biol Chem*. 2000;**275(27)**:20346-54.

Chapter 5 – References

- Sies H, Stahl W, Sevanian A. Nutritional, dietary and postprandial oxidative stress. *J Nutr.* 2005;**135**(5):969-72.
- Sinha P, Hutter G, Kottgen E, Dietel M, Schadendorf D, Lage H. Increased expression of annexin I and thioredoxin detected by two-dimensional gel electrophoresis of drug resistant human stomach cancer cells. *J Biochem Biophys Methods.* 1998;**37**(3):105-16.
- Sharma A, Rajappa M, Saxena A, Sharma M. Antioxidant status in advanced cervical cancer patients undergoing neoadjuvant chemoradiation. *Br J Biomed Sci.* 2007;**64**(1):23-7.
- Shearer MJ. Role of vitamin K and Gla proteins in the pathophysiology of osteoporosis and vascular calcification. *Curr Opin Clin Nutr Metab Care.* 2000;**3**(6):433-438.
- Shigenaga MK, Gimeno CJ, Ames BN. Urinary 8-hydroxy-2'-deoxyguanosine as a biological marker of in vivo oxidative DNA damage. *Proc Natl Acad Sci U S A.* 1989;**86**(24):9697-701.
- Smith IE, Dowsett M. Aromatase inhibitors in breast cancer. *N Engl J Med.* 2003;**348**:2431-42.
- Sommer R, Tautz D. Minimal homology requirements for PCR primers. *Nucleic Acids Res.* 1989;**17**(16):6749.
- Song SH, Lee KH, Kang MS, Lee YJ. Role of paxillin in metabolic oxidative stress induced cytoskeletal reorganization: involvement of SAPK signal transduction pathway and PTP-PEST gene expression. *Free Radic Biol Med.* 2000;**29**(1):61-70.

- Spitz DR, Phillips JW, Adams DT, Sherman CM, Deen DF, Li GC. Cellular resistance to oxidative stress is accompanied by resistance to cisplatin: the significance of increased catalase activity and total glutathione in hydrogen peroxide-resistant fibroblasts. *J Cell Physiol.* 1993;156(1):72-9.
- Sripathy SP, Chaplin LJ, Gaikwad NW, Rogan EG, Montano MM. hPMC2 is required for recruiting an ER beta coactivator complex to mediate transcriptional upregulation of NQO1 and protection against oxidative DNA damage by tamoxifen. *Oncogene.* 2008;27:6376–6384
- Staka CM, Nicholson RI, Gee JM. Acquired resistance to oestrogen deprivation: role for growth factor signalling kinases/oestrogen receptor cross-talk revealed in new MCF-7X model. *Endocr Relat Cancer.* 2005;12 Suppl 1:S85-97.
- Su WC, Sun TP, Wu FY. The in vitro and in vivo cytotoxicity of menadione (vitamin K3) against rat transplantable hepatoma induced by 3'-methyl-4-dimethyl-aminoazobenzene. *Gaoxiong Yi Xue Ke Xue Za Zhi.* 1991;7(9):454-9.
- Suematsu M, Suzuki H, Delano FA, Schmid-Schonbein GW. The inflammatory aspect of the microcirculation in hypertension: oxidative stress, leukocytes/endothelial interaction, apoptosis. *Microcirculation.* 2002;9(4):259-76.
- Suggs SV, Wallace RB, Hirose T, Kawashima EH, Itakura K. Use of synthetic oligonucleotides as hybridization probes: isolation of cloned cDNA

Chapter 5 – References

- sequences for human beta 2-microglobulin. *Proc Natl Acad Sci U S A*. 1981;**78**(11):6613-7.
- Sule AA, Tai DY, Tze CC, Deepa B, Leow M. Potentially fatal paracetamol overdose and successful treatment with 3 days of intravenous N acetylcysteine regime--a case report. *Ann Acad Med Singapore*. 2006;**35**(2):108-11.
- Sun JS, Tsuang YH, Huang WC, Chen LT, Hang YS, Lu FJ. Menadione induced cytotoxicity to rat osteoblasts. *Cell Mol Life Sci*. 1997;**53**(11 12):967-76.
- Supinski G. Free radical induced respiratory muscle dysfunction. *Mol Cell Biochem*. 1998;**179**(1-2):99-110.
- Sureda FX, Gabriel C, Comas J, Pallas M, Escubedo E, Camarasa J, Camins A. Evaluation of free radical production, mitochondrial membrane potential and cytoplasmic calcium in mammalian neurons by flow cytometry. *Brain Res Brain Res Protoc*. 1999;**4**(3):280-7.
- Szatrowski TP, Nathan CF. Production of large amounts of hydrogen peroxide by human tumor cells. *Cancer Res*. 1991;**51**(3):794-8.
- Thor H, Smith MT, Hartzell P, Bellomo G, Jewell SA, Orrenius S. The metabolism of menadione (2-methyl-1,4-naphthoquinone) by isolated hepatocytes. A study of the implications of oxidative stress in intact cells. *J Biol Chem*. 1982;**257**(20):12419-25.
- Toufektsian MC, Boucher FR, Tanguy S, Morel S, de Leiris JG. Cardiac toxicity of singlet oxygen: implication in reperfusion injury. *Antioxid Redox Signal*. 2001;**3**(1):63-9.

Chapter 5 – References

- Townsend DM, Tew KD, Tapiero H. The importance of glutathione in human disease. *Biomed Pharmacother.* 2003;**57**:145-155.
- Toyokuni S, Okamoto K, Yodoi J, Hiai H. Persistent oxidative stress in cancer. *FEBS letters.* 1994;**385**:1-3.
- Tsai MJ, O'Malley BW. Molecular mechanisms of action of steroid/thyroid receptor superfamily members. *Annu Rev Biochem.* 1994;**63**:451-86.
- Ullrich A, Coussens L, Hayflick JS, Dull TJ, Gray A, Tam AW, Lee J, Yarden Y, Libermann TA, Schlessinger J, et al. Human epidermal growth factor receptor cDNA sequence and aberrant expression of the amplified gene in A431 epidermoid carcinoma cells. *Nature.* 1984;**309**(5967):418-25.
- Ungheri D, Pisani C, Sanson G, Bertani A, Schioppacassi G, Delgado R, Sironi M, Ghezzi P. Protective effect of n-acetylcysteine in a model of influenza infection in mice. *Int J Immunopathol Pharmacol.* 2000;**13**(3):123-128.
- Valko M, Rhodes CJ, Moncol J, Izakovic M, Mazur M. Free radicals, metals and antioxidants in oxidative stress-induced cancer. *Chem Biol Interact.* 2006;**160**(1):1-40.
- Vasquez-Vivar J, Kalyanaraman B, Martasek P, Hogg N, Masters BS, Karoui H, Tordo P, Pritchard KA Jr. Superoxide generation by endothelial nitric oxide synthase: the influence of cofactors. *Proc Natl Acad Sci USA.* 1998;**95**(16):9220-5.
- Wakeling AE, Dukes M, Bowler J. A potent specific pure antiestrogen with clinical potential. *Cancer Res.* 1991;**51**(15):3867-73.

Chapter 5 – References

- Wan XS, Zhou Z, Kennedy AR. Adaptation of the dichlorofluorescein assay for detection of radiation-induced oxidative stress in cultured cells. *Radiat Res.* 2003;**160(6)**:622-30.
- Wang M, Dhingra K, Hittelman WN, Liehr JG, de Andrade M, Li D. Lipid peroxidation-induced putative malondialdehyde-DNA adducts in human breast tissues. *Cancer Epidemiol Biomarkers Prev.* 1996;**5(9)**:705-10.
- Wang T, Tamae D, LeBon T, Shively JE, Yen Y, Li JJ. The role of peroxiredoxin II in radiation-resistant MCF-7 breast cancer cells. *Cancer Res.* 2005;**65(22)**:10338-46.
- Wei H, Cai Q, Tian L, Lebwohl M. Tamoxifen reduces endogenous and UV light induced oxidative damage to DNA, lipid and protein *in vitro* and *in vivo*. *Carcinogenesis.* 1998;**19(6)**:1013-8.
- Wells G, Berry JM, Bradshaw TD, Burger AM, Seaton A, Wang B, Westwell AD, Stevens MFG. 4-Substituted 4-hydroxycyclohexa-2,5-dien-1-ones with selective activities against colon and renal cancer cell lines. *J Med Chem.* 2003;**46(4)**:532-541.
- Witschi A, Junker E, Schranz C, Speck RF, Lauterburg BH. Supplementation of N acetylcysteine fails to increase glutathione in lymphocytes and plasma of patients with AIDS. *AIDS Res Hum Retroviruses.* 1995;**11(1)**:141-3.
- Wolf DM, Jordan VC. The estrogen receptor from a tamoxifen stimulated MCF-7 tumor variant contains a point mutation in the ligand binding domain. *Breast Cancer Res Treat.* 1994;**31(1)**:129-38.

Chapter 5 – References

- Wu FY, Liao WC, Chang HM. Comparison of antitumor activity of vitamins K1, K2 and K3 on human tumor cells by two (MTT and SRB) cell viability assays. *Life Sci.* 1993a;**52(22)**:1797-804.
- Wu FY, Chang NT, Chen WJ, Juan CC. Vitamin K3-induced cell cycle arrest and apoptotic cell death are accompanied by altered expression of c-fos and c- myc in nasopharyngeal carcinoma cells. *Oncogene.* 1993b;**8(8)**:2237-44.
- Xiong Y, Lei M, Fu S, Fu Y. Effect of diabetic duration on serum concentrations of endogenous inhibitor of nitric oxide synthase in patients and rats with diabetes. *Life Sci.* 2005;**77**:149-159.
- Yang Y, Sharma A, Sharma R, Patrick B, Singhal SS, Zimniak P, Awasthi S, Awasthi YC. Cells preconditioned with mild, transient UVA irradiation acquire resistance to oxidative stress and UVA-induced apoptosis: role of 4-hydroxynonenal in UVA-mediated signaling for apoptosis. *J Biol Chem.* 2003;**278(42)**:41380-8.
- Yokomizo A, Ono M, Nanri H, Makino Y, Ohga T, Wada M, Okamoto T, Yodoi J, Kuwano M, Kohno K. Cellular levels of thioredoxin associated with drug sensitivity to cisplatin, mitomycin C, doxorubicin, and etoposide. *Cancer Res.* 1995;**55(19)**:4293-6.
- Zalba G, San Jose G, Moreno MU, Fortuno MA, Fortuno A, Beaumont FJ, Diez J. Oxidative stress in arterial hypertension: role of NAD(P)H oxidase. *Hypertension.* 2001;**38(6)**:1395-9.

Chapter 5 – References

Zhou Y, Eppenberger-Castori S, Eppenberger U and Benz CC. The NFkB pathway and endocrine-resistant breast cancer. *Conference paper*. 2005;12:37-46.

Zunino SJ, Ducore JM, Storms DH. Parthenolide induces significant apoptosis and production of reactive oxygen species in high-risk pre-B leukaemia cells. *Cancer Lett*. 2007;254(1):119-27.

Websites:

<http://www.abcam.com/Ki67-antibody-Proliferation-Marker-ab15580.html>

<http://info.cancerresearchuk.org/cancerandresearch/learnaboutcancer/whatisancer/historyofcancer/>

<http://info.cancerresearchuk.org/cancerstats/types/breast/>

<http://www.genecards.org/>

<http://www.genesifter.net/web/>

<http://www.ncbi.nlm.nih.gov/sites/entrez?db=pubmed>

***Appendix I – Compilation of Signal Transduction
pathway genes related to Oxidative Stress (n =117)***

Table 1. Cell signalling proteins associated with oxidative stress.

Alias	Name
ADAM12	metallopeptidase domain 12 (meltrin alpha)
AT1	angiotensin II receptor, type 1
AKT1	v-akt murine thymoma viral oncogene homolog 1
AKT3	v-akt murine thymoma viral oncogene homolog 3 (protein kinase B, gamma)
ALS2	Amyotrophic lateral sclerosis 2 (juvenile)
AP-1	activating transcription factor 1
AP2A1	Adaptor-related protein complex 2, alpha 1 subunit
Apaf-1	apoptotic peptidase activating factor
APOA1	Apolipoprotein A-I
APP	Amyloid beta (A4) precursor protein
ARHGAP26	Rho GTPase activating protein 26
ATF4	activating transcription factor 4 (tax-responsive enhancer element B67)
ATF6	Activating transcription factor 6
BRCA2	breast cancer 2, early onset
BTK	Bruton agammaglobulinemia tyrosine kinase
CASP3	Caspase 3, apoptosis-related cysteine peptidase
CASP8	Caspase 8, apoptosis-related cysteine peptidase
CASP9	caspase 9, apoptosis-related cysteine peptidase
c-fos	v-fos FBJ murine osteosarcoma viral oncogene homolog
CREB1	AMP responsive element binding protein 1
DAG	dystroglycan 1 (dystrophin-associated glycoprotein 1)
DDAH2	dimethylarginine dimethylaminohydrolase 2
EGFR	Epidermal growth factor receptor
EGR-1	early growth response 1
ELK1	ELK1, members of ETS oncogene family
ERBB2	erythroblastic leukemia viral oncogene homolog 2
ERBB3	v-erb-b2 erythroblastic leukemia viral oncogene homolog 3
ERBB4	v-erb-b2 erythroblastic leukemia viral oncogene homolog 4
ERN1	Endoplasmic reticulum to nucleus signalling 1
ER	Estrogen Receptor 1
ET1	Endothelin-1
FGR	Gardner-Rasheed feline sarcoma viral (v-fgr) oncogene homolog
FRA1	FOS-like antigen 1
FYN	FYN oncogene related to SRC, FGR, YES
G3BP	Ras-GTPase-activating protein SH3-domain-binding protein
GCLC	Glutamate-cysteine ligase, catalytic subunit
GCSH	glycine cleavage system protein H (aminomethyl carrier)
GPAM	Glycerol-3-phosphate acyltransferase, mitochondrial
GPR132	G protein-coupled receptor 132
GR	Nuclear receptor subfamily 3, group C, member 1 (glucocorticoid receptor)
GRAP2	GRB-related adaptor 2
GRB2	Growth factor receptor-bound protein 2
GRLF1	glucocorticoid receptor DNA binding factor 1
GSH	GS homeobox 1
HBEGF	heparin-binding EGF-like growth factor
HCK	hemopoietic cell kinase
HGF	Hepatocyte growth factor (hepapoietin A; scatter factor)
HRAS	Harvey rat sarcoma viral oncogene homolog
ICAM	intercellular adhesion molecule 1 (CD54), human rhinovirus receptor
IGF1	Insulin-like growth factor 1 (somatomedin C)
IGFBP2	Insulin-like growth factor binding protein 2, 36kDa
IGFBP7	Insulin-like growth factor receptor binding protein 7
IKIP	IKK interacting protein
INrf2	kelch-like ECH-associated protein 1
JAK2	Janus kinase 2 (a protein tyrosine kinase)
JNKK	mitogen-activated protein kinase kinase 4
JUN	v-jun sarcoma virus 17 oncogene homolog (avian)

JUNB	Jun B proto-oncogene
LDLR	low density lipoprotein receptor (familial hypercholesterolemia)
LPA	endothelial differentiation, lysophosphatidic acid G-protein-coupled receptor 2
LYN	v-src-1 Yamaguchi sarcoma viral related oncogene homolog
MafF,	v-maf musculoaponeurotic fibrosarcoma oncogene homolog F (avian)
MafG	v-maf musculoaponeurotic fibrosarcoma oncogene homolog G (avian)
MafK	v-maf musculoaponeurotic fibrosarcoma oncogene homolog K (avian)
MAP3K5	mitogen-activated protein kinase kinase kinase 5
MAPK1	Mitogen-activated protein kinase 1
MAPK10	Mitogen-activated protein kinase 10
MAPK14	Mitogen-activated protein kinase 14
MAPK3	Mitogen-activated protein kinase 3
MAPK7	mitogen-activated protein kinase 7
MAPK8	Mitogen-activated protein kinase 8
MDA7	interleukin 24
MEK	mitogen-activated protein kinase kinase 1
MEKK	mitogen-activated protein kinase kinase kinase 1
MT1A	Metallothionein 1A (functional)
MT1A	metallothionein 2A
MT1H	metallothionein 1H
MTF1	metal-regulatory transcription factor 1
MYB	v-myb myeloblastosis viral oncogene homolog (avian)
MYC	v-myc myelocytomatosis viral oncogene homolog (avian)
NFE2	nuclear factor (erythroid-derived 2), 45kDa
NFE2L2	Nuclear factor (erythroid-derived 2)-like 2
NFIX	Nuclear factor I/X (CCAAT-binding transcription factor)
NFKBIA	Nuclear factor of kappa light polypeptide gene enhancer in B-cells inhibitor A
NGF	nerve growth factor, beta polypeptide
nPKC-eta	protein kinase C, eta
P53	Tumor Protein p53 (Li-Fraumeni syndrome)
PAFR	platelet-activating factor receptor
PAK1	p21/Cdc42/Rac1-activated kinase 1 (STE20 homolog, yeast)
PDGF1	platelet-derived growth factor alpha polypeptide
PECAM1	platelet/endothelial cell adhesion molecule (CD31 antigen)
PI3K	Phosphoinositide-3-kinase, catalytic, gamma polypeptide
PIP3-E	phosphoinositide-binding protein PIP3-E
PKC-alpha	protein kinase C, alpha
PKC-beta	protein kinase C, beta 1
PKC-gamma	protein kinase C, gamma
PLA2	phospholipase A2, group IIA (platelets, synovial fluid)
PLCG1	phospholipase C, gamma 1
PPARA	peroxisome proliferative activated receptor, alpha
PRKCD	protein kinase C, delta
PYK2	proline-rich tyrosine kinase 2
RAC1	Ras-related C3 botulinum toxin substrate 1
RAF1	v-raf-1 murine leukemia viral oncogene homolog 1
ROCK	Rho-associated, coiled-coil containing protein kinase 1
SELE	selectin E (endothelial adhesion molecule 1)
SHC	Src homology 2 domain containing transforming protein 1
SOS1	son of sevenless homolog 1
SP1	Sp1 transcription factor
SRC1	viral oncogene homolog (avian)
SYK	spleen tyrosine kinase
TGFB1	Transforming growth factor, beta induced, 68kDa
TGFB1	transforming growth factor, beta 1 (Camurati-Engelmann disease)
TNF	tumor necrosis factor (TNF superfamily, member 2)
Traf2	TNF receptor-associated factor 2
VCAM1	vascular cell adhesion molecule 1
YBX1	Y box binding protein 1
ZAP70	Zeta-chain (TCR) associated protein kinase 70kDa

Appendix II – Methodology Recipes

csFCS

csFCS was achieved by initially preparing 100ml aliquots of standard FCS (pH 4.2) left at 4°C for 30minutes to equilibrate. A charcoal (11.1%) and dextran C (0.06%) solution was prepared with distilled water and Norit A, and mixed well for 1 hour, whereby 5ml of this charcoal solution (5%) was added to each 100ml aliquot csFCS and incubated (with mild agitation) at 4°C for a further 16 hours. Any traces of charcoal were removed by centrifugation (12000g for 40minutes) followed by filtering through grade 4 filter paper. The charcoal solution was then readjusted to pH7.2 and passed through 0.2µM membrane filter to remove any impurities and contaminating micro-organisms.

TESPA coating

TESPA coating of coverslips was carried out by an initial 5 seconds dipping a solution in 6ml TESPA of 300ml Acetone, with 2 minutes subsequent washing in Acetone alone, followed by 2x1minute washes in ultrapure distilled water before sterilisation by Autoclaving before use.

